THE ROLE OF BIOMEMBRANES AND BIOPHYSICS IN IMMUNE CELL SIGNALING

EDITED BY: Yan Shi, Erdinc Sezgin and Wei Chen
PUBLISHED IN: Frontiers in Immunology and Frontiers in Physiology

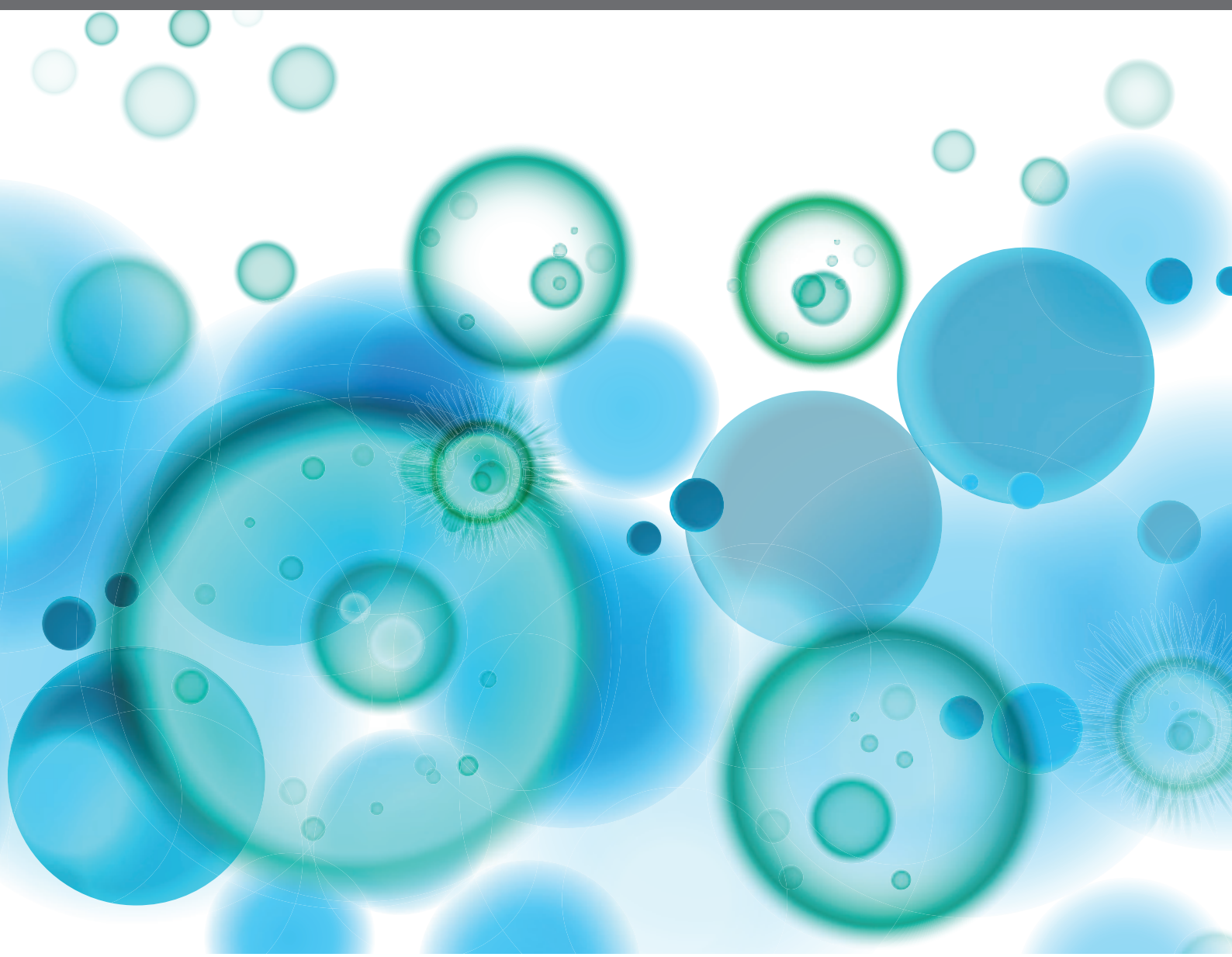

frontiers Research Topics

frontiers

ISSN 1664-8714
ISBN 978-2-88971-634-0
DOI 10.3389/978-2-88971-634-0

About Frontiers

Frontiers is more than just an open-access publisher of scholarly articles: it is a pioneering approach to the world of academia, radically improving the way scholarly research is managed. The grand vision of Frontiers is a world where all people have an equal opportunity to seek, share and generate knowledge. Frontiers provides immediate and permanent online open access to all its publications, but this alone is not enough to realize our grand goals.

Frontiers Journal Series

The Frontiers Journal Series is a multi-tier and interdisciplinary set of open-access, online journals, promising a paradigm shift from the current review, selection and dissemination processes in academic publishing. All Frontiers journals are driven by researchers for researchers; therefore, they constitute a service to the scholarly community. At the same time, the Frontiers Journal Series operates on a revolutionary invention, the tiered publishing system, initially addressing specific communities of scholars, and gradually climbing up to broader public understanding, thus serving the interests of the lay society, too.

Dedication to Quality

Each Frontiers article is a landmark of the highest quality, thanks to genuinely collaborative interactions between authors and review editors, who include some of the world's best academicians. Research must be certified by peers before entering a stream of knowledge that may eventually reach the public - and shape society; therefore, Frontiers only applies the most rigorous and unbiased reviews.
Frontiers revolutionizes research publishing by freely delivering the most outstanding research, evaluated with no bias from both the academic and social point of view. By applying the most advanced information technologies, Frontiers is catapulting scholarly publishing into a new generation.

What are Frontiers Research Topics?

Frontiers Research Topics are very popular trademarks of the Frontiers Journals Series: they are collections of at least ten articles, all centered on a particular subject. With their unique mix of varied contributions from Original Research to Review Articles, Frontiers Research Topics unify the most influential researchers, the latest key findings and historical advances in a hot research area! Find out more on how to host your own Frontiers Research Topic or contribute to one as an author by contacting the Frontiers Editorial Office: frontiersin.org/about/contact

THE ROLE OF BIOMEMBRANES AND BIOPHYSICS IN IMMUNE CELL SIGNALING

Topic Editors:
Yan Shi, Tsinghua University, China
Erdinc Sezgin, Karolinska Institutet (KI), Sweden
Wei Chen, Zhejiang University, China

Citation: Shi, Y., Sezgin, E., Chen, W., eds. (2021). The Role of Biomembranes and Biophysics in Immune Cell Signaling. Lausanne: Frontiers Media SA.
doi: 10.3389/978-2-88971-634-0

Table of Contents

frontiers in Immunology

EDITORIAL
published: 24 September 2021
doi: 10.3389/fimmu.2021.740373

Editorial: The Role of Biomembranes and Biophysics in Immune Cell Signaling

Yan Shi[1,2*†], *Erdinc Sezgin*[3*†] *and Wei Chen*[4*†]

[1] Department of Basic Medical Sciences, Institute for Immunology, Beijing Key Lab for Immunological Research on Chronic Diseases, School of Medicine, Tsinghua University, Beijing, China, [2] Department of Microbiology, Immunology and Infectious Diseases, Snyder Institute, University of Calgary, Calgary, AB, Canada, [3] Science for Life Laboratory, Department of Women's and Children's Health, Karolinska Institutet, Solna, Sweden, [4] Department of Cell Biology and Department of Cardiology of the Second Affiliated Hospital, Zhejiang University School of Medicine, Hangzhou, China

Keywords: cell membrane, lipid domains, membrane biophysics, receptor signaling, T cell receptor

Editorial on the Research Topic

The Role of Biomembranes and Biophysics in Immune Cell Signaling

OPEN ACCESS

Edited by:
Harry W. Schroeder, University of Alabama at Birmingham, United States

Reviewed by:
Nicolas Destainville, Université de Toulouse, France

***Correspondence:**
Yan Shi
yanshiemail@mail.tsinghua.edu.cn
Erdinc Sezgin
erdinc.sezgin@ki.se
Wei Chen
jackweichen@zju.edu.cn

†These authors have contributed equally to this work

Specialty section:
This article was submitted to B Cell Biology, a section of the journal Frontiers in Immunology

Received: *13 July 2021*
Accepted: *06 September 2021*
Published: *24 September 2021*

Citation:
Shi Y, Sezgin E and Chen W (2021) Editorial: The Role of Biomembranes and Biophysics in Immune Cell Signaling. Front. Immunol. 12:740373. doi: 10.3389/fimmu.2021.740373

The plasma membrane is the ultimate demarcation between "in" and "out" for cellular life forms. It is also the platform on which "cross border" communications take place, such as receptor ligand interactions. Here, several thousand species of membrane proteins anchored by their transmembrane domains on this platform specifically sense complex biological, biochemical, and biophysical cues in the extracellular environment and trigger signaling cascades to determine various cellular functions. While modern technologies permit our study into the structure, dynamic, and function of these proteins, the reality is, the behaviors of this platform itself are likely more complex and in most cases heavily shielded from our probing eyes. The challenge of studying how membrane properties affect membrane-receptor functions is multi-faceted, and this is rooted in the complex heterogeneity of the membrane itself. As each layer of complexity can affect cellular signaling, the question becomes where we shall start to look. One of the issues is the limited availability of suitable tools. The most evident one is the resolution power constrained by optical diffraction, the size below which most biophysical events take place on the membrane. Another challenge is that the tools required for biophysical sensing and manipulation are often of limited sensitivity of mechanical forces. In addition, different from protein and nucleic acid related research, whereby clear causality can be established when all variables are controlled, membrane biophysics is intrinsically chaotic with numerous factors working at the same time in a promiscuous manner and events are often transitional.

In this Research Topic collection, the coverage reflects the complexity of this battle ground. Significant attention is paid to the instrument development that is arguably more important to this research scheme than conventional biochemistry-based research fields. In this editorial, we attempt to establish a progressive line based on three dimensions of complexity in biomembrane research, and settle the contributors' insights into suitable spots on this logic chain.

Singer and Nicolson's mosaic model is straight forward: that lipid species are randomly distributed and proteins are present free from additional constraints. This view, however, is too simplistic. It is generally accepted that membrane and membrane proteins have several layers of complexity. 1. Heterogeneity of membrane bilayer. 2. Lipid-protein interface and secondary membrane structure. 3. Receptor signaling in a lipid environment.

First layer of complexity comes from the lipid domains. One of the key features of eukaryotic cell forms is the emergence of cholesterol synthesis, typically *via* mevalonate pathway in animals. This simple lipid species changes the membrane behavior substantially and is a key player on the bilayer asymmetry.

In mammalian membrane, due to their peculiar packing requirement, sphingolipids are only present on the outer leaflets. The presence of sphingolipids and cholesterol forms the first layer of complexity: lipid ordered domains, roughly equivalent of lipid rafts. Physiological ordered domains on a cell surface likely involve coupling between outer and inner leaflets, cytosolic components such as cytoskeleton and several classes of transmembrane and membrane-associated proteins. However, the fact remains that in giant unilamellar vesicles with defined ternary mixtures of saturated and unsaturated lipids with cholesterol, the phase separation still takes place. Intriguingly, on >1000 component giant plasma membrane vesicles (cell-derived vesicles that preserve largely cellular plasma membrane composition), phase separation is still observed and the ordered domains to some degree can be regarded as "raft"-like (although larger). The domain behavior in model systems (such as size, shape etc.) can be modulated *via* changing the environmental conditions or adding external components (1–3). The ordered domains have several essential features: they probably sort the inner leaflet lipid species across the hydrophobic core, yet this interleaflet coupling still needs extensive work both in model systems and in live cell membranes. In this regard, role of membrane asymmetry on membrane domains is also largely unexplored. Recent work shows that plasma membrane is asymmetric not only in lipid head groups but also in acyl chain length and saturation (4). Therefore, it will be exciting to see future work on how this multi-layer asymmetry affects the interleaflet coupling, domain formation and their physicochemical properties. The ordered domains are also assumed to be linked to cortical cytoskeleton *via* linker such as ERM (ezrin/radixin/moesin) as a result of inner leaflet lipid tuning. In laying the biophysical grounds to establish a model that explains microvilli on T cells, Cebecauer provided a sophisticated overview how this may work. Sphingolipid-dependent lipid domains are distinguished from the rest of the membrane by a lipid-lipid interface holing a definitive line tension. This tension creates a circular entrapping effect that drives lipid domains upwards. The accumulation of PIP2 likely draws in FERM (Band 4.1 ERM)-domain containing proteins that drive the growth of microvilli on T cells. The underlying principle is likely applicable to ordered domains without invoking the extreme curvature as in microvilli formation. Taking the angle of membrane cholesterol, Zhang et al. discussed how receptors may be regulated by this lipid domain. A key point, even from the narrow confines of cholesterol, is that its impact on receptor signaling can be extremely complex and stimulation-dependent. Cholesterol by itself inhibits TCR β chain from entering a "primed" state. On the other hand, it is also essential to potentiate T cell functions probably through enhancing TCR and lipid domain clustering. Such regulation is likely involved in BCR and FCR signaling. From the biochemical standpoint, cholesterol stiffens the local lipid environment, which may be a key platform for the receptor ligation to transduce mechanical force across the membrane. From a theoretical perspective, Lamerton et al. discussed the concept of protein and lipid clustering. At the lipid level, clustering may be lipid rafts from a different viewing angle, particularly when defined as saturated acyl tails working together with cholesterol to form densely packed lipid domains.

The second layer of complexity is the interaction of lipid membrane and proteins. Proteins in this case can be separated into two groups per their association with the membrane. The first group is those contained within the bilayer, such as Bin-Amphiphysin-Rvs family proteins that intrinsically alter membrane curvature. They interact with cytoskeletal regulators which control actin nucleation and F-actin remodeling. Realistically, all transmembrane proteins likely impact biophysical properties of lipid membranes to various extents, however, we shall refrain from that discussion as the reciprocity therein becomes too compounded for this editorial. The second group of proteins are those approaching the membrane from the inside, mainly those of cortical cytoskeleton. Chief among which are the ERM proteins. Their central involvement can be deduced from their structure. N-terminal FERM domains are known to bind a diverse set of cytosolic tails of transmembrane proteins, such as CD44 and EGFR. Critically, FERM domain has specificity to PIP2 (phosphatidylinositol (4,5) biphosphate), a lipid species known to sort per influence of lipid orders. The C-terminal of ERM proteins is a C-ERMAD domain, which binds to F-actin. FERM and C-ERMAD domains self-associate and remain soluble in cytosol. Binding of FERM to PIP2 activates those proteins. This design creates numerous interactions as a consequence of membrane dynamics on the inner leaflet and is likely responsible for the more complex membrane protrusions, such as filapodia, lamina podia, and as the "favorite child" of this collection, T cell microvilli. Orbach and Su presented an abstract, yet vivid, reconstitution on how those microvilli come to being on T cells surface. The role of those often ignored features in T cell biology is also convincingly illustrated and it is understood that such a finger-like feature may increase the "scanning" of antigen presenting cells. From a different perspective, these membrane protrusions may represent an underappreciated hand in organizing lipid domains and receptor complex components, which may have different preferences to a particular lipid order. A key event described by the kinetic-segregation model is the separation of CD45 from the rest of signaling complex, which likely maintains a state of high phosphorylation for the key factors associated with TCR/CD3 signaling. Apparently, structural features of microvilli favor this segregation. Of particular interest is the piece by Dam et al. that discussed a phenomenon related to this topic (5). Supported lipid bilayers are commonly used a surrogate of MHC/peptide to interact with TCR. Such a design had led to an unexpected finding that exclusion of CD45 from the TCR complex is sufficient to trigger ligand free activation. Dam et al.'s data suggested that this might be due to intrinsic binding to nickel-chelating lipids, rather than specific TCR interactions, which serves a reminder that some biophysical analyses must be carefully controlled to avoid artifacts.

The third layer of complexity is how lipid environment impacts receptor signaling. Starting from a resting receptor, there are two parameters to be determined. 1. Their preference with reference to ordered domains. 2. Their state of aggregation prior to ligand binding. Upon ligand binding, biophysical properties of the membrane will significantly alter receptors' signaling potential. In the case of TCR, the story is complex. For a simple treatment of cholesterol depletion, T cell activation can be either diminished or

enhanced. This outcome is setup-dependent, revealing that there is much more information yet to be extracted. Likely, the association of TCR β chain with cholesterol is inhibitory (this is still being debated). The activation step requires a step that escapes this association. Yet, src family kinases are located in ordered domains, and at minimum final assembly of signaling complex requires proper arrangements of TCR, CD3 chains, transmembrane phosphatases, upstream ITAM-specific kinases, downstream targets including LAT platform, as well as several enzymes involved in PI metabolism. If the lipid order is integrated into TCR signaling, there must be some type of rearrangement of each component, not only for their positioning against each other, but also for their interfaces toward the lipid environment – a complexity likely beyond our current comprehension. Equally important, the formation of the signaling complex is also regulated by the cytoskeleton, which to some degree controls the formation of transmembrane receptors. Either through individual dissection, or a grand design of a formidably intricate experiment, solving the details of this process will be the final answer to TCR activation. At the moment, we know the lipid composition is critical to TCR activation. For instance *the in-situ* TCR-pMHC binding strength is likely lipid-dependent (Zhang et al.). This step perhaps introduces a conformational change that turns both TCR ectodomains and the CD3 chains, exposing ITAM motifs folded into negatively charged inner leaflet. Membrane bilayer could also provide physical platform to produce and transmit biomechanical force to regulate TCR antigen recognition by inducing TCR/CD3 and pMHC conformational changes and to trigger signaling. As to be expected, biophysical properties can affect receptor signaling, thus impacting several categories of immune dysfunctions and diseases. In this series, Gunasinghe et al. gave a comprehensive review that can serve as an insightful reference for those interested in biomechanical dysfunctions in chronic diseases. Shi and Ruan presented another possibility in addition of organizing role of ordered domains in receptor signaling, that the presence of lipid domains may be an intrinsic property that prevents receptor from spontaneous activation. Receptor activation may in some cases a simple instruction from ligands to avoid this suppression. Whether this proposal can stand the test of time will depend on experiments of several major receptor ligand interactions, especially with the aid of recent instrument development.

With all the challenges discussed, we remain enthusiastic that biophysical research on membrane is entering a new era. This confidence is supported by the rapid arrival of new instruments. Compared with other research fields, instrument and protocol developments are the lifeline of new discoveries. A sobering example is the transition in membrane domain research from the sole dependence of detergent solubilizing extraction to polarity sensing lipid dyes such as laurdan, as well as, sub-optical diffraction imaging, as illustrated by Lamerton et al. in this series. With a focus on cytoskeletal interaction with plasma membrane, Schneider et al. discussed at depth the new imaging tools currently available, starting from more conventional TIRF, SPT to more sophisticated fluorescence fluctuation-based FCS in combination with STED and fluorescence energy transfer-based techniques. This discussion should be of considerable value in helping select best and latest tools for all of us. Another interesting piece by Stanly et al. discussed a new development in optical diffraction tomography in studying intracellular sphericity, as well as refractive index in diseased platelets, pointing to an uncommon biophysical angle of evaluation (6). Using FLIM and FRET techniques, Vleeshouwers et al. presented new findings on how prostaglandin E2 receptors regulate podosome dissolution *via* microtubules. While this study is not directly focused on biomembrane, it nevertheless reflects the additional dimension biophysics in cell biology, such as how both two systems of cytoskeleton, actin and microtubules, take part in cellular adhesion.

In the original proposal to start this Research Topic, it was our intension to gather thoughts on biophysical analyses of cellular membranes, as the area is relatively uncoordinated in protocols, standards and concepts. It was recognized that coordination can only be started with a substantive exchange. At this moment of closing off this series, we are excited by the breadth and insight of submissions collected. This effort, in our view, is one of the very rare series solely focused on biophysics on cellular membrane and a good foundation for future growth of this research scheme.

AUTHOR CONTRIBUTIONS

All authors contributed equally. All authors contributed to the article and approved the submitted version.

REFERENCES

1. Cornell CE, Skinkle AD, He S, Levental I, Levental KR, Keller SL. Tuning Length Scales of Small Domains in Cell-Derived Membranes and Synthetic Model Membranes. *Biophys J* (2018) 115:690–701. doi: 10.1016/j.bpj.2018.06.027
2. Destainville N, Manghi M, Cornet J. A Rationale for Mesoscopic Domain Formation in Biomembranes. *Biomolecules* (2018) 8(4):104. doi: 10.20944/preprints201807.0492.v1
3. Shimobayashi SF, Ichikawa M, Taniguchi T. Direct Observations of Transition Dynamics From Macro- to Micro-Phase Separation in Asymmetric Lipid Bilayers Induced by Externally Added Glycolipids. *EPL (Europhysics Lett)* (2016) 113:56005. doi: 10.1209/0295-5075/113/56005
4. Lorent JH, Levental KR, Ganesan L, Rivera-Longsworth G, Sezgin E, Doktorova M, et al. Plasma Membranes Are Asymmetric in Lipid Unsaturation, Packing and Protein Shape. *Nat Chem Biol* (2020) 16:644–52. doi: 10.1038/s41589-020-0529-6
5. Dam T, Junghans V, Humphrey J, Chouliara M, Jonsson P. Calcium Signaling in T Cells Is Induced by Binding to Nickel-Chelating Lipids in Supported Lipid Bilayers. *Front Physiol* (2020) 11:613367.
6. Stanly TA, Suman R, Rani GF, O'Toole PJ, Kaye PM, Hitchcock IS. Quantitative Optical Diffraction Tomography Imaging of Mouse Platelets. *Front Physiol* (2020) 11:568087.

Conflict of Interest: The authors declare that the research was conducted in the absence of any commercial or financial relationships that could be construed as a potential conflict of interest.

frontiers in Immunology

PERSPECTIVE
published: 09 September 2020
doi: 10.3389/fimmu.2020.01909

Toward a Membrane-Centric Biology

Yan Shi [1,2,3,4,5]* *and Hefei Ruan* [1,2,3,4]

[1] Tsinghua-Peking University Joint Center for Life Sciences, Tsinghua University, Beijing, China, [2] Department of Basic Medical Sciences, Tsinghua University, Beijing, China, [3] Institute for Immunology, Tsinghua University, Beijing, China, [4] Beijing Key Lab for Immunological Research on Chronic Diseases, School of Medicine, Tsinghua University, Beijing, China, [5] Department of Microbiology, Immunology and Infectious Diseases, Snyder Institute, University of Calgary, Calgary, AB, Canada

With advancements of modern biophysical tools and superresolution imaging, cell biology is entering a new phase of research with technological power fitting for membrane dynamics analyses. However, our current knowledge base of cellular signaling events is mostly built on a network of protein interactions, which is incompatible with the essential roles of membrane activities in those events. The lack of a theoretical platform is rendering biophysical analyses of membrane biology supplementary to the protein-centric paradigm. We hypothesize a framework of signaling events mediated by lipid dynamics and argue that this is the evolutionarily obligatory developmental path of cellular complexity buildup. In this framework, receptors are the late comers, integrating into the pre-existing membrane based signaling events using their lipid interface as the point of entry. We further suggest that the reason for cell surface receptors to remain silent at the resting state is via the suppression effects of their surrounding lipids. The avoidance of such a suppression, via ligand binding or lipid domain disruption, enables the receptors to autonomously integrate themselves into the preexisting networks of signaling cascades.

Keywords: plasma membrane, lipid rafts, evolution, receptor ligand model, lipid interaction, receptor activation mechanism

OPEN ACCESS

Edited by:
Junji Xing,
Houston Methodist Research Institute, United States

Reviewed by:
Chaofeng Han,
State Key Laboratory of Medical Immunology, Second Military Medical University, China
Chunfu Zheng,
Fujian Medical University, China

***Correspondence:**
Yan Shi
yanshiemail@mail.tsinghua.edu.cn

Specialty section:
This article was submitted to Molecular Innate Immunity, a section of the journal Frontiers in Immunology

Received: *21 May 2020*
Accepted: *16 July 2020*
Published: *09 September 2020*

Citation:
Shi Y and Ruan H (2020) Toward a Membrane-Centric Biology. Front. Immunol. 11:1909. doi: 10.3389/fimmu.2020.01909

INTRODUCTION

The main goal of this piece is to gather sufficient consensus regarding how biophysicists, or other specialists so inclined, may approach life science research with a stronger footing of legitimacy. In recent years, with advancements in superresolution imaging and computational biology, biophysicists are given enormous probing power in our life science work. In comparison, traditional biologists using more conventional tools are still making ground-breaking discoveries at a pace appreciably faster than most of us. A sobering dichotomy is evident that findings made with biophysical approaches are being regarded as "supplemental" to other paradigms. Using T cell biology as an example, whereas many papers have been published in this area regarding membrane behavior upon T cell receptor activation, the whole theoretical framework of T cell activation can be completely explained without any reference to biophysical properties. Points of interest in biophysics or membrane biology are generated to explain the details of how polypeptides work. While we know for certain that this cannot be true, our strongest protest may be the insistence that "no signaling can be fully understood without its membrane platform." *C'est la vie*, such a defensive stand will not change the "outsider looking-in" mentality. We need to move biophysics and membrane biology to the frontlines of biological research. The questions are "why hasn't it happened?" and "what is the main roadblock?"

MAIN TEXT

The current state of biological research is protein-centric. The cause lies in its history and the availability of investigative tools. Yet, conceptual inertia is not beyond reproach. Our inability to delineate biological events with models built from membrane biology is the core deficiency. It is time that we collectively reflect on this dilemma. In this opinion piece, we make a call for change.

Membrane Structure, Critical Behavior, and Their Preservation in Biology

Let's start with the eukaryotic membrane. In the 70s, Singer and Nicolson presented the mosaic model in which the membrane bilayer was regarded as a fluid mixture of lipids and proteins (1). With many years of work into the heterogeneity of vesicular and plasma membranes, Kai Simons et al. in 1997 proposed the concept of ordered and disordered membrane phases generically known as the lipid raft theory (2). Aki Kusumi, mainly using particle tracking, refined this model with an additional detail that lipid domains are stabilized by membrane lipid binding to cortical cytoskeleton, or the picket and fence model (3). As those theories are discussed at length elsewhere and readers of this writing are well versed in this stream of concepts, we simplify our discussion with the most accepted membrane model (4). Eukaryotic membrane inner leaflets are occupied by mostly phospholipids with negative charge and are active in signal exchange in abundance. In comparison the outer leaflets are structurally dynamic. There, sphingolipids and gangliosides are more enriched, perhaps due to their enlarged head groups more suited to the positive curvature. Cholesterol, nimble in size and low in charge, is free to move laterally (5) or change leaflets via overcoming the energy barrier set by hydrophobic core of the bilayer (6). The rendezvous of sphingolipids, cholesterol, and saturated phospholipids at physiological temperatures forms the structure of ordered lipid domains. The formation of ordered vs. disordered lipid domains can be explained by the combined entropic diffusion and energy conservation in special lipid pairing (7, 8). Remarkably, this feature is common to all eukaryotes despite the vast different collections of lipid species in distinct cell types. About 5% of genes are dedicated to maintain it (4). As current efforts have not been able to fully mimic domains found in live cells with defined lipids, the remarkable preservation implies an extreme cellular dedication in their maintenance. This point alone should give us a strong clue that this is something central to all aspects of eukaryotic biology.

Another intrigue of the lipid domains is the critical behavior which refers to the state where at physiological temperature, lipid domain formation (demixing) and dissolution (mixing) are at a critical point (7). This feature, coupled to cytoskeletal association, was vividly demonstrated with STED superresolution microscopy, and with a clear linear correlation to the temperature (9). Such a delicate feature allows large phase transition with minimal energy input. For instance, minute disturbance of receptor ligand interaction may force such a phase change, an ingenious system of signal amplification (receptor ligation can be viewed as a localized suppression of entropy, or cooling). We shall return to this point later. Nevertheless, it should be noted that such a behavior is unimaginable in a cohort of protein molecules.

Current Status of Understanding

Since the proposal of lipid rafts, biologists have tried to incorporate this feature into their models of membrane signaling. To circumvent the optical diffraction limit which makes visual observations of resting cell lipid rafts impossible, two surrogates have been developed. One is to isolate detergent-resistant membrane domains, hoping to capture proteins associated with or free from lipid rafts at the moment of cell lysis (10). The other, used by some, is to observe domain coalescence at the point of "signalosome" formation (11) or visible lipid domains found on GPMV (12). One of the most influential conclusions is the partition of protein molecules into different phases of membrane domains. From those experiments, it was understood that the transition of those protein molecules with reference to lipid domains is associated with their state of activation. Some are activated in disordered phase, such as EGFR (13), while in others transition into or residence inside the ordered domain is required for their activation, such as death receptor Fas, IFNγR, and Wnt receptor (14–16). In addition, protein signaling complex formation with the participation of numerous components is also controlled by the coalescence of lipid rafts, such as in TCR activation (17). Regardless of the study subject, in a protein-centric world, those events are regarded as the consequence of receptor ligation and protein–protein interaction, which is taken as the driving force of lipid domain alteration.

Those observations, however, are not without their own peril. First, the selection of detergents has a tremendous effect on the observed association, demanding caution in data interpretation. Perhaps more importantly, this "snap photo" approach will leave out spatial temporal regulation. Using TCR as an example, the signaling is mediated by TCR ligation by the MHC/peptide complex, yet the signal is initiated at Src family kinase activation of the tyrosine residues in the ITAM motifs. Thereafter, the signal has several bifurcations or multiplications; some of downstream events such as Lck and LAT are clearly dependent on lipid domains (18), while others such as TCR itself and CD45 are not (19, 20). Likely due to those technical limitations, some conclusions are not always in agreement. In a remarkable demonstration of collegiality among biophysicists, those differences are accepted as limits of one's own research unable to explain seemingly contradicting results. In fact, those differences *en masse* reflect the lack of more sophisticated tools as well as a biophysical explanation of how membranes work in this setting. Happily, the constraint posed by tool selection is being rapidly lifted in recent years. A particular case in point is the newly gained ability to study the dynamics of lipid rafts on the cell membrane, which in our opinion is the technological foundation to introduce membrane dynamics into core concepts of biology.

Evidence of Membrane Lipid Interface Is a Biological Switch

Imagine a simplest eukaryotic cell with no cell surface receptor and driven by a few signaling pathways that support the basic

biology. All those regulations are anchored to membrane sensing. Earliest multicellular animals were found about 600 million years ago. Shortly after, about 550 million years ago, life rapidly diversified during the Cambrian explosion. Around that time two rounds of whole genome duplication likely provided a genetic playground for the emergence of vertebrates (20). It is hard to imagine that receptor ligand interactions would have been the dominant way of communication prior to these junctures. The definition of receptor-ligand interaction is that they must be evolutionarily coupled. As a single cell is exposed to an unmalleable environment, this co-evolution lacked a driving force. On the flip side, receptor-independent sensing of environment, such as phagocytosis (21, 22), was a daily occurrence that had propelled the evolution for at least 1.4 billion years. Many prominent signaling pathways came before this time, including GTPase (23), MAPK (24), phagocytosis (21), TNFRF (25), Jak/Stat (26) pathways, metalloproteases, (27) and metabolic events with a possible exception of Wnt pathway (28). All those pathways are regulated by membrane events. In our own research, we first discovered that solid particle binding to plasma membrane induces the accumulation of lipid rafts which triggers phagocytosis (29, 30). Based on this finding, we further revealed that immune receptors had evolved out of a primordial phagocytic signaling that uses the membrane anchoring protein moesin to sense the PIP2 accumulation in the inner leaflet as a result of particle binding. Moesin binding to PIP2 opens its ITAM motif, for downstream signaling, including Syk and PI3K. Remarkably, all those events are used verbatim in immune signaling of all classes, including BCR, TCR, and Fc receptors (21). Therefore, the adaptive immunity hijacked the machinery of the ancient phagocytosis following membrane sensing. If the intracellular events are regulated by membrane activities, what argues against the notion that modern immune receptors initiate signaling with the same mechanism?

Let's look at another set of events observed by most if not all whom have attempted: the consequence of lipid domain perturbation, mostly in the form of cholesterol depletion. EGFR (31–33), TNFR1 (34), TLRs (35, 36), TCR (19, 37, 38), TGFβR (39–41), and shedding events (42–44) are triggered by lipid domain disruption. **Figure 1** illustrates our own findings. There are certainly good examples where clustering toward lipid rafts is induced by ligand binding. Linked to the observation that those receptors are sequestered in their own lipid environment at the resting state, one can reasonably predict: 1. Some receptors are self-activating depending on the lipid environment or phase transition. 2. For one receptor to be accepted as useful contributor to biology, it would have to obey the suppression of the membrane. Therefore, membrane lipid phases are an ingrained tool of suppression of receptors. Kai Simons noted that due to the size of lipid domains, each raft would contain very few polypeptides (45). Therefore, those receptors are blocked by their spatial separation. Once the blockage is released, such as in the case of domain disruption, they become activated. Fessler and Parks used a number of examples to show how lipid perturbation itself is sufficient to activate many receptors (46). Yet, they stopped at the last step to connect the final dots that lipid perturbation-mediated receptor activation and ligand/receptor-based activation may be fundamentally the same at least for some receptor families. To extrapolate this idea further, we can imagine that a receptor ligation interaction, rather than bringing in certain conformations to accommodate their interaction binding partners, could easily regulate its lipid interface to avoid the suppression. In light of the critical behavior in membrane lipids, such a minute change can cause the clustering of signaling molecules as a consequence of lipid domain alteration at the energy level fitting for receptor ligand interaction. This hypothesis, with modern tools, should be testable *in situ* or on a model membrane without the need of biological feedback, which often causes protein-centric analyses becoming embroiled in incessant cycles of amplification. If a receptor/lipid interface event is established as being autonomous, this binary regulation certainly carries an enormous power of prediction, with a simplistic elegance not seen in sometimes chaotic search of how each protein receptor works with its downstream partners (**Figure 2**). At minimum, it explains why several thousand signaling receptors can stay silently together on a cell, and during an activation event, several signaling cascades are triggered at the same time, as those involved are likely gated by their own membrane sequestration. This is not to say that receptors are mere puppets in this chain of events; they certainly play their role in the clustering and their own complex formation as they also possess ranges of lipid specificities and membrane dynamics (47, 48). But the activation initiation point can be explained by lipid receptor interface, or the sum of "collectives" of protein-lipid interaction following the introduction of a ligand.

Toward a Simple Beginning

Our lab has preliminary data to suggest that "suppression avoidance" is a core mechanism of some cell death receptors, and the cellular signaling is initiated at the simple phase change between the receptor and its surrounding lipid species. This type of effort, while fulfilling the common wisdom that receptor activation is responding to its ligand, is probably also suited to explain some activation triggers, particularly those that are not protein in nature. In such a scenario, many "ligands" can activate their "receptors" via lipid alteration without the need of direct engagement. For instance, a long acyl chain fatty acid can alter the domain features, which allows a particularly strong signaling receptor to become activated in response to lipid domain change. Macroscopically, this would look like a perfect receptor/ligand interaction. Current dogma would require the search of how this pair of receptor/ligand works, but the "suppression avoidance" model would relieve ourselves from this futility. In fact, some of the low-hanging fruits should be easy to spot.

We are not arguing against the vast network of protein signaling in biology. However, from an evolutionary perspective, membrane triggered events should be highly relevant and they set the basic signaling principles in the cell. The numerical imbalance between the vast number of cell/vesicle surface receptors and limited signaling pathways clearly tells us that the former hijacked the latter, to develop the mesmerizingly

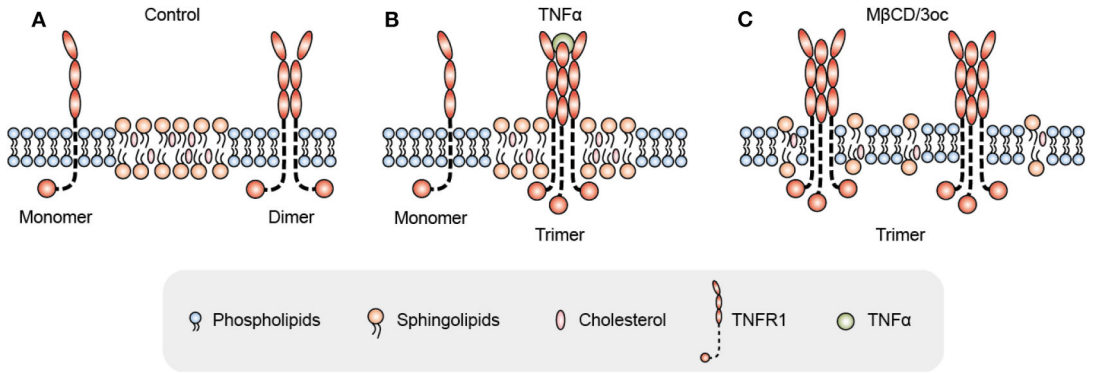

FIGURE 1 | Proposed mechanism for TNFR1 signal activation initiated as a negotiation between the receptor and its surrounding lipid species. **(A)** In the resting state, TNFR1 mainly exists as monomers and dimers on the cell membrane under the suppression of dense lipid rafts. **(B)** Under TNFα ligand stimulation, TNFR1 negotiates with lipid domains by changing its transmembrane domain conformation, and then enters lipid rafts for trimerization. **(C)** When the lipid rafts are disrupted by MβCD or 3oc [N-(3-oxododecanoyl) homoserine lactone], TNFR1 spontaneously trimerizes and activates signals without ligands as the membrane suppression is relieved.

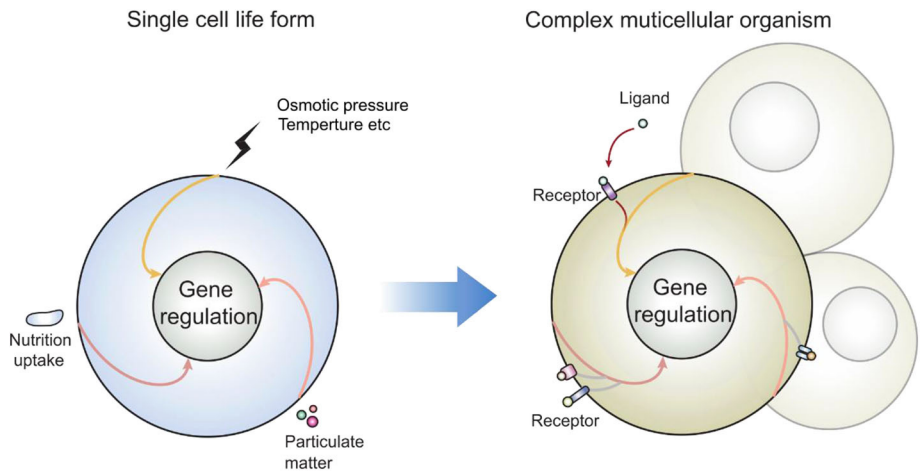

FIGURE 2 | How receptors may enter the preexisting signal cascades: as many signaling events present in modern day eukaryotic cells predate the multicellular life forms, those enclosed single cells interacted with the environment via lipid membrane. Those signal cascades are therefore coupled to membrane sensing, particularly in response to lipid domain alteration. New receptors cannot reinvent a new signal cascade; rather than producing protein molecules as adaptors, they can also regulate their own lipid interface, which is the legitimate and built-in mechanism of cell activation.

complex activation patterns in modern eukaryotic cells. Similar to the preservation of amino acid codons, those basic signaling events cannot be altered in the biological continuum. Then it is reasonable to question how the late comers, the receptor-ligand interaction, came into the theme. For our purpose, if they also use the lipid interface as the initiation point, then we have the theoretical prowess to establish a model toward a membrane-based biology, to smooth out rough edges and peculiarities in the protein-centric paradigm.

This opinion piece may be deemed inaccurate or even false in the future. However, as a research discipline with cutting edge tools and deals with some of the most autonomous events that formed the platform for other late developed biology, our collective attempt to create a landscape for this new frontier, no matter how juvenile at the beginning, is certainly worthwhile.

DATA AVAILABILITY STATEMENT

The original contributions presented in the study are included in the article/supplementary material, further inquiries can be directed to the corresponding author/s.

AUTHOR CONTRIBUTIONS

YS conceptualized the theory and wrote the manuscript with assistance from HR. All authors contributed to the article and approved the submitted version.

FUNDING

YS was supported by the joint Peking-Tsinghua Center for Life Sciences, the National Natural Science Foundation of China

General Program (31370878), State Key Program (31630023), and Innovative Research Group Program (81621002), by grants from CIHR (PJT-156334 and PJT-166155) and NSERC (RGPIN/03748-2018). HR was supported by China Postdoctoral Science Foundation (No. 2019M650718).

ACKNOWLEDGMENTS

We thank Drs. Erdinc Sezgin, Jack Wei Chen, Xiaoyu Hu, and Yonghui Zhang for discussion and feedback. We thank Ying Xu for the drawings.

REFERENCES

1. Singer SJ, Nicolson GL. The fluid mosaic model of the structure of cell membranes. *Science.* (1972) 175:720–31. doi: 10.1126/science.175.4023.720
2. Simons K, Ikonen E. Functional rafts in cell membranes. *Nature.* (1997) 387:569–72. doi: 10.1038/42408
3. Ritchie K, Iino R, Fujiwara T, Murase K, Kusumi A. The fence and picket structure of the plasma membrane of live cells as revealed by single molecule techniques (Review). *Mol Membr Biol.* (2003) 20:13–8. doi: 10.1080/0968768021000055698
4. van Meer G, Voelker DR, Feigenson GW. Membrane lipids: where they are and how they behave. *Nat Rev Mol Cell Biol.* (2008) 9:112–24. doi: 10.1038/nrm2330
5. Scheidt HA, Huster D, Gawrisch K. Diffusion of cholesterol and its precursors in lipid membranes studied by 1H pulsed field gradient magic angle spinning NMR. *Biophys J.* (2005) 89:2504–12. doi: 10.1529/biophysj.105.062018
6. Gu RX, Baoukina S, Tieleman DP. Cholesterol flip-flop in heterogeneous membranes. *J Chem Theory Comput.* (2019) 15:2064–70. doi: 10.1021/acs.jctc.8b00933
7. Machta BB, Papanikolaou S, Sethna JP, Veatch SL. Minimal model of plasma membrane heterogeneity requires coupling cortical actin to criticality. *Biophys J.* (2011) 100:1668–77. doi: 10.1016/j.bpj.2011.02.029
8. Crow KD, Wagner GP, SMBE Tri-National Young Investigators. Proceedings of the SMBE Tri-National Young Investigators' Workshop 2005. What is the role of genome duplication in the evolution of complexity and diversity? *Mol Biol Evol.* (2006) 23:887–92. doi: 10.1093/molbev/msj083
9. Honigmann A, Sadeghi S, Keller J, Hell SW, Eggeling C, Vink R. A lipid bound actin meshwork organizes liquid phase separation in model membranes. *Elife.* (2014) 3:e01671. doi: 10.7554/eLife.01671.013
10. Thomas S, Preda-Pais A, Casares S, Brumeanu TD. Analysis of lipid rafts in T cells. *Mol Immunol.* (2004) 41:399–409. doi: 10.1016/j.molimm.2004.03.022
11. Dykstra M, Cherukuri A, Sohn HW, Tzeng SJ, Pierce SK. Location is everything: lipid rafts and immune cell signaling. *Annu Rev Immunol.* (2003) 21:457–81. doi: 10.1146/annurev.immunol.21.120601.141021
12. Baumgart T, Hammond AT, Sengupta P, Hess ST, Holowka DA, Baird BA, et al. Large-scale fluid/fluid phase separation of proteins and lipids in giant plasma membrane vesicles. *Proc Natl Acad Sci USA.* (2007) 104:3165–70. doi: 10.1073/pnas.0611357104
13. Irwin ME, Mueller KL, Bohin N, Ge Y, Boerner JL. Lipid raft localization of EGFR alters the response of cancer cells to the EGFR tyrosine kinase inhibitor gefitinib. *J Cell Physiol.* (2011) 226:2316–28. doi: 10.1002/jcp.22570
14. Gajate C, Mollinedo F. Lipid raft-mediated Fas/CD95 apoptotic signaling in leukemic cells and normal leukocytes and therapeutic implications. *J Leukoc Biol.* (2015) 98:739–59. doi: 10.1189/jlb.2MR0215-055R
15. Blouin CM, Hamon Y, Gonnord P, Boularan C, Kagan J, De Lesegno C V, et al. Glycosylation-Dependent IFN-γR partitioning in lipid and actin nanodomains is critical for JAK activation. *Cell.* (2016) 166:920–34. doi: 10.1016/j.cell.2016.07.003
16. Sezgin E, Azbazdar Y, Ng XW, Teh C, Simons K, Weidinger G, et al. Binding of canonical Wnt ligands to their receptor complexes occurs in ordered plasma membrane environments. *FEBS J.* (2017) 284:2513–26. doi: 10.1111/febs.14139
17. Jury EC, Flores-Borja F, Kabouridis PS. Lipid rafts in T cell signalling and disease. *Semin Cell Dev Biol.* (2007) 18:608–15. doi: 10.1016/j.semcdb.2007.08.002
18. Razzaq TM, Ozegbe P, Jury EC, Sembi P, Blackwell NM, Kabouridis PS. Regulation of T-cell receptor signalling by membrane microdomains. *Immunology.* (2004) 113:413–26. doi: 10.1111/j.1365-2567.2004.01998.x
19. Swamy M, Beck-Garcia K, Beck-Garcia E, Hartl FA, Morath A, Yousefi O S, et al. A cholesterol-based allostery model of T cell receptor phosphorylation. *Immunity.* (2016) 44:1091–101. doi: 10.1016/j.immuni.2016.04.011
20. Zhang M, Moran M, Round J, Low TA, Patel VP, Tomassian T, et al. CD45 signals outside of lipid rafts to promote ERK activation, synaptic raft clustering, and IL-2 production. *J Immunol.* (2005) 174:1479–90. doi: 10.4049/jimmunol.174.3.1479
21. Mu L, Tu Z, Miao L, Ruan H, Kang N, Hei Y, et al. A phosphatidylinositol 4,5-bisphosphate redistribution-based sensing mechanism initiates a phagocytosis programing. *Nat Commun.* (2018) 9:4259. doi: 10.1038/s41467-018-06744-7
22. Yutin N, Wolf MY, Wolf YI, Koonin EV. The origins of phagocytosis and eukaryogenesis. *Biol Direct.* (2009) 4:9. doi: 10.1186/1745-6150-4-9
23. Harris SD. Cdc42/Rho GTPases in fungi: variations on a common theme. *Mol Microbiol.* (2011) 79:1123–7. doi: 10.1111/j.1365-2958.2010.07525.x
24. Li M, Liu J, Zhang C. Evolutionary history of the vertebrate mitogen activated protein kinases family. *PLoS ONE.* (2011) 6:e26999. doi: 10.1371/journal.pone.0026999
25. Quistad SD, Traylor-Knowles N. Precambrian origins of the TNFR superfamily. *Cell Death Discov.* (2016) 2:16058. doi: 10.1038/cddiscovery.2016.58
26. Liongue C, Ward AC. Evolution of the JAK-STAT pathway. *JAKSTAT.* (2013) 2:e22756. doi: 10.4161/jkst.22756
27. Fanjul-Fernández M, Folgueras AR, Cabrera S, López-Otín C. Matrix metalloproteinases: evolution, gene regulation and functional analysis in mouse models. *Biochim Biophys Acta.* (2010) 1803:3–19. doi: 10.1016/j.bbamcr.2009.07.004
28. Holstein TW. The evolution of the Wnt pathway. *Cold Spring Harb Perspect Biol.* (2012) 4:a007922. doi: 10.1101/cshperspect.a007922
29. Ng G, Sharma K, Ward SM, Desrosiers MD, Stephens LA, Schoel WM, et al. Receptor-independent, direct membrane binding leads to cell-surface lipid sorting and Syk kinase activation in dendritic cells. *Immunity.* (2008) 29:807–18. doi: 10.1016/j.immuni.2008.09.013
30. Flach TL, Ng G, Hari A, Desrosiers MD, Zhang P, Ward SM, et al. Alum interaction with dendritic cell membrane lipids is essential for its adjuvanticity. *Nat Med.* (2011) 17:479–87. doi: 10.1038/nm.2306
31. Chen X, Resh MD. Cholesterol depletion from the plasma membrane triggers ligand-independent activation of the epidermal growth factor receptor. *J Biol Chem.* (2002) 277:49631–37. doi: 10.1074/jbc.M208327200
32. Furuchi T, Anderson RG. Cholesterol depletion of caveolae causes hyperactivation of extracellular signal-related kinase (ERK). *J Biol Chem.* (1998) 273:21099–104. doi: 10.1074/jbc.273.33.21099
33. Lambert S, Vind-Kezunovic D, Karvinen S, Gniadecki R. Ligand-independent activation of the EGFR by lipid raft disruption. *J Invest Dermatol.* (2006) 126:954–62. doi: 10.1038/sj.jid.5700168
34. Song D, Meng J, Cheng J, Fan Z, Chen P, Ruan H, et al. Pseudomonas aeruginosa quorum-sensing metabolite induces host immune cell death through cell surface lipid domain dissolution. *Nat Microbiol.* (2019) 4:97–111. doi: 10.1038/s41564-018-0290-8
35. Smoak KA, Aloor JJ, Madenspacher J, Merrick BA, Collins JB, Zhu X, et al. Myeloid differentiation primary response protein 88 couples reverse cholesterol transport to inflammation. *Cell Metab.* (2010) 11:493–502. doi: 10.1016/j.cmet.2010.04.006
36. Jackson SK, Abate W, Parton J, Jones S, Harwood JL. Lysophospholipid metabolism facilitates Toll-like receptor 4 membrane translocation to regulate the inflammatory response. *J Leukoc Biol.* (2008) 84:86–92. doi: 10.1189/jlb.0907601

37. Rouquette-Jazdanian AK, Pelassy C, Breittmayer JP, Aussel C. Full CD3/TCR activation through cholesterol-depleted lipid rafts. *Cell Signal.* (2007) 19:1404–18. doi: 10.1016/j.cellsig.2007.01.015
38. Mahammad S, Dinic J, Adler J, Parmryd I. Limited cholesterol depletion causes aggregation of plasma membrane lipid rafts inducing T cell activation. *Biochim Biophys Acta.* (2010) 1801:625–34. doi: 10.1016/j.bbalip.2010.02.003
39. Shapira KE, Ehrlich M, Henis YI. Cholesterol depletion enhances TGF-β Smad signaling by increasing c-Jun expression through a PKR-dependent mechanism. *Mol Biol Cell.* (2018) 29:2494–507. doi: 10.1091/mbc.E18-03-0175
40. Chen CL, Huang SS, Huang JS. Cholesterol modulates cellular TGF-beta responsiveness by altering TGF-beta binding to TGF-beta receptors. *J Cell Physiol.* (2008) 215:223–33. doi: 10.1002/jcp.21303
41. Chen CL, Liu IH, Fliesler SJ, Han X, Huang SS, Huang JS. Cholesterol suppresses cellular TGF-beta responsiveness: implications in atherogenesis. *J Cell Sci.* (2007) 120(Pt 20):3509–21. doi: 10.1242/jcs.006916
42. Matthews V, Schuster B, Schütze S, Bussmeyer I, Ludwig A, Hundhausen C, et al. Cellular cholesterol depletion triggers shedding of the human interleukin-6 receptor by ADAM10 and ADAM17 (TACE). *J Biol Chem.* (2003) 278:38829–39. doi: 10.1074/jbc.M210584200
43. von Tresckow B, Kallen KJ, von Strandmann EP, Borchmann P, Lange H, Engert A, et al. Depletion of cellular cholesterol and lipid rafts increases shedding of CD30. *J Immunol.* (2004) 172:4324–31. doi: 10.4049/jimmunol.172.7.4324
44. Murai T, Maruyama Y, Mio K, Nishiyama H, Suga M, Sato C. Low cholesterol triggers membrane microdomain-dependent CD44 shedding and suppresses tumor cell migration. *J Biol Chem.* (2011) 286:1999–2007. doi: 10.1074/jbc.M110.184010
45. Simons K, Toomre D. Lipid rafts and signal transduction. *Nat Rev Mol Cell Biol.* (2000) 1:31–9. doi: 10.1038/35036052
46. Fessler MB, Parks JS. Intracellular lipid flux and membrane microdomains as organizing principles in inflammatory cell signaling. *J Immunol.* (2011) 187:1529–35. doi: 10.4049/jimmunol.1100253
47. Contreras FX, Ernst AM, Haberkant P, Björkholm P, Lindahl E, Gönen B, et al. Molecular recognition of a single sphingolipid species by a protein's transmembrane domain. *Nature.* (2012) 481:525–9. doi: 10.1038/nature10742
48. Lozano MM, Hovis JS, Moss FR 3rd, Boxer SG. Dynamic reorganization and correlation among lipid raft components. *J Am Chem Soc.* (2016) 138:9996–10001. doi: 10.1021/jacs.6b05540

Conflict of Interest: The authors declare that the research was conducted in the absence of any commercial or financial relationships that could be construed as a potential conflict of interest.

frontiers in Immunology

REVIEW
published: 11 September 2020
doi: 10.3389/fimmu.2020.02187

Surfing on Membrane Waves: Microvilli, Curved Membranes, and Immune Signaling

Ron Orbach[1] *and Xiaolei Su*[1,2]*

[1] Department of Cell Biology, Yale School of Medicine, New Haven, CT, United States, [2] Yale Cancer Center, Yale University, New Haven, CT, United States

Microvilli are finger-like membrane protrusions, supported by the actin cytoskeleton, and found on almost all cell types. A growing body of evidence suggests that the dynamic lymphocyte microvilli, with their highly curved membranes, play an important role in signal transduction leading to immune responses. Nevertheless, challenges in modulating local membrane curvature and monitoring the high dynamicity of microvilli hampered the investigation of the curvature-generation mechanism and its functional consequences in signaling. These technical barriers have been partially overcome by recent advancements in adapted super-resolution microscopy. Here, we review the up-to-date progress in understanding the mechanisms and functional consequences of microvillus formation in T cell signaling. We discuss how the deformation of local membranes could potentially affect the organization of signaling proteins and their biochemical activities. We propose that curved membranes, together with the underlying cytoskeleton, shape microvilli into a unique compartment that sense and process signals leading to lymphocyte activation.

Keywords: microvilli, actin, membrane curvature, BAR protein, WASp, TCR, super-resolution microscopy, T-cell signaling

OPEN ACCESS

Edited by:
Erdinc Sezgin,
Karolinska Institutet (KI), Sweden

Reviewed by:
Pablo F. Céspedes-Donoso,
University of Oxford, United Kingdom
Ana Mafalda Santos,
University of Oxford, United Kingdom

***Correspondence:**
Xiaolei Su
xiaolei.su@yale.edu

Specialty section:
This article was submitted to T Cell Biology, a section of the journal Frontiers in Immunology

Received: *30 May 2020*
Accepted: *11 August 2020*
Published: *11 September 2020*

Citation:
Orbach R and Su X (2020) Surfing on Membrane Waves: Microvilli, Curved Membranes, and Immune Signaling. Front. Immunol. 11:2187. doi: 10.3389/fimmu.2020.02187

INTRODUCTION

Sea looks calm miles away but wavy inches ahead; same applies to the plasma membrane. A variety of membrane protrusions have been identified on the cell surface, including microvilli, filopodia, lamellipodia, and cilia (see **Table 1**). Those structures play a classical function in sensing the environmental cues as well as facilitating cell migration. Meanwhile, accumulating evidence suggests that membrane protrusions also play an active role in regulating biochemical reactions that transduce membrane-proximal signaling (1–3), and dysregulation of their formation has been associated with diseases like Huntington's disease, PAPA syndrome, Wiskott–Aldrich syndrome (WAS), and renal dysfunction (4–6).

In the immune system, microvilli are among the most common types of membrane protrusions found on lymphocytes. Although they have been well-described by electron microscopy (EM) studies (7), the biochemical and signaling functions of microvilli remained neglected until recently. In this review, we discuss the potential of physical feature of microvilli in regulating chemical reactions that transduce membrane-proximal signaling. We also summarize the development of new techniques for imaging cell surface topography at high spatial or temporal resolutions, and for modulating membrane curvature in a precision manner, which could provide powerful tools for investigating the signaling function of microvilli.

FORMATION OF DYNAMIC MICROVILLI

Microvilli are thin finger-like membrane protrusions that are found on the surface of a wide variety of cell types (8), including intestinal epithelial cells (9), dendritic cells (10), and neurons (11). They are supported by actin filaments (F-actin) that are organized in parallel bundles of 10–30 filaments (12, 13), which resemble the actin network that constitutes filopodia (14). However, filopodia often protrude from the lamellipodial and lamellar actin network (15), while the microvilli actin network does not (16, 17). In the case of lymphocytes, EM studies showed the presence of microvilli on the surface of both T cells and B cells (18). The diameter of the microvilli ranges from 50 to 550 nm, as revealed by EM and fluorescence microscopy studies, while their length varies between 100 nm to several microns (**Figure 1**) (7, 13, 19, 20). Thus, microvilli dramatically increase the cell surface area, while having a negligible effect on the cytosolic volume. Furthermore, actin depolymerizing toxin Latrunculin A (LatA) eliminates most microvilli within 1 min in a reversible manner, suggesting that microvilli are highly dynamic structures (13). Recent technological advances in lattice light-sheet microscopy allow 3D real-time tracing of such dynamic microvilli (20). It was discovered that microvilli move laterally on the plasma membrane and survey antigen-presenting cells (APCs) within 1 min, which is, coincidently or not, the half-life of T cell–APC contact duration *in vivo* (20). Therefore, the dynamics of microvilli fits well into their function in searching antigens.

Despite a handful of studies on microvilli morphology, our knowledge on the regulatory mechanism of microvilli size, structure, and dynamics is still limited. Evidently, their fate following the formation of immunological synapse is still a matter of debate. Cai et al. (20) demonstrated that there is no change in the microvilli density before and after the immunological synapse is formed. In contrast, Kim et al. (21) showed that at an early stage of synapse development microvilli polarize toward the synapse, but as the synapse matures, most of the microvilli disappear. The later was further supported by a recent study by Ghosh et al. (22), showing the loss of the microvilli after T cell receptor (TCR) stimulation.

The microvilli are also regulated by cytokines and chemokines. Westerberg et al. (23) found that CD40 antibody together with IL-4 induces microvilli on the surface of B cells. On the other hand, the chemokines stromal derived factor 1α (SDF-1α) and B lymphocyte chemokine (BLC) induce resorption of microvilli (24, 25), which promotes B cell homing by transition from rolling adhesion to integrin-mediated adhesion. Not surprisingly, members of the ezrin-radixin-moesin (ERM) family, which link the cortical F-actin cytoskeleton to the plasma membrane, were found to regulate microvilli assembly, namely, dephosphorylation of ERM proteins (ezrin, T567; radixin, T564, moesin, T558), induced by chemokines, results in resorption of microvilli within a few seconds (25, 26). Because ERM dephosphorylation can be triggered by TCR activation (27), ERM could mediate TCR-induced microvilli resorption (22).

Interestingly, changes in the microvilli shape and density are also linked to several diseases. Uneven distribution of long microvilli was observed on B cells from hairy cell leukemia patients (28–31). Moreover, changes in microvilli morphology were observed in WAS, a severe immunodeficiency disorder that is caused by defective or missing Wiskott–Aldrich syndrome protein (WASp). WASp activates Arp2/3 complex by inducing a conformational change of Arp2/3 and by delivering the first actin monomer of the nascent filament (32–36). On the

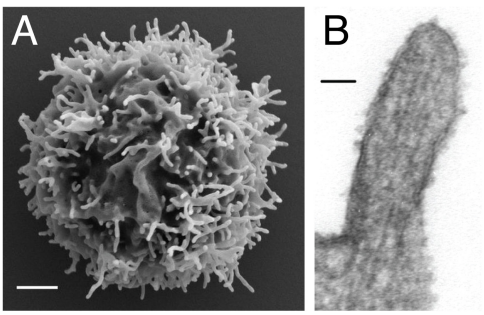

FIGURE 1 | Microvilli decorating the plasma membrane of lymphocytes. **(A)** Scanning electron microscopy micrograph showing microvilli that protrude from the cell surface of resting peripheral blood human T cells. Scale bar: 1 μm. Reproduced from Jung et al. (19). Copyright 2016 National Academy of Sciences. **(B)** Transmission electron microscopy micrograph showing the parallel arrangement of F-actin within the microvilli of 300.19 cell (Abelson-transformed murine pre-B lymphoma) Scale bar: 50 nm. Republished with permission of ASH from Ref. (13).

TABLE 1 | Comparison between common types of membrane protrusions.

	Microvilli	Filopodia	Lamellipodia	Cilia
Cell type	Most cells	Motile cells	Motile cells	All vertebrate cells, except for hematopoietic cells
Function	Signaling and motility	Sensory and guiding organelle	Motility	Signaling and motility
Diameter	50–350 nm	100–400 nm	Sheet-like structure	∼250 nm
Length	<4 μm	Up to 40 μm		1–10 μm
Cytoskeleton core structure	Actin	Actin	Actin	Microtubule
Organization	Parallel bundles	Parallel bundles	Branched network	Motile cilia: "9 + 2" Primary cilia: "9 + 0"
Other		Often emerge from lamellipodial sheets		Emerge from basal body

other hand, WASp could directly promote actin polymerization independently of Arp2/3 (37). It has been demonstrated that lymphocytes derived from patients with WAS, either in resting or activated states, exhibit various microvillar morphological abnormalities. These abnormalities include a decrease in microvilli density and length, as well as formation of dysmorphic structures (5, 24, 38–42). However, knockdown of Arp2 in Jurkat T cells caused no significant effect on microvilli assembly (43), which suggests that WASp might regulate microvilli formation independent of Arp2/3. Meanwhile, further studies are required to confirm the Arp2 phenotype in primary T cells.

CAN MICROVILLI SERVE AS A SIGNALING CENTER?

The notion that microvilli could serve as a signaling center was primed by studies showing that certain signaling proteins are enriched in microvilli. Immunogold EM studies demonstrated the enrichment of various receptors and adhesion molecules on the microvilli, including insulin receptors, selectin, integrin, and the T cell co-receptor CD4 (44–49). Mass-spectrometry analysis was also implemented to compare the protein composition between isolated microvilli and whole cell, from both human peripheral blood T-lymphocytes and a mouse pre-B lymphocyte line (50). It revealed that microvilli are enriched of GTP-binding proteins, cytoskeletal proteins, and transmembrane proteins as compared to the cell body (after removing the nucleus). This study provides the first global mapping of the microvilli proteome. However, it should be noted that using the cell body as a control could lead to the identification of membrane-associated proteins rather than microvilli-specific proteins, because the surface-to-volume ratio is much higher in microvilli as compared to the cytoplasm. It should be also noted that the identification of membrane proteins by mass-spectrometry remains as a challenge because of the proteins limited solubility in aqueous buffer (51). Therefore, certain hits might be missing in the dataset. Thus, orthogonal approaches will be needed to verify the microvilli-enriched proteins.

For many years the dynamic nature of microvilli together with their small dimensions have hindered the structural and functional characterization of microvilli. Although EM provides high spatial resolutions, understanding the signaling function of microvilli requires characterizing microvilli morphology and signaling protein localization with high temporal resolutions. The advancement of fluorescence microscopy techniques in the past decades has enabled an investigation of membrane morphology and protein localization in microvilli at either high temporal or spatial resolutions, though the combination of both is still technically challenging (19–22, 52, 53).

The Haran group comprehensively characterized the localization of TCR signaling proteins on the microvilli by a unique imaging technique that allows accurate mapping of membrane protein localization. By combining variable-angle total internal reflection microscopy and stochastic localization nanoscopy, the authors reconstructed 3D topographical maps of T cells (19, 22). They have shown that TCR, co-receptor CD4, kinase Lck, adaptor LAT, and adhesion receptor CD2 are highly enriched in the microvilli. On the sub-microvilli scale, the Jun group, using Total Internal Reflection Fluorescence (TIRF) microscopy, showed that TCR is specifically enriched on the microvilli tip (**Figure 2**) (21). Thus, the tip localization of TCR could promote searching of antigens and establishing contacts with APCs (20). The Haran group also found that treatment with LatA or expressing a dominant negative form of ezrin, both of which reduce microvilli, leads to a random distribution of TCR throughout the plasma membrane. Intriguingly, the authors showed that following TCR stimulation, T cells lose their microvilli, which consequently leads to an even distribution of TCRαβ throughout the plasma membrane (22). This result suggests that microvilli-dependent TCR enrichment could be regulated by TCR triggering.

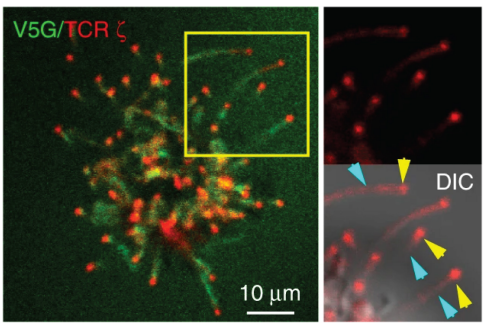

FIGURE 2 | TCR localizes to the microvilli tip. Jurkat T cells expressing GFP-V5G and TCRζ-tdTomato were imaged at the terminal stage of T cell activation. Reproduced from Kim et al. (21) licensed under Creative Commons (CC BY 4.0).

The "kinetic-segregation" model serves as one of the prevalent mechanisms explaining TCR triggering (54–57). A key part to this model is the segregation of the large tyrosine phosphatase CD45 from the TCR-pMHC contact zone. Therefore, multiple groups have investigated the localization of CD45 in the context of microvilli and showed that the segregation between TCR and CD45 occurs a few seconds after contacts are established (58–61). Interestingly, although it has been assumed and supported by experimental data that CD45 is evenly distributed on the cell surface in resting T cells (19, 60), a new study revealed, using expansion microscopy, that CD45 is excluded from the microvilli tip even before contacts are established with APC (53). These discrepancies could be caused by differences in T cell subtypes, activation methods, and resolution of individual imaging techniques.

Summarizing localization studies above, key components mediating TCR-proximal signaling reside in microvilli. These include TCR itself, kinase Lck, and adaptor LAT. It is expected that cytosolic proteins that are associated with these membrane proteins, including ZAP70, Grb2, Sos1, PLCγ1, Gads, and SLP76, are likely to be enriched in microvilli as well. The physical proximity of these molecules could increase the rate of chemical reactions and efficiency of signal transduction. Microvilli, therefore, could serve as a compartment to enrich

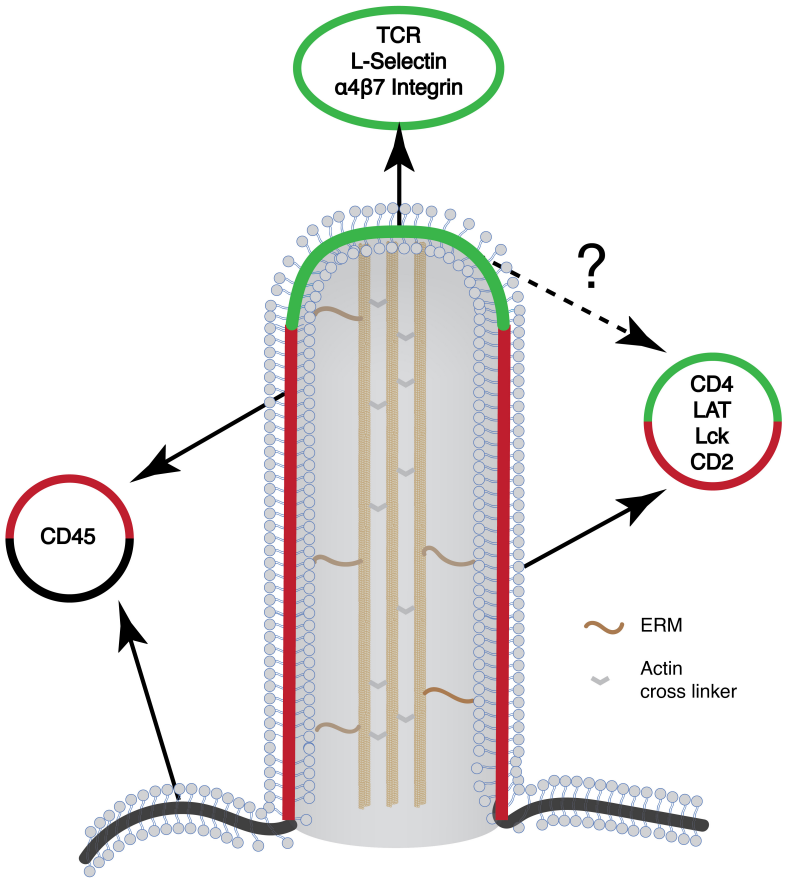

FIGURE 3 | Schematic of the microvilli and the organization of different signaling proteins on the microvilli. Many of the signaling molecules that are involved in T cell activation preferentially localize to the microvilli. Yet, their organization within the microvilli is not known (marked in question mark). Green, microvilli tip region; red, microvilli body; black, plasma membrane.

signaling proteins to promote TCR signaling (**Figure 3**). In this regard, T cell microclusters are another entity that has been proposed for promoting TCR signaling (62, 63). Because both microvilli-localized proteins and T cell microcluster components display a puncta-like structure on the cell membrane, it raises an interesting question on the relationship between the two. Current evidence suggests that these two entities are different but related structures. The microvilli-enriched proteins are mostly characterized in resting T cells and microvilli disappear, at least in some studies, after TCR activation (22). In contrast, T cell microclusters are formed after TCR activation (62, 63). They also displayed limited mobility as compared to the highly mobile microvilli (20). Meanwhile, the "pre-enrichment" of signaling components in microvilli could facilitate T microcluster formation upon TCR activation.

Besides a potential signaling function in T cells, microvilli have also been proposed by the Jun Lab to serve as precursors for generating TCR-enriched extracellular vesicles (or synaptosomes) that activate dendritic cells (21). It remains to be determined whether the synaptosomes are similar or different to other TCR-enriched microvesicles (synaptic ectosomes) that were described by the Dustin Lab (64). Ectosomes are generated by the ESCRT complex, of which TSG101 facilitates the sorting of TCR into the ectosomes whereas Vps4 facilitates the scission of ectosomes from the plasma membrane. Interestingly, CD40L, a key effector delivered by helper T cells to activate APC, is also enriched in the microvilli and ectosomes, though CD40L is spatially segregated from TCR in ectosomes (65). This probably suggests that TCR and CD40L are independently sorted into microvilli, whereas the exact mechanism needs to be determined. It also remains as an intriguing question on how many microvilli and their associated TCRs end up in synaptosomes or ectosomes. Is ESCRT, a general membrane-shaping machinery, involved in microvilli dynamics regulation and resorption? Answering these questions will help to generate a complete picture of the microvilli life cycle during T cell activation (65).

MECHANISMS FOR INDUCING MEMBRANE CURVATURE AND PROTEIN ENRICHMENT

Highly curved membranes represent a unique feature of microvilli, which could also serve as a platform for enriching proteins in microvilli. Several mechanisms have been proposed for generating curved membranes. Polymerization of actin

filaments drives membrane protrusion; in parallel, membrane-associated proteins can also induce membrane curvature by the insertion of conical transmembrane proteins or hydrophobic protein domains into the membrane (66, 67). Intriguingly, intrinsically disordered domains, when attached to membranes, can drive membrane protrusion either with a positive or negative curvature (68–70).

The Bin-Amphiphysin-Rvs (BAR) superfamily is a key player involved in regulation, formation, and detection of cell membrane curvature (71). In this superfamily, the N-BAR and the F-BAR are associated with positive curvatures (e.g., membrane invagination or endocytic pits). In contrast, the I-BAR subfamily of proteins is associated with negative curvatures as found in various membrane protrusions (72). Many members of the BAR superfamily contain the structurally conserved SH2 or SH3 domains that recruit their binding partners to the curved membranes (73). One particular interesting example is the I-BAR protein IRSp53 (also known as BAIAP2) that binds cytoskeletal effectors such as N-WASP through its SH3 domain (74). In an *in vitro* biochemical assay, IRSp53 induces tubular membrane protrusions with similar dimensions of microvilli (75). IRSp53 is localized to filopodia when ectopically expressed in neuronal NSC34 cells (76) and regulates filopodia dynamics (77). Interestingly, IRSp53 is also expressed in T cells (78), raising its possible role in regulating microvilli formation. Surprisingly, the N-BAR protein sorting nexin 9 (SNX9), which is expected to recognize positive curvatures, is involved the biogenesis of filopodia (79). In a cell-free system for reconstituting actin bundles of filopodia (80), immunodepletion of SNX9 resulted in shorter actin bundles. Moreover, SNX9 localizes to the filopodial tip and shaft in RPE-1 cells (79). The positive role of SNX9 in filopodia formation is dependent on its activity in stimulating N-WASp and Arp2/3 (81), which probably overrides the curvature-sensing function of the N-BAR domain. In terms of the function of SNX9 in T cells, SNX9 was found to interact with WASp, p85, and CD28 to form a signaling complex on endocytic vesicles when T cells are activated by soluble CD3/CD28 antibodies (82). It remains to be determined if SNX9 can regulate microvilli when T cells are activated by surface or bilayer-presented stimuli because stimuli with a physical support could cause different outcomes as compared to those in a soluble format. Previous reports showed that TCR is internalized through endocytosis when T cells are treated with soluble MHC tetramer (83), whereas TCR is sorted into extracellular microvesicles when T cells are activated by supported lipid bilayer (SLB)-presented pMHC (64).

While the BAR proteins sense membrane curvature within the nanometer scale, there are proteins that can also sense a larger length scale. Septins and stage V sporulation protein M (SpoVM) sense positive micron-scale curvatures (84, 85). It was suggested that these nanometer-sized proteins sense micron-scale curvature by polymerization into micro-scale filaments. In contrast, the protein machinery that directly senses micron- or submicron-scale negative curvatures remains to be determined.

What is the cellular function of membrane deformation? Various studies have highlighted the role of membrane curvature in regulating sorting of transmembrane proteins (86–89). Using patterned nanostructure surfaces, Zhao et al. (90) found that the protein machinery mediating clathrin-mediated endocytosis prefers a positive curvature with a radius below 200 nm. Liang et al. (91) discovered that small GTPase Ras senses membrane curvatures in an isoform-dependent manner. One isoform binds to membranes with low curvatures, whereas the other binds to membranes with high curvatures. The effect of local membrane curvature may also influence cell polarization. For many years it had been assumed that cell polarization is induced exclusively by a gradient of a chemoattractant. A recent report revealed that chemical signaling is not sufficient for inducing cell polarization of neutrophils and $CD8^+$ T cells (92). Instead, the authors found that polarization initiates with the formation of curved membranes, which recruits BAR domain protein SRGAP2, activates PI4KA, and results in PtdIns4P polarization. Furthermore, to understand the mechanism by which membrane curvature affects actin-dependent processes, such as endocytosis, focal adhesion maturation, and stress fiber organization, Lou et al. (93) have used patterned nanostructure surfaces to study actin rearrangement. Intriguingly, the authors found that the actin nucleator Arp2/3 and its regulators N-WASP and cortactin are recruited by BAR proteins to membranes with positive curvatures (with radii <200 nm). Consequently, branched actin networks assemble around curved membranes, depleting the monomeric actin pool for assembling stress fibers and mature focal adhesions. Interestingly, members of the formin family, which promote the polymerization of linear F-actin, showed no preferential localization to curved membranes.

The lipid composition of the plasma membrane also influences membrane geometry and protein localization. The size of the lipid headgroups, their charge, as well as the saturation state of acyl chains determines lipid shapes, and consequently the local membrane curvature (66, 94). Lipids with small headgroups such as cardiolipin, phosphatidylethanolamine, ceramide, diacylglycerol, and phosphatic acid induce negative membrane curvatures, whereas lipids with large headgroups like lysophosphatidylcholine and phosphatidylinositol phosphate induce positive curvatures (95). Some of these lipids can also recruit proteins to the membrane. For example, the negatively charged lipids phosphatidylserine and phosphatidylinositol 4,5-bisphosphate recruit positively charged proteins by electrostatic interactions (96–98). Sphingomyelin was found to selectively localize to the microvilli of epithelial cells and to induce microvilli formation through the indirect recruitment of ERM proteins (99). Whether this is also the case in lymphocytes and what the role of sphingomyelinase is in regulating microvilli formation need to be further explored. On the other hand, lipids can mediate the exclusion of proteins from curved membranes. A recent intriguing study from Jung et al. showed that CD45 is excluded out of the tip of microvilli in a cholesterol-dependent manner (53). Although the localization of cholesterol needs to be determined in the context of microvilli, cholesterol was previously reported to be enriched in the negative curved membranes in vitro or in silico (100, 101), where it, together with sphingomyelin, also thickens the membrane (102, 103). The thickened membrane caused by the accumulation of cholesterol was suggested to exclude CD45 of which the transmembrane domain is not long enough to be integrated into the thickened membrane. Depletion of cholesterol by cyclodextrin reduced the

exclusion of CD45 from the tip, accompanied by a decrease in the membrane thickness and number of microvilli (53, 104). Besides the contribution from individual lipids, membrane tension, by serving as a physical barrier, can antagonize actin based-protrusion (105).

The composition and organization of the glycocalyx layer, which covers the outer leaflet of the plasma membrane, also contributes to cell morphology and membrane protrusions (106). Mucins are flexible transmembrane glycoprotein polymers within the glycocalyx that are enriched on the surface of many membrane protrusions, such as epithelial microvilli (107). A recent study has demonstrated the role of the mucins in generating forces driving the tubularization of the plasma membrane (108). In contrast, rigid glycoproteins have not shown similar phenomenon as the mucins. In the case of T cells, many cell surface proteins are highly glycosylated, among which CD43 and CD45 are the most abundant glycoproteins (109, 110). Notably, different isoforms of CD45 are expressed at different T cell development stages, and these isoforms differ significantly in their extracellular domain sizes (58, 111). It remains as an interesting question whether these isoforms contribute differently to microvilli formation.

APPROACHES TO MANIPULATE MICROVILLI AND MEMBRANE CURVATURE

Investigation of the microvilli function can be extremely challenging due to limited tools to specifically manipulate them in cells without perturbing other actin-based processes. Moreover, their small dimensions ($r < 200$ nm) and unique architecture (i.e., negative membrane curvature viewed from inside of microvilli) hamper the application of traditional *in vitro* reconstitution approach to the study of microvilli. Nevertheless, methods for studying filopodia, which present similar structural properties as the microvilli, as well as other recent technological advances that enable the accurate shaping of membranes, can be implemented to interrogate microvilli.

Genetic Approaches

In microvilli the actin filaments are organized in parallel bundles (13). Various crosslinkers such as fascin, fimbrin, and espin promote the formation of actin bundles (112–115). While direct evidence is required, these actin crosslinkers can be attractive targets for specifically modulating microvilli shape and density, as demonstrated in filopodia (113). The ERM family, another component involved in microvilli formation, plays a major role in connecting actin cytoskeleton to the cell membrane. Overexpressing a dominant-negative form of ezrin dramatically reduces microvilli formation (24). Yet, a recent finding suggests that the enrichment of ezrin around membrane protrusions is facilitated by I-BAR-domain proteins (116).

Pharmacological Approaches

Complementing genetic manipulations, pharmacological treatments perturbing membrane composition or cytoskeleton can modulate microvilli in a rapid fashion. Greicius et al. (104) reported a decrease in microvilli density by depleting cholesterol using cyclodextrin. A similar effect could be achieved by using the actin depolymerizing toxin LatA (13, 19). However, both drugs are expected to affect the whole membrane structure, actin network, and surface presence of many signaling proteins, all of which may complicate the interpretation of the results regarding microvilli-specific functions. Recently, an inhibitor of the crosslinker protein fascin has been identified, which could be potentially used to manipulate microvilli. This inhibitor blocks the activity of fascin to bundle actin filaments *in vitro,* and filopodial formation in multiple cell lines. Furthermore, it blocks cancer cell metastasis, potentially by inhibiting filopodia formation (117).

Physical Approaches

In vitro assays have been developed to isolate the effect of membrane curvature from complex cellular environment. Yet, while methods to generate positive membrane curvature are well established, it is not the case with negative membrane curvatures, especially in the range of microvillus sizes ($r < 200$ nm). In one approach, a giant unilamellar vesicle (GUV) is held by a micropipette at one side and pulled, on the other side, by a polystyrene bead holding by optical traps (**Figure 4A**). A membrane nanotube can be generated with controlled radii, ranging from 7 to 100 nm, by adjusting the micropipette pressure (118). Similarly, an optical trap has been used to pull short tethers ($r < 100$ nm) from the cell membrane (119). Meanwhile, these manipulations are technically challenging and may be time-consuming. GUVs are also sensitive to osmotic changes and therefore can bring difficulty to long-duration experiments. Alternative approaches to study negative curvature

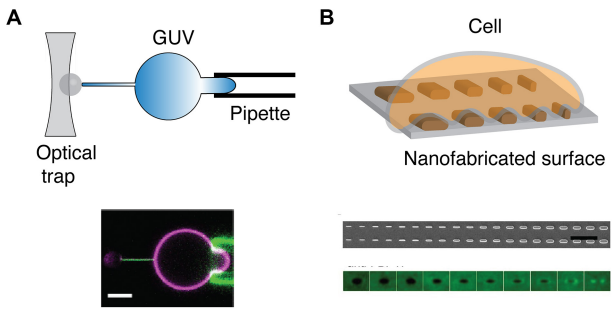

FIGURE 4 | Methods to physically manipulate membrane curvature. **(A)** Schematic of optical trap that is used to pull a thin nanotube from GUV held by a pipette (top). Confocal microscopy reveals that GFP-IRSp53 BAR protein localizes to nanotube pulled from GUV (magenta) that is held by a pipette (bottom). Scale bar: 5 μm. Reproduced from Prévost et al. (118) licensed under Creative Commons (CC BY 4.0). **(B)** Schematic of a cell on a nanofabricated surface with structures of different radii (top). Scanning electron microscopy microfabricated of nanofabricated chip with a gradient nanobar array with a variable width from 100 to 1,000 nm (100 nm increment; bar length: 2 μm) (middle). The averaged nanobar images of anti-FBP17 immunostaining for 10 different nanobar widths. FBP17 localizes to positively curved structures with a width <400 nm (bottom). Reproduced from (93). Copyright 2019 National Academy of Sciences.

employ substrates that serve as a mold to induce membrane curvature on artificial membranes and cells (**Figure 4B**). Focused ion beam has been applied to etch an array of invaginations with a radius of 100 nm on a glass surface (120). The fabricated substrate can then be covered with SLB to mimic the highly curved membranes in microvilli. Another promising means to induce membrane curvature is by using nanofabricated substrates (90, 121). Yet, the diffusion of membrane components may be affected by the substrate (122, 123), which should be carefully evaluated beforehand.

OUTLOOK

Looking forward, significant questions remain to be addressed in terms of the mechanism and signaling function of T cell microvilli:

(1) What are the mechanisms that regulate microvilli formation and dynamics? Besides identifying the key protein and lipid components regulating microvilli, it will also be necessary to understand the relationship between microvilli and other membrane structures, for example, the recently identified CD2 Corolla which seems to be devoid of microvilli (124).

(2) How do microvilli regulate the localization and oligomerization state of proteins and lipids? Phase separation, or the formation of liquid-like microclusters, emerges as a new principle in regulating TCR signaling (125, 126). The unique membrane topology in microvilli could play an important role in regulating the assembly of signaling microclusters. On the other hand, microvilli could bring proteins physically close even if there are no direct interactions between those proteins. Future co-localization studies should be best performed in the context of microvilli to understand the exact nature of the entities that are examined. In addition, many other tiny and transient proteo-lipid nanodomains have been identified on the plasma membrane (127–130). It remains as an open question on the relationship between these structures and the microvilli-localized proteins.

(3) How do microvilli modulate chemical reactions? The src-family kinase Lck has been shown to be enriched in microvilli (22). Future studies are expected to reveal the microvilli localization or even sub-microvilli localization (tip, side, or base) of other enzymes in the TCR signaling (e.g., PLCγ1, ZAP70, SHP1, CBL), together with their corresponding substrates. Elegant reconstitution approaches will be needed to recapitulate the essential physical and chemical environment of microvilli to understand how curved membranes in microvilli affect the specific activity of kinases, phosphatases, and lipases.

(4) How do microvilli regulate TCR signal transduction? As protrusive structures that search the surrounding space and make contacts with the APCs, microvilli are constantly experiencing mechanical forces from the environment (131). These forces may be involved in the regulation of cell recognition and calcium flux, as found in the microvillar photoreceptor cells (132). Moreover, TCRs on the tip of the microvilli receive stimuli from APCs. Meanwhile, what happens after antigen recognition remains unclear. How is signal transduced from the tip of microvilli to the cell body? Do microvilli participate in kinetic proof-reading since microvilli are enriched with proteins mediating multiple steps along the TCR pathway? Do microvilli serve as a signaling unit that integrates signals from TCR and co-receptors first before sending them to the cell body, or are different signals transduced individually across the microvilli? With these questions being addressed, the current map of T cell membrane signaling is likely to be significantly expanded from a 2D surface to a 3D world.

AUTHOR CONTRIBUTIONS

RO and XS conceived and wrote the manuscript. Both authors contributed to the article and approved the submitted version.

FUNDING

XS was supported by the American Cancer Society Institutional Research Grant, the Charles H. Hood Foundation Child Health Research Awards, the Andrew McDonough B+ Foundation Research Grant, the Gilead Sciences Research Scholars Program in Hematology/Oncology, and the Rally Foundation a Collaborative Pediatric Cancer Research Awards Program.

ACKNOWLEDGMENTS

The authors thank the Su lab for fruitful discussions.

REFERENCES

1. Mim C, Unger VM. Membrane curvature and its generation by BAR proteins. *Trends Biochem Sci.* (2012) 37:526–33. doi: 10.1016/j.tibs.2012.09.001
2. Jarsch IK, Daste F, Gallop JL. Membrane curvature in cell biology: an integration of molecular mechanisms. *J Cell Biol.* (2016) 214:375–87. doi: 10.1083/jcb.201604003
3. Pettmann J, Santos AM, Dushek O, Davis SJ. Membrane ultrastructure and T cell activation. *Front Immunol.* (2018) 9:1263. doi: 10.3389/fimmu.2018.02152
4. Liu S, Xiong X, Zhao X, Yang X, Wang H. F-BAR family proteins, emerging regulators for cell membrane dynamic changes-from structure to human diseases. *J Hematol Oncol.* (2015) 8:47. doi: 10.1186/s13045-015-0144-2
5. Molina IJ, Kenney DM, Rosen FS, Remold-O'Donnell E. T cell lines characterize events in the pathogenesis of the Wiskott-Aldrich syndrome. *J Exp Med.* (1992) 176:867–74. doi: 10.1084/jem.176.3.867
6. Varkey J, Isas JM, Mizuno N, Jensen MB, Bhatia VK, Jao CC, et al. Membrane curvature induction and tubulation are common features of synucleins and apolipoproteins. *J Biol Chem.* (2010) 285:32486–93. doi: 10.1074/jbc.m110.139576

7. Polliack A, Lampen N, Clarkson BD, Harven ED, Bentwich Z, Siegal FP, et al. Identification of human B and T lymphocytes by scanning electron microscopy. *J Exp Med*. (1973) 138:607–24. doi: 10.1084/jem.138.3.607
8. Gorelik J, Shevchuk AI, Frolenkov GI, Diakonov IA, Lab MJ, Kros CJ, et al. Dynamic assembly of surface structures in living cells. *Proc Natl Acad Sci USA*. (2003) 100:5819–22. doi: 10.1073/pnas.1030502100
9. Sauvanet C, Wayt J, Pelaseyed T, Bretscher A. Structure, regulation, and functional diversity of microvilli on the apical domain of epithelial cells. *Annu Rev Cell Dev Biol*. (2015) 31:593–621. doi: 10.1146/annurev-cellbio-100814-125234
10. Fisher PJ, Bulur PA, Vuk-Pavlovic S, Prendergast FG, Dietz AB. Dendritic cell microvilli: a novel membrane structure associated with the multifocal synapse and T-cell clustering. *Blood*. (2008) 112:5037–45. doi: 10.1182/blood-2008-04-149526
11. Elsaesser R, Paysan J. The sense of smell, its signalling pathways, and the dichotomy of cilia and microvilli in olfactory sensory cells. *BMC neuroscience*. (2007) 8(Suppl. 3):S1. doi: 10.1186/1471-2202-8-s3-s1
12. Mooseker MS, Tilney LG. Organization of an actin filament-membrane complex. Filament polarity and membrane attachment in the microvilli of intestinal epithelial cells. *J Cell Biol*. (1975) 67:725–43. doi: 10.1083/jcb.67.3.725
13. Majstoravich S, Zhang J, Nicholson-Dykstra S, Linder S, Friedrich W, Siminovitch KA, et al. Lymphocyte microvilli are dynamic, actin-dependent structures that do not require Wiskott-Aldrich syndrome protein (WASp) for their morphology. *Blood*. (2004) 104:1396–403. doi: 10.1182/blood-2004-02-0437
14. Lewis AK, Bridgman PC. Nerve growth cone lamellipodia contain two populations of actin filaments that differ in organization and polarity. *J Cell Biol*. (1992) 119:1219–43. doi: 10.1083/jcb.119.5.1219
15. Svitkina TM, Bulanova EA, Chaga OY, Vignjevic DM, Kojima S, Vasiliev JM, et al. Mechanism of filopodia initiation by reorganization of a dendritic network. *J Cell Biol*. (2003) 160:409–21. doi: 10.1083/jcb.200210174
16. Hirokawa N, Tilney LG, Fujiwara K, Heuser JE. Organization of actin, myosin, and intermediate filaments in the brush border of intestinal epithelial cells. *J Cell Biol*. (1982) 94:425–43. doi: 10.1083/jcb.94.2.425
17. Chhabra ES, Higgs HN. The many faces of actin: matching assembly factors with cellular structures. *Nat Cell Biol*. (2007) 9:1110–21. doi: 10.1038/ncb1007-1110
18. Alexander E, Sanders S, Braylan R. Purported difference between human T-and B-cell surface morphology is an artefact. *Nature*. (1976) 261:239–41. doi: 10.1038/261239a0
19. Jung Y, Riven I, Feigelson SW, Kartvelishvily E, Tohya K, Miyasaka M, et al. Three-dimensional localization of T-cell receptors in relation to microvilli using a combination of superresolution microscopies. *Proc Natl Acad Sci USA*. (2016) 113:E5916–24. doi: 10.1073/pnas.1605399113
20. Cai E, Marchuk K, Beemiller P, Beppler C, Rubashkin MG, Weaver VM, et al. Visualizing dynamic microvillar search and stabilization during ligand detection by T cells. *Science*. (2017) 356:eaal3118. doi: 10.1126/science.aal3118
21. Kim H-R, Mun Y, Lee K-S, Park Y-J, Park J-S, Park J-H, et al. T cell microvilli constitute immunological synaptosomes that carry messages to antigen-presenting cells. *Nat Commun*. (2018) 9:3630. doi: 10.1038/s41467-018-06090-8
22. Ghosh S, Bartolo VD, Tubul L, Shimoni E, Kartvelishvily E, Dadosh T, et al. Dependent assembly of T cell receptor signaling and co-stimulatory molecules on microvilli prior to activation. *Cell Rep*. (2020) 30:3434–47.e6. doi: 10.1016/j.celrep.2020.02.069
23. Westerberg L, Greicius G, Snapper SB, Aspenström P, Severinson E. Cdc42, Rac1, and the Wiskott-Aldrich syndrome protein are involved in the cytoskeletal regulation of B lymphocytes. *Blood*. (2001) 98:1086–94. doi: 10.1182/blood.v98.4.1086
24. Brown MJ, Nijhara R, Hallam JA, Gignac M, Yamada KM, Erlandsen SL, et al. Chemokine stimulation of human peripheral blood T lymphocytes induces rapid dephosphorylation of ERM proteins, which facilitates loss of microvilli and polarization. *Blood*. (2003) 102:3890–9. doi: 10.1182/blood-2002-12-3807
25. Parameswaran N, Matsui K, Gupta N. Conformational switching in ezrin regulates morphological and cytoskeletal changes required for B cell chemotaxis. *J Immunol*. (2011) 186:4088–97. doi: 10.4049/jimmunol.1001139
26. Nijhara R, van Hennik PB, Gignac ML, Kruhlak MJ, Hordijk PL, Delon J, et al. Rac1 mediates collapse of microvilli on chemokine-activated T lymphocytes. *J Immunol*. (2004) 173:4985–93. doi: 10.4049/jimmunol.173.8.4985
27. Faure S, Salazar-Fontana LI, Semichon M, Tybulewicz VLJ, Bismuth G, Trautmann A, et al. ERM proteins regulate cytoskeleton relaxation promoting T cell-APC conjugation. *Nat Immunol*. (2004) 5:272–9. doi: 10.1038/ni1039
28. Sasaki M, Sugimoto K, Mori T, Karasawa K, Oshimi K. Effective treatment of a refractory hairy cell leukemia variant with splenic pre-irradiation and alemtuzumab. *Acta Haematol*. (2008) 119:48–53. doi: 10.1159/000115785
29. Tabata R, Tabata C, Iwama H, Yasumizu R, Kojima M. CD27-positive hairy cell leukemia-Japanese variant. *Virchows Arch*. (2016) 468:375–9. doi: 10.1007/s00428-015-1881-x
30. Machii T, Yamaguchi M, Inoue R, Tokumine Y, Kuratsune H, Nagai H, et al. Polyclonal B-cell lymphocytosis with features resembling hairy cell leukemia-Japanese variant. *Blood*. (1997) 89:2008–14.
31. Polliack A, Tadmor T. Surface topography of hairy cell leukemia cells compared to other leukemias as seen by scanning electron microscopy. *Leuk Lymphoma*. (2011) 52(Suppl. 2):14–7. doi: 10.3109/10428194.2011.565095
32. Machesky LM, Insall RH. Scar1 and the related Wiskott-Aldrich syndrome protein, WASP, regulate the actin cytoskeleton through the Arp2/3 complex. *Curr Biol*. (1998) 8:1347–56. doi: 10.1016/s0960-9822(98)00015-3
33. Marchand JB, Kaiser DA, Pollard TD, Higgs HN. Interaction of WASP/Scar proteins with actin and vertebrate Arp2/3 complex. *Nat Cell Biol*. (2001) 3:76–82. doi: 10.1038/35050590
34. Rodal AA, Sokolova O, Robins DB, Daugherty KM, Hippenmeyer S, Riezman H, et al. Conformational changes in the Arp2/3 complex leading to actin nucleation. *Nat Struct Mol Biol*. (2005) 12:26–31. doi: 10.1038/nsmb870
35. Dayel MJ, Mullins RD. Activation of Arp2/3 complex: addition of the first subunit of the new filament by a WASP protein triggers rapid ATP hydrolysis on Arp2. *PLoS Biol*. (2004) 2:E91. doi: 10.1371/journal.pbio.0020091
36. Padrick SB, Doolittle LK, Brautigam CA, King DS, Rosen MK. Arp2/3 complex is bound and activated by two WASP proteins. *Proc Natl Acad Sci USA*. (2011) 108:E472–9. doi: 10.1073/pnas.1100236108
37. Urbanek AN, Smith AP, Allwood EG, Booth WI, Ayscough KR. A novel actin-binding motif in Las17/WASP nucleates actin filaments independently of Arp2/3. *Curr Biol*. (2013) 23:196–203. doi: 10.1016/j.cub.2012.12.024
38. Kenney D, Cairns L, Remold-O'Donnell E, Peterson J, Rosen FS, Parkman R. Morphological abnormalities in the lymphocytes of patients with the Wiskott-Aldrich syndrome. *Blood*. (1986) 68:1329–32.
39. Gallego MD, Santamaría M, Peña J, Molina IJ. Defective actin reorganization and polymerization of Wiskott-Aldrich T cells in response to CD3-mediated stimulation. *Blood*. (1997) 90:3089–97.
40. Facchetti F, Blanzuoli L, Vermi W, Notarangelo LD, Giliani S, Fiorini M, et al. Defective actin polymerization in EBV-transformed B-cell lines from patients with the Wiskott-Aldrich syndrome. *J Pathol*. (1998) 185:99–107. doi: 10.1002/(sici)1096-9896(199805)185:13.0.co;2-l
41. Burns SO, Killock DJ, Moulding DA, Metelo J, Nunes J, Taylor RR, et al. A congenital activating mutant of WASp causes altered plasma membrane topography and adhesion under flow in lymphocytes. *Blood*. (2010) 115:5355–65. doi: 10.1182/blood-2009-08-236174
42. Westerberg L, Larsson M, Hardy SJ, Fernández C, Thrasher AJ, Severinson E. Wiskott-Aldrich syndrome protein deficiency leads to reduced B-cell adhesion, migration, and homing, and a delayed humoral immune response. *Blood*. (2005) 105:1144–52. doi: 10.1182/blood-2004-03-1003
43. Nicholson-Dykstra SM, Higgs HN. Arp2 depletion inhibits sheet-like protrusions but not linear protrusions of fibroblasts and lymphocytes. *Cell Motil Cytoskeleton*. (2008) 65:904–22. doi: 10.1002/cm.20312
44. Carpentier JL, Obberghen EV, Gorden P, Orci L. Surface redistribution of 125I-insulin in cultured human lymphocytes. *J Cell Biol*. (1981) 91:17–25. doi: 10.1083/jcb.91.1.17
45. Hasslen SR, von Andrian UH, Butcher EC, Nelson RD, Erlandsen SL. Spatial distribution of L-selectin (CD62L) on human lymphocytes and transfected murine L1-2 cells. *Histochem J*. (1995) 27:547–54.

46. von Andrian UH, Hasslen SR, Nelson RD, Erlandsen SL, Butcher EC. A central role for microvillous receptor presentation in leukocyte adhesion under flow. *Cell*. (1995) 82:989–99. doi: 10.1016/0092-8674(95)90278-3
47. Berlin C, Bargatze RF, Campbell JJ, von Andrian UH, Szabo MC, Hasslen SR, et al. alpha 4 integrins mediate lymphocyte attachment and rolling under physiologic flow. *Cell*. (1995) 80:413–22. doi: 10.1016/0092-8674(95)90491-3
48. Singer II, Scott S, Kawka DW, Chin J, Daugherty BL, DeMartino JA, et al. CCR5, CXCR4, and CD4 are clustered and closely apposed on microvilli of human macrophages and T cells. *J Virol*. (2001) 75:3779–90. doi: 10.1128/jvi.75.8.3779-3790.2001
49. Foti M, Phelouzat M-A, Holm A, Rasmusson BJ, Carpentier J-L. p56Lck anchors CD4 to distinct microdomains on microvilli. *Proc Natl Acad Sci USA*. (2002) 99:2008–13. doi: 10.1073/pnas.042689099
50. Hao J-J, Wang G, Pisitkun T, Patino-Lopez G, Nagashima K, Knepper MA, et al. Enrichment of distinct microfilament-associated and GTP-binding-proteins in membrane/microvilli fractions from lymphoid cells. *J Proteome Res*. (2008) 7:2911–27. doi: 10.1021/pr800016a
51. Alfonso-Garrido J, Garcia-Calvo E, Luque-Garcia JL. Sample preparation strategies for improving the identification of membrane proteins by mass spectrometry. *Anal Bioanal Chem*. (2015) 407:4893–905. doi: 10.1007/s00216-015-8732-0
52. Razvag Y, Neve-Oz Y, Sajman J, Yakovian O, Reches M, Sherman E. T Cell activation through isolated tight contacts. *Cell Rep*. (2019) 29:3506–21.e6. doi: 10.1016/j.celrep.2019.11.022
53. Jung Y, Wen L, Altman A, Ley K. CD45 pre-exclusion from the tips of microvilli establishes a phosphatase-free zone for early TCR triggering. *bioRxiv* [Preprint]. (2020). doi: 10.1101/2020.05.21.109074
54. Davis SJ, van der Merwe PA. The kinetic-segregation model: TCR triggering and beyond. *Nat Immunol*. (2006) 7:803–9. doi: 10.1038/ni1369
55. van der Merwe PA, Davis SJ, Shaw AS, Dustin ML. Cytoskeletal polarization and redistribution of cell-surface molecules during T cell antigen recognition. *Semin Immunol*. (2000) 12:5–21. doi: 10.1006/smim.2000.0203
56. Davis SJ, van der Merwe PA. The structure and ligand interactions of CD2: implications for T-cell function. *Immunol Today*. (1996) 17:177–87. doi: 10.1016/0167-5699(96)80617-7
57. Choudhuri K, Wiseman D, Brown MH, Gould K, van der Merwe PA. T-cell receptor triggering is critically dependent on the dimensions of its peptide-MHC ligand. *Nature*. (2005) 436:578–82. doi: 10.1038/nature03843
58. Chang VT, Fernandes RA, Ganzinger KA, Lee SF, Siebold C, McColl J, et al. Initiation of T cell signaling by CD45 segregation at "close contacts". *Nat Immunol*. (2016) 17:574–82. doi: 10.1038/ni.3392
59. Razvag Y, Neve-Oz Y, Sajman J, Reches M, Sherman E. Nanoscale kinetic segregation of TCR and CD45 in engaged microvilli facilitates early T cell activation. *Nat Commun*. (2018) 9:732. doi: 10.1038/s41467-018-03127-w
60. Fernandes RA, Ganzinger KA, Tzou JC, Jönsson P, Lee SF, Palayret M, et al. A cell topography-based mechanism for ligand discrimination by the T cell receptor. *Proc Natl Acad Sci USA*. (2019) 116:14002–10. doi: 10.1073/pnas.1817255116
61. Bakalar MH, Joffe AM, Schmid EM, Son S, Podolski M, Fletcher DA. Size-dependent segregation controls macrophage phagocytosis of antibody-opsonized targets. *Cell*. (2018) 174:131–42.e13. doi: 10.1016/j.cell.2018.05.059
62. Bunnell SC, Hong DI, Kardon JR, Yamazaki T, McGlade CJ, Barr VA, et al. T cell receptor ligation induces the formation of dynamically regulated signaling assemblies. *J Cell Biol*. (2002) 158:1263–75. doi: 10.1083/jcb.200203043
63. Campi G, Varma R, Dustin ML. Actin and agonist MHC–peptide complex–dependent T cell receptor microclusters as scaffolds for signaling. *J Exp Med*. (2005) 202:1031–6. doi: 10.1084/jem.20051182
64. Choudhuri K, Llodrá J, Roth EW, Tsai J, Gordo S, Wucherpfennig KW, et al. Polarized release of T-cell-receptor-enriched microvesicles at the immunological synapse. *Nature*. (2014) 507:118–23. doi: 10.1038/nature12951
65. Saliba DG, Céspedes-Donoso PF, Bálint Š, Compeer EB, Korobchevskaya K, Valvo S, et al. Composition and structure of synaptic ectosomes exporting antigen receptor linked to functional CD40 ligand from helper T cells. *eLife*. (2019) 8:247. doi: 10.7554/elife.47528
66. McMahon HT, Gallop JL. Membrane curvature and mechanisms of dynamic cell membrane remodelling. *Nature*. (2005) 438:590–6. doi: 10.1038/nature04396
67. Wolf D, Hofbrucker-MacKenzie SA, Izadi M, Seemann E, Steiniger F, Schwintzer L, et al. Ankyrin repeat-containing N-Ank proteins shape cellular membranes. *Nat Cell Biol*. (2019) 21:1191–205. doi: 10.1038/s41556-019-0381-7
68. Snead WT, Zeno WF, Kago G, Perkins RW, Richter JB, Zhao C, et al. BAR scaffolds drive membrane fission by crowding disordered domains. *J Cell Biol*. (2019) 218:664–82. doi: 10.1083/jcb.201807119
69. Busch DJ, Houser JR, Hayden CC, Sherman MB, Lafer EM, Stachowiak JC. Intrinsically disordered proteins drive membrane curvature. *Nat Commun*. (2015) 6:7875. doi: 10.1038/ncomms8875
70. Yuan F, Alimohamadi H, Bakka B, Trementozzi AN, Fawzi NL, Rangamani P, et al. Membrane bending by protein phase separation. *bioRxiv* [Preprint]. (2020). doi: 10.1101/2020.05.21.109751
71. Frost A, Unger VM, Camilli PD. The BAR domain superfamily: membrane-molding macromolecules. *Cell*. (2009) 137:191–6. doi: 10.1016/j.cell.2009.04.010
72. Saarikangas J, Zhao H, Pykäläinen A, Laurinmäki P, Mattila PK, Kinnunen PKJ, et al. Molecular mechanisms of membrane deformation by I-BAR domain proteins. *Curr Biol*. (2009) 19:95–107. doi: 10.1016/j.cub.2008.12.029
73. Carman PJ, Dominguez R. BAR domain proteins-a linkage between cellular membranes, signaling pathways, and the actin cytoskeleton. *Biophys Rev*. (2018) 10:1587–604. doi: 10.1007/s12551-018-0467-7
74. Lim KB, Bu W, Goh WI, Koh E, Ong SH, Pawson T, et al. The Cdc42 effector IRSp53 generates filopodia by coupling membrane protrusion with actin dynamics. *J Biol Chem*. (2008) 283:20454–72. doi: 10.1074/jbc.m710185200
75. Mattila PK, Pykäläinen A, Saarikangas J, Paavilainen VO, Vihinen H, Jokitalo E, et al. Missing-in-metastasis and IRSp53 deform PI(4,5)P2-rich membranes by an inverse BAR domain-like mechanism. *J Cell Biol*. (2007) 176:953–64. doi: 10.1083/jcb.200609176
76. Crespi A, Ferrari I, Lonati P, Disanza A, Fornasari D, Scita G, et al. LIN7 regulates the filopodium- and neurite-promoting activity of IRSp53. *J Cell Sci*. (2012) 125:4543–54. doi: 10.1242/jcs.106484
77. Kast DJ, Dominguez R. IRSp53 coordinates AMPK and 14-3-3 signaling to regulate filopodia dynamics and directed cell migration. *Mol Biol Cell*. (2019) 30:1285–97. doi: 10.1091/mbc.e18-09-0600
78. Thomas A, Mariani-Floderer C, López-Huertas MR, Gros N, Hamard-Péron E, Favard C, et al. Involvement of the Rac1-IRSp53-Wave2-Arp2/3 Signaling Pathway in HIV-1 Gag particle release in CD4 T Cells. *J Virol*. (2015) 89:8162–81. doi: 10.1128/jvi.00469-15
79. Jarsch IK, Gadsby JR, Nuccitelli A, Mason J, Shimo H, Pilloux L, et al. A direct role for SNX9 in the biogenesis of filopodia. *J Cell Biol*. (2020) 219:931. doi: 10.1083/jcb.201909178
80. Lee K, Gallop JL, Rambani K, Kirschner MW. Self-assembly of filopodia-like structures on supported lipid bilayers. *Science*. (2010) 329:1341–5. doi: 10.1126/science.1191710
81. Yarar D, Waterman-Storer CM, Schmid SL. SNX9 couples actin assembly to phosphoinositide signals and is required for membrane remodeling during endocytosis. *Dev Cell*. (2007) 13:43–56. doi: 10.1016/j.devcel.2007.04.014
82. Badour K, McGavin MKH, Zhang J, Freeman S, Vieira C, Filipp D, et al. Interaction of the Wiskott-Aldrich syndrome protein with sorting nexin 9 is required for CD28 endocytosis and cosignaling in T cells. *Proc Natl Acad Sci USA*. (2007) 104:1593–8. doi: 10.1073/pnas.0610543104
83. Weder P, Schumacher TNM, Spits H, Luiten RM. Testing for HLA/peptide tetramer-binding to the T cell receptor complex on human T lymphocytes. *Results Immunol*. (2012) 2:88–96. doi: 10.1016/j.rinim.2012.04.001
84. Ramamurthi KS, Lecuyer S, Stone HA, Losick R. Geometric cue for protein localization in a bacterium. *Science*. (2009) 323:1354–7. doi: 10.1126/science.1169218
85. Bridges AA, Jentzsch MS, Oakes PW, Occhipinti P, Gladfelter AS. Micron-scale plasma membrane curvature is recognized by the septin cytoskeleton. *J Cell Biol*. (2016) 213:23–32. doi: 10.1083/jcb.201512029
86. Hägerstrand H, Mrówczyńska L, Salzer U, Prohaska R, Michelsen KA, Kralj-Iglič V, et al. Curvature-dependent lateral distribution of raft markers in the human erythrocyte membrane. *Mol Membr Biol*. (2009) 23:277–88. doi: 10.1080/09687860600682536

87. Aimon S, Callan-Jones A, Berthaud A, Pinot M, Toombes GES, Bassereau P. Membrane shape modulates transmembrane protein distribution. *Dev Cell*. (2014) 28:212–8. doi: 10.1016/j.devcel.2013.12.012
88. Strahl H, Ronneau S, González BS, Klutsch D, Schaffner-Barbero C, Hamoen LW. Transmembrane protein sorting driven by membrane curvature. *Nat Commun*. (2015) 6:1–9. doi: 10.1038/ncomms9728
89. Rosholm KR, Leijnse N, Mantsiou A, Tkach V, Pedersen SL, Wirth VF, et al. Membrane curvature regulates ligand-specific membrane sorting of GPCRs in living cells. *Nat Chem Biol*. (2017) 13:724–9. doi: 10.1038/nchembio.2372
90. Zhao W, Hanson L, Lou H-Y, Akamatsu M, Chowdary PD, Santoro F, et al. Nanoscale manipulation of membrane curvature for probing endocytosis in live cells. *Nat Nanotechnol*. (2017) 12:750–6. doi: 10.1038/nnano.2017.98
91. Liang H, Mu H, Jean-Francois F, Lakshman B, Sarkar-Banerjee S, Zhuang Y, et al. Membrane curvature sensing of the lipid-anchored K-Ras small GTPase. *Life Sci Alliance*. (2019) 2:e201900343. doi: 10.26508/lsa.201900343
92. Ren C, Yuan Q, Braun M, Zhang X, Petri B, Zhang J, et al. Leukocyte cytoskeleton polarization is initiated by plasma membrane curvature from cell attachment. *Dev Cell*. (2019) 49:206–19.e7. doi: 10.1016/j.devcel.2019.02.023
93. Lou H-Y, Zhao W, Li X, Duan L, Powers A, Akamatsu M, et al. Membrane curvature underlies actin reorganization in response to nanoscale surface topography. *Proc Natl Acad Sci USA*. (2019) 116:23143–51. doi: 10.1073/pnas.1910166116
94. Hirama T, Lu SM, Kay JG, Maekawa M, Kozlov MM, Grinstein S, et al. Membrane curvature induced by proximity of anionic phospholipids can initiate endocytosis. *Nat Commun*. (2017) 8:1393. doi: 10.1038/s41467-017-01554-9
95. Zimmerberg J, Kozlov MM. How proteins produce cellular membrane curvature. *Nat Rev Mol Cell Biol*. (2006) 7:9–19. doi: 10.1038/nrm1784
96. Heo WD, Inoue T, Park WS, Kim ML, Park BO, Wandless TJ, et al. PI(3,4,5)P3 and PI(4,5)P2 lipids target proteins with polybasic clusters to the plasma membrane. *Science*. (2006) 314:1458–61. doi: 10.1126/science.1134389
97. Yeung T, Gilbert GE, Shi J, Silvius J, Kapus A, Grinstein S. Membrane phosphatidylserine regulates surface charge and protein localization. *Science*. (2008) 319:210–3. doi: 10.1126/science.1152066
98. Fairn GD, Hermansson M, Somerharju P, Grinstein S. Phosphatidylserine is polarized and required for proper Cdc42 localization and for development of cell polarity. *Nat Cell Biol*. (2011) 13:1424–30. doi: 10.1038/ncb2351
99. Ikenouchi J, Hirata M, Yonemura S, Umeda M. Sphingomyelin clustering is essential for the formation of microvilli. *J Cell Sci*. (2013) 126:3585–92. doi: 10.1242/jcs.122325
100. Wang W, Yang L, Huang HW. Evidence of cholesterol accumulated in high curvature regions: implications to the curvature elastic enregy for lipid mixtures. *Biophys J*. (2007) 92:2319–30. doi: 10.1529/biophysj.106097923
101. Koldsø H, Shorthouse D, Hélie J, Sansom MSP. Lipid clustering correlates with membrane curvature as revealed by molecular simulations of complex lipid bilayers. *PLoS Comput. Biol.* (2014) 10:e1003911. doi: 10.1371/journal.pcbi.1003911
102. Favela-Rosales F, Galván-Hernández A, Hernández-Cobos J, Kobayashi N, Carbajal-Tinoco MD, Nakabayashi S, et al. A molecular dynamics study proposing the existence of statistical structural heterogeneity due to chain orientation in the POPC-cholesterol bilayer. *Biophys Chem*. (2020) 257:106275. doi: 10.1016/j.bpc.2019.106275
103. Smondyrev AM, Berkowitz ML. Structure of dipalmitoylphosphatidylcholine/cholesterol bilayer at low and high cholesterol concentrations: molecular dynamics simulation. *Biophys J*. (1999) 77:2075–89. doi: 10.1016/s0006-3495(99)77049-9
104. Greicius G, Westerberg L, Davey EJ, Buentke E, Scheynius A, Thyberg J, et al. Microvilli structures on B lymphocytes: inducible functional domains? *Int Immunol*. (2004) 16:353–64. doi: 10.1093/intimm/dxh031
105. Keren K, Pincus Z, Allen GM, Barnhart EL, Marriott G, Mogilner A, et al. Mechanism of shape determination in motile cells. *Nature*. (2008) 453:475–80. doi: 10.1038/nature06952
106. Möckl L. The emerging role of the mammalian glycocalyx in functional membrane organization and immune system regulation. *Front Cell Dev Biol*. (2020) 8:253. doi: 10.3389/fcell.2020.00253
107. Kesimer M, Ehre C, Burns KA, Davis CW, Sheehan JK, Pickles RJ. Molecular organization of the mucins and glycocalyx underlying mucus transport over mucosal surfaces of the airways. *Mucosal Immunol*. (2013) 6:379–92. doi: 10.1038/mi.2012.81
108. Shurer CR, Kuo JC-H, Roberts LM, Gandhi JG, Colville MJ, Enoki TA, et al. Physical principles of membrane shape regulation by the glycocalyx. *Cell*. (2019) 177:1757–70.e21. doi: 10.1016/j.cell.2019.04.017
109. Clark MC, Baum LG. T cells modulate glycans on CD43 and CD45 during development and activation, signal regulation, and survival. *Ann N Y Acad Sci USA*. (2012) 1253:58–67. doi: 10.1111/j.1749-6632.2011.06304.x
110. Pereira MS, Alves I, Vicente M, Campar A, Silva MC, Padrão NA, et al. Glycans as key checkpoints of T cell activity and function. *Front Immunol*. (2018) 9:2754. doi: 10.3389/fimmu.2018.02754
111. McCall MN, Shotton DM, Barclay AN. Expression of soluble isoforms of rat CD45. Analysis by electron microscopy and use in epitope mapping of anti-CD45R monoclonal antibodies. *Immunology*. (1992) 76:310–7.
112. Yamashiro-Matsumura S, Matsumura F. Purification and characterization of an F-actin-bundling 55-kilodalton protein from HeLa cells. *J Biol Chem*. (1985) 260:5087–97.
113. Vignjevic D, Kojima S, Aratyn Y, Danciu O, Svitkina T, Borisy GG. Role of fascin in filopodial protrusion. *J Cell Biol*. (2006) 174:863–75. doi: 10.1083/jcb.200603013
114. Loomis PA, Zheng L, Sekerková G, Changyaleket B, Mugnaini E, Bartles JR. Espin cross-links cause the elongation of microvillus-type parallel actin bundles in vivo. *J Cell Biol*. (2003) 163:1045–55. doi: 10.1083/jcb.200309093
115. Tilney MS, Tilney LG, Stephens RE, Merte C, Drenckhahn D, Cotanche DA, et al. Preliminary biochemical characterization of the stereocilia and cuticular plate of hair cells of the chick cochlea. *J Cell Biol*. (1989) 109:1711–23. doi: 10.1083/jcb.109.4.1711
116. Tsai F-C, Bertin A, Bousquet H, Manzi J, Senju Y, Tsai M-C, et al. Ezrin enrichment on curved membranes requires a specific conformation or interaction with a curvature-sensitive partner. *eLife*. (2018) 7:129. doi: 10.7554/elife.37262
117. Huang F-K, Han S, Xing B, Huang J, Liu B, Bordeleau F, et al. Targeted inhibition of fascin function blocks tumour invasion and metastatic colonization. *Nat Commun*. (2015) 6:7465. doi: 10.1038/ncomms8465
118. Prévost C, Zhao H, Manzi J, Lemichez E, Lappalainen P, Callan-Jones A, et al. IRSp53 senses negative membrane curvature and phase separates along membrane tubules. *Nat Commun*. (2015) 6:8529. doi: 10.1038/ncomms9529
119. Shi Z, Graber ZT, Baumgart T, Stone HA, Cohen AE. Cell membranes resist flow. *Cell*. (2018) 175:1769–79.e13. doi: 10.1016/j.cell.2018.09.054
120. Lee I-H, Kai H, Carlson L-A, Groves JT, Hurley JH. Negative membrane curvature catalyzes nucleation of endosomal sorting complex required for transport (ESCRT)-III assembly. *Proc Natl Acad Sci USA*. (2015) 112:15892–7. doi: 10.1073/pnas.1518765113
121. Li X, Matino L, Zhang W, Klausen L, McGuire AF, Lubrano C, et al. A nanostructure platform for live-cell manipulation of membrane curvature. *Nat Protoc*. (2019) 14:1772–802. doi: 10.1038/s41596-019-0161-7
122. Przybylo M, Sıkora J, Humpolíckova J, Benda A, Zan A, Hof M. Lipid diffusion in giant unilamellar vesicles is more than 2 times faster than in supported phospholipid bilayers under identical conditions. *Langmuir*. (2006) 22:9096–9. doi: 10.1021/la061934p
123. Hsieh C-L, Spindler S, Ehrig J, Sandoghdar V. Tracking single particles on supported lipid membranes: multimobility diffusion and nanoscopic confinement. *J Phys Chem B*. (2014) 118:1545–54. doi: 10.1021/jp412203t
124. Demetriou P, Abu-Shah E, McCuaig S, Mayya V, Valvo S, Korobchevskaya K, et al. CD2 expression acts as a quantitative checkpoint for immunological synapse structure and T-cell activation. *Biorxiv* [Preprint]. (2019). doi: 10.1101/589440

125. Lillemeier BF, Mörtelmaier MA, Forstner MB, Huppa JB, Groves JT, Davis MM. TCR and Lat are expressed on separate protein islands on T cell membranes and concatenate during activation. *Nat Immunol*. (2010) 11:90–6. doi: 10.1038/ni.1832
126. Su X, Ditlev JA, Hui E, Xing W, Banjade S, Okrut J, et al. Phase separation of signaling molecules promotes T cell receptor signal transduction. *Science*. (2016) 352:595–9. doi: 10.1126/science.aad9964
127. Eggeling C, Ringemann C, Medda R, Schwarzmann G, Sandhoff K, Polyakova S, et al. Direct observation of the nanoscale dynamics of membrane lipids in a living cell. *Nature*. (2008) 457:1159–62. doi: 10.1038/nature07596
128. Honigmann A, Mueller V, Ta H, Schoenle A, Sezgin E, Hell SW, et al. Scanning STED-FCS reveals spatiotemporal heterogeneity of lipid interaction in the plasma membrane of living cells. *Nat Commun*. (2014) 5:5412. doi: 10.1038/ncomms6412
129. Brameshuber M, Kellner F, Rossboth BK, Ta H, Alge K, Sevcsik E, et al. Monomeric TCRs drive T cell antigen recognition. *Nat Immunol*. (2018) 19:487–96. doi: 10.1038/s41590-018-0092-4
130. Reth M. Matching cellular dimensions with molecular sizes. *Nat Immunol*. (2013) 14:765–7. doi: 10.1038/ni.2621
131. Harrison DL, Fang Y, Huang J. T-cell mechanobiology: force sensation, potentiation, and translation. *Front Phys*. (2019) 7:835. doi: 10.3389/fphy.2019.00045
132. Hardie RC, Franze K. Photomechanical responses in *Drosophila* photoreceptors. *Science*. (2012) 338:260–3. doi: 10.1126/science.1222376

Conflict of Interest: The authors declare that the research was conducted in the absence of any commercial or financial relationships that could be construed as a potential conflict of interest.

frontiers in Physiology

ORIGINAL RESEARCH
published: 16 September 2020
doi: 10.3389/fphys.2020.568087

Quantitative Optical Diffraction Tomography Imaging of Mouse Platelets

*Tess A. Stanly[1], Rakesh Suman[2], Gulab Fatima Rani[3], Peter J. O'Toole[2], Paul M. Kaye[3] and Ian S. Hitchcock[1]**

[1] York Biomedical Research Institute, Department of Biology, University of York, York, United Kingdom, [2] Technology Facility, Department of Biology, University of York, York, United Kingdom, [3] York Biomedical Research Institute, Hull York Medical School, University of York, York, United Kingdom

Platelets are specialized anucleate cells that play a major role in hemostasis following vessel injury. More recently, platelets have also been implicated in innate immunity and inflammation by directly interacting with immune cells and releasing proinflammatory signals. It is likely therefore that in certain pathologies, such as chronic parasitic infections and myeloid malignancies, platelets can act as mediators for hemostatic and proinflammatory responses. Fortunately, murine platelet function *ex vivo* is highly analogous to human, providing a robust model for functional comparison. However, traditional methods of studying platelet phenotype, function and activation status often rely on using large numbers of whole isolated platelet populations, which severely limits the number and type of assays that can be performed with mouse blood. Here, using cutting edge 3D quantitative phase imaging, holotomography, that uses optical diffraction tomography (ODT), we were able to identify and quantify differences in single unlabeled, live platelets with minimal experimental interference. We analyzed platelets directly isolated from whole blood of mice with either a JAK2V617F-positive myeloproliferative neoplasm (MPN) or *Leishmania donovani* infection. Image analysis of the platelets indicates previously uncharacterized differences in platelet morphology, including altered cell volume and sphericity, as well as changes in biophysical parameters such as refractive index (RI) and dry mass. Together, these data indicate that, by using holotomography, we were able to identify clear disparities in activation status and potential functional ability in disease states compared to control at the level of single platelets.

Keywords: platelets, holotomography, MPN, JAK2V617F, leishmaniasis

OPEN ACCESS

Edited by:
Yan Shi,
Tsinghua University, China

Reviewed by:
Zahid Yaqoob,
Massachusetts Institute of Technology, United States
Jinghe Yuan,
Institute of Chemistry (CAS), China

****Correspondence:***
Ian S. Hitchcock
ian.hitchcock@york.ac.uk

Specialty section:
This article was submitted to Membrane Physiology and Membrane Biophysics, a section of the journal Frontiers in Physiology

Received: *08 June 2020*
Accepted: *25 August 2020*
Published: *16 September 2020*

Citation:
Stanly TA, Suman R, Rani GF, O'Toole PJ, Kaye PM and Hitchcock IS (2020) Quantitative Optical Diffraction Tomography Imaging of Mouse Platelets. Front. Physiol. 11:568087. doi: 10.3389/fphys.2020.568087

INTRODUCTION

Maintaining blood flow in basal states and preventing excessive blood loss following injury relies on an orchestrated response from different cell types and non-cellular components, such as clotting factors. Platelets are key cells in this process, becoming rapidly activated following injury and form a platelet plug to reduce blood loss, as well as initiating secondary hemostasis to promote the formation of a stable fibrin-rich thrombus (Machlus and Italiano, 2013). Maintaining

a physiological number of functional platelets is essential for hemostasis. However, a wide variety of pathological conditions lead to rapid and sustained changes in platelet counts and functionality. Thrombocytopenia (sustained reduction in platelets of $<100 \times 10^3/\mu L$ whole blood in humans) is common in autoimmune conditions as well as acute and chronic infections by bacterial, parasitic and viral pathogens including *Salmonella, Staphylococcus aureus, Plasmodium, Leishmania,* and dengue virus (Varma and Naseem, 2010; Cox et al., 2011; Lacerda et al., 2011; Liu et al., 2016; Kullaya et al., 2018; Riswari et al., 2019).

Conversely, thrombocytosis (sustained excess platelet count $>450 \times 10^3/\mu L$ whole blood in humans) is common in myeloproliferative neoplasms (MPNs), such as essential thrombocythemia (ET). Furthermore, platelet production by megakaryocytes can be significantly altered by bone marrow failure syndromes, whereas inflammatory conditions often impact platelet functionality. In addition to being essential for hemostasis, there is now compelling evidence suggesting key roles for platelets in other processes including wound healing, angiogenesis, inflammation, and innate immunity (Machlus and Italiano, 2013; van der Meijden and Heemskerk, 2019). Platelets express a range of receptors that allow them to interact with and respond to pathogens and assist in regulating an immune response (Assinger, 2014; Hamzeh-Cognasse et al., 2015; van der Meijden and Heemskerk, 2019). There is complex interplay between platelets and bacteria during infections, where the interaction of platelets with immune cells, such as neutrophils generate neutrophil traps/net or release immunomodulatory factors for trapping and clearance of bacteria. Platelets can also bind directly to the bacteria to form clots during inflammatory endocarditis. Platelets assist the formation of the traps, and concurrently the nets contribute to platelet activation, linking inflammation to thrombosis (Gros et al., 2015; Hamzeh-Cognasse et al., 2015).

As platelet production and function is comparable between mice and humans, murine models provide an excellent platform to study the effects of diverse pathologies on platelet form and function. However, traditional methods used for studying platelet phenotype, function and activation status often rely on using large numbers of whole isolated platelet populations. The limited volume of the blood obtained for isolation of platelets severely restricts the number and type of assays that can be performed with mouse blood. Super-resolution imaging techniques have recently enabled the study of structural changes in the protein distribution or cytoskeleton changes of platelets in disease models (Poulter et al., 2015; Bergstrand et al., 2019; Khan and Pike, 2020), However, it is important to note that with improvements in resolution, the post-isolation processing which entails fixation, permeabilization and labeling, can often lead to artifacts if not carefully controlled (Schnell et al., 2012; Stanly et al., 2016; Pereira et al., 2019; Khan and Pike, 2020).

Here, using cutting edge 3D quantitative phase imaging, holotomography, which uses optical diffraction tomography (ODT), we were able to identify and quantify differences in single unlabeled platelets from very small sample volumes. The technique measures 3D differences in the refractive index (RI) tomograms that are generated due to alterations in the diffraction patterns obtained from the cells. This allows the measurement of cellular changes under live conditions, without experimental interferences such as labeling or fixation. With this label-free imaging of the samples we can obtain quantitative information such as cellular dry mass (cytoplasmic concentration) and information on the cell size or structure (Kim et al., 2017; Lee et al., 2019).

Using this technique, we analyzed platelets directly isolated from the whole blood of two different pathological mouse models. In the first model, *Jak/2E/B6 Stella-Cre* mice express a mutated version of human JAK2 (JAK2V617F) under the control of the endogenous *Jak2* promoter (Li et al., 2010). These mice develop symptoms similar to a JAK2V617F-positive MPN, including increased platelets and erythrocytes, megakaryocyte hyperplasia and markers of chronic systemic inflammation. However, the role of JAK2V617F in platelet function remains unclear. *In vitro* analysis of platelets isolated from MPN patients suggests there may be defects in signal transduction and integrin activity (Moore et al., 2013; Lucchesi et al., 2020). While in JAK2V617F-positive mouse models, studies have suggested changes in platelet aggregation *in vitro* (Hobbs et al., 2013) and others identify aberrant hemostasis *in vivo*, but no clear platelet phenotype (Etheridge et al., 2014; Lamrani et al., 2014). Furthermore, as chronic inflammation is now considered a key characteristic of MPNs, the proinflammatory environment may lead to functional changes in platelet activity, leading to the increased incidence of bleeding abnormalities in these patients, as reviewed in Hasselbalch (2012, 2014).

We also analyzed platelets taken from a mouse model of visceral leishmaniasis (VL). In humans, VL causes thrombocytopenia and anemia, a phenotype also mirrored in experimental murine models of *Leishmania donovani*, which is thought to be caused by defective medullary erythropoiesis and thrombocytopenia (Varma and Naseem, 2010; Preham et al., 2018; Rani et al., 2019). The cause of severe thrombocytopenia in the mouse models of VL is unclear, but is likely to be multifactorial, with the parasite infection leading to significant changes in the bone marrow microenvironment and increased macrophage activity that would likely lead to excessive platelet clearance.

In this study, using holotomography, we were able to identify distinct platelet phenotypes in both disease mouse models that may not have been identifiable using current standard assays.

MATERIALS AND METHODS

Ethics Statement

All animal care and experimental procedures were performed under UK Home Office License (Ref # PPL 7008596 and P49487014) and with approval from the Animal Welfare and Ethical Review Board of the Department of Biology, University of York.

Mice

C57BL/6 (WT) and Jak/2E/B6 Stella-Cre (Li et al., 2010; Kent et al., 2013) (herein referred to as VF) mice were bred at

the University of York. For platelet experiments, heterozygous VF mice where used, which exhibit a JAK2V617F+ ET-like phenotype with modest platelet increases, splenomegaly and transformation to myelofibrosis.

For *L. donovani* infection experiments, C57BL/6 female mice at 6–8 weeks of age used for the study. Mice were infected with 3×10^7 amastigotes of the Ethiopian strain of *L. donovani* (LV9) via lateral tail vein, as described (Hasselbalch, 2014). All mice were maintained in individually ventilated cages (at ACDP CL3, where necessary for infection control). All experimental mice were killed 4 weeks post infection.

Platelet Isolation

The WT and VF mice were euthanized with pentobarbital, followed by collection of whole blood into acid citrate dextrose (ACD) via cardiac punctures. The collected blood was topped up with equal volume of wash buffer (150 mM NaCl, 20 mM HEPES, at RT, pH 6.5) and centrifuged at 60 *g* for 7 min at room temperature without breaks. The platelet rich plasma (PRP) was collected and centrifuged at 240 *g* for 10 min at room temperature to separate platelets and plasma. The platelet pellet was resuspended in wash buffer containing 1 U/ml of apyrase (Sigma-Aldrich, United Kingdom) and 1 μM of prostaglandin E1 (Sigma-Aldrich, United Kingdom) (Prévost et al., 2007).

For *L. donovani* infected mice, whole blood was collected via cardiac puncture after anesthetizing the mice with isoflurane inhalation in a secure chamber (Apollo TEC3 Isoflurane Vaporize, Sound Veterinary Equipment, Rowville, VIC, Australia). Blood was collected in 5 ml polystyrene tubes (Falcon™) coated with ACD and isolated as above into wash buffer without apyrase and prostaglandin E1.

Twenty microliter of the isolated platelets were then added to a TomoDish (Tomocube Inc.) fluidic chamber assembly, where the sample is sandwiched between two #1.5H coverslips.

Platelet Fixation and Granule Labeling

For monitoring the effect of fixation on platelets, 10 μl isolated platelets in wash buffer were added to the TomoDish with a coverslip and imaged, followed by addition of 10 μl 8% PFA to the flow chamber in the TomoDish allowing it to diffuse in, making a 4% PFA final concentration within the chamber. This was allowed to incubate and imaged every 10 min for a total of 30 min at room temperature (RT).

For labeling the granules, the isolated platelets were incubated, for 30 min at 37°C, 5% CO_2, with 50 μM Mepacrine (Q3251-25G, Sigma-Aldrich, United Kingdom) to label dense granules or 10 μg/ml of BQ-BSA Green (D12050, Invitrogen, Fisher Scientific) to label the alpha granules. After incubation, the platelets were washed and plated onto the TomoDish with 4% PFA for 10 min at RT. The fixative was removed, and the platelets were then imaged in wash buffer.

Microscopy

3D Quantitative phase images of platelets were generated using a commercial holotomographic microscope (HT-2H, Tomocube Inc.) that employs ODT using two UPLSAP 60X (NA 1.2) Water dipping lenses (Olympus, Tokyo, Japan). Full details of the optical configuration have been previously described here (Kim et al., 2013; Lim et al., 2015). Samples in wash buffer were mounted on specialized TomoDishes with No1.5H coverslips at RT.

Statistics

The data were plotted using GraphPad Prism 8 and data analyzed using unpaired or paired two-tailed *t*-tests as indicated in figure legends.

RESULTS

3D Holotomography Image Acquisition and Data Analysis

Briefly, the HT-2H microscope is based on a Mach–Zehnder interferometer equipped with a digital micromirror device (DMD) (**Figure 1A**). Using a coherent monochromatic laser (λ = 532 nm) divided into a sample and reference beam, 2D holographic QPI images were generated at multiple illumination angles (**Figure 1B**) where the incidence light is accurately controlled by the DMD (Shin et al., 2015). The light beam diffracted by the sample was collected using a high numerical aperture (NA = 1.2) objective lens UPLSAP 60XW (Olympus, Tokyo, Japan), with the subsequent holograms recorded on a CMOS sensor. A 3D RI tomogram was then reconstructed from the series of off-axis holograms using the TomoStudio™ software (Tomocube Inc.) (**Figure 1C**). Further details of the algorithms used and principles of ODT can be found here (Shin et al., 2016).

The 3D RI Tomograms of individual platelets were visualized and segmented to measure three-dimensional morphological parameters, mean RI and dry mass within the TomoStudio™ software (**Figures 1D,E** and **Supplementary Videos 1A,B**).

Platelets From Myeloid Malignancies Show Changes in Platelet Morphologies and Intracellular Components

Aberrant hemostasis and thrombosis is one of the most common causes of morbidity and mortality in JAK2V617F-positive MPN patients. Although some differences have been identified in platelet protein expression levels that would lead to a prothrombotic phenotype, the actual structure or morphology of these platelets has yet not been visualized. In order to study the differences in these platelets from WT vs. VF mice, we used a previously characterized murine model system for JAK2V617F+ mice (Li et al., 2010). Maximum RI projection images of unfixed platelets, freshly isolated from WT and VF mice indicated no visible change in the morphology (**Figure 2A**). However, quantitative analysis of the RI projection data indicated that had higher intensity compared to WT platelets (**Figure 2B**; $P < 0.001$), suggesting differences in composition between platelets from these two strains. There were no significant differences between WT and VF platelets in surface area or volume, but VF platelets had a significant increase in sphericity (unpaired two-tailed *t*-test, $P = 0.1921$, $P = 0.5062$, and

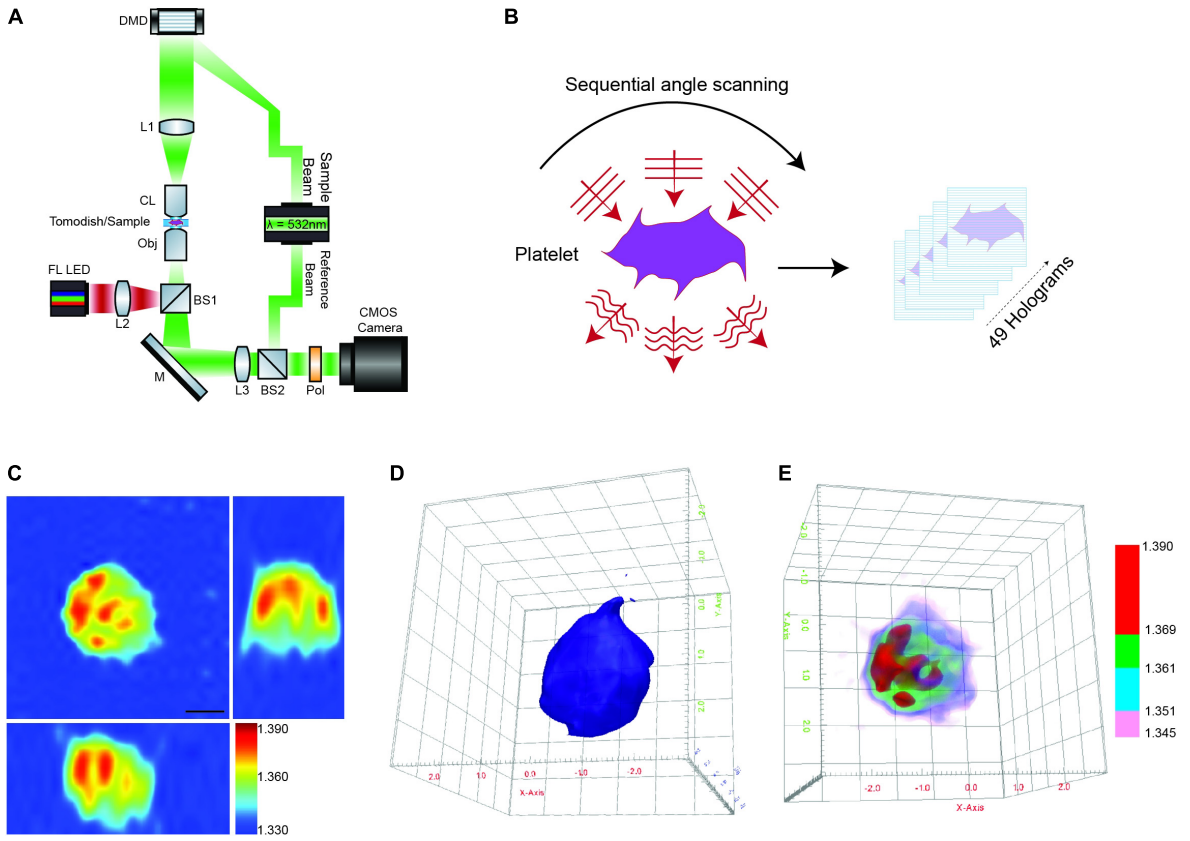

FIGURE 1 | Label-free 3D ODT imaging of platelets. **(A)** Simplified schematic of a holotomographic microscope based on Mach-Zehnder interferometric microscopy. λ-532 nm, laser light source; DMD, digital micromirror device; L1–L3, lenses; CL, condenser lens 60× NA 1.2; Obj, objective lens 60× NA 1.2; M, mirror; BS1-2, beam splitter; Pol, polarizer; FL LED, fluorescence light source. **(B)** Image acquisition/scanning of the sample based on sequential imaging at multiple angles to yield a total of 49 holograms. **(C)** Representative cross-sectional 3D RI tomogram image of a platelet. Color bar represents refractive index. **(D)** Example of 3D surface rendering of the platelet sample used to measure morphological parameters (see also **Supplementary Video 1A**). **(E)** Representative RI based rendering, where the pseudo coloring represents different bands of refractive index to highlight intracellular features of the platelet (see also **Supplementary Video 1B**).

$P = 0.0063$, respectively; **Figure 2C**). Thus, platelets in VF mice are altered in shape but not size.

We next created 3D iso-surface rendered images of the platelets based on a range of RIs, to provide data about cytosolic differences between cells (Kim et al., 2017; Lee et al., 2019). The 3D iso-surface rendered images of the platelets from WT and JAK2V617F mice show a clear difference in the organization of RI materials within the platelets (**Figure 2D**). corresponding with the RI values (**Figure 2E**; unpaired two-tailed t-test, $P \leq 0.0001$) and a significant increase in the dry mass (unpaired two-tailed t-test, $P \leq 0.0001$).

Bioactive molecules, such as those stored in alpha granules [containing membrane associated proteins – integrins, P-selectin, and soluble factors – vWF, factor V to name a few (Blair and Flaumenhaft, 2009; Flaumenhaft and Sharda, 2018)] and dense granules [mainly contain calcium, serotonin, histamines, etc., (Flaumenhaft and Sharda, 2018)], are key components within the platelets that make them active and respond to specific agonists (Hamzeh-Cognasse et al., 2015). In order to identify these granules and map the RI, we labeled the granules using membrane permeable dyes (Hanby et al., 2017) and fixed the platelets with 4% PFA for 10 min. The PFA fixation at 10 min does not affect the size, shape, RI and dry mass of the platelets but leaving them from longer than 10 min significantly alters these parameters (**Supplementary Figures S1A–E**). Unfortunately, although we could detect alpha and dense granules within the platelets, we were unable to measure the exact RI for the granules (**Supplementary Figures S1F,G**).

L. donovani Infected Mice Have Altered Platelet Morphologies and Intracellular Features

To determine whether similar changes occurred in another pathological setting characterized by alterations in platelet numbers, we examined platelets from mice with experimental VL (Hasselbalch, 2014; Preham et al., 2018).

Visible changes in the morphology of the platelets was observed in maximum RI projection images of the platelets freshly isolated from naïve and *L. donovani*-infected WT C57BL/6 mice (**Figure 3A**). In contrast to VF mice (**Figure 2**), platelets from *L. donovani*-infected mice have a much lower mean

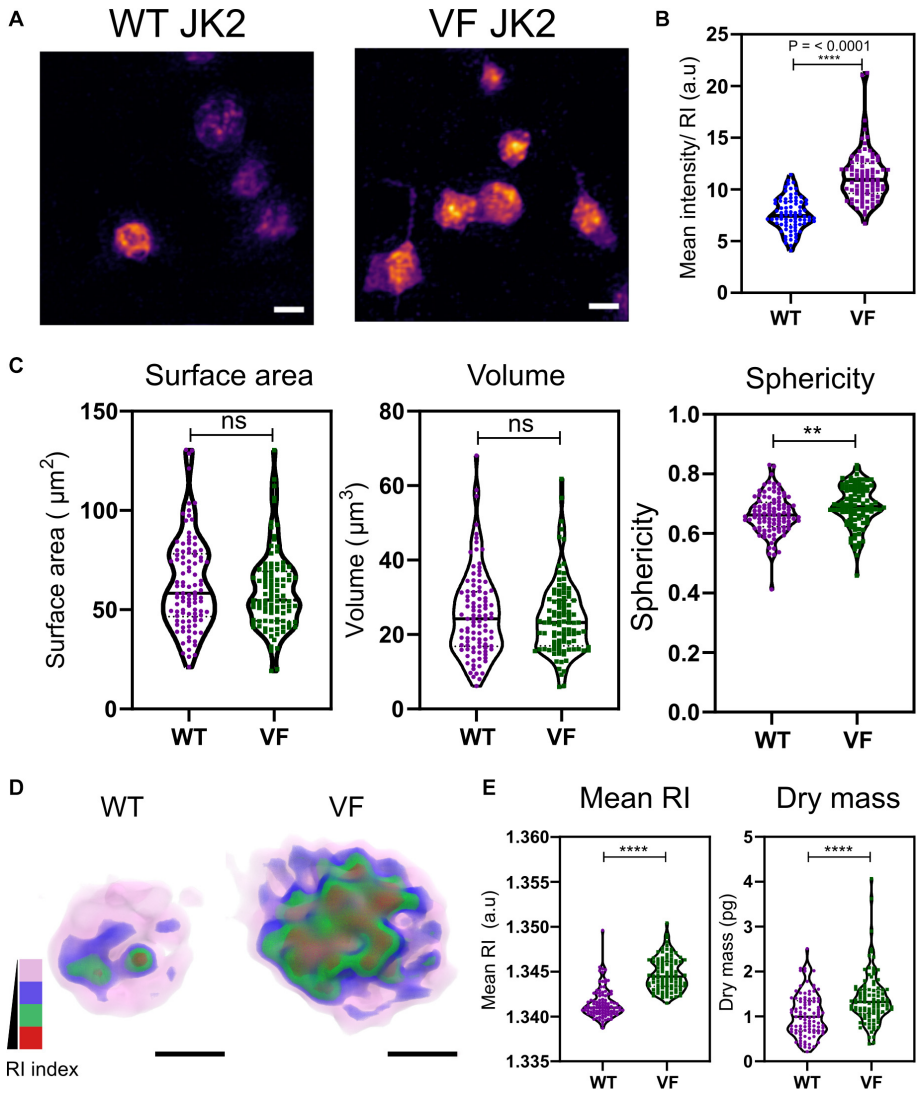

FIGURE 2 | Morphological and biophysical differences in platelets from WT and JAK2V617F+ (VF) from murine blood. **(A)** Max RI projections of the 3D phase images of platelets from WT and VF mice. **(B)** The mean intensity values from the RI projections between WT and VF platelets (unpaired two-tailed *t*-test, $P \leq 0.0001$, $n = 80$ platelets). **(C)** Morphological changes of platelets from WT and VF mice in surface area platelets (unpaired two-tailed *t*-test, $P = 0.1921$), volume (unpaired two-tailed *t*-test, $P = 0.5062$), and sphericity (unpaired two-tailed *t*-test, $P = 0.0063$ $n = 102$ platelets, median represented by black line in the violin plot. Scale bar 2 µm. **(D)** 3D rendered iso-surface image of platelets from WT and VF mice based on RI. **(E)** Changes in mean RI (unpaired two-tailed *t*-test, $P \leq 0.0001$) and dry mass (unpaired two-tailed *t*-test, $P \leq 0.0001$) of the platelets. Scale bar 1 µm, RI scales; Pink: 1.3426–1.3483, blue: 1.3484–1.3519, green: 1.3520–1.3565, red: 1.3566–1.3628. $^{**}P \leq 0.01$, $^{****}P \leq 0.0001$.

intensity (unpaired two-tailed *t*-test, $P = 0.0038$; **Figure 3B**). Platelets from infected mice had increased surface area and volume but reduced sphericity (unpaired two-tailed *t*-test all $P \leq 0.0001$; **Figure 3C**) Thus, platelets from infected mice had an increase in size as well as an altered intracellular environment and a suggestion, based on sphericity, of activation.

Similar to the VF model, we also studied changes in the cytosolic parameters. Platelets from naïve and *L. donovani*-infected mice also showed a visible difference in the RI (**Figure 3D**), with a significant reduction in higher RI based structures (unpaired two-tailed *t*-test, $P \leq 0.0001$; **Figure 3E**). Unlike VF platelets, platelets from *L. donovani*-infected mice had an increase in dry mass (unpaired two-tailed *t*-test, $P \leq 0.0001$; **Figure 3E**).

DISCUSSION

Imaging based techniques are rising in popularity with the advancement of super-resolution imaging and the amount of quantitative information concerning the functioning of the cells that can be derived from such experiments. The field of platelet biology has taken advantage of these tools and a vast array of new and exciting information relating to the changes in the internal

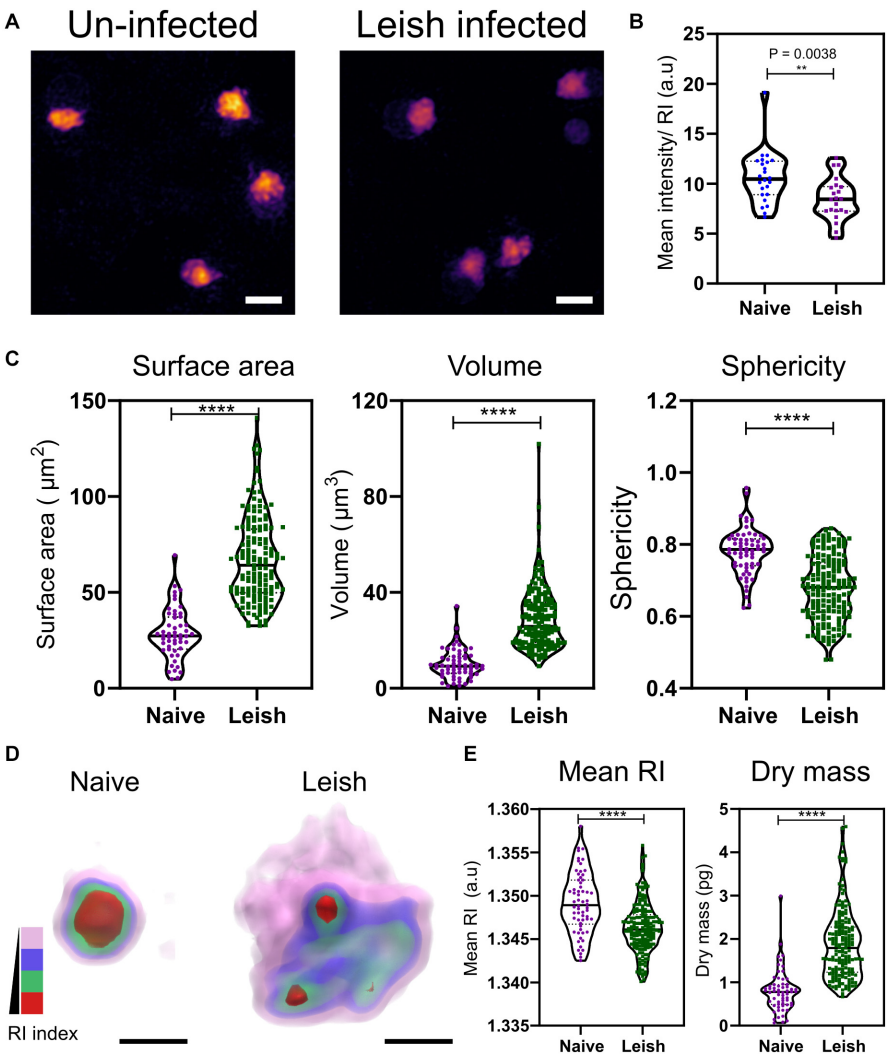

FIGURE 3 | Morphological and biophysical differences in platelets from naïve and Leishmania infected mice. **(A,B)** Max RI projections of the 3D phase images of platelets from Naïve and *L. donovani* infected mice $n = 23$ platelets. **(C)** Morphological changes seen in platelets in surface area, volume, and sphericity. $n = 62$ platelets, 10 platelets from each WT mice in study (6 mice) and $n = 172$ platelets from 17 *L. donovani* infected mice, median represented by black line in the violin plot. Scale bar 2 µm. **(D)** 3D rendered iso-surface image of platelets from naïve and *L. donovani* infected mice based on RI. Scale bar 1 µm. **(E)** Changes in mean RI (unpaired two-tailed *t*-test, $P \leq 0.0001$), and dry mass (unpaired two-tailed *t*-test, $P \leq 0.0001$) of the platelets. RI index scales; Pink: 1.3406–1.3525, blue: 1.3525–1.3621, green: 1.3622–1.3735, red: 1.3736–1.3822. $^{**}P \leq 0.01$, $^{****}P \leq 0.0001$.

structure and function of platelets or platelet proteins during activation processes or disorders has recently been produced (Poulter et al., 2015; Westmoreland et al., 2016; Knight et al., 2017; Bergstrand et al., 2019; Khan and Pike, 2020). With fluorescence based imaging, the protein of interest often requires the samples to have a fluorescent tag – either genetically modified or by immuno-labeling, to provide the contrast required for visualization. In our study, we use 3D holotomography, a RI-based imaging technique, that requires no labeling or post-isolation processing, enabling us to study alterations in the cell morphology and changes in biophysical parameter of unaltered cells or platelets in health and disease.

Obtaining enough platelets from mice to perform standard *in vitro* functional assays, such as lumi-aggregometry or western blotting, has always been significant restraint for platelet studies. As a result, researchers are often limited to a single assay for each mouse. However, the assays outlined here can be performed with a minimum volume of 10–20 µl/chamber, allowing sampling of 100–200 platelets at single cell level, sufficient to generate quantitative information relating to platelet morphology and RI/dry mass. Therefore, this imaging technique can serve as a valuable additional or complementary technique to other *in vitro* platelet function assays.

Here, we used this technique to study the morphological changes and alterations in the cellular composition of platelets directly isolated from two murine disease models. We isolated and imaged platelets from mice with either somatic mutations in JAK2, JAK2V617F, that cause MPNs or platelets from mice

with experimental VL following infection with *L. donovani*. Both of these models have characteristic alterations in their platelets, leading to either thrombocytosis or thrombocytopenia with chronic inflammation giving rise to these fatal thrombotic or bleeding disorders (Goncalves et al., 2011; Hasselbalch, 2012, 2014; Etheridge et al., 2014).

Under normal physiological conditions, the vascular endothelium continuously suppresses platelet activation via expression of ectonucleotidases, thrombomodulin, or by releasing prostaglandin I2 and nitric oxide. This is usually altered when there is an inflammatory environment or vascular injury that contributes to a prothrombotic phenotype, as seen in bleeding disorders (van der Meijden and Heemskerk, 2019). We have previously shown, using an alternative murine JAK2V617F-positive MPN model, that expression of the mutated protein in platelets did not have a significant effect on aggregation *in vitro*, and aberrant hemostasis was largely due to extreme thrombocytosis-induced acquired von Willebrand's disease and an inflamed endothelial environment (Etheridge et al., 2014). An inflamed endothelium is common in MPNs due to a chronic inflammatory environment and often leads to atherosclerosis and secondary cancers (Hasselbalch, 2012, 2014). This inflammatory environment is characterized by increases in circulating thrombomodulin, selectins and von Willebrand factor. This is turn activates the endothelial cells lining the blood vessels, leukocytes and platelets (Hasselbalch, 2014). Thus the platelets have a significant role to play in the MPN bleeding complications, often with progression to secondary complications (Hasselbalch, 2012; Etheridge et al., 2014). In our study, platelets isolated from VF mice do not have a characteristic change in morphology, but do show an increase in the mean RI and dry mass (**Figure 2**) indicating intracellular changes within the platelets, which may largely be due to platelets being primed by the inflammatory environment for further activation and function.

The larger the size of the platelets, the greater is reactivity and prothrombotic ability (Slavka et al., 2011; Machlus and Italiano, 2013). Platelets from *L. donovani* infected C57BL/6 mice were found to be much larger in size and less spherical compared to the naïve platelets (**Figure 3**), presenting a much more morphologically activated state, accompanied by changes in the intracellular content. The larger platelets were also seen in H&E staining of blood smears from infected mice (Rani et al., 2019 and Rani G et al., unpublished). The mechanism(s) underlying these changes in platelets during infection remain to be determined. The inflammatory response to *L. major* infection has previously been associated with platelet activation, release of platelet derived growth factor (PDGF) and amplification of monocyte recruitment via CCL-2 (Goncalves et al., 2011). Platelet activation is also known to alter sialylation of surface glycoproteins allowing recruitment to the inflamed liver and clearance by hepatocytes via Ashwell-Morrell Receptor (Rani et al., 2019 and Rani G et al., unpublished). Furthermore, an increase in the number of IgG-bound platelets in *L. donovani* infected mice likely underpins enhanced clearance of activated platelets, leading to severe thrombocytopenia in these models. The presence of larger platelets, as seen in our results, could also be due to newly formed platelets owing to increased turnover and changes in platelet biogenesis [Rani et al. (unpublished); and Slavka et al. (2011)].

In both models studied, we noticed a different platelet RI for the WT and naïve mice and a non-linear relationship of RI and dry mass between naïve and *L. donovani* infected platelets (**Figures 2**, **3**). We currently do not know the effect of the different platelet isolation methods and buffers (see "Materials and Methods") have on the RI of the platelets. We speculate this to be one of the reasons resulting in the RI difference. Day to day calibration of the system based on the "buffer background" is done prior to imaging which could also cause these minor alterations in the resulting RI between the two models.

Based on ODT literature, RI and dry mass are linearly proportional (Kim et al., 2016, 2017; Lee et al., 2019). In the *L. donovani* infection model, this does not seem to be the case. The naïve platelets, in the infection model, show a broad distribution of RI data sets – some with higher RI and others lower. The corresponding dry mass shows a tighter distribution of the data set. This difference is noted in both models, with the WT mice having a tighter RI range and a broader dry mass in contrast to the naïve platelets. But strangely, this occurs only in the WT and naïve platelets, while the VF and *L. donovani* infected platelets do not show this pattern. Human platelets isolated from different donors have been shown to have some variation in their morphological and cytosolic parameters and also have altered activation patterns when stimulated (Lee et al., 2019). Therefore, the differences in our results may be an inherent property of the normal, uninfected platelets that may have gone unnoticed with other platelet assays. Thus, from these two differences highlighted in our results, we can only compare and contrast RI data from within one experimental data.

Both mouse models used in our study share several hematological pathologies such as splenomegaly, largely associated with thrombocytopenia in leishmaniasis, and an inflammatory environment (Hasselbalch, 2012; Sangkhae et al., 2015; Preham et al., 2018). This inflammatory environment causes an influx of immune cell responses, where platelets can act as mediators for generating these responses (Garraud and Cognasse, 2015; Gros et al., 2015). The role of platelets in innate immunity is largely due to their capacity to internalize viruses and bacteria, release of bioactive molecules stored in their granules and interaction with other cells, i.e., leukocytes to combat a potential threat (Li et al., 2012; Ali et al., 2015). Overall, the complex nature of platelet function as either pro- or anti-inflammatory, or the platelets having a beneficial or detrimental effect is entirely dependent on the cause of the inflammation and the pathophysiology of the disease as described in the review by Gros et al. (2015). Here, using our label-free method of RI imaging, we were able to highlight that platelets isolated from our hematological and inflammatory disease models appear different in structure and size and cytosolic concentrations, compared to WT controls. Although there are some limitations in using the fluorescence-based imaging with this platform, there is more RI based information and real-time cell dynamics that can be tracked over time (Lee et al., 2019), allowing this method to be used for studying the effect of different drugs on the activation states of platelets. The technique also highlights the amount of valuable information that can be derived from only a fraction of

the platelets isolated from mice, which will aid in complementing other functional assays of platelet activation.

DATA AVAILABILITY STATEMENT

All datasets presented in this study are included in the article/**Supplementary Material**.

ETHICS STATEMENT

The animal study was reviewed and approved by the UK Home Office Animal Welfare and Ethical Review Board of the Department of Biology, University of York.

AUTHOR CONTRIBUTIONS

TS contributed to the experimental design, experimental work, imaging, data analysis, and manuscript preparation. RS contributed to the imaging and data analysis. GR contributed to the experimental work and manuscript preparation. PO'T contributed to the experimental work. PK contributed to the *L. donovani* project supervision and manuscript preparation. IH contributed to the project supervision, experimental design, and manuscript preparation. All authors contributed to the article and approved the submitted version.

FUNDING

This work was supported by grants from the Cancer Research UK (A24593 to IH) and the Wellcome Trust (WT1063203 to PK). GR was supported by a training scholarship from the Higher Education Commission of Pakistan.

ACKNOWLEDGMENTS

We thank the Biological Services Facility for care and providing the mice for the experiments and the Department of Biology, Technology Facility. Katiuska Daniela Pulgar Prieto for assistance with animal work.

SUPPLEMENTARY MATERIAL

The Supplementary Material for this article can be found online at: https://www.frontiersin.org/articles/10.3389/fphys.2020.568087/full#supplementary-material

FIGURE S1 | Four percentage PFA fixation on platelets at varying time scales. **(A–E)** Morphological and biochemical parameters affected by PFA fixation **(A)** Surface area (P = 0.3263, 0.0010, 0.0083), **(B)** Volume (P = 0.4913, <0.0001, 0.0004), **(C)** Sphericity (P = 0.1521, 0.0027, 0.0103), **(D)** RI (P = 0.4214, 0.9495, 0.6858), and **(E)** Dry mass (P = 0.7976, 0.0005, 0.0001). Paired two tailed t-test was performed for all, n = 30. RI: Pink: 1.3444–1.3525, blue: 1.3526–1.3621, brown: 1.3622–1.3719, red: 1.3720–1.3775.

REFERENCES

Ali, R. A., Wuescher, L. M., and Worth, R. G. (2015). Platelets: essential components of the immune system. *Curr. Trends Immunol.* 16, 65–78.

Assinger, A. (2014). Platelets and infection - An emerging role of platelets in viral infection. *Front. Immunol.* 5:649. doi: 10.3389/fimmu.2014.00649

Bergstrand, J., Xu, L., Miao, X., Li, N., Öktem, O., Franzén, B., et al. (2019). Super-resolution microscopy can identify specific protein distribution patterns in platelets incubated with cancer cells. *Nanoscale* 11, 10023–10033. doi: 10.1039/c9nr01967g

Blair, P., and Flaumenhaft, R. (2009). Platelet α-granules: basic biology and clinical correlates. *Blood Rev.* 23, 177–189. doi: 10.1016/j.blre.2009.04.001

Cox, D., Kerrigan, S. W., and Watson, S. P. (2011). Platelets and the innate immune system: mechanisms of bacterial-induced platelet activation. *J. Thromb. Haemost.* 9, 1097–1107. doi: 10.1111/j.1538-7836.2011.04264.x

Etheridge, S. L., Roh, M. E., Cosgrove, M. E., Sangkhae, V., Fox, N. E., Chen, J., et al. (2014). JAK2V617F-positive endothelial cells contribute to clotting abnormalities in myeloproliferative neoplasms. *Proc. Natl. Acad. Sci. U.S.A.* 111, 2295–2300. doi: 10.1073/pnas.1312148111

Flaumenhaft, R., and Sharda, A. (2018). The life cycle of platelet granules. *F1000Research* 7:236. doi: 10.12688/f1000research.13283.1

Garraud, O., and Cognasse, F. (2015). Are platelets cells? And if yes, are they immune cells? *Front. Immunol.* 6:70. doi: 10.3389/fimmu.2015.00070

Goncalves, R., Zhang, X., Cohen, H., Debrabant, A., and Mosser, D. M. (2011). Platelet activation attracts a subpopulation of effector monocytes to sites of Leishmania major infection. *J. Exp. Med.* 208, 1253–1265. doi: 10.1084/jem.20101751

Gros, A., Ollivier, V., and Ho-Tin-Noé, B. (2015). Platelets in inflammation: regulation of leukocyte activities and vascular repair. *Front. Immunol.* 5:678. doi: 10.3389/fimmu.2014.00678

Hamzeh-Cognasse, H., Damien, P., Chabert, A., Pozzetto, B., Cognasse, F., and Garraud, O. (2015). Platelets and infections - Complex interactions with bacteria. *Front. Immunol.* 6:82. doi: 10.3389/fimmu.2015.00082

Hanby, H. A., Bao, J., Noh, J. Y., Jarocha, D., Poncz, M., Weiss, M. J., et al. (2017). Platelet dense granules begin to selectively accumulate mepacrine during proplatelet formation. *Blood Adv.* 1, 1478–1490. doi: 10.1182/bloodadvances.2017006726

Hasselbalch, H. C. (2012). Perspectives on chronic inflammation in essential thrombocythemia, polycythemia vera, and myelofibrosis: is chronic inflammation a trigger and driver of clonal evolution and development of accelerated atherosclerosis and second cancer? *Blood* 119, 3219–3225. doi: 10.1182/blood-2011-11-394775

Hasselbalch, H. C. (2014). The platelet-cancer loop in myeloproliferative cancer. Is thrombocythemia an enhancer of cancer invasiveness and metastasis in essential thrombocythemia, polycythemia vera and myelofibrosis? *Leuk. Res.* 38, 1230–1236. doi: 10.1016/j.leukres.2014.07.006

Hobbs, C. M., Manning, H., Bennett, C., Vasquez, L., Severin, S., Brain, L., et al. (2013). JAK2V617F leads to intrinsic changes in platelet formation and reactivity in a knock-in mouse model of essential thrombocythemia. *Blood* 122, 3787–3797. doi: 10.1182/blood-2013-06-501452

Kent, D. G., Li, J., Tanna, H., Fink, J., Kirschner, K., Pask, D. C., et al. (2013). Self-renewal of single mouse hematopoietic stem cells is reduced by JAK2V617F without compromising progenitor cell expansion. *PLoS Biol.* 11:e1001576. doi: 10.1371/journal.pbio.1001576

Khan, A. O., and Pike, J. A. (2020). Super-resolution imaging and quantification of megakaryocytes and platelets. *Platelets* 31, 559–569. doi: 10.1080/09537104.2020.1732321

Kim, D., Lee, S., Lee, M., Oh, J., Yang, S.-A., and Park, Y. (2017). Refractive index as an intrinsic imaging contrast for 3-D label-free live cell imaging. *bioRxiv* [Preprint]. doi: 10.1101/106328

Kim, K., Yoon, H., Diez-Silva, M., Dao, M., Dasari, R. R., and Park, Y. (2013). High-resolution three-dimensional imaging of red blood cells parasitized by Plasmodium falciparum and in situ hemozoin crystals using optical diffraction tomography. *J. Biomed. Opt.* 19:011005. doi: 10.1117/1.jbo.19.1.011005

Kim, K., Yoon, J., Shin, S., Lee, S., Yang, S.-A., and Park, Y. (2016). Optical diffraction tomography techniques for the study of cell pathophysiology. *J. Biomed. Photonics Eng.* 2:e020201. doi: 10.18287/jbpe16.02.020201

Knight, A. E., Gomez, K., and Cutler, D. F. (2017). Super-resolution microscopy in the diagnosis of platelet granule disorders. *Expert Rev. Hematol.* 10, 375–381. doi: 10.1080/17474086.2017.1315302

Kullaya, V., De Jonge, M. I., Langereis, J. D., Van Der Gaast-De Jongh, C. E., Büll, C., Adema, G. J., et al. (2018). Desialylation of platelets by pneumococcal neuraminidase a induces ADP-dependent platelet hyperreactivity. *Infect. Immun.* 86:e00213-18. doi: 10.1128/IAI.00213-18

Lacerda, M. V. G., Mourão, M. P. G., Coelho, H. C., and Santos, J. B. (2011). Thrombocytopenia in malaria: who cares? *Mem. Inst. Oswaldo Cruz* 106(Suppl. 1), 52–63. doi: 10.1590/S0074-02762011000900007

Lamrani, L., Lacout, C., Ollivier, V., Denis, C. V., Gardiner, E., Ho Tin Noe, B., et al. (2014). Hemostatic disorders in a JAK2V617F-driven mouse model of myeloproliferative neoplasm. *Blood* 124, 1136–1145. doi: 10.1182/blood-2013-10-530832

Lee, S., Jang, S., and Park, Y. (2019). Measuring three-dimensional dynamics of platelet activation using 3-D quantitative phase imaging. *bioRxiv* [Preprint]. doi: 10.1101/827436

Li, C., Li, J., Li, Y., Lang, S., Yougbare, I., Zhu, G., et al. (2012). Crosstalk between platelets and the immune system: old systems with new discoveries. *Adv. Hematol.* 2012:384685. doi: 10.1155/2012/384685

Li, J., Spensberger, D., Ahn, J. S., Anand, S., Beer, P. A., Ghevaert, C., et al. (2010). JAK2 V617F impairs hematopoietic stem cell function in a conditional knock-in mouse model of JAK2 V617F-positive essential thrombocythemia. *Blood* 116, 1528–1538. doi: 10.1182/blood-2009-12-259747

Lim, J., Lee, K., Jin, K. H., Shin, S., Lee, S., Park, Y., et al. (2015). Comparative study of iterative reconstruction algorithms for missing cone problems in optical diffraction tomography. *Opt. Express* 23, 16933–16948. doi: 10.1364/oe.23.016933

Liu, Y., Chen, S., Sun, Y., Lin, Q., Liao, X., Zhang, J., et al. (2016). Clinical characteristics of immune thrombocytopenia associated with autoimmune disease: a retrospective study. *Medicine* 95:e5565. doi: 10.1097/MD.0000000000005565

Lucchesi, A., Carloni, S., De Matteis, S., Ghetti, M., Musuraca, G., Poggiaspalla, M., et al. (2020). Unexpected low expression of platelet fibrinogen receptor in patients with chronic myeloproliferative neoplasms: how does it change with aspirin? *Br. J. Haematol.* 189, 335–338. doi: 10.1111/bjh.16335

Machlus, K. R., and Italiano, J. E. (2013). The incredible journey: from megakaryocyte development to platelet formation. *J. Cell Biol.* 201, 785–796.

Moore, S. F., Hunter, R. W., Harper, M. T., Savage, J. S., Siddiq, S., Westbury, S. K., et al. (2013). Dysfunction of the PI3 kinase/Rap1/integrin aIIbb3 pathway underlies ex vivo platelet hypoactivity in essential thrombocythemia. *Blood* 121, 1209–1219. doi: 10.1182/blood-2012-05-431288

Pereira, P. M., Albrecht, D., Culley, S., Jacobs, C., Marsh, M., Mercer, J., et al. (2019). Fix your membrane receptor imaging: actin cytoskeleton and CD4 membrane organization disruption by chemical fixation. *Front. Immunol.* 10:675. doi: 10.3389/fimmu.2019.00675

Poulter, N. S., Pollitt, A. Y., Davies, A., Malinova, D., Nash, G. B., Hannon, M. J., et al. (2015). Platelet actin nodules are podosome-like structures dependent on Wiskott-Aldrich syndrome protein and ARP2/3 complex. *Nat. Commun.* 6, 1–15.

Preham, O., Pinho, F. A., Pinto, A. I., Rani, G. F., Brown, N., Hitchcock, I. S., et al. (2018). CD4+ T cells alter the stromal microenvironment and repress medullary erythropoiesis in murine visceral leishmaniasis. *Front. Immunol.* 9:2958. doi: 10.3389/fimmu.2018.02958

Prévost, N., Kato, H., Bodin, L., and Shattil, S. J. (2007). Platelet integrin adhesive functions and signaling. *Methods Enzymol.* 426, 103–115. doi: 10.1016/S0076-6879(07)26006-9

Rani, G. F., Preham, O., Hitchcock, I., and Kaye, P. (2019). Understanding the mechanisms underlying thrombocytopenia in visceral leishmaniasis. *Blood* 134(Suppl._1), 2378. doi: 10.1182/blood-2019-128133

Riswari, S. F., Tunjungputri, R. N., Kullaya, V., Garishah, F. M., Utari, G. S. R., Farhanah, N., et al. (2019). Desialylation of platelets induced by von willebrand factor is a novel mechanism of platelet clearance in dengue. *PLoS Pathog.* 15:e1007500. doi: 10.1371/journal.ppat.1007500

Sangkhae, V., Etheridge, S. L., Kaushansky, K., and Hitchcock, I. S. (2015). The thrombopoietin receptor, MPL, is critical for development of a JAK2 V 617 F-induced myeloproliferative neoplasm. *Blood* 124, 3956–3964.

Schnell, U., Dijk, F., Sjollema, K. A., and Giepmans, B. N. G. (2012). Immunolabeling artifacts and the need for live-cell imaging. *Nat. Methods* 9, 152–158.

Shin, S., Kim, K., Kim, T., Yoon, J., Hong, K., Park, J., et al. (2016). Optical diffraction tomography using a digital micromirror device for stable measurements of 4D refractive index tomography of cells. *Quant. Phase Imaging* 2:971814. doi: 10.1117/12.2216769

Shin, S., Kim, K., Yoon, J., and Park, Y. (2015). Active illumination using a digital micromirror device for quantitative phase imaging. *Opt. Lett.* 40, 5407–5410. doi: 10.1364/ol.40.005407

Slavka, G., Perkmann, T., Haslacher, H., Greisenegger, S., Marsik, C., Wagner, O. F., et al. (2011). Mean platelet volume may represent a predictive parameter for overall vascular mortality and ischemic heart disease. *Arterioscler. Thromb. Vasc. Biol.* 31, 1215–1218. doi: 10.1161/ATVBAHA.110.221788

Stanly, T. A., Fritzsche, M., Banerji, S., García, E., Bernardino de la Serna, J., Jackson, D. G., et al. (2016). Critical importance of appropriate fixation conditions for faithful imaging of receptor microclusters. *Biol. Open* 5, 1343–1350.

van der Meijden, P. E. J., and Heemskerk, J. W. M. (2019). Platelet biology and functions: new concepts and clinical perspectives. *Nat. Rev. Cardiol.* 16, 166–179. doi: 10.1038/s41569-018-0110-0

Varma, N., and Naseem, S. (2010). Hematologic changes in visceral Leishmaniasis/Kala Azar. *Indian J. Hematol. Blood Transfus.* 26, 78–82. doi: 10.1007/s12288-010-0027-1

Westmoreland, D., Shaw, M., Grimes, W., Metcalf, D. J., Burden, J. J., Gomez, K., et al. (2016). Super-resolution microscopy as a potential approach to diagnosis of platelet granule disorders. *J. Thromb. Haemost.* 14, 839–849. doi: 10.1111/jth.13269

Conflict of Interest: The authors declare that the research was conducted in the absence of any commercial or financial relationships that could be construed as a potential conflict of interest.

frontiers in Immunology

REVIEW
published: 11 January 2021
doi: 10.3389/fimmu.2020.612542

Quantitative Bio-Imaging Tools to Dissect the Interplay of Membrane and Cytoskeletal Actin Dynamics in Immune Cells

Falk Schneider[1†], *Huw Colin-York*[1,2†] *and Marco Fritzsche*[1,2,3*]

[1] Medical Research Council (MRC) Human Immunology Unit, Weatherall Institute of Molecular Medicine, University of Oxford, Oxford, United Kingdom, [2] Kennedy Institute for Rheumatology, University of Oxford, Oxford, United Kingdom, [3] Rosalind Franklin Institute, Harwell Campus, Didcot, United Kingdom

Cellular function is reliant on the dynamic interplay between the plasma membrane and the actin cytoskeleton. This critical relationship is of particular importance in immune cells, where both the cytoskeleton and the plasma membrane work in concert to organize and potentiate immune signaling events. Despite their importance, there remains a critical gap in understanding how these respective dynamics are coupled, and how this coupling in turn may influence immune cell function from the bottom up. In this review, we highlight recent optical technologies that could provide strategies to investigate the simultaneous dynamics of both the cytoskeleton and membrane as well as their interplay, focusing on current and future applications in immune cells. We provide a guide of the spatio-temporal scale of each technique as well as highlighting novel probes and labels that have the potential to provide insights into membrane and cytoskeletal dynamics. The quantitative biophysical tools presented here provide a new and exciting route to uncover the relationship between plasma membrane and cytoskeletal dynamics that underlies immune cell function.

Keywords: plasma membrane, actin cytoskeleton, fluorescence correlation spectroscopy, fluorescence recovery after photobleaching, immune cells, metal induced energy transfer, volumetric imaging, quantitative imaging

OPEN ACCESS

Edited by:
Wei Chen,
Zhejiang University, China

Reviewed by:
Jon C. D. Houtman,
The University of Iowa, United States
Christoph Wülfing,
University of Bristol, United Kingdom

***Correspondence:**
Marco Fritzsche
marco.fritzsche@kennedy.ox.ac.uk

†The authors have contributed equally to this work

Specialty section:
This article was submitted to T Cell Biology, a section of the journal Frontiers in Immunology

Received: *30 September 2020*
Accepted: *23 November 2020*
Published: *11 January 2021*

Citation:
Schneider F, Colin-York H and Fritzsche M (2021) Quantitative Bio-Imaging Tools to Dissect the Interplay of Membrane and Cytoskeletal Actin Dynamics in Immune Cells. Front. Immunol. 11:612542. doi: 10.3389/fimmu.2020.612542

INTRODUCTION

Life is dynamic. Cellular components are in constant motion bridging various time- and length-scales. This includes the plasma membrane and the cortical actin cytoskeleton, which form a dynamic interface between the cell and its environment, working together to control cellular signaling and morphology as well as to maintain the mechanical integrity of the cell. It is becoming increasingly clear that the dynamics of the cortical actin cytoskeleton and the plasma membrane are intimately linked to immune cell function, playing a critical role in, for instance, the regulation of receptor organization, granule section, and specific cytoskeletal protrusions (1–4). Despite their individual importance, how both the membrane and the cortical actin cytoskeleton dynamics are coupled, and how feedback between the two structures shapes their interplay in immune cells remains unknown. Crucially, to understand the functional significance of this interplay,

measurement techniques are required that allow the dynamics of actin and membrane to be captured simultaneously, enabling their direct correlation in both space and time.

Actin-Membrane Interactions at a Glance

The interactions between the membrane and the actin cortex are numerous and complex and have been the subject of intense research (5, 6) (**Figure 1A**). Underlying the plasma membrane the actin cortex exists as a densely cross-linked meshwork of filamentous actin (F-actin) formed by the polymerization of globular actin (G-actin) monomers undergoing constant turnover on the second time-scale (7). The dynamic architecture of the actin cortex is governed by two primary modes of F-actin polymerization driven by either Arp2/3 or formin nucleation leading to constantly varying actin mesh-sizes from tens of nanometers to microns (8). The dynamic nature of the cortex as well as its mechanical plasticity is largely mediated by a variety of myosin motors that cross-link individual filaments and induce active mechanical stress within the network (8).

Biochemically linking the actin cortex and the plasma membrane are a series of specific protein-protein and protein-lipid interactions (9). One of the most important membrane

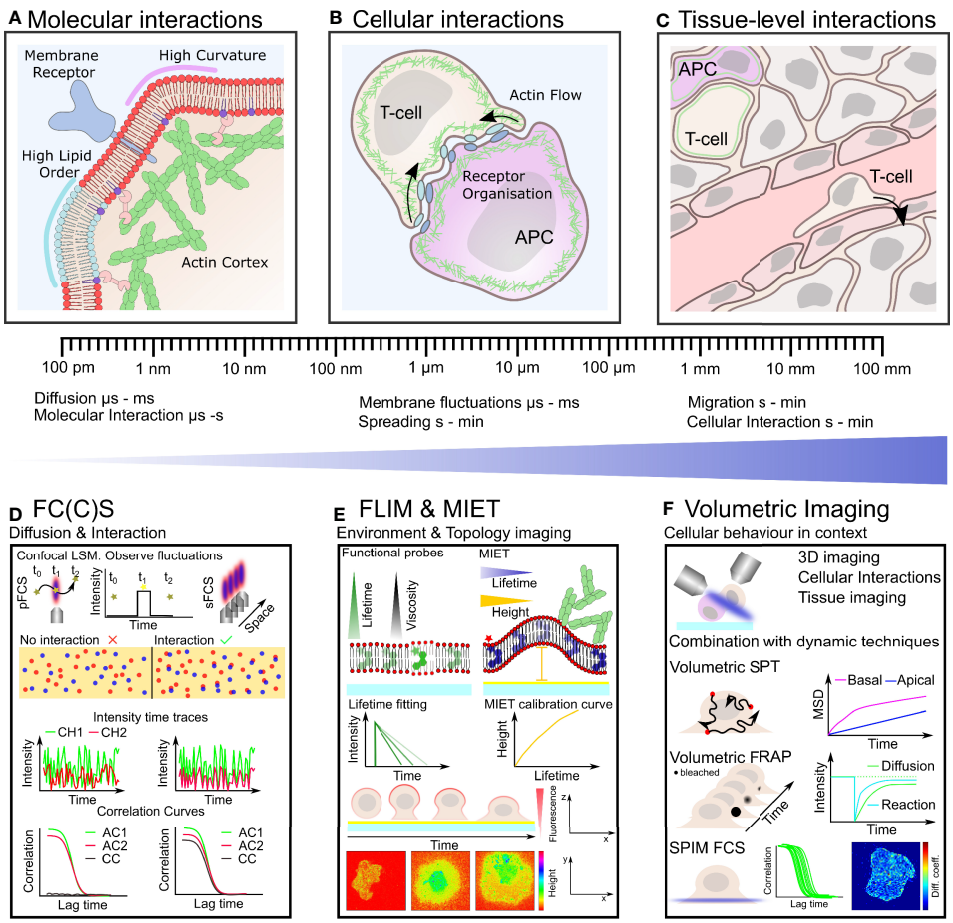

FIGURE 1 | Plasma membrane organization and actin cytoskeletal dynamics are intrinsically linked to immune cell organization and function over many length- and time-scales **(A–C)**. Techniques with the ability to quantify simultaneous dynamics present an exciting route to understand the interplay of cortical actin and plasma membrane in immune cells **(D–F)**. **(A)** On the nano-scale actin filaments are turning over and binding the plasma membrane influencing its organization which in turn impacts on actin organization and the distribution of receptors, lipids and other membrane constituents. **(B)** Defined actin and membrane flows, organization and their integrity are crucial for cell-cell contacts such as during immunological synapse formation on the meso-scale. **(C)** Within tissue, immune cells must navigate through biophysically diverse environments, relying on both a dynamic plasma membrane and actin cytoskeleton to carry out their function. **(D)** Fluorescence correlation spectroscopy (FCS) and FCCS measure fluctuation of fluorescently labeled molecules diffusing through the focus of a confocal microscope. Typical transit times range from µs to hundreds of ms highlighting the large dynamic range and unrivaled temporal resolution of these techniques. Auto-correlation (AC) of the intensity traces (in two spectral channels CH1 and CH2) allows to calculate diffusion coefficients and interactions (cross-correlation, CC). **(E)** Fluorescence lifetime imaging (FLIM) allows to monitor changes in fluorescence lifetime. Acquiring FLIM images typically takes seconds to minutes. Functional probes can change their lifetime in accordance to their environment sensing, for example, viscosity. In metal induced energy transfer (MIET) the lifetime change is correlate with the distance to the surface and allows the recalculation of heights yielding the membrane topology, for example, during cell spreading. **(F)** Volumetric imaging using, for instance, a light-sheet approach allows to image the cellular context in 3D at moderate time resolution (down to seconds). Combination with the dynamics techniques, single particle tracking (SPT), fluorescence recovery after photobleaching (FRAP), and FC(C)S represents a promising route for mapping plasma membrane and actin dynamics in the full physiological setting by correlating their time- and length-scales.

components mediating this interaction is the glycolipid phosphatidylinositol-bisphosphate, PIP2. By binding the ERM (ezrin, radixin, and moesin) proteins, an actin binding family of proteins, PIP2 provides a linkage between cytoskeleton and membrane (**Figure 1A**). In addition to the ERM proteins, WASP and WAVE, key regulators of Arp2/3 driven actin polymerization, are also able to bind PIP2 in the membrane, leading to active polymerization of F-actin at the plasma membrane (6). Notably, the conserved diversity of specific linkages between cortex and membrane is indicative of the importance of the tight coupling of these structures for their function within the cell.

In addition to the specific molecular interactions between the plasma membrane and actin cortex, there are a number of more general biophysical interactions that have been well characterized *in vitro* (10), for example, the local charge of the membrane has been shown to influence actin binding (11). Furthermore, curvature introduced by the polymerization of the actin cytoskeleton during the formation of specific protrusions can influence the diffusion and distribution of membrane proteins (12, 13). Conversely, membrane curvature induced by the physical membrane microenvironment can lead to actin polymerization (14). Local changes in actin polymerization can also induce changes in the rate and diffusion mode of lipid and protein components as well as the membrane tension (15–18). Crucially, membrane composition, dynamics, and organization influence the underlying actin cytoskeleton. Similarly, the dynamics and architecture of the actin cytoskeleton has been shown to influence the plasma membrane (19). Therefore, the complex interplay between membrane and cortical cytoskeleton makes assessing causal links challenging, highlighting the unmet need for techniques that allow the dynamics of both components to be quantified simultaneously in space and time.

Actin-Membrane Interactions in Immune Cells

Many stages of the immune response, for example, antigen recognition, rely on the integration of information by immune cells from their environment, often involving the formation of highly specialized cell-cell contacts, such as the immunological synapse (IS) that forms between T-cells, B-cells, and antigen presenting cells (APCs) (**Figure 1B**). At these contacts, immunological signaling is initiated and propagated *via* the interactions of a wide array of molecules, occurring on and in the proximity of the plasma membrane. Owing to this, the dynamics of both the plasma membrane and the underlying actin cytoskeleton have a profound impact on the organization and dynamics of crucial signaling molecules. The process of immune cell activation spans a range of time- and length-scales starting with nano-scale reorganization and receptor engagement (sub-second), actin polymerization driven retrograde flow (seconds), to micron-scale cellular activation, spreading, and cytokine secretion (up to hours) (20–22).

During T-cell activation and IS formation, one of the key steps in the adaptive immune response, there has been increasing interest in the role of specific cytoskeletal protrusions in the initiation and orchestration of early T-cell signaling at the plasma membrane (23–25). Microvilli at the T-cell surface have been shown to provide an efficient means of environment scanning, while association of ERM proteins to the plasma membrane interface has been shown to lead to the accumulation of signaling molecules at microvilli (23, 24, 26). Following T-cell receptor (TCR) triggering, the T-cell undergoes a dramatic morphological change driven by the rapid polymerization of F-actin. This results in the formation of an increased contact area between the two cells, which is characterized by the retrograde flow of actin filaments within a lamellipodial structure at its periphery as well as a ramified actin network at its center (27). Crucially, TCRs are trafficked in coordination with the F-actin flow toward the center of the IS and the continued flow of actin has been shown to be necessary for continued activation, sustaining PLCγ1 signaling (28–30). Notably, once the IS has formed, recent evidence suggests that tension generated by specific dynamic actin structures influence the symmetry and lifetime of the IS (31).

In contrast to its polymerization, the depletion of actin has also been shown to play a role in immune cell function. Targeted killing by cytotoxic T lymphocytes requires the precise spatio-temporal control of actin depletion with recent studies pointing to a complex and intricate mechanism, whereby the density of the cortical actin underlying the membrane is tuned by the interaction of the kinase PIP5K and the loss of the charged PIP2 lipid (32, 33).

Like the cortical actin cytoskeleton the plasma membrane is a dynamic structure, constantly in motion and continuously reorganizing (34, 35). The presence of defined domains or rafts (tens of nanometer in diameter) has been evoked to explain a number of phenomena, including lateral heterogeneity of the plasma membrane and, for example, the non-random distribution of membrane proteins on the cell surface (35–38). Along these lines, the reorganization of immune receptors by specific incorporation into such structures has been described (39–41). This is based on a biophysical property of the membrane and the proteins themselves: proteins can exhibit a preference for different lipid environments preferring, for instance, a densely packed lipid environment (liquid ordered phase, highly viscous) enriched in saturated lipids and cholesterol (42, 43). In contrast, other proteins can prefer the liquid disordered membrane environment, rather associating with loosely packed, unsaturated lipids resulting in a low viscosity environment. This could act as means of increasing interaction likelihood and forming signaling platforms (44, 45). The degree of order and the viscosity of the membrane are primarily tuned by the cholesterol content and in addition likely by its specific interactions with proteins and lipids (46–48). Intriguingly, the attachment of actin filaments to the membrane has been seen to influence membrane organization, resulting in the formation of ordered domains (49, 50), providing a potential mechanism for actin to indirectly influence membrane protein organization.

As is evident, studies of the dynamics of the cytoskeleton and membrane have led to important insights into the function of immune cells (51–53). Despite this, there are only a limited number of studies that have attempted to address the correlated biophysical and biochemical dynamic mechanisms whereby membrane and actin work together in immune cells. Recent advances in correlative imaging such as the combination of super-resolution microscopy and electron microscopy have allowed for detailed insights into

structural links between plasma membrane and cortical actin organization (54–56). However, these approaches only allow snapshots of a constantly evolving structure and thus do not allow the dynamic interplay to be followed live, and therefore make assessing causality challenging. Furthermore, little is known about how these interactions influence the behavior of cells in more complex tissue environments or in their full physiological setting, with our knowledge often restricted to *in vitro* single cell studies (**Figure 1C**). This has primarily been due to a lack of accessible technologies with sufficient temporal (< ms binding and transport events) and spatial resolution (single proteins on the order of nanometres can effect changes on cellular level beyond tenth of micrometers) to assess the correlated dynamics of the plasma membrane and the actin cytoskeleton without perturbing the system. In addition to this, such lack of technology has been confounded by a lack of membrane and actin probes that can operate at physiological conditions and offer reliable performance within the cellular environment.

Here, we review recent advances in both dynamic measurement techniques and actin/membrane probes that have not yet been widely applied to study immune cells. In our view, these methods present a significant opportunity to address the complex interplay between these two systems crucial to the immune response by simultaneous quantification of both membrane and actin dynamics.

FROM FLUORESCENCE IMAGING TO QUANTIFICATION OF DYNAMICS

Live-cell fluorescence imaging is the method of choice to understand the behavior of dynamic biological processes owing to the specificity of labeling structures of interest and the minimal invasiveness of the approach. Observing events crucial to the immune response occurring in live cells has long been performed by employing fluorescence microscopy with confocal and total internal reflection fluorescence (TIRF) time-lapse imaging due to their optical sectioning capabilities yielding key insights into the dynamic nature of these processes (57, 58). This approach has revealed, for example, the formation and trafficking of T-cell receptor clusters (21, 59), which is crucial for initiation and continuation of signaling and has been shown to be strongly regulated by the dynamic interplay of the membrane and cortical actin cytoskeleton flows (60, 61). Despite their success, imaging alone restricts the level of quantitative information that can be extracted from the biological system of interest, for instance, due to the limited time resolution of time-lapse imaging acquisitions (tens of ms to s).

An alternative quantitative route to assessing transient processes such as cellular reorganization driven by molecular diffusion, binding-kinetics, or flow has been the use of dynamic techniques such as single particle tracking (SPT), fluorescence recovery after photobleaching (FRAP), or fluorescence fluctuation spectroscopy (FFS) approaches. For a detailed technical description, we refer the reader to (62–64). In immunology, these traditional techniques and their advancements have, for instance, been used to investigate the diffusion properties of key signaling molecules such as BCR, CD1d, TCR, CD45, or Lck in live cells (65–74).

Fluorescence Fluctuation Based Approaches to Assess Simultaneous Dynamics

The spatial heterogeneity across microns along with fast molecular interactions within the cell membrane represent a challenge to all dynamic techniques which rely on maintaining single molecule sensitivity in the crowded cellular environment. Similar to fluorescence time-lapse imaging FRAP and SPT are conventionally limited to resolving processes in the ms time regime. Using fluctuation based techniques such as fluorescence correlation spectroscopy (FCS) offers unmatched temporal resolution (down to ns) to cover the range from very fast molecular binding dynamics (μs) to motion of large protein complexes in the membrane (hundreds of ms). Unfortunately, the spatial resolution remains diffraction limited (~200 nm). Thus, inherently one will average many molecular interactions missing precise details on dynamics and potential sub 100 nm spatial heterogeneity which could be functionally important, for instance, during receptor-ligand engagement. The combination of stimulated emission depletion (STED) super-resolution microscopy with FCS has proven itself as a valuable remedy and a tool to assess nano-scale diffusion directly at the relevant spatio-temporal scales (75, 76). It has revealed a vast heterogeneity in diffusion behaviors of membrane constituents caused by interactions with lipid domains, transmembrane proteins, or the cortical actin cytoskeleton (16, 17, 77). While STED-FCS offers very high spatial resolution in living specimens (<50 nm), it is limited by comparatively high light exposure, requires dedicated equipment (depletion beam), and necessitates special dyes (75).

By sampling not only a single point, but rather a linear or circular region, scanning fluorescence correlation spectroscopy (sFCS) studies offer not only increased statistical power over conventional FCS but also limited phototoxicity (78, 79), and allow spatial heterogeneities in molecular diffusion dynamics to be accounted for (**Figure 1D**). The increased statistical power of sFCS can be exploited to decipher the diffusion mode of the molecule of interest (determining if a molecule undergoes free Brownian or hindered diffusion (80) due to nano-scale interactions). On the one hand, changes in diffusion behavior can initiate signaling pathways and on the other hand can be indicative of a cellular state such as activation (81, 82). Similar to STED-FCS, the statistical analysis of sFCS data can yield details of dynamic molecular organization but notably does not rely on any special equipment or dyes and can be performed on any turn-key confocal laser scanning microscope (79, 80). Critically, two-color scanning fluorescence cross-correlation spectroscopy (sFCCS) data can be used to characterize the dynamics of two species of interest, exploring their interplay in detail (83–86) (**Figure 1D**). Super-resolved (STED) cross-correlation studies have not yet been achieved, but in combination with beam scanning bare potential to uncover short-lived interactions (87, 88). Together with harnessing the statistical power of scanning approaches, we anticipate that the advances in fast photon-counting acquisitions,

high-count rate FCS and thus fast photon filtering may pave the way to the realization of such techniques (89, 90). Cross-correlation studies offer a unique opportunity to quantify cytoskeletal and membrane dynamics simultaneously, for example, probing the dynamic interactions between signaling molecules at the plasma membrane and the flow of the actin cytoskeleton during synapse formation, allowing cross-correlation on short (μs to ms) time-scales. Such correlated, simultaneous acquisitions represent a promising way to dissect causation and may decipher when the actin cytoskeleton is driving the membrane organization and vice versa.

Imaging larger regions allows for the mapping of diffusion across space and delivers increased spatial information at the expense of temporal resolution (> ms). Both TIRF and single-plane illumination (SPIM) schemes have been combined with camera based FCS acquisitions yielding similar and even larger statistics compared to sFCS (91–93). Crucially, these techniques provide subcellular or cellular imaging, contextualizing the dynamic measurements and allowing routine correlation with specific compartments of the cell. Expanding such approaches using image mean squared displacement (iMSD) analysis can even yield insights into the diffusion modes with a statistical power similar to STED-FCS and sFCS (94, 95). For camera based acquisitions the frame time (of about 1 ms minimum) represents the most common bottleneck for resolving fast diffusion (96). Given recent advances in camera technology this will likely not pose a limitation for much longer. For example, interferometric scattering (iSCAT) microscopy, which relies on collecting scattered light from the sample rather than fluorescence emission, allows frame rates of multiple kilo Hertz covering most of the range of dynamic processes in biology (97–99).

Exploiting Fluorescence Lifetime to Measure Dynamics and Topology

The time a fluorophore spends in the excited state is termed fluorescence lifetime and can be used as an additional means for introducing contrast in fluorescence microscopy with the fluorescence lifetime strongly depending on the environmental conditions and fluorophore properties (62). The unrivaled temporal resolution of fluorescence fluctuation approaches offer a promising route to decipher lateral membrane organization. Yet, biology operates in all three spatial dimensions, for example, actin polymerization causing plasma membrane deformations, and the aforementioned methods are largely blind to changes in axial organization. In the following, we discuss a possible remedy exploiting fluorescence lifetime modulation.

The recent advances in commercially available fluorescence lifetime imaging (FLIM) platforms enable fast acquisitions (few seconds per frame) and easy access to this microscopy modality (100). Typically, fluorescence lifetime information is used as an intrinsic method to generate contrast in unlabeled samples (using auto-fluorescence) or in conjunction with Foerster resonance energy transfer (FRET), where the lifetime shortening of the fluorescence donor is used to calculate the distance between two fluorochromes (donor and acceptor) revealing molecular interactions or conformational changes (101) (**Figure 1E**). A versatile variation of FRET makes use of the lifetime and fluorescence quenching abilities of thin metal films on the glass coverslip. In metal induced energy transfer (MIET), the lifetime can be used to calculate the height (distance from the quenching surface) of a fluorophore with nanometer precision across a range of 0-150 nm (102) (**Figure 1E**). The dynamic range and localisation precision can be tuned by the coating material (most commonly gold and more recently graphene) (103–105). MIET displays a great opportunity to explore membrane topology and curvature (106), for example, in common T cell surface interaction studies using plasma membrane markers, as has been applied to study the epithelial-to-mesenchymal transition of epithelial cells (107). This becomes even more powerful when combined with two-color labeling (108, 109), allowing the simultaneous spatio-temporal quantification of the actin cortex and plasma membrane topology, which may elucidate microvilli structures and allow axial mapping of segregation and IS organization (109). Specifically, it could be used to differentiate actual protein clusters from axially stacked molecules (as in microvilli). MIET can be combined with FCS (or rather its cousin fluorescence lifetime correlation spectroscopy) allowing for height dependant dynamic measurements, giving the opportunity to separate receptor dynamics proximal and distal from the surface within one measurement in a few seconds, allowing key insights into the mobility of receptors in the vicinity of specific actin structures (110). As a further extension, the combination of fluorescence lifetime imaging with functional probes paves the way for some exciting applications, whereby membrane topology can be correlated with other readouts, such as membrane tension, curvature, or order (see below).

Fast Volumetric Imaging and Its Combination With Dynamic Techniques

The aforementioned approaches give highly detailed insights on fast time- and short length-scales. Nevertheless, the actin cortex plasma membrane interplay also affects larger-scale cellular dynamics such as pushing/pulling of the membrane, cell migration and sampling of the immediate surroundings (see introduction) (**Figure 1C**). The investigation of these processes necessitate tools that are able to operate in in all three dimension (3D), capturing the complex geometries and topologies of cellular and multicellular samples. In biology, 3D (volumetric) imaging has typically been achieved using axial scanning confocal microscopy, and more recently using super-resolution techniques such as 3D-SIM. Unfortunately, such techniques are often restricted to relatively long (several seconds to minutes) scan times, limiting their application to slowly evolving biological systems. To investigate transient processes in a more physiological setting (compared to a planar coverslip), great advances in volumetric and *in vivo* imaging have been made, primarily based on the use of light sheet technologies, allowing for rapid 3D acquisition (111–116) (**Figure 1F**). These volumetric imaging approaches present an opportunity to overcome a long-standing issue for the investigation of plasma membrane and actin cortex interactions in lymphocytes such as T-cells. Typically, due to restrictions imposed by conventional imaging methods, specific activation is achieved by replacing the antigen presenting cell by a coverslip coated with an activing molecule or a supported lipid

bilayer presenting target molecules (117, 118). This approach has led to a great number of important insights into immune cell biology, yet it omits a large proportion of the biological complexity and three-dimensional geometry present within the physiological interactions between immune cells and target cells. Consequently, the opportunity to investigating plasma membrane and actin cortex interactions in physiological geometry using volumetric imaging is likely to yield great insights (33, 119, 120).

Crucially, instead of acquiring time-lapse imaging alone, combing the aforementioned dynamic techniques such as FCS, FRAP, or SPT with light-sheet imaging has the great advantage of providing spatial context for the observations (121). Notably, in contrast to FCS, the FRAP method can not only extract the dynamics of one species of interest, but can also quantify reaction processes, such as the binding of actin monomers within the actin cortex (122). The combination of FRAP with volumetric imaging therefore represents an exciting opportunity to correlate diffusive processes, for example, at the plasma membrane with the reaction driven turnover of the actin cortex beneath. Such technologies will likely be key in providing insights into the correlated dynamics of immune cell membrane and actin cytoskeleton within physiologically relevant environments (123).

All these techniques and ideas, of course, rely on appropriate and non-perturbing labeling strategies. Excitingly, a large variety of actin and membrane labels are now available.

Labels and Probes for Quantification of Plasma Membrane Dynamics

A variety of approaches can be chosen to label the plasma membrane. Broadly speaking, labels can be divided in specific labels, binding to or mimicking a certain lipid, and non-specific labels, displaying usually hydrophobic compounds, which insert into the membrane. The former can be used to study a specific lipid or pathway, the latter as a general membrane label.

Non-specific labels such as DiO or DiI have been around for decades and have even been used for *in vivo* cell tracking (124, 125). They conveniently incorporate quickly into the membrane by incubation alone which works well with model membranes but can require optimisation for live-cell membrane staining (126). Homogeneous membrane labeling can also be achieved using various other commercial compounds such as the CellMask™ dyes (Life Technologies). More recently, the MemBright dyes were developed allowing for higher photo-stability, lower working concentration and super-resolution microscopy applications (127). Alternatively, specific labels can be used to mimic the structure of a lipid or membrane constituent. This can be a lipid modified with an organic dye, a protein domain specifically binding to a lipid or even an antibody (126, 128). Labeled lipid analogs have enabled insightful studies of the dynamic nano-scale organization of the membrane (76, 77, 87). Nevertheless, due to the comparable size of dye and lipid it cannot be excluded that the analog does not exactly represent the native lipid. An important constituent of the plasma membrane with an abundance of about 30%–40% is cholesterol (35, 46). A variety of probes and cholesterol binding proteins are available (47, 129), however how cholesterol is distributed laterally and axially in the plasma membrane remains under heated debate.

It should be noted that fluorescent WGA conjugates are commonly used to stain the plasma membrane. This protein displays a lectin and rather binds the membrane adjacent glycocalyx thus spatial variations can occur within one cell and definitely when comparing different cell types (127). Some proteins have specific domains to interact with lipids. Such proteins can be tagged with a fluorescent protein and in this way be engineered to become a lipid reporter. These are convenient probes as the cells do not require any further labeling, but overexpression of such reporters may sequester the native lipid species, infer with endogenous signaling and membrane binding and lipid species specificity is often modulated by multiple components. Lipid binding domains include C1-domain (DAG), C2-domain (phospholipids), FYVE- and PX-domain (PI3P), PH-domain (phosphoinositide polyphosphates), and Annexin V (PS) (128, 130, 131).

A variety of compounds exists that not only label the membrane but also report on its properties (environment-sensitive dyes), known as functional probes. Polarity-sensitive dyes, for example, change their fluorescence properties depending on the local order (molecular packing, accessibility of the hydrophobic core to water from the exterior medium) of the surrounding membrane (132, 133). This results in quantifiable changes in fluorescence spectra or lifetimes and can be combined with super-resolution microscopy (134, 135). Other probes sense different membrane properties such as tension or viscosity (136, 137). Work with probes that change their spectrum upon changes in the local environment is experimentally convenient as it only requires acquisition in two optimized spectral channels (even though spectral detection is preferred) (138). Unfortunately, these dyes typically have a very broad emission spectrum that makes it difficult to simultaneously quantitatively image another structure such as actin in addition. Therefore, we anticipate again that lifetime-based probes and acquisitions may show better sensitivity (139, 140).

Approaches for Quantifying F- and G-Actin Dynamics

Visualizing the dynamics of the actin cytoskeleton in living cells remains challenging, largely owing to the rapid turn-over of the molecular components of the cytoskeleton. Two main strategies exists for the visualization of actin within living cells: either genetic approaches modifying G-actin monomers directly with a fluorescent protein or a self-labeling tag (SNAP/Halo), or by using a variety of indirect filamentous F-actin binding labels, for example, the short peptides Lifeact or F-tractin, which are additionally modified with a fluorescent protein (141–143). As with lipid labeling, care must be taken to use the appropriate strategy for the desired dynamic output, for instance, FRAP or FCS studies assessing actin diffusion must utilize a direct G-actin approach to ensure that the measured diffusion is that of G-actin and not the indirect actin probe e.g. Lifeact-filament binding. A recent versatile approach is the visualization of membrane proximal F-actin by a membrane-bound F-tractin reporter (MPAct) as this directly reports on plasma membrane cortex interactions (144).

This enables to investigate actin cortex remodeling in proximity of the membrane, which could yield novel insights into actin-rich protrusions and their dynamic reorganization during T-cell activation. Labeling F-actin in live cells can also be performed with a small organic molecule, SiR-actin (143). This is derived from a toxin and has the advantage that it can simply be added to the cell of interest, is cell permeable and can readily be used with super-resolution STED microscopy (145). Because of its mode of binding to actin filaments, it may perturb native actin dynamics. A rather recent approach displays the use of anti-actin nanobodies (Chromotek) (146–148) or direct delivery of mRNA encoding for labeled Lifeact with certain advantages for primary cells (IBIDI). In immunology both Lifeact and F-tractin have been widely applied to visualize F-actin dynamics (141, 149). More recently, Lifeact has also been implicated in changing endogenous actin dynamics (150–152). As with any secondary labeling, careful optimisation and controls are necessary. When investigating F-actin a comparison with a (fixed) phalloidin stain can serve as a control.

Common to all labeling strategies applied to fluorescence microscopy in living cells should be the use of probes that do not disturb the native behavior of the tagged molecule and do not influence the biological system. As mentioned above, lipids and the attached fluorescent dyes are of a comparable size, and thus measures should be taken to ensure that the lipid behaves as its native counterpart. Often a variety of chemical structures need to be screened in order to optimize labeling of a target molecule (i.e. signaling function, cellular localisation, molecular interactions and so forth need to be preserved and checked) (77, 129). Similar issues arise with the use of fluorescent proteins which can sterically hinder their target protein or artificially cause oligomerisation (153). Therefore, it is advisable to use flexible linkers and trial multiple labeling strategies, for example, C- and N-terminal tagging (154, 155). Overall, we would like to emphasize that controls ensuring the preserved function are of the utmost importance.

Perturbation Studies Using Biochemical- and Photo-Manipulation

Specific labeling of molecules allows the membrane or the cytoskeleton to be studied in different physiological settings. A common additional step of the analysis is to perform perturbations, disturbing the steady-state of the actin assembly or membrane structure or even the actin-membrane interplay. By systematically perturbing different components of the system independently, the impact of each on the signaling and function within the living cell can be inferred and key-components, for example, as drug targets be identified.

Perturbations at the plasma membrane are commonly performed by altering the lipid composition. For transient changes, lipid species can simply be fed but recent evidence shows that the cells quickly counteract this to preserve the biophysical properties of the membrane (156). More commonly, certain membrane constituents are depleted. For instance, cholesterol which is a major component of the plasma membrane, playing an important role in signaling, and is proposed to be the major organizer of nanodomains aka rafts and has a profound effect on the overall biophysical properties such as viscosity and rigidity of the plasma membrane is a common target (46, 157). Treatments with cholesterol oxidase or methyl-β-cyclodextrin are routinely used to deplete cholesterol directly at the plasma membrane (158) for studying fast time scales such as seconds to minutes. Alternatively, drugs such as statins which interfere with cholesterol synthesis in the cell enable investigations of longer time scales up to hours and days (35). In that way, changes in cellular function, membrane organization or signaling upon variations in cholesterol content can be probed (77, 159). Analogously the role of sphingomyelin can be studied by treating the cell with sphingomyelinase or drugs such as fumonisin B1 or myriocin, respectively (35, 47, 77, 160).

Similarly, the actin cytoskeleton and its turnover can be targeted with various drugs or genetically modified (161, 162). For instance, Latruncullin B along with Cytochlasins or Phalloidin can be used to rapidly block F-actin polymerization (163), specifically inhibiting the addition of new actin monomers to the barbed end of F-actin (27, 28, 163). In contrast, Jasplakinolide can be used to stabilize actin filaments and promote polymerization (2, 164). Other drugs can be used to tune the cortex structure by influencing the nucleation of F-actin. For example, CK666 can inhibit actin branching by binding to Arp2/3 which can in turn be used to study the influence of the cortex organization and ultra-structure on the nano-scale diffusion behavior within the membrane (16, 165, 166). Furthermore, the formin inhibitor SMIFH2 can be used to remodel actin filaments and cortex structure (167, 168). In addition, a number of drugs can be used to target myosin molecular motors that drive stress generation within cortex. Specifically, both blebbistatin (169), an inhibitor of myosin II ATPase activity, and the rho kinase inhibitor Y27632 (170), are commonly used to perturb the ability of myosin II to actively generate stress within the cortex.

While these studies provided profound insights, for example, into actin reorganization during T-cell activation (27, 168), such perturbations using small molecules and enzymes affect the cell as a whole and can have unwanted side effects: For example, SMIFH2 has recently been indicated to inhibit myosins in addition to formins (171). Because of this, care needs to be taken when interpreting their effect on the structure or process of interest. A remedy to looking at global changes may come with the introduction of more photo-caged compounds or photo-activatable proteins, offering the potential for spatio-temporal control of perturbations (172–174). In addition, model systems such as cell-derived vesicles offer more control but do not allow to measure a living system (17, 35, 175).

DISCUSSION AND FUTURE PERSPECTIVES

The communication of immune cells with their environment, other immune cells and target cells involves a diversity of complex receptor-ligand interactions. These interactions all take place within the context of the plasma membrane and the underlying actin cortex. Consequently, their dynamics are intimately linked to the biophysical properties of both the membrane and the actin cytoskeleton and are constantly influencing one another. In this review, we have sought to highlight tools and technologies that present exciting opportunities to uncover the correlated dynamics

of the plasma membrane and the cortical actin cytoskeleton at the immune cell interface for the first time, harnessing the power of simultaneous acquisitions. In particular, the presented methodologies provide a route to pick apart the key determinants of actin-membrane dynamics, unraveling the causal mechanistic relationships between the two systems. Crucially, these technologies operate across a wide range of length- and time-scales, allowing the investigation of nanoscale interactions on the sub-millisecond time scale up to large scale whole-cell measurements using volumetric imaging. Armed with these new technologies, immunologists can address key questions regarding the interactions of molecules on or in the proximity of the plasma membrane. The ubiquity of membrane interactions in immune cell functions means these techniques have the potential to provide insight into a wide range of immunological cell types, in both the adaptive and innate immune response.

As detailed, these new technologies together with novel functional probes allow the assessment of important biophysical parameters such as lipid order, charge, viscosity, and membrane tension. Many of these parameters have been implicated in immune cell function, thus their systematic probing using these newly available tools is timely (176–178). Coupled with established immunological methods, such as fluorescence-activated cell sorting (FACS), these techniques provide a powerful route to better understand the function of a wide range of immune cells.

To maximize the gains from the presented techniques, they must be applied at the appropriate time- and length-scales. FCS, for instance, operates at the µs to ms time scales and sub-micron spatial-scales, and FRAP rather on ms to s and on micron scales. MIET offers high sensitivity in the axial direction, but remains diffraction limited laterally, and temporal resolution is limited by the sample signal and lifetime acquisition (~s). Volumetric imaging can be extremely rapid, but in most cases cannot surpass the diffraction limit in spatial resolution. 3D-SIM is promising in the regard of isotropic sub-diffraction resolution but sacrifices temporal resolution (179, 180). Therefore, care needs to be taken to answer the right questions with the right tools. In addition to this, as discussed, probes and labels should be chosen such that they maximize the potential of the applied technique, for example, in FCS, dyes with a high molecular brightness and high photo-stability are desirable, whereas dyes utilized for FRAP should allow for efficient photobleaching. For MIET, fluorescent dyes showing a single exponential lifetime decay curve are desirable to allow for more straightforward reconstruction of the topological features from the quenched lifetimes. In addition, the labeling density should be considered: SPT, for example, can only be applied in the case that single molecules (single emitters) can be tracked, whereas FRAP and FCS can operate over a much wider range of molecular densities. Lastly, as for any multi-color microscopy experiments, the emission spectra and the possible overlap of the utilized dyes should be taken into account. Especially for dynamic techniques spectral bleed-through can result in the measurement of false positive interactions.

While these techniques present exciting opportunities for single cells and subcellular context, future work should focus on extending the capabilities of these methods to operate in more complex, more relevant multi-cellular environments including tissues and living organisms. Indeed, work in this direction is well underway with the introduction of rapid volumetric imaging systems like those presented here. We believe that great potential lies in the combination and integration of large scale volumetric imaging with technologies such as FC(C)S, FRAP and SPT, providing quantification of key biophysical parameters throughout the functionally diverse life cycles of immune cells.

AUTHOR CONTRIBUTIONS

FS, HC-Y, and MF wrote the manuscript. All authors contributed to the article and approved the submitted version.

ACKNOWLEDGMENTS

FS, HC-Y, and MF thank the Rosalind Franklin Institute and Kennedy Trust for Rheumatology Research, as well as the Wellcome Trust (212343/Z/18/Z), and EPSRC (EP/S004459/1) for funding.

REFERENCES

1. Kumari S, Curado S, Mayya V, Dustin ML. T cell antigen receptor activation and actin cytoskeleton remodeling. *Biochim Biophys Acta - Biomembr* (2014) 1838:546–56. doi: 10.1016/j.bbamem.2013.05.004
2. Colin-York H, Javanmardi Y, Skamrahl M, Kumari S, Chang VT, Khuon S, et al. Cytoskeletal Control of Antigen-Dependent T Cell Activation. *Cell Rep* (2019) 26:3369–79.e5. doi: 10.1016/j.celrep.2019.02.074
3. Mattila PK, Batista FD, Treanor B. Dynamics of the actin cytoskeleton mediates receptor cross talk: An emerging concept in tuning receptor signaling. *J Cell Biol* (2016) 212:267–80. doi: 10.1083/jcb.201504137
4. Gawden-Bone C, Griffiths GM. Phospholipids: Pulling back the actin curtain for granule delivery to the immune synapse. *Front Immunol* (2019) 10:700. doi: 10.3389/fimmu.2019.00700
5. Köster DV, Mayor S. Cortical actin and the plasma membrane: inextricably intertwined. *Curr Opin Cell Biol* (2016) 38:81–9. doi: 10.1016/j.ceb.2016.02.021
6. Saarikangas J, Zhao H, Lappalainen P. Regulation of the actin cytoskeleton-plasma membrane interplay by phosphoinositides. *Physiol Rev* (2010) 90:259–89. doi: 10.1152/physrev.00036.2009
7. Rottner K, Faix J, Bogdan S, Linder S, Kerkhoff E. Actin assembly mechanisms at a glance. *J Cell Sci* (2017) 130:3427–35. doi: 10.1242/jcs.206433
8. Chugh P, Paluch EK. The actin cortex at a glance. *J Cell Sci* (2018) 131: jcs186254. doi: 10.1242/jcs.186254
9. Fehon RG, McClatchey AI, Bretscher A. Organizing the cell cortex: the role of ERM proteins. *Nat Rev Mol Cell Biol* (2010) 11:276–87. doi: 10.1038/nrm2866
10. Mueller J, Szep G, Nemethova M, de Vries I, Lieber AD, Winkler C, et al. Load Adaptation of Lamellipodial Actin Networks. *Cell* (2017) 171:188–200. doi: 10.1016/j.cell.2017.07.051
11. Schroer CFE, Baldauf L, van Buren L, Wassenaar TA, Melo MN, Koenderink GH, et al. Charge-dependent interactions of monomeric and filamentous actin with lipid bilayers. *Proc Natl Acad Sci U S A* (2020) 117:5861–72. doi: 10.1073/pnas.1914884117
12. Mogilner A, Rubinstein B. The physics of filopodial protrusion. *Biophys J* (2005) 89:782–95. doi: 10.1529/biophysj.104.056515
13. Jung Y, Riven I, Feigelson SW, Kartvelishvily E, Tohya K, Miyasaka M, et al. Three-dimensional localization of T-cell receptors in relation to microvilli using a combination of superresolution microscopies. *Proc Natl Acad Sci U S A* (2016) 113:E5916–24. doi: 10.1073/pnas.1605399113

14. Schaumann EN, Tian B. Actin-packed topography: Cytoskeletal response to curvature. *Proc Natl Acad Sci U S A* (2019) 116:22897–8. doi: 10.1073/pnas.1916656116
15. Wen PJ, Grenklo S, Arpino G, Tan X, Liao H-S, Heureaux J, et al. Actin dynamics provides membrane tension to merge fusing vesicles into the plasma membrane. *Nat Commun* (2016) 7:12604. doi: 10.1038/ncomms12604
16. Andrade DM, Clausen MP, Keller J, Mueller V, Wu C, Bear JE, et al. Cortical actin networks induce spatio-temporal confinement of phospholipids in the plasma membrane – a minimally invasive investigation by STED-FCS. *Sci Rep* (2015) 5:11454. doi: 10.1038/srep11454
17. Schneider F, Waithe D, Clausen MP, Galiani S, Koller T, Ozhan G, et al. Diffusion of lipids and GPI-anchored proteins in actin-free plasma membrane vesicles measured by STED-FCS. *Mol Biol Cell* (2017) 28:1507–18. doi: 10.1091/mbc.e16-07-0536
18. Simon C, Caorsi V, Campillo C, Sykes C. Interplay between membrane tension and the actin cytoskeleton determines shape changes. *Phys Biol* (2018) 15:065004. doi: 10.1088/1478-3975/aad1ab
19. Simon C, Kusters R, Caorsi V, Allard A, Abou-Ghali M, Manzi J, et al. Actin dynamics drive cell-like membrane deformation. *Nat Phys* (2019) 8:602–9. doi: 10.1038/s41567-019-0464-1
20. Fooksman DR, Vardhana S, Vasiliver-Shamis G, Liese J, Blair DA, Waite J, et al. Functional Anatomy of T Cell Activation and Synapse Formation. *Annu Rev Immunol* (2010) 28:79–105. doi: 10.1146/annurev-immunol-030409-101308
21. Varma R, Campi G, Yokosuka T, Saito T, Dustin ML. T Cell Receptor-Proximal Signals Are Sustained in Peripheral Microclusters and Terminated in the Central Supramolecular Activation Cluster. *Immunity* (2006) 25:117–27. doi: 10.1016/j.immuni.2006.04.010
22. Bálint S, Müller S, Fischer R, Kessler BM, Harkiolaki M, Valitutti S, et al. Supramolecular attack particles are autonomous killing entities released from cytotoxic T cells. *Science (80-)* (2020) 368:897–901. doi: 10.1126/science.aay9207
23. Cai E, Marchuk K, Beemiller P, Beppler C, Rubashkin MG, Weaver VM, et al. Visualizing dynamic microvillar search and stabilization during ligand detection by T cells. *Science* (2017) 356:eaal3118. doi: 10.1126/science.aal3118
24. Ghosh S, Di Bartolo V, Tubul L, Shimoni E, Kartvelishvily E, Dadosh T, et al. ERM-Dependent Assembly of T Cell Receptor Signaling and Co-stimulatory Molecules on Microvilli prior to Activation. *Cell Rep* (2020) 30:3434–47. doi: 10.1016/j.celrep.2020.02.069
25. Jung Y, Wen L, Altman A, Ley K. CD45 Pre-Exclusion from the Tips of Microvilli Establishes a Phosphatase-Free Zone for Early TCR Triggering. *BioRxiv* (2020) 2020.05.21.109074. doi: 10.1101/2020.05.21.109074
26. Orbach R, Su X. Surfing on Membrane Waves: Microvilli, Curved Membranes, and Immune Signaling. *Front Immunol* (2020) 11:2187. doi: 10.3389/fimmu.2020.02187
27. Fritzsche M, Fernandes RA, Chang VT, Colin-York H, Clausen MP, Felce JH, et al. Cytoskeletal actin dynamics shape a ramifying actin network underpinning immunological synapse formation. *Sci Adv* (2017) 3: e1603032. doi: 10.1126/sciadv.1603032
28. Yi J, Wu XS, Crites T, Hammer JA. Actin retrograde flow and actomyosin II arc contraction drive receptor cluster dynamics at the immunological synapse in Jurkat T cells. *Mol Biol Cell* (2012) 23:834–52. doi: 10.1091/mbc.E11-08-0731
29. Babich A, Li S, O'Connor RS, Milone MC, Freedman BD. Burkhardt JK. F-actin polymerization and retrograde flow drive sustained PLCγ1 signaling during T cell activation. *J Cell Biol* (2012) 197:775–87. doi: 10.1083/jcb.201201018
30. Sims TN, Soos TJ, Xenias HS, Dubin-Thaler B, Hofman JM, Waite JC, et al. Opposing Effects of PKCθ and WASp on Symmetry Breaking and Relocation of the Immunological Synapse. *Cell* (2007) 129:773–85. doi: 10.1016/j.cell.2007.03.037
31. Kumari S, Mak M, Poh Y, Tohme M, Watson N, Melo M, et al. Cytoskeletal tension actively sustains the migratory T-cell synaptic contact. *EMBO J* (2020) 39:1–18. doi: 10.15252/embj.2019102783
32. Gawden-Bone CM, Frazer GL, Richard AC, Ma CY, Strege K, Griffiths GM. PIP5 Kinases Regulate Membrane Phosphoinositide and Actin Composition for Targeted Granule Secretion by Cytotoxic Lymphocytes. *Immunity* (2018) 49:427–37. doi: 10.1016/j.immuni.2018.08.017
33. Ritter AT, Asano Y, Stinchcombe JC, Dieckmann NMG, Chen BC, Gawden-Bone C, et al. Actin Depletion Initiates Events Leading to Granule Secretion at the Immunological Synapse. *Immunity* (2015) 42:864–76. doi: 10.1016/j.immuni.2015.04.013
34. Lorent JH, Levental KR, Ganesan L, Rivera-Longsworth G, Sezgin E, Doktorova M, et al. Plasma membranes are asymmetric in lipid unsaturation, packing and protein shape. *Nat Chem Biol* (2020) 16:644–52. doi: 10.1038/s41589-020-0529-6
35. Sezgin E, Levental I, Mayor S, Eggeling C. The mystery of membrane organization: composition, regulation and roles of lipid rafts. *Nat Rev Mol Cell Biol* (2017) 18:361–74. doi: 10.1038/nrm.2017.16
36. Dinic J, Riehl A, Adler J, Parmryd I. The T cell receptor resides in ordered plasma membrane nanodomains that aggregate upon patching of the receptor. *Sci Rep* (2015) 5:10082. doi: 10.1038/srep10082
37. Klammt C, Lillemeier BF. How membrane structures control T cell signaling. *Front Immunol* (2012) 3:291. doi: 10.3389/fimmu.2012.00291
38. Meiri KF. Lipid rafts and regulation of the cytoskeleton during T cell activation. *Philos Trans R Soc B Biol Sci* (2005) 360:1663–72. doi: 10.1098/rstb.2005.1704
39. Montixi C, Langlet C, Bernard AM, Thimonier J, Dubois C, Wurbel MA, et al. Engagement of T cell receptor triggers its recruitment to low-density detergent-insoluble membrane domains. *EMBO J* (1998) 17:5334–48. doi: 10.1093/emboj/17.18.5334
40. Drevot P, Langlet C, Guo XJ, Bernard AM, Colard O, Chauvin JP, et al. TCR signal initiation machinery is pre-assembled and activated in a subset of membrane rafts. *EMBO J* (2002) 21:1899–908. doi: 10.1093/emboj/21.8.1899
41. Gaus K, Chklovskaia E, Fazekas De St. Groth B, Jessup W, Harder T. Condensation of the plasma membrane at the site of T lymphocyte activation. *J Cell Biol* (2005) 171:121–31. doi: 10.1083/jcb.200505047
42. Lorent JH, Diaz-Rohrer B, Lin X, Spring K, Gorfe AA, Levental KR, et al. Structural determinants and functional consequences of protein affinity for membrane rafts. *Nat Commun* (2017) 8:1219. doi: 10.1038/s41467-017-01328-3
43. Sezgin E, Levental I, Grzybek M, Schwarzmann G, Mueller V, Honigmann A, et al. Partitioning, diffusion, and ligand binding of raft lipid analogs in model and cellular plasma membranes. *Biochim Biophys Acta* (2012) 1818:1777–84. doi: 10.1016/j.bbamem.2012.03.007
44. Jacobson K, Mouritsen OG, Anderson RGW. Lipid rafts: at a crossroad between cell biology and physics. *Nat Cell Biol* (2007) 9:7–14. doi: 10.1038/ncb0107-7
45. Ventimiglia LN, Alonso MA. The role of membrane rafts in Lck transport, regulation and signalling in T-cells. *Biochem J* (2013) 454:169–79. doi: 10.1042/bj20130468
46. Pinkwart K, Schneider F, Lukoseviciute M, Sauka-Spengler T, Lyman E, Eggeling C, et al. Nanoscale dynamics of cholesterol in the cell membrane. *J Biol Chem* (2019) 294:12599–609. doi: 10.1074/jbc.RA119.009683
47. Endapally S, Frias D, Grzemska M, Gay A, Tomchick DR, Radhakrishnan A. Molecular Discrimination between Two Conformations of Sphingomyelin in Plasma Membranes. *Cell* (2019) 176:1040–53. doi: 10.1016/j.cell.2018.12.042
48. Subczynski WK, Pasenkiewicz-Gierula M, Widomska J, Mainali L, Raguz M. High Cholesterol/Low Cholesterol: Effects in Biological Membranes Review. *Cell Biochem Biophys* (2017) 75:1–17. doi: 10.1007/s12013-017-0792-7
49. Dinic J, Ashrafzadeh P, Parmryd I. Actin filaments attachment at the plasma membrane in live cells cause the formation of ordered lipid domains. *Biochim Biophys Acta - Biomembr* (2013) 1828:1102–11. doi: 10.1016/j.bbamem.2012.12.004
50. Honigmann A, Sadeghi S, Keller J, Hell SW, Eggeling C, Vink R. A lipid bound actin meshwork organizes liquid phase separation in model membranes. *Elife* (2014) 2014:1–16. doi: 10.7554/eLife.01671
51. Zumerle S, Molon B, Viola A. Membrane rafts in T cell activation: A spotlight on CD28 costimulation. *Front Immunol* (2017) 8:1467. doi: 10.3389/fimmu.2017.01467
52. Wickramarachchi DC, Theofilopoulos AN, Kono DH. Immune pathology associated with altered actin cytoskeleton regulation. *Autoimmunity* (2010) 43:64–75. doi: 10.3109/08916930903374634

53. Beemiller P, Krummel MF. Mediation of T-cell activation by actin meshworks. *Cold Spring Harb Perspect Biol* (2010) 2:1–14. doi: 10.1101/cshperspect.a002444
54. Joosten B, Willemse M, Fransen J, Cambi A, van den Dries K. Super-Resolution Correlative Light and Electron Microscopy (SR-CLEM) Reveals Novel Ultrastructural Insights Into Dendritic Cell Podosomes. *Front Immunol* (2018) 9:1908. doi: 10.3389/fimmu.2018.01908
55. Dobbie IM. Bridging the resolution gap: correlative super-resolution imaging. *Nat Rev Microbiol* (2019) 17:337. doi: 10.1038/s41579-019-0203-8
56. Ganeva I, Kukulski W. Membrane Architecture in the Spotlight of Correlative Microscopy. *Trends Cell Biol* (2020) 30:577–87. doi: 10.1016/j.tcb.2020.04.003
57. Ojcius DM, Niedergang F, Subtil A, Hellio R, Dautry-Varsat A. Immunology and the confocal microscope. *Res Immunol* (1996) 147:175–88. doi: 10.1016/0923-2494(96)83169-5
58. Lee KH, Holdorf AD, Dustin ML, Chan AC, Allen PM, Shaw AS. T cell receptor signaling precedes immunological synapse formation. *Science (80-)* (2002) 295:1539–42. doi: 10.1126/science.1067710
59. Harwood NE, Batista FD. Early Events in B Cell Activation. *Annu Rev Immunol* (2010) 28:185–210. doi: 10.1146/annurev-immunol-030409-101216
60. Beemiller P, Krummel MF. Regulation of T-cell receptor signaling by the actin cytoskeleton and poroelastic cytoplasm. *Immunol Rev* (2013) 256:148–59. doi: 10.1111/imr.12120
61. Roy NH, Burkhardt JK. The actin cytoskeleton: A mechanical intermediate for signal integration at the immunological synapse. *Front Cell Dev Biol* (2018) 6:116. doi: 10.3389/fcell.2018.00116
62. Lackowicz J. *Principles of Fluorescence Spectroscopy. 3rd ed.* JR Lakowicz, editor. Boston, MA: Springer US (2006). doi: 10.1007/978-0-387-46312-4
63. Manzo C, Garcia-Parajo MF. A review of progress in single particle tracking: from methods to biophysical insights. *Rep Prog Phys* (2015) 78:124601. doi: 10.1088/0034-4885/78/12/124601
64. Dorsch S, Klotz KN, Engelhardt S, Lohse MJ, Bünemann M. Analysis of receptor oligomerization by FRAP microscopy. *Nat Methods* (2009) 6:225–30. doi: 10.1038/nmeth.1304
65. Favier B, Burroughs NJ, Wedderburn L, Valitutti S. TCR dynamics on the surface of living T cells. *Int Immunol* (2001) 13:1525–32. doi: 10.1093/intimm/13.12.1525
66. Schwarzenbacher M, Kaltenbrunner M, Brameshuber M, Hesch C, Paster W, Weghuber J, et al. Micropatterning for quantitative analysis of protein-protein interactions in living cells. *Nat Methods* (2008) 5:1053–60. doi: 10.1038/nmeth.1268
67. Tolentino TP, Wu J, Zarnitsyna VI, Fang Y, Dustin ML, Zhu C. Measuring diffusion and binding kinetics by contact area FRAP. *Biophys J* (2008) 95:920–30. doi: 10.1529/biophysj.107.114447
68. Treanor B, Depoil D, Gonzalez-Granja A, Barral P, Weber M, Dushek O, et al. The Membrane Skeleton Controls Diffusion Dynamics and Signaling through the B Cell Receptor. *Immunity* (2010) 32:187–99. doi: 10.1016/j.immuni.2009.12.005
69. Zimmermann L, Paster W, Weghuber J, Eckerstorfer P, Stockinger H, Schütz GJ. Direct observation and quantitative analysis of Lck exchange between plasma membrane and cytosol in living T cells. *J Biol Chem* (2010) 285:6063–70. doi: 10.1074/jbc.M109.025981
70. Hiramoto-Yamaki N, Tanaka KAK, Suzuki KGN, Hirosawa KM, Miyahara MSH, Kalay Z, et al. Ultrafast Diffusion of a Fluorescent Cholesterol Analog in Compartmentalized Plasma Membranes. *Traffic* (2014) 15:583–612. doi: 10.1111/tra.12163
71. Kapoor-Kaushik N, Hinde E, Compeer EB, Yamamoto Y, Kraus F, Yang Z, et al. Distinct Mechanisms Regulate Lck Spatial Organization in Activated T Cells. *Front Immunol* (2016) 7:83. doi: 10.3389/fimmu.2016.00083
72. Ma Y, Benda A, Nicovich PR, Gaus K. Measuring membrane association and protein diffusion within membranes with supercritical angle fluorescence microscopy. *BioMed Opt Express* (2016) 7:1561. doi: 10.1364/BOE.7.001561
73. Ponjavic A, McColl J, Carr AR, Santos AM, Kulenkampff K, Lippert A, et al. Single-Molecule Light-Sheet Imaging of Suspended T Cells. *Biophys J* (2018) 114:2200–11. doi: 10.1016/j.bpj.2018.02.044
74. Bedard M, Shrestha D, Priestman DA, Wang Y, Schneider F, Matute JD, et al. Sterile activation of invariant natural killer T cells by ER-stressed antigen-presenting cells. *Proc Natl Acad Sci* (2019) 116:23671–81. doi: 10.1073/pnas.1910097116
75. Sezgin E, Schneider F, Galiani S, Urbančič I, Waithe D, Lagerholm BC, et al. Measuring nanoscale diffusion dynamics in cellular membranes with super-resolution STED–FCS. *Nat Protoc* (2019) 14:1054–83. doi: 10.1038/s41596-019-0127-9
76. Eggeling C, Ringemann C, Medda R, Schwarzmann G, Sandhoff K, Polyakova S, et al. Direct observation of the nanoscale dynamics of membrane lipids in a living cell. *Nature* (2009) 457:1159–62. doi: 10.1038/nature07596
77. Mueller V, Ringemann C, Honigmann A, Schwarzmann G, Medda R, Leutenegger M, et al. STED Nanoscopy Reveals Molecular Details of Cholesterol- and Cytoskeleton-Modulated Lipid Interactions in Living Cells. *Biophys J* (2011) 101:1651–60. doi: 10.1016/j.bpj.2011.09.006
78. Ruan Q, Cheng MA, Levi M, Gratton E, Mantulin WW. Spatial-temporal studies of membrane dynamics: scanning fluorescence correlation spectroscopy (SFCS). *Biophys J* (2004) 87:1260–7. doi: 10.1529/biophysj.103.036483
79. Waithe D, Schneider F, Chojnacki J, Clausen MP, Shrestha D, de la Serna JB, et al. Optimized processing and analysis of conventional confocal microscopy generated scanning FCS data. *Methods* (2017) 140–141:62–73. doi: 10.1016/j.ymeth.2017.09.010
80. Schneider F, Waithe D, Lagerholm BC, Shrestha D, Sezgin E, Eggeling C, et al. Statistical Analysis of Scanning Fluorescence Correlation Spectroscopy Data Differentiates Free from Hindered Diffusion. *ACS Nano* (2018) 12:8540–6. doi: 10.1021/acsnano.8b04080
81. Blouin CM, Hamon Y, Gonnord P, Boularan C, Kagan J, Viaris de Lesegno C, et al. Glycosylation-Dependent IFN-γR Partitioning in Lipid and Actin Nanodomains Is Critical for JAK Activation. *Cell* (2016) 166:920–34. doi: 10.1016/j.cell.2016.07.003
82. Guzmán C, Šolman M, Ligabue A, Blaževitš O, Andrade DM, Reymond L, et al. The efficacy of raf kinase recruitment to the GTPase H-ras depends on H-ras membrane conformer-specific nanoclustering. *J Biol Chem* (2014) 289:9519–33. doi: 10.1074/jbc.M113.537001
83. Ries J, Yu SR, Burkhardt M, Brand M, Schwille P. Modular scanning FCS quantifies receptor-ligand interactions in living multicellular organisms. *Nat Methods* (2009) 6:643–5. doi: 10.1038/nmeth.1355
84. Di Bona M, Mancini MA, Mazza D, Vicidomini G, Diaspro A, Lanzanò L. Measuring Mobility in Chromatin by Intensity-Sorted FCS. *Biophys J* (2019) 116:987–99. doi: 10.1016/j.bpj.2019.02.003
85. Dörlich RM, Chen Q, Niklas Hedde P, Schuster V, Hippler M, Wesslowski J, et al. Dual-color dual-focus line-scanning FCS for quantitative analysis of receptor-ligand interactions in living specimens. *Sci Rep* (2015) 5:10149. doi: 10.1038/srep10149
86. Dunsing V, Mayer M, Liebsch F, Multhaup G, Chiantia S. Direct evidence of amyloid precursor–like protein 1 trans interactions in cell–cell adhesion platforms investigated via fluorescence fluctuation spectroscopy. *Mol Biol Cell* (2017) 28:3609–20. doi: 10.1091/mbc.E17-07-0459
87. Honigmann A, Mueller V, Ta H, Schoenle A, Sezgin E, Hell SW, et al. Scanning STED-FCS reveals spatiotemporal heterogeneity of lipid interaction in the plasma membrane of living cells. *Nat Commun* (2014) 5:5412. doi: 10.1038/ncomms6412
88. Schneider F, Waithe D, Galiani S, Bernardino de la Serna J, Sezgin E, Eggeling C. Nanoscale Spatiotemporal Diffusion Modes Measured by Simultaneous Confocal and Stimulated Emission Depletion Nanoscopy Imaging. *Nano Lett* (2018) 18:4233–40. doi: 10.1021/acs.nanolett.8b01190
89. Lanzanò L, Scipioni L, Di Bona M, Bianchini P, Bizzarri R, Cardarelli F, et al. Measurement of nanoscale three-dimensional diffusion in the interior of living cells by STED-FCS. *Nat Commun* (2017) 8:65. doi: 10.1038/s41467-017-00117-2
90. Schneider F, Hernandez-Varas P, Christoffer Lagerholm B, Shrestha D, Sezgin E, Julia Roberti M, et al. High photon count rates improve the quality of super-resolution fluorescence fluctuation spectroscopy. *J Phys D Appl Phys* (2020) 53:164003. doi: 10.1088/1361-6463/ab6cca
91. Bag N, Holowka DA, Baird BA. Imaging FCS delineates subtle heterogeneity in plasma membranes of resting mast cells. *Mol Biol Cell* (2020) 31:709–23. doi: 10.1091/mbc.E19-10-0559
92. Wohland T, Shi X, Sankaran J, Stelzer EHK. Single Plane Illumination Fluorescence Correlation Spectroscopy (SPIM-FCS) probes inhomogeneous three-dimensional environments. *Opt Express* (2010) 18:10627. doi: 10.1364/oe.18.010627

93. Bag N, Sankaran J, Paul A, Kraut RS, Wohland T. Calibration and limits of camera-based fluorescence correlation spectroscopy: A supported lipid bilayer study. *ChemPhysChem* (2012) 13:2784–94. doi: 10.1002/cphc.201200032
94. Di Rienzo C, Gratton E, Beltram F, Cardarelli F. Fast spatiotemporal correlation spectroscopy to determine protein lateral diffusion laws in live cell membranes. *Proc Natl Acad Sci* (2013) 110:12307–12. doi: 10.1073/pnas.1222097110
95. Di Rienzo C, Gratton E, Beltram F, Cardarelli F. Spatiotemporal Fluctuation Analysis: A Powerful Tool for the Future Nanoscopy of Molecular Processes. *Biophys J* (2016) 111:679–85. doi: 10.1016/j.bpj.2016.07.015
96. Di Rienzo C, Gratton E, Beltram F, Cardarelli F. From Fast Fluorescence Imaging to Molecular Diffusion Law on Live Cell Membranes in a Commercial Microscope. *J Vis Exp* (2014) e51994:1–12. doi: 10.3791/51994
97. Ortega-Arroyo J, Kukura P. Interferometric scattering microscopy (iSCAT): new frontiers in ultrafast and ultrasensitive optical microscopy. *Phys Chem Chem Phys* (2012) 14:15625. doi: 10.1039/c2cp41013c
98. Reina F, Galiani S, Shrestha D, Sezgin E, De Wit G, Cole D, et al. Complementary studies of lipid membrane dynamics using iSCAT and super-resolved fluorescence correlation spectroscopy. *J Phys D Appl Phys* (2018) 51:235401. doi: 10.1088/1361-6463/aac04f
99. Taylor RW, Mahmoodabadi RG, Rauschenberger V, Giessl A, Schambony A, Sandoghdar V. Interferometric scattering microscopy reveals microsecond nanoscopic protein motion on a live cell membrane. *Nat Photonics* (2019) 13:480–7. doi: 10.1038/s41566-019-0414-6
100. Alvarez LAJ, Widzgowski B, Ossato G, van den BB, Jalink K, Kuschel L, et al. SP8 FALCON : a novel concept in fluorescence lifetime imaging enabling video-rate confocal FLIM. *Nat Methods* (2019). doi: 10.1038/d42473-019-00261
101. Sun Y, Day RN, Periasamy A. Investigating protein-protein interactions in living cells using fluorescence lifetime imaging microscopy. *Nat Protoc* (2011) 6:1324–40. doi: 10.1038/nprot.2011.364
102. Chizhik AI, Rother J, Gregor I, Janshoff A, Enderlein J. Metal-induced energy transfer for live cell nanoscopy. *Nat Photonics* (2014) 8:124–7. doi: 10.1038/nphoton.2013.345
103. Benda A, Fagul'ová V, Deyneka A, Enderlein J, Hof M. Fluorescence lifetime correlation spectroscopy combined with lifetime tuning: New perspectives in supported phospholipid bilayer research. *Langmuir* (2006) 22:9580–5. doi: 10.1021/la061573d
104. Kułakowska A, Jurkiewicz P, Sýkora J, Benda A, Mely Y, Hof M. Fluorescence lifetime tuning-a novel approach to study flip-flop kinetics in supported phospholipid bilayers. *J Fluoresc* (2010) 20:563–9. doi: 10.1007/s10895-009-0581-9
105. Ghosh A, Sharma A, Chizhik AI, Isbaner S, Ruhlandt D, Tsukanov R, et al. Graphene-based metal-induced energy transfer for sub-nanometre optical localization. *Nat Photonics* (2019) 13:860–5. doi: 10.1038/s41566-019-0510-7
106. Jarsch IK, Daste F, Gallop JL. Membrane curvature in cell biology: An integration of molecular mechanisms. *J Cell Biol* (2016) 214:375–87. doi: 10.1083/jcb.201604003
107. Baronsky T, Ruhlandt D, Brueckner BR, Schäfer J, Karedla N, Haehnel D, et al. Cell-Substrate Dynamics of the Epithelial-to- Mesenchymal Transition. *Nano Lett* (2017) 17(5):3320–6. doi: 10.1021/acs.nanolett.7b01558
108. Chizhik AM, Wollnik C, Ruhlandt D, Karedla N, Chizhik AI, Hauke L, et al. Dual-color metal-induced and förster resonance energy transfer for cell nanoscopy. *Mol Biol Cell* (2018) 29:846–51. doi: 10.1091/mbc.E17-05-0314. mbc.E17-05-0314.
109. Chizhik AM, Ruhlandt D, Pfaff J, Karedla N, Chizhik AI, Gregor I, et al. Three Dimensional Reconstruction of Nuclear Envelope Architecture Using Dual-Color Metal-Induced Energy Transfer Imaging. *ACS Nano* (2017) 11:11839–46. doi: 10.1021/acsnano.7b04671. acsnano.7b04671.
110. Ghosh A, Karedla N, Thiele JC, Gregor I, Enderlein J. Fluorescence lifetime correlation spectroscopy: Basics and applications. *Methods* (2018) 140–141:32–9. doi: 10.1016/j.ymeth.2018.02.009
111. Chang BJ, Kittisopikul M, Dean KM, Roudot P, Welf ES, Fiolka R. Universal light-sheet generation with field synthesis. *Nat Methods* (2019) 16(3):235–8. doi: 10.1038/s41592-019-0327-9
112. Millett-Sikking A, York A. *AndrewGYork/high_na_single_objective_lightsheet: Work-in-progress (Version 0.0.1)*. Zenodo (2019). doi: 10.5281/zenodo.3244421
113. Yang B, Millett-Sikking A, Lange M, Solak AC, Kobayashi H, York A, et al. High-Resolution , Large Field-of-View , and Multi-View Single Objective Light-Sheet Microscopy. *bioRxiv* (2020), 1–10. doi: 10.1101/2020.09.22.309229
114. McDole K, Guignard L, Amat F, Berger A, Malandain G, Royer LA, et al. In Toto Imaging and Reconstruction of Post-Implantation Mouse Development at the Single-Cell Level. *Cell* (2018) 175:859–76.e33. doi: 10.1016/j.cell.2018.09.031
115. Voleti V, Patel KB, Li W, Perez Campos C, Bharadwaj S, Yu H, et al. Real-time volumetric microscopy of in vivo dynamics and large-scale samples with SCAPE 2.0. *Nat Methods* (2019) 16:1054–62. doi: 10.1038/s41592-019-0579-4
116. Chen BCB-C, Legant WR, Wang K, Shao L, Milkie DE, Davidson MW, et al. Lattice light-sheet microscopy: Imaging molecules to embryos at high spatiotemporal resolution. *Science* (2014) 346:1257998–1257998. doi: 10.1126/science.1257998
117. Groves JT, Dustin ML. Supported planar bilayers in studies on immune cell adhesion and communication. *J Immunol Methods* (2003) 278:19–32. doi: 10.1016/S0022-1759(03)00193-5
118. Santos AM, Ponjavic A, Fritzsche M, Fernandes RA, de la Serna JB, Wilcock MJ, et al. Capturing resting T cells: the perils of PLL. *Nat Immunol* (2018) 19:203–5. doi: 10.1038/s41590-018-0048-8
119. Jenkins E, Santos AM, O'Brien-Ball C, Felce JH, Wilcock MJ, Hatherley D, et al. Reconstitution of immune cell interactions in free-standing membranes. *J Cell Sci* (2019) 132:jcs219709. doi: 10.1242/jcs.219709
120. Roybal KT, Mace EM, Mantell JM, Verkade P, Orange JS, Wülfing C. Early signaling in primary t cells activated by antigen presenting cells is associated with a deep and transient lamellal actin network. *PLoS One* (2015) 10:1–22. doi: 10.1371/journal.pone.0133299
121. Rosenberg J, Cao G, Borja-Prieto F, Huang J. Lattice Light-Sheet Microscopy Multi-dimensional Analyses (LaMDA) of T-Cell Receptor Dynamics Predict T-Cell Signaling States. *Cell Syst* (2020) 10:433–44. doi: 10.1016/j.cels.2020.04.006
122. Fritzsche M, Charras G. Dissecting protein reaction dynamics in living cells by fluorescence recovery after photobleaching. *Nat Protoc* (2015) 10:660–80. doi: 10.1038/nprot.2015.042
123. Hobson CM, O'Brien ET, Falvo MR, Superfine R. Combined Selective Plane Illumination Microscopy and FRAP Maps Intranuclear Diffusion of NLS-GFP. *Biophys J* (2020) 119:514–24. doi: 10.1016/j.bpj.2020.07.001
124. Sims PJ, Waggoner AS, Wang CH, Hoffman JF. Mechanism by which cyanine dyes measure membrane potential in red blood cells and phosphatidylcholine vesicles. *Biochemistry* (1974) 13:3315–30. doi: 10.1021/bi00713a022
125. Hume RI, Honig MG. Fluorescent Carbocyanine Dyes Allow Living Neurons of Identified Origin to Be Studied in Long-Term Cultures. *J Cell Biol* (1986) 103:171–87. doi: 10.1083/jcb.103.1.171
126. Klymchenko AS, Kreder R. Fluorescent probes for lipid rafts: From model membranes to living cells. *Chem Biol* (2014) 21:97–113. doi: 10.1016/j.chembiol.2013.11.009
127. Collot M, Ashokkumar P, Anton H, Boutant E, Faklaris O, Galli T, et al. MemBright: A Family of Fluorescent Membrane Probes for Advanced Cellular Imaging and Neuroscience. *Cell Chem Biol* (2019) 26:600–14. doi: 10.1016/j.chembiol.2019.01.009
128. Maekawa M, Fairn GD. Molecular probes to visualize the location, organization and dynamics of lipids. *J Cell Sci* (2014) 127:4801–12. doi: 10.1242/jcs.150524
129. Sezgin E, Can FB, Schneider F, Clausen MP, Galiani S, Stanly TA, et al. A comparative study on fluorescent cholesterol analogs as versatile cellular reporters. *J Lipid Res* (2016) 57:299–309. doi: 10.1194/jlr.M065326
130. Hurley JH, Misra S. Signaling and subcellular targeting by membrane-binding domains. *Annu Rev Biophys Biomol Struct* (2000) 29:49–79. doi: 10.1146/annurev.biophys.29.1.49
131. Várnai P, Gulyás G, Tóth DJ, Sohn M, Sengupta N, Balla T. Quantifying lipid changes in various membrane compartments using lipid binding protein domains. *Cell Calcium* (2017) 64:72–82. doi: 10.1016/j.ceca.2016.12.008
132. Parasassi T, Krasnowska EK. Laurdan and Prodan as polarity-sensitive fluorescent membrane probes. *J Fluoresc* (1998) 8:365–73. doi: 10.1023/A:1020528716621
133. Sezgin E, Sadowski T, Simons K. Measuring lipid packing of model and cellular membranes with environment sensitive probes. *Langmuir* (2014) 30:8160–6. doi: 10.1021/la501226v

134. Sezgin E, Schneider F, Zilles V, Urbančič I, Garcia E, Waithe D, et al. Polarity-Sensitive Probes for Superresolution Stimulated Emission Depletion Microscopy. *Biophys J* (2017) 113:1321–30. doi: 10.1016/j.bpj.2017.06.050
135. Danylchuk DI, Moon S, Xu K, Klymchenko AS. Switchable Solvatochromic Probes for Live-Cell Super-resolution Imaging of Plasma Membrane Organization. *Angew Chemie* (2019) 131:15062–6. doi: 10.1002/ange.201907690
136. Colom A, Derivery E, Soleimanpour S, Tomba C, Molin MD, Sakai N, et al. A fluorescent membrane tension probe. *Nat Chem* (2018) 10:1118–25. doi: 10.1038/s41557-018-0127-3
137. Dal Molin M, Verolet Q, Colom A, Letrun R, Derivery E, Gonzalez-Gaitan M, et al. Fluorescent Flippers for Mechanosensitive Membrane Probes. *J Am Chem Soc* (2015) 137:568–71. doi: 10.1021/ja5107018
138. Sezgin E, Waithe D, Bernardino de la Serna J, Eggeling C. Spectral Imaging to Measure Heterogeneity in Membrane Lipid Packing. *ChemPhysChem* (2015) 16:1387–94. doi: 10.1002/cphc.201402794
139. Steinkühler J, Sezgin E, Urbančič I, Eggeling C, Dimova R. Mechanical properties of plasma membrane vesicles correlate with lipid order and viscosity and depend on cell density. *Commun Biol* (2019) 2:1–18. doi: 10.1101/669085
140. Owen DM, Lanigan PMP, Dunsby C, Munro I, Grant D, Neil MAA, et al. Fluorescence lifetime imaging provides enhanced contrast when imaging the phase-sensitive dye di-4-ANEPPDHQ in model membranes and live cells. *Biophys J* (2006) 90:L80–2. doi: 10.1529/biophysj.106.084673
141. Riedl J, Crevenna AH, Kessenbrock K, Yu JH, Neukirchen D, Bista M, et al. Lifeact: A versatile marker to visualize F-actin. *Nat Methods* (2008) 5:605–7. doi: 10.1038/nmeth.1220
142. Johnson HW, Schell MJ. Neuronal IP 3 3-Kinase is an F-actin–bundling Protein: Role in Dendritic Targeting and Regulation of Spine Morphology. *Mol Biol Cell* (2009) 20:5166–80. doi: 10.1091/mbc.e09-01-0083
143. Melak M, Plessner M, Grosse R. Actin visualization at a glance. *J Cell Sci* (2017) 130:525–30. doi: 10.1242/jcs.189068
144. Bisaria A, Hayer A, Garbett D, Cohen D, Meyer T. Membrane-proximal F-actin restricts local membrane protrusions and directs cell migration. *Science (80-)* (2020) 368:1205–10. doi: 10.1126/science.aay7794
145. D'Este E, Kamin D, Göttfert F, El-Hady A, Hell SW. STED Nanoscopy Reveals the Ubiquity of Subcortical Cytoskeleton Periodicity in Living Neurons. *Cell Rep* (2015) 10:1246–51. doi: 10.1016/j.celrep.2015.02.007
146. Plessner M, Melak M, Chinchilla P, Baarlink C, Grosse R. Nuclear F-actin formation and reorganization upon cell spreading. *J Biol Chem* (2015) 290:11209–16. doi: 10.1074/jbc.M114.627166
147. Rocchetti A, Hawes C, Kriechbaumer V. Fluorescent labelling of the actin cytoskeleton in plants using a cameloid antibody. *Plant Methods* (2014) 10:12. doi: 10.1186/1746-4811-10-12
148. Schiavon C, Zhang T, Zhao B, Andrade L, Wu M, Sung T-C, et al. Actin chromobody imaging reveals sub-organellar actin dynamics. *Nat Methods* (2019) 17:917–21. doi: 10.1101/639278
149. Colin-York H, Kumari S, Barbieri L, Cords L, Fritzsche M. Distinct actin cytoskeleton behaviour in primary and immortalised T-cells. *J Cell Sci* (2019) 133:jcs232322. doi: 10.1242/jcs.232322
150. Courtemanche N, Pollard TD, Chen Q. Avoiding artefacts when counting polymerized actin in live cells with LifeAct fused to fluorescent proteins. *Nat Cell Biol* (2016) 18:676–83. doi: 10.1038/ncb3351
151. Spracklen AJ, Fagan TN, Lovander KE, Tootle TL. The pros and cons of common actin labeling tools for visualizing actin dynamics during Drosophila oogenesis. *Dev Biol* (2014) 393:209–26. doi: 10.1016/j.ydbio.2014.06.022
152. Montes-Rodriguez A, Kost B. Direct comparison of the performance of commonly employed in vivo F-actin markers (Lifeact-YFP, YFP-mTn and YFP-FABD2) in tobacco pollen tubes. *Front Plant Sci* (2017) 8:1349. doi: 10.3389/fpls.2017.01349
153. Ai HW, Baird MA, Shen Y, Davidson MW, Campbell RE. Engineering and characterizing monomeric fluorescent proteins for live-cell imaging applications. *Nat Protoc* (2014) 9:910–28. doi: 10.1038/nprot.2014.054
154. Snapp E. Design and Use of Fluorescent Fusion Proteins in Cell Biology. *Curr Protoc Cell Biol* (2005) 27:21.4.1–21.4.13. doi: 10.1002/0471143030.cb2104s27
155. Ooi A, Wong A, Esau L, Lemtiri-Chlieh F. Gehring C. A Guide to Transient Expression of Membrane Proteins in HEK-293 Cells for Functional Characterization. *Front Physiol* (2016) 7:300. doi: 10.3389/fphys.2016.00300
156. Levental KR, Malmberg E, Symons JL, Fan YY, Chapkin RS, Ernst R, et al. Lipidomic and biophysical homeostasis of mammalian membranes counteracts dietary lipid perturbations to maintain cellular fitness. *Nat Commun* (2020) 11:1–13. doi: 10.1038/s41467-020-15203-1
157. Lingwood D, Simons K. Lipid rafts as a membrane-organizing principle. *Science* (2010) 327:46–50. doi: 10.1126/science.1174621
158. Neuvonen M, Manna M, Mokkila S, Javanainen M, Rog T, Liu Z, et al. Enzymatic oxidation of cholesterol: Properties and functional effects of cholestenone in cell membranes. *PLoS One* (2014) 9:e103743. doi: 10.1371/journal.pone.0103743
159. Rouquette-Jazdanian AK, Pelassy C, Breittmayer JP, Aussel C. Revaluation of the role of cholesterol in stabilizing rafts implicated in T cell receptor signaling. *Cell Signal* (2006) 18:105–22. doi: 10.1016/j.cellsig.2005.03.024
160. Storti B, Di Rienzo C, Cardarelli F, Bizzarri R, Beltram F. Unveiling TRPV1 spatio-temporal organization in live cell membranes. *PLoS One* (2015) 10: e0116900. doi: 10.1371/journal.pone.0116900
161. Silvestre F, Tosti E. Impact of marine drugs on cytoskeleton-mediated reproductive events. *Mar Drugs* (2010) 8:881–915. doi: 10.3390/md8040881
162. Harterink M, Da Silva ME, Will L, Turan J, Ibrahim A, Lang AE, et al. DeActs: Genetically encoded tools for perturbing the actin cytoskeleton in single cells. *Nat Methods* (2017) 14:479–82. doi: 10.1038/nmeth.4257
163. Cooper JA. Effects of cytochalasin and phalloidin on actin. *J Cell Biol* (1987) 105:1473–8. doi: 10.1083/jcb.105.4.1473
164. Holzinger A. Jasplakinolide: An Actin-Specific Reagent that Promotes Actin Polymerization. In: RH Gavin, editor. *Cytoskeleton Methods and Protocols*. Totowa, NJ: Humana Press (2009). p. 71–87. doi: 10.1007/978-1-60761-376-3_4
165. Fritzsche M, Erlenkämper C, Moeendarbary E, Charras G, Kruse K. Actin kinetics shapes cortical network structure and mechanics. *Sci Adv* (2016) 2: e1501337. doi: 10.1126/sciadv.1501337
166. Fritzsche M, Li D, Colin-York H, Chang VT, Moeendarbary E, Felce JH, et al. Self-organizing actin patterns shape membrane architecture but not cell mechanics. *Nat Commun* (2017) 8:14347. doi: 10.1038/ncomms14347
167. Isogai T, Van Der Kammen R, Innocenti M. SMIFH2 has effects on Formins and p53 that perturb the cell cytoskeleton. *Sci Rep* (2015) 5:9802. doi: 10.1038/srep09802
168. Murugesan S, Hong J, Yi J, Li D, Beach JR, Shao L, et al. Formin-generated actomyosin arcs propel t cell receptor microcluster movement at the immune synapse. *J Cell Biol* (2016) 215:383–99. doi: 10.1083/jcb.201603080
169. Kovács M, Tóth J, Hetényi C, Málnási-Csizmadia A, Sellers JR. Mechanism of Blebbistatin Inhibition of Myosin II. *J Biol Chem* (2004) 279:35557–63. doi: 10.1074/jbc.M405319200
170. Ishizaki T, Uehata M, Tamechika I, Keel J, Nonomura K, Maekawa M, et al. Pharmacological properties of Y-27632, a specific inhibitor of rho-associated kinases. *Mol Pharmacol* (2000) 57:976–83.
171. Sellers JR, Shi S, Nishimura Y, Zhang F, Liu R, Takagi Y, et al. The Formin Inhibitor, SMIFH2, Inhibits Members of the Myosin Superfamily. *Biophys J* (2020) 118:125a. doi: 10.1016/j.bpj.2019.11.817
172. Ross TD, Lee HJ, Qu Z, Banks RA, Phillips R, Thomson M. Controlling organization and forces in active matter through optically defined boundaries. *Nature* (2019) 572:224–9. doi: 10.1038/s41586-019-1447-1
173. Schuhmacher M, Grasskamp AT, Barahtjan P, Wagner N, Lombardot B, Schuhmacher JS, et al. Live-cell lipid biochemistry reveals a role of diacylglycerol side-chain composition for cellular lipid dynamics and protein affinities. *Proc Natl Acad Sci U S A* (2020) 117:7729–38. doi: 10.1073/pnas.1912684117
174. Ballister ER, Aonbangkhen C, Mayo AM, Lampson MA, Chenoweth DM. Localized light-induced protein dimerization in living cells using a photocaged dimerizer. *Nat Commun* (2014) 5:5475. doi: 10.1038/ncomms6475
175. Sezgin E, Kaiser H-J, Baumgart T, Schwille P, Simons K, Levental I. Elucidating membrane structure and protein behavior using giant plasma membrane vesicles. *Nat Protoc* (2012) 7:1042–51. doi: 10.1038/nprot.2012.059
176. Rossy J, Laufer JM, Legler DF. Role of mechanotransduction and tension in t cell function. *Front Immunol* (2018) 9:2638. doi: 10.3389/fimmu.2018.02638
177. Rudd-Schmidt JA, Hodel AW, Noori T, Lopez JA, Cho H-J, Verschoor S, et al. Lipid order and charge protect killer T cells from accidental death. *Nat Commun* (2019) 10:5396. doi: 10.1038/s41467-019-13385-x
178. Limozin L, Puech PH. Membrane Organization and Physical Regulation of Lymphocyte Antigen Receptors: A Biophysicist's Perspective. *J Membr Biol* (2019) 252:397–412. doi: 10.1007/s00232-019-00085-2
179. Wu Y, Shroff H. Faster, sharper, and deeper: structured illumination microscopy for biological imaging. *Nat Methods* (2018) 15:1011–9. doi: 10.1038/s41592-018-0211-z

180. Kraus F, Miron E, Demmerle J, Chitiashvili T, Budco A, Alle Q, et al. Quantitative 3D structured illumination microscopy of nuclear structures. *Nat Protoc* (2017) 12:1011–28. doi: 10.1038/nprot.2017.020

Conflict of Interest: The authors declare that the research was conducted in the absence of any commercial or financial relationships that could be construed as a potential conflict of interest.

frontiers in Physiology

BRIEF RESEARCH REPORT
published: 21 January 2021
doi: 10.3389/fphys.2020.613367

Calcium Signaling in T Cells Is Induced by Binding to Nickel-Chelating Lipids in Supported Lipid Bilayers

*Tommy Dam[1], Victoria Junghans[1], Jane Humphrey[2], Manto Chouliara[1] and Peter Jönsson[1]**

[1] Department of Chemistry, Lund University, Lund, Sweden, [2] Department of Chemistry, University of Cambridge, Cambridge, United Kingdom

Supported lipid bilayers (SLBs) are one of the most common cell-membrane model systems to study cell-cell interactions. Nickel-chelating lipids are frequently used to functionalize the SLB with polyhistidine-tagged ligands. We show here that these lipids by themselves can induce calcium signaling in T cells, also when having protein ligands on the SLB. This is important to avoid "false" signaling events in cell studies with SLBs, but also to better understand the molecular mechanisms involved in T-cell signaling. Jurkat T cells transfected with the non-signaling molecule rat CD48 were found to bind to ligand-free SLBs containing ≥2 wt% nickel-chelating lipids upon which calcium signaling was induced. This signaling fraction steadily increased from 24 to 60% when increasing the amount of nickel-chelating lipids from 2 to 10 wt%. Both the signaling fraction and signaling time did not change significantly compared to ligand-free SLBs when adding the CD48-ligand rat CD2 to the SLB. Blocking the SLB with bovine serum albumin reduced the signaling fraction to 11%, while preserving CD2 binding and the exclusion of the phosphatase CD45 from the cell-SLB contacts. Thus, CD45 exclusion alone was not sufficient to result in calcium signaling. In addition, more cells signaled on ligand-free SLBs with copper-chelating lipids instead of nickel-chelating lipids and the signaling was found to be predominantly via T-cell receptor (TCR) triggering. Hence, it is possible that the nickel-chelating lipids act as ligands to the cell's TCRs, an interaction that needs to be blocked to avoid unwanted cell activation.

Keywords: calcium signal, T-cell receptor, CD45, kinetic segregation model, CD2, ligand-independent activation

OPEN ACCESS

Edited by:
Erdinc Sezgin, Karolinska Institutet (KI), Sweden

Reviewed by:
Ryugo Tero, Toyohashi University of Technology, Japan
Jaydeep Kumar Basu, Indian Institute of Science (IISc), India

***Correspondence:**
Peter Jönsson
peter.jonsson@fkem1.lu.se

Specialty section:
This article was submitted to Membrane Physiology and Membrane Biophysics, a section of the journal Frontiers in Physiology

Received: *02 October 2020*
Accepted: *30 December 2020*
Published: *21 January 2021*

Citation:
Dam T, Junghans V, Humphrey J, Chouliara M and Jönsson P (2021) Calcium Signaling in T Cells Is Induced by Binding to Nickel-Chelating Lipids in Supported Lipid Bilayers. Front. Physiol. 11:613367. doi: 10.3389/fphys.2020.613367

INTRODUCTION

T-cell activation is initiated by the binding of T-cell receptors (TCRs) to their cognate antigen on a meeting cell. This results in phosphorylation of cytoplasmic immunoreceptor tyrosine-based activation motifs (ITAMs) in the TCR complex, which starts a cascade of chemical reactions resulting in the release of calcium from endoplasmic reticulum Ca^{2+} stores (Chakraborty and Weiss, 2014). The depleted Ca^{2+} stores in turn activate different Ca^{2+} release-activated calcium channels in the plasma membrane to sustain the Ca^{2+} level, ultimately resulting in cytokine production and cell activation (Lewis, 2001; Oh-hora and Rao, 2008). In a resting T cell the ITAMs are

kept unphosphorylated by the phosphatase CD45, which according to the kinetic segregation mechanism is excluded due to its large size from the close contacts formed when the TCR binds antigen (Davis and van der Merwe, 2006). TCR triggering and subsequent calcium signaling has traditionally been studied *in vitro* by ligating the TCR to antibodies coated on a glass slide, but has also been achieved using supported lipid bilayers (SLBs) containing peptide-presenting major histocompatibility complex molecules specific for the TCR (Grakoui et al., 1999; Huppa et al., 2010; O'Donoghue et al., 2013). However, recent studies have shown that T-cell signaling can also be induced without directly binding to the TCR (Chang et al., 2016; Ponjavic et al., 2018; Santos et al., 2018; Fernandes et al., 2019). The mechanism for this ligand-independent triggering is due to exclusion of CD45 from the closed contacts formed between the T cell and a functionalized surface. If the area of the close contact is sufficiently large then the TCR will have time to be net phosphorylated and triggered before it diffuses out of the contact (Davis and van der Merwe, 2006).

Supported lipid bilayers are one of the most common membrane model systems and have been used extensively to study cell-cell interactions (Castellana and Cremer, 2006; Dustin, 2009; Jönsson et al., 2016; Biswas and Groves, 2019; Jenkins et al., 2019) including ligand-independent triggering (Chang et al., 2016; Fernandes et al., 2019). Protein ligands are typically anchored to the SLB via polyhistidine-tags that bind to nickel-chelating lipids [DGS-NTA(Ni)] in the SLB (Nye and Groves, 2008). However, ligand-free SLBs containing 5% DGS-NTA(Ni) have previously been observed to bind Jurkat T cells and even induce calcium signaling in the cells (Ponjavic et al., 2018). SLBs will generally not be ligand-free, but instead functionalized with protein ligands that could shield the influence of the nickel-chelating lipids on the cell. The aim of this study was to investigate how DGS-NTA(Ni) influences calcium signaling when there are also receptor-binding ligands on the SLB and to better understand the mechanism behind this. This is important to understand how to keep SLB-binding cells in a resting state and to avoid unwanted cell signaling, but also to utilize this phenomenon as an artificial means to study the molecular mechanisms of T-cell signaling.

As a model system we used Jurkat T cells expressing non-signaling rat CD48 that binds fluorescently labeled rat CD2, which was anchored to an SLB at different concentrations. The rat CD2-CD48 (CD2-CD58 in humans) interaction is argued to align immune-cell surfaces *in vivo* to facilitate the interaction between TCRs and antigen (James and Vale, 2012; Jönsson et al., 2016). It also creates a ∼15 nm cell gap that effectively excludes CD45, an event that by itself can induce T-cell signaling by ligand-independent triggering (Chang et al., 2016; Fernandes et al., 2019). The cells were loaded with a calcium-sensitive dye that upon calcium signaling in the cells gave rise to a sharp increase in intensity. The cells were added to SLB systems with different amounts of DGS-NTA(Ni) and CD2 densities and both the fraction of cells that signaled as well as the time between cell binding and signaling was monitored. It was found that DGS-NTA(Ni) can significantly induce calcium signaling in the cells even when having CD2 in the SLB. It was furthermore demonstrated that DGS-NTA(Ni) dominated over signaling caused by ligand-independent triggering due to CD2 binding CD48 for the current system, and the fraction of signaling cells decreased to 11% when blocking the SLB with bovine serum albumin (BSA) before adding the cells. The signaling was also found to be predominantly via TCR triggering since TCR-deficient J.RT3-T3.5 cells signaled significantly less on DGS-NTA(Ni). To further investigate the mechanism by which DGS-NTA(Ni) induces calcium signaling we labeled the cells with fluorescent antibodies against CD45 and monitored how these molecules distributed in the cell-SLB contact of the different SLBs. CD45 was observed to be excluded from the cell-SLB contacts at a similar level for all CD2-containing systems, independent of the signaling fraction, indicating that the main mechanism for calcium signaling induced by DGS-NTA(Ni) in this study is not ligand-independent triggering but could instead be due to TCR binding.

METHOD

Cell Lines, Culture and Flow Cytometry

E6.1 Jurkat T cells (ATCC) expressing non-signaling rat CD48 and human leukocyte antigen DQ8-glia-α1 (HLA-DQ8-glia-α1) were made as described by Junghans et al. (2020). The cells were kept in RPMI 1640 medium (Sigma-Aldrich), which was supplemented with 10% fetal bovine serum (FBS; Sigma-Aldrich), 2% L-glutamine (Sigma-Aldrich), 1% sodium pyruvate (Sigma-Aldrich), 1% HEPES (Sigma-Aldrich), and 1% Penicillin-Streptomycin (Sigma-Aldrich). The Jurkat T cells were cultured at 37°C and 5% CO_2 and had a concentration of 5×10^5 cells/ml on the day of the experiment. THP-1 cells and J.RT3-T3.5 cells (ATCC) were cultured using the same conditions and supplemented cell medium as described above.

The amount of CD48, TCR, and CD45 on the cells was determined using flow cytometry and Quantibrite analysis (BD Biosciences). 0.5×10^6 Jurkat T cells were centrifuged for 3 min at 1,200 rpm and washed twice with phosphate-buffered saline (PBS, Merck) containing 0.05% sodium azide. The cells were labeled for 45 min at 4°C with isotype phycoerythrin (PE) α-mouse IgG1 (clone MOPC-21, #400112, BioLegend, 1:10 dilution), PE α-rat CD48 (clone OX-45, #MA5-17528, Thermo Fisher Scientific; 1:10 dilution), PE α-human CD45 (clone 2D1, #368509, BioLegend, 1:10 dilution) and PE α-human CD3 (clone OKT3, #317307, BioLegend, 1:10 dilution) and washed twice with PBS + 0.05% sodium azide before analysis in a BD Accuri C6 Flow Cytometer (BD Biosciences). BD Quantibrite PE beads (#340495, BD Biosciences) were used for quantification purposes and measured alongside the antibody-stained cells. This allowed for the calculation of the total number of antibodies per cell, which, at saturating concentrations of antibodies, was assumed to be equal to the total number of receptors per cell (Poncelet and Carayon, 1985). With the OKT3 antibody targeting CD3ε the TCR number per cell was obtained by dividing the CD3

count by two. All data were analyzed using FlowJo (v10.5.2, BD Biosciences) and Microsoft Excel (Microsoft).

Calcium Imaging and Antibody Labeling

The cells were prepared for calcium imaging following the protocol outlined by Santos et al. (2018) with minor modifications. Approximately 1×10^6 Jurkat cells were loaded with 1 μl of a 1 mM Fluo4-AM solution (#F-14217, Invitrogen) with 100 μl of supplement-free RPMI 1640 medium (Sigma-Aldrich) and 100 μl HEPES buffer saline solution (HBS; 10 mM HEPES, 150 mM NaCl, pH 7.4) supplemented with 2.5 mM probenecid (AAT Bioquest). The cell solution was incubated for 10 min at 37°C followed by a 20 min incubation at room temperature. The cells were washed three times with HBS buffer + 2.5 mM probenecid before being resuspended in 200 μl of HBS-probenecid buffer solution. 15 μl of the Fluo4-AM-loaded cell solution was added to different surfaces enclosed by a press-to-seal silicon well (4.5 mm in diameter, 1.6 mm in depth, Grace Bio-Labs).

To measure the distribution of CD45 and TCR in the cell-SLB contacts 0.25×10^6 Jurkat T cells were labeled either with 6 μg/ml of Alexa Fluor 488 conjugated anti-CD45 antibodies (clone HI30, #304017, BioLegend) or 8 μg/ml of Alexa Fluor 488 conjugated anti-CD3 antibodies (clone OKT3, #16-0037-85, Invitrogen). The anti-CD3 antibodies were fluorescently labeled using an Alexa Fluor 488 antibody labeling kit (#A20181, Invitrogen). The cells were centrifuged for 2 min at 2,000 rpm and resuspended in 250 μl HBS buffer, labeled with the respective antibody on ice for 30 min and washed with HBS buffer. The cells were added to the SLBs 15 min prior to imaging.

Supported Lipid Bilayers

Supported lipid bilayers were made using vesicle fusion and rupture on clean glass. In short, small unilamellar vesicles containing a mixture of 1-palmitoyl-2-oleoyl-*sn*-glycero-3-phosphocholine (POPC, Avanti Polar Lipids) and 1,2-dioleoyl-sn-glycero-3-[(N-(5-amino-1-carboxypentyl)iminodiacetic acid)succinyl] (DGS-NTA(Ni), #790404C; Avanti Polar Lipids) were made at different ratios. In addition, for one experiment a lipid mixture of 10 wt% of the anionic lipid 1,2-dioleoyl-*sn*-glycero-3-phospho-L-serine (DOPS, Avanti Lipids) and 90 wt% POPC was used. Glass cover slides (24 mm × 40 mm, thickness 1.5, Menzel-Gläzer) were cleaned for 30 min using a 80°C mixture of 75% sulfuric acid (99.9%, Sigma-Aldrich) and 25% hydrogen peroxide (30%, Sigma-Aldrich) and four press-to-seal silicon wells (4.5 mm in diameter, 1.6 mm in depth, Grace Bio-Labs) were attached to the clean glass slide. SLBs were formed by adding the different vesicle solutions in HBS buffer (0.5 mg lipids per ml) to each well and incubating for 1 h.

Rat CD2 molecules containing a double polyhistidine-tag (12xH) at the C-terminus and the human L3-12 TCR containing one polyhistidine-tag (6xH) each on the C-terminus of the α- and β-chain were made as described in Junghans et al. (2020) and were fluorescently labeled using an Alexa Fluor 647 antibody labeling kit (#A20186, Invitrogen). Depending on the desired ligand density, between 0.3 and 2.5 μg/ml of CD2 in HBS buffer was incubated with the SLB for 15–30 min before rinsing. The density of the CD2 molecules on the SLB was obtained from the intensity of single CD2 molecules on glass as described previously (Junghans et al., 2018, 2020). The successful formation of a mobile SLB was confirmed by fluorescence recovery after photobleaching before each experiment (Jönsson et al., 2008).

Blocking of the SLB was done with a 5% BSA solution (#A5611, Sigma-Aldrich) in HBS buffer, which was incubated with the SLB for 30 min before washing the sample. Stripping of the nickel ions from DGS-NTA(Ni) was performed with 100 mM ethylenediaminetetraacetic acid (EDTA) in HBS buffer. The EDTA solution was incubated with the SLB for 10 min before washing, a procedure that was repeated twice before adding the Jurkat T cells. In all the washing experiments the cells were added to the SLB 15 min before washing with HBS buffer.

For a subset of experiments, the Ni^{2+} ions in DGS-NTA(Ni) were replaced with either Cu^{2+} or Co^{2+} ions. A 5 wt% DGS-NTA(Ni) SLB was first washed with 100 mM EDTA as described above. The SLB was then reloaded with metal ions by incubating the SLB with a 5 mM solution of either (i) $CoCl_2$ (Sigma-Aldrich), (ii) $NiCl_2$ (Sigma-Aldrich), or (iii) $CuCl_2$ (Sigma-Aldrich) in HBS, adjusted to a pH of 7.4 with tris(hydroxymethyl)aminomethane (TRIS, Sigma-Aldrich), for 40 min before rinsing again with HBS. It was verified using fluorescence recovery after photobleaching that all the different DGS-NTA complexes bound polyhistidine-tagged CD2.

Imaging

A customized inverted Nikon Eclipse Ti microscope with a motorized stage was used for imaging of the samples using either total internal reflection fluorescence (TIRF) or epi-fluorescence microscopy. An Oxxius LBX diode laser operating at 488 nm was used to monitor the Fluo4-AM signal inside the cells as well as the anti-CD45 and anti-CD3 antibodies at the cell surface. An Oxxius LBX diode laser operating at 638 nm was used to monitor CD2 on the SLB. The images were acquired on a Photometrics Prime 95B sCMOS camera.

Cell-SLB contacts were monitored with an 100x oil immersion objective (NA 1.49, Nikon Corporation) in TIRF mode, whereas to obtain signaling fractions of triggered Jurkat T cells, the cells, containing Fluo4-AM, were visualized with a 10x air objective (Nikon Corporation) in epi-fluorescence mode. To capture the increase in Fluo4-AM intensity upon binding of Ca^{2+} ions a 150 frame long time-lapse video with a time between frames of 5 or 6 s was started at the time of cell addition to the sample. The motorized stage was used to measure four samples in each experiment. In each experiment, one of the four surfaces was coated with the anti-CD3 antibody OKT3 (clone OKT3, #16-0037-85, Invitrogen) at a concentration of 10 μg/mL for 60 min as a positive control to confirm the ability of the cells to be activated. All images were acquired with an exposure time of 100 ms via μManager version 1.4 (Edelstein et al., 2010).

Image Analysis

Calcium signaling from the bound cells was analyzed using a custom-written MATLAB script (R2020a, MathWorks). Only the first 150 cells binding to the surface were used in the

analysis, which were detected using the script pkfnd in MATLAB (Blair and Dufresne, 2020; **Supplementary Figure 1**). Cells that signaled directly on landing or were present already at frame 1 were removed from the analysis and were not included in the 150 cells that were analyzed. The intensity for each cell was plotted as a function of time. When the intensity increased above a user-set threshold value and remained above this value the cell was considered to have bound to the surface. When the intensity increased more than 2.5 times above the baseline, non-activated intensity of the bound cell, the cell was considered to have signaled (**Supplementary Figure 1**). The intensity vs. time plot for each cell was saved and inspected manually to verify that the script had classified the cell correctly (**Supplementary Figures 2, 3**). All images had the background intensity subtracted using a rolling ball radius of 50 pixels in ImageJ (1.53e) (Schneider et al., 2012).

The accumulation of CD2 in the cell contacts was detected using a customized MATLAB script as described in detail elsewhere (Jönsson et al., 2016). In short, the outline of the cell-SLB contact was created by thresholding the intensity of CD2 in the SLB to detect regions of CD2 accumulation. The average intensity in each contact was saved yielding the sum of bound and free ligands in the contact. The intensity outside the contact gave the free ligand density, which was corrected for ligand exclusion in the cell-SLB contact by 25% (Junghans et al., 2020). The intensities were converted to protein densities using the single molecule intensity from one protein as described by Junghans et al. (2018, 2020).

A line profile of the intensity through each of the cell-SLB contacts was used to analyze the anti-CD45 antibody distribution. The exclusion of CD45 from the contact was determined as $1-I_{in}/I_{out}$, where I_{in} is the intensity inside the contact and I_{out} is the maximum intensity of the anti-CD45 signal in the area outside the contact.

RESULTS

Cell Signaling on Ligand-Free SLBs

It was first assessed at what concentration of DGS-NTA(Ni) in the SLB the cells attach. Jurkat T cells on SLBs without DGS-NTA(Ni) could be washed off after being added to the SLB (**Supplementary Figure 4**). When having 1 wt% DGS-NTA(Ni) approximately half of the cells remained after washing, which increased to 90% and higher for SLBs with ≥2 wt% DGS-NTA(Ni) (**Supplementary Figure 4**). When blocking the SLBs with 5% BSA before adding the cells, the majority of cells could be washed off (**Supplementary Figure 4**). The same was true when washing the SLBs with EDTA that strips the nickel ions from the DGS-NTA(Ni) (**Supplementary Figure 4**). In addition, replacing the net negatively charged DGS-NTA(Ni) with 10 wt% of the anionic lipid DOPS did not result in cell attachment (**Supplementary Figure 4**), altogether indicating that it is the nickel ions in DGS-NTA(Ni) that are responsible for the cell attachment. The cell attachment was furthermore not restricted to Jurkat T cells since the human monocytic cell line THP-1 also bound to DGS-NTA(Ni) SLBs, and the cells could be detached after washing with EDTA (**Supplementary Figure 4**).

Having established that SLBs containing ≥2 wt% DGS-NTA(Ni) bind T cells, we investigated whether they also induces calcium signaling in the cells (**Figure 1A**). It was found that all SLBs induced calcium signaling, but to various extents. The fraction of signaling cells increased with the concentration of DGS-NTA(Ni) in the SLB and was 24 ± 5% (mean ± s.d.), 41 ± 11%, and 60 ± 10% at 2, 5, and 10 wt% DGS-NTA(Ni), respectively (**Figure 1B** and **Supplementary Movie 1–3**). This is similar to what was previously observed by Ponjavic et al. (2018) who observed a signaling fraction of around 50% for a ligand-free SLB containing 5% DGS-NTA(Ni). The fraction of cells showing calcium signaling on glass coated with the anti-CD3 antibody OKT3 was higher with 89 ± 7% (**Figure 1B** and **Supplementary Movie 4**). Whereas the signaling fraction increased with the amount of DGS-NTA(Ni) in the SLB no significant trend in the time between cell landing and signaling was observed between the different SLBs (**Figure 1C**). There was a higher spread in the signaling times for cells on SLBs compared to cells binding to OKT3-coated glass, the latter also having an average signaling time that was more than twice as fast as that of the SLBs.

In addition, SLBs containing 5 wt% DGS-NTA chelated with either (i) Co^{2+}, (ii) Ni^{2+}, or (iii) Cu^{2+} were also made. All three DGS-NTA complexes showed significant signaling, with DGS-NTA(Cu) signaling significantly more than the two other complexes (**Figure 1D**). This is in agreement with the protein affinity for Cu^{2+} being the highest of these three metal ions in immobilized metal ion affinity chromatography (Porath, 1992), illustrating that other factors than just the positive charge of the nickel ions in DGS-NTA(Ni) influences calcium signaling. It is possible that DGS-NTA(Ni) could induce calcium signaling by another mechanism than TCR triggering, for example by acting on mechanosensitive calcium channels in the plasma membrane (Pottosin et al., 2015). To investigate this, calcium signaling experiments were performed on a 5 wt% DGS-NTA(Ni) SLB with the Jurkat T cell mutant J.RT3-T3.5 that lacks the beta chain of the TCR. The J.RT3-T3.5 cells showed considerably lower signaling than Jurkat T cells with 7 ± 2% (mean ± s.d., $n = 2$) of the J.RT3-T3.5 cells signaling on 5 wt% DGS-NTA (**Figure 1E**), indicating that DGS-NTA(Ni) signaling is mainly via TCR triggering.

DGS-NTA(Ni) Dominates Signaling Also With Ligands in the SLB

It was shown in the previous section that DGS-NTA(Ni)-containing SLBs alone can induce T-cell signaling and that the fraction of cells that signal increases with the amount of DGS-NTA(Ni) in the SLB. However, SLBs will in general be functionalized with protein ligands, which might be able to shield and reduce interactions between the DGS-NTA(Ni) and the cell. To investigate the influence of ligands on calcium signaling by DGS-NTA(Ni) we next investigated how the fraction of signaling Jurkat T cells, transfected with the non-signaling receptor CD48, depends on the amount of the ligand CD2 in the SLB (**Figure 2A**). SLBs containing up to 2,000 CD2 molecules per μm^2 were made and the ligands were observed to bind to CD48 in the contacting

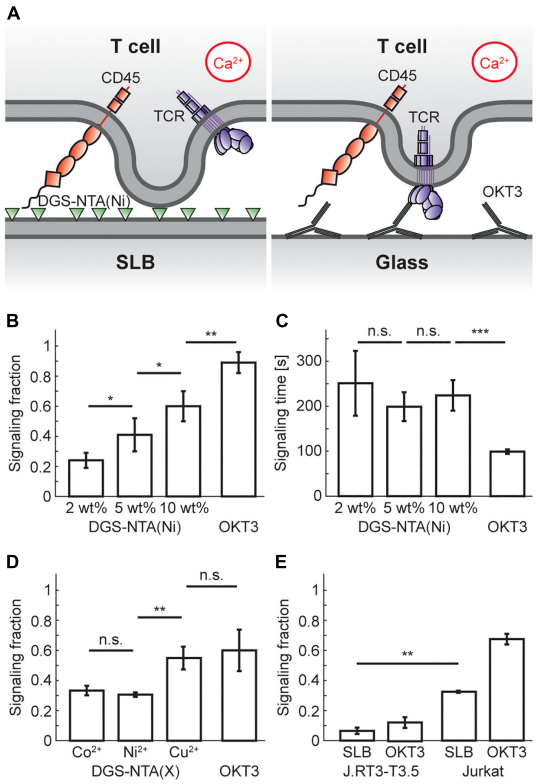

FIGURE 1 | T-cell signaling fraction increases with concentration of DGS-NTA(Ni) in the SLB. **(A)** Schematic illustration showing calcium signaling by either (*left*) DGS-NTA(Ni) in an SLB or (*right*) anti-CD3 antibodies on glass. **(B)** The fraction of signaling T cells for either ligand-free SLBs with DGS-NTA(Ni) or OKT3 on a glass slide (mean signaling fraction ± s.d.). **(C)** The time between cell landing and calcium signaling for either ligand-free SLBs with DGS-NTA(Ni) or OKT3 on a glass slide (mean signaling time ± s.d.). **(D)** The signaling fraction binding to a ligand-free SLB containing 5 wt% DGS-NTA(X), with X being either Co^{2+}, Ni^{2+} or Cu^{2+}. **(E)** The signaling fraction of J.RT3-T3.5 cells (*left*) and Jurkat T cells (*right*) on SLBs with ligand-free 5 wt% DGS-NTA(Ni) and on OKT3-coated glass. Data are shown for three to five experiments, except for E which is from two experiments, with 150 cells in each experiment. A two-sample *t*-test in MATLAB was used for statistical analysis with: * <0.05, ** <0.01, *** <0.001.

T cells (**Figure 2B**). The relative accumulation of CD2 in the cell-SLB contacts could also be presented in a Zhu-Golan plot (**Figure 2C**). The slope of the Zhu-Golan plot corresponds to $-1/K_d$ of the CD2-CD48 interaction, where K_d is the two-dimensional dissociation coefficient, whereas the intersect with the *x*-axis gives the density of mobile CD48 receptors on the cell (Zhu et al., 2007). A linear fit to the data in **Figure 2C** gave a K_d of 5 molecules per μm^2, which agrees with what has previously been measured for this interaction (Junghans et al., 2020). From the *x*-intersect a density of mobile CD48 receptors of 36 molecules per μm^2 was obtained. Assuming a cell area of 700 μm^2 and a fraction of mobile CD48 receptors of 60% (Junghans et al., 2020) this gave a total number of 42,000 CD48 molecules per cell. This is comparable to an average number of 47,000 CD48 molecules per cell measured using flow cytometry (**Supplementary Figure 5**).

The concentration of CD2 in the SLB did not change the fraction of signaling cells compared to ligand-free SLBs (**Figure 2D** and **Supplementary Movie 5,6**). Thus, SLBs with similar amounts of CD2 did signal approximately 50% more on SLBs containing 10 wt% DGS-NTA(Ni) compared to SLBs containing 5 wt% DGS-NTA(Ni). There was also no statistical difference for the signaling time with and without ligand, accessed by a two-sample *t*-test, although there was a larger spread in this data (**Figure 2E**). At a density of 2,000 CD2 molecules per μm^2 the average distance between two CD2 molecules is 22 nm, which appears to be enough for the cell surface to be able to interact with DGS-NTA(Ni) in the SLB. It is also worth stressing that there are of the order of 100,000 DGS-NTA(Ni) molecules per μm^2 in a 10 wt% DGS-NTA(Ni) SLB, and the number of available DGS-NTA(Ni) molecules in the SLB is thus negligibly affected by CD2 binding under these conditions.

BSA Blocking Reduces Calcium Signaling Without Affecting CD45 Exclusion

When blocking the CD2-functionalized SLBs with BSA before adding the cells (**Figure 3A**) the majority of cells still bound to the SLB, but, the signaling cell fraction decreased to on average 11% (**Figure 3B** and **Supplementary Movie 7**). This was not dependent on whether the SLB contained 5 or 10 wt% DGS-NTA(Ni). There appeared to be a weak increase in signaling fraction with CD2 density, but, the correlation between signaling fraction and CD2 density in **Figure 3B** was not statistically significant. A reduction of signaling to ∼10% was also observed by Ponjavic et al. (2018) when blocking a ligand-free SLB containing 5% DGS-NTA(Ni) with BSA solution, which could indicate that this value is approximately the background signaling level for these cells and that the signaling fraction above this value for the blocked SLBs is due to ligand-independent triggering caused by CD2 binding CD48.

Since the exclusion of the phosphatase CD45 from cell-SLB contacts has previously been shown to be a key event in inducing T-cell signaling (James and Vale, 2012; Cordoba et al., 2013; Chang et al., 2016) we labeled the cells with fluorescently labeled antibodies against CD45 to study the distribution of CD45 in- and outside the cell-SLB contacts. Similar to previous observations we found that CD45 was excluded from cell-SLB contacts created by CD2-CD48 binding (Chang et al., 2016; Bakalar et al., 2018; Fernandes et al., 2019; **Figure 3C**). Although the signaling fraction of cells varied significantly between SLBs with and without BSA the exclusion level of CD45 was 79% in both cases [±5% (6%) s.d., $n = 32$ (47) for a 5 wt% DGS-NTA(Ni) SLB containing ∼1,000 CD2 molecules per μm^2 with (without) BSA]. In contrast, antibodies against the TCR complex showed no clear exclusion in the cell-SLB contact (**Supplementary Figure 6**). Although the size of the antibody can potentially influence the distribution of CD45 in the contact, the found exclusion levels are nonetheless comparable to the CD45 exclusion that has previously been observed for other systems having CD2 binding CD48 on T cells (Chang et al., 2016; Fernandes et al., 2019).

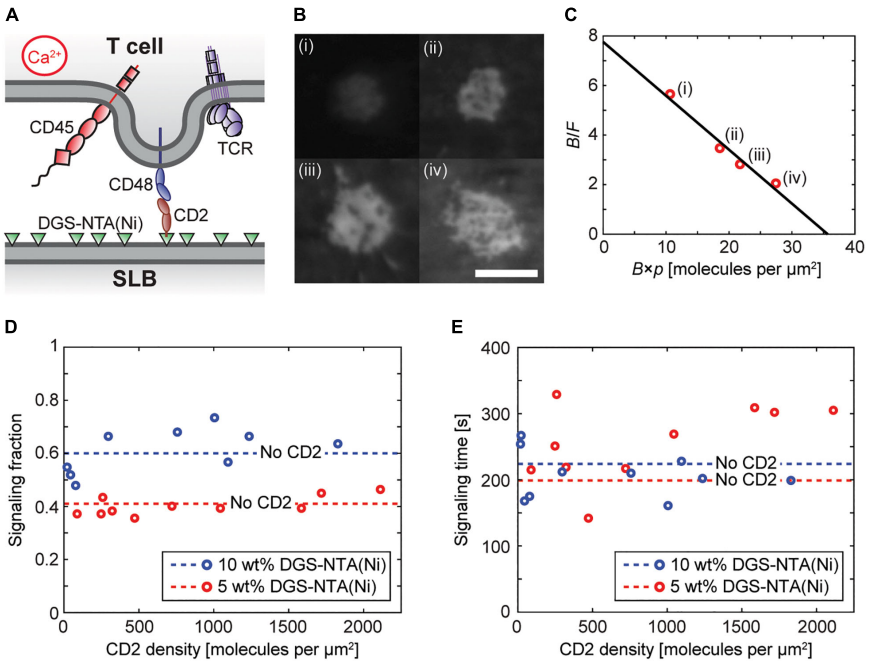

FIGURE 2 | DGS-NTA(Ni) dominates over ligand binding in inducing calcium signaling. **(A)** An illustration of a Jurkat T cell interacting with a rat CD2-functionalized SLB to induce calcium signaling. **(B)** Fluorescence images of accumulated CD2 in four different cell-SLB contacts with varying free (bound) CD2 density: (i) 68 (381) CD2 molecules per μm^2, (ii) 189 (659) CD2 molecules per μm^2, (iii) 249 (697) CD2 molecules per μm^2, and (iv) 361 (739) CD2 molecules per μm^2. The average cell-SLB contact area increased from 19 to 26 μm^2 between (i) and (iv). The scale bar is 5 μm and the scale is the same for all images. **(C)** Zhu-Golan plot for the data in (B) (red circles) with: *F*, free CD2 density; *B*, bound CD2 density; and *p*, the fraction of the cell surface area within the cell-SLB contact. The solid line is a linear fit to the data. **(D,E)** The signaling fraction and average signaling time at different densities of CD2 on SLBs containing 5 wt% DGS-NTA(Ni) (red circles) and 10 wt% DGS-NTA(Ni) (blue circles). Each data point represents one experiment with 150 analyzed cells. The dashed lines represent the average values on a ligand-free SLB [5 wt% DGS-NTA(Ni): blue dashed line, 10 wt% DGS-NTA(Ni): red dashed line].

DISCUSSION

We demonstrate how nickel-chelating lipids in an SLB can induce calcium signaling in T cells even when having protein ligands on the SLB. The fraction of cells that signaled increased with the concentration of nickel-chelating lipids and reached 60% for an SLB with 10 wt% DGS-NTA(Ni), independently of whether the SLB was functionalized with protein ligands or not. This was lower than the ∼90% signaling fraction we obtained for the same cells when using glass coated with the anti-CD3 antibody OKT3, but still of the same magnitude as observed in other studies where non-TCR ligands were responsible for inducing calcium signaling (Chang et al., 2016; Ponjavic et al., 2018). When blocking the SLB with BSA the signaling fraction decreased to 11%, indicating that ligand binding only weakly, if at all, induces calcium signaling for the current system and conditions. A reduction in signaling by nickel-chelating lipids is expected by using other blocking molecules as well, for example including polyethylene glycosylated lipids in the SLB or having higher levels of non-binding ligands. The difference in signaling fraction does not appear to be due to different levels of CD45 exclusion in the various systems, since both BSA blocked and unblocked SLBs containing CD2 showed a similar level of exclusion of CD45. This indicates that the calcium signaling induced by DGS-NTA(Ni) is caused by a different mechanism than in ligand-independent triggering. However, DGS-NTA(Ni) appears to induce signaling via TCR triggering since the fraction of signaling cells decreased significantly when using TCR-deficient J.RT3-T3.5 cells instead of Jurkat T cells. A similar signaling fraction and signaling time, both with and without BSA blocking (**Supplementary Movies 8, 9**), was furthermore observed when instead of CD2 having L3-12 TCR in the SLB, which bound to non-signaling HLA-DQ8-glia-α1 on the Jurkat T cell, and which was expressed at considerably higher levels than that of CD48 (Junghans et al., 2020).

To what extent DGS-NTA(Ni) influences calcium signaling will likely depend on both the state of the cell, its T-cell type and the experimental conditions, and for this reason it is mainly the relative changes that are of general interest. We can nevertheless say that for our system signaling via binding of the TCRs directly to antibodies on glass was the most potent, followed by DGS-NTA(Ni) and then lastly CD45 exclusion in close contacts according to ligand-independent triggering. That ligand-independent triggering caused by CD2-CD48 binding is not clearly observable in this study is in contrast to previous studies where it has been shown that creating close contacts that exclude CD45 to a similar degree as found here will trigger the TCR and induce calcium signaling for a majority of the bound cells (Chang et al., 2016; Fernandes et al., 2019). One reason for this could be that the cells used in this study express lower amounts of TCR (on average ∼4,000 TCRs per cell with

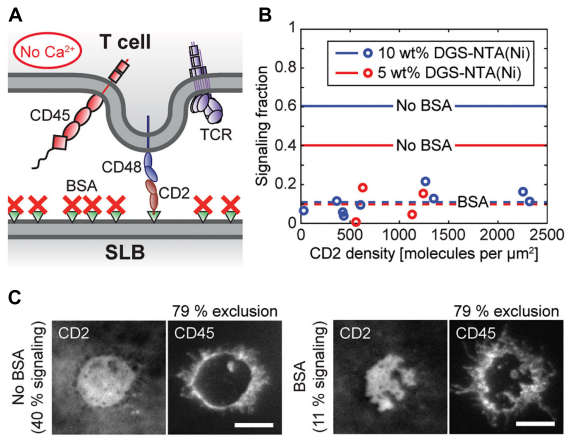

FIGURE 3 | Calcium signaling is significantly reduced upon blocking the SLB with BSA, without affecting CD45 exclusion. **(A)** Schematic illustration of the BSA-blocked and CD2-functionalized SLB in contact with a T cell. **(B)** The signaling fraction of cells on BSA-blocked SLBs containing either 5 wt% DGS-NTA(Ni) (red circles) or 10 wt% DGS-NTA(Ni) (blue circles) at different CD2 densities. Each data point represents one experiment with 150 analyzed cells. The solid lines represent the average values on a non-blocked SLB [5 wt% DGS-NTA(Ni): blue line, 10 wt% DGS-NTA(Ni): red line], whereas the dashed lines correspond to the average signaling fraction for the BSA-blocked SLBs. **(C)** Fluorescence images of two representative cell-SLB contacts in the CD2 and the CD45 channel without (*left*) and with (*right*) BSA blocking. The SLBs contained 5 wt% DGS-NTA(Ni) and had ∼1,000 CD2 molecules per μm^2. The scale bars are 5 μm.

the flow cytometry peak corresponding to ∼8,000 TCRs per cell; **Supplementary Figure 5**) compared to the Jurkat T cells and primary CD4+ T cells used in these studies (12,000–14,000 TCRs per cell for the Jurkat T cells and ∼40,000 TCRs per cell for the primary CD4+ T cells; (Fernandes et al., 2019) and personal communication with Ricardo A. Fernandes). It was found in Fernandes et al. (2019) that an average of 16 TCRs were residing in the close contact zones upon calcium signaling indicating that calcium signaling depends on multiple TCRs being triggered in close proximity. That triggering of multiple TCRs in close proximity is connected to T-cell activation has also been demonstrated in other studies (Manz et al., 2011; Lin et al., 2019). It is therefore possible that the lower density of TCR for the cells in this study is not sufficient to give rise to enough TCR triggering events to initiate calcium signaling by ligand-independent triggering alone. It should also be noted that in Chang et al. (2016), the dependence of bilayer contact on CD2-CD48 binding *per se* was controlled for by showing that cells lacking CD48 did not settle on CD2-presenting bilayers. This indicates that the interaction between the cells and DGS-NTA(Ni) was weaker for these cells than what is observed in this study for similar levels of DGS-NTA(Ni) in the SLB. Why signaling takes place when T cells bind to OKT3-coated glass or to SLBs with DGS-NTA(Ni) in this study can only be speculated about. However, one possibility is that both these systems engage the TCR to some extent, which via conformational changes could make the TCR more sensitive to signaling (Mariuzza et al., 2020). It could also be, in line with the low amount of TCR on the cells, that binding the TCR locally increases the concentration of triggered TCRs above the threshold needed to induce calcium signaling.

In summary, we show that DGS-NTA(Ni) can have a significant effect on binding T cells and induce calcium signaling even when having ligands in the SLB. The molecular mechanism by which this happens can only be speculated about but appears not to be due to increasing the level of CD45 exclusion, although this is likely one crucial part for signaling on the ligand-free SLBs. It is instead possible that the charged DGS-NTA(Ni) acts as a weak ligand for the TCR which can induce calcium signaling unless the nickel-chelating lipids are blocked. The amount of calcium signaling induced by DGS-NTA(Ni) vs. ligand-independent triggering can vary between different cells and conditions. However, it should generally be of importance to keep the nickel-chelating lipids in the SLB blocked in order to ensure minimum influence on the cells and to keep them in a resting state when binding to protein ligands on the SLB.

DATA AVAILABILITY STATEMENT

The raw data supporting the conclusions of this article are available upon request from the corresponding author, without undue reservation.

AUTHOR CONTRIBUTIONS

TD, VJ, PJ, and JH: conceptualization. TD and MC: formal analysis. TD: investigation. PJ and VJ: resources and supervision. TD and PJ: writing – original draft and visualization. TD, PJ, and VJ: writing – review and editing. PJ: project administration and funding acquisition. All authors contributed to the article and approved the submitted version.

FUNDING

PJ has received funding from the European Research Council (ERC) under the European Union's Horizon 2020 Research and Innovation Program (grant agreement no. 757797) and the Swedish Research Council (grant number no. 2018-03872).

ACKNOWLEDGMENTS

The authors thank S. Davis, K. Ganzinger, and R. Fernandes for general input on the manuscript and A. Ponjavic and E. Jenkins for useful discussions on calcium-signaling measurements and analysis.

SUPPLEMENTARY MATERIAL

The Supplementary Material for this article can be found online at: https://www.frontiersin.org/articles/10.3389/fphys.2020.613367/full#supplementary-material

REFERENCES

Bakalar, M. H., Joffe, A. M., Schmid, E. M., Son, S., Podolski, M., and Fletcher, D. A. (2018). Size-dependent segregation controls macrophage phagocytosis of antibody-opsonized targets. *Cell* 174, 131–142.e13. doi: 10.1016/j.cell.2018.05.059

Biswas, K. H., and Groves, J. T. (2019). Hybrid live cell–supported membrane interfaces for signaling studies. *Annu. Rev. Biophys.* 48, 537–562. doi: 10.1146/annurev-biophys-070317-033330

Blair, D., and Dufresne, E. (2020). *The Matlab Particle Tracking Code Repository*. Available online at: http://site.physics.georgetown.edu/matlab/code.html (accessed September 18, 2020).

Castellana, E. T., and Cremer, P. S. (2006). Solid supported lipid bilayers: from biophysical studies to sensor design. *Surf. Sci. Rep.* 61, 429–444. doi: 10.1016/j.surfrep.2006.06.001

Chakraborty, A. K., and Weiss, A. (2014). Insights into the initiation of TCR signaling. *Nat. Immunol.* 15, 798–807. doi: 10.1038/ni.2940

Chang, V. T., Fernandes, R. A., Ganzinger, K. A., Lee, S. F., Siebold, C., McColl, J., et al. (2016). Initiation of T cell signaling by CD45 segregation at "close contacts." *Nat. Immunol.* 17, 574–582. doi: 10.1038/ni.3392

Cordoba, S. P., Choudhuri, K., Zhang, H., Bridge, M., Basat, A. B., Dustin, M. L., et al. (2013). The large ectodomains of CD45 and CD148 regulate their segregation from and inhibition of ligated T-cell receptor. *Blood* 121, 4295–4302. doi: 10.1182/blood-2012-07-442251

Davis, S. J., and van der Merwe, P. A. (2006). The kinetic-segregation model: TCR triggering and beyond. *Nat. Immunol.* 7, 803–809. doi: 10.1038/ni1369

Dustin, M. L. (2009). Supported bilayers at the vanguard of immune cell activation studies. *J. Struct. Biol.* 168, 152–160. doi: 10.1016/j.jsb.2009.05.007

Edelstein, A., Amodaj, N., Hoover, K., Vale, R., and Stuurman, N. (2010). Computer control of microscopes using manager. *Curr. Protoc. Mol. Biol.* 92, 1–22. doi: 10.1002/0471142727.mb1420s92

Fernandes, R. A., Ganzinger, K. A., Tzou, J. C., Jönsson, P., Lee, S. F., Palayret, M., et al. (2019). A cell topography-based mechanism for ligand discrimination by the T cell receptor. *Proc. Natl. Acad. Sci. U.S.A.* 116, 14002–14010. doi: 10.1073/pnas.1817255116

Grakoui, A., Bromley, S. K., Sumen, C., Davis, M. M., Shaw, A. S., Allen, P. M., et al. (1999). The immunological synapse: a molecular machine controlling T cell activation. *Science* 285, 221–227. doi: 10.1126/science.285.5425.221

Huppa, J. B., Axmann, M., Mörtelmaier, M. A., Lillemeier, B. F., Newell, E. W., Brameshuber, M., et al. (2010). TCR–peptide–MHC interactions in situ show accelerated kinetics and increased affinity. *Nature* 463, 963–967. doi: 10.1038/nature08746

James, J. R., and Vale, R. D. (2012). Biophysical mechanism of T-cell receptor triggering in a reconstituted system. *Nature* 487, 64–69. doi: 10.1038/nature11220

Jenkins, E., Santos, A. M., O'Brien-Ball, C., Felce, J. H., Wilcock, M. J., Hatherley, D., et al. (2019). Reconstitution of immune cell interactions in free-standing membranes. *J. Cell Sci.* 132:jcs219709. doi: 10.1242/jcs.219709

Jönsson, P., Jonsson, M. P., Tegenfeldt, J. O., and Höök, F. A. (2008). Method improving the accuracy of fluorescence recovery after photobleaching analysis. *Biophys. J.* 95, 5334–5348. doi: 10.1529/biophysj.108.134874

Jönsson, P., Southcombe, J. H., Santos, A. M., Huo, J., Fernandes, R. A., McColl, J., et al. (2016). Remarkably low affinity of CD4/peptide-major histocompatibility complex class II protein interactions. *Proc. Natl. Acad. Sci. U.S.A.* 113, 5682–5687. doi: 10.1073/pnas.1513918113

Junghans, V., Chouliara, M., Santos, A. M., Hatherley, D., Petersen, J., Dam, T., et al. (2020). Effects of a local auxiliary protein on the two-dimensional affinity of a TCR–peptide MHC interaction. *J. Cell Sci.* 133:jcs245985. doi: 10.1242/jcs.245985

Junghans, V., Hladilkova, J., Santos, A. M., Lund, M., Davis, S. J., and Jönsson, P. (2018). Hydrodynamic trapping measures the interaction between membrane-associated molecules. *Sci. Rep.* 8:12479. doi: 10.1038/s41598-018-30285-0

Lewis, R. S. (2001). Calcium signaling in T cells. *Annu. Rev. Immunol.* 19, 497–521. doi: 10.1146/annurev.immunol.19.1.497

Lin, J. J. Y., Low-Nam, S. T., Alfieri, K. N., McAffee, D. B., Fay, N. C., and Groves, J. T. (2019). Mapping the stochastic sequence of individual ligand-receptor binding events to cellular activation: T cells act on the rare events. *Sci. Signal.* 12, 1–14. doi: 10.1126/scisignal.aat8715

Manz, B. N., Jackson, B. L., Petit, R. S., Dustin, M. L., and Groves, J. (2011). T-cell triggering thresholds are modulated by the number of antigen within individual T-cell receptor clusters. *Proc. Natl. Acad. Sci. U.S.A.* 108, 9089–9094. doi: 10.1073/pnas.1018771108

Mariuzza, R. A., Agnihotri, P., and Orban, J. (2020). The structural basis of T-cell receptor (TCR) activation: an enduring enigma. *J. Biol. Chem.* 295, 914–925. doi: 10.1074/jbc.REV119.009411

Nye, J. A., and Groves, J. T. (2008). Kinetic control of histidine-tagged protein surface density on supported lipid bilayers. *Langmuir* 24, 4145–4149. doi: 10.1021/la703788h

O'Donoghue, G. P., Pielak, R. M., Smoligovets, A. A., Lin, J. J., and Groves, J. T. (2013). Direct single molecule measurement of TCR triggering by agonist pMHC in living primary T cells. *eLife* 2:e00778. doi: 10.7554/eLife.00778

Oh-hora, M., and Rao, A. (2008). Calcium signaling in lymphocytes. *Curr. Opin. Immunol.* 20, 250–258. doi: 10.1016/j.coi.2008.04.004

Poncelet, P., and Carayon, P. (1985). Cytofluorometric quantification of cell-surface antigens by indirect immunofluorescence using monoclonal antibodies. *J. Immunol. Methods* 85, 65–74. doi: 10.1016/0022-1759(85)90274-1

Ponjavic, A., McColl, J., Carr, A. R., Santos, A. M., Kulenkampff, K., Lippert, A., et al. (2018). Single-Molecule Light-Sheet Imaging of Suspended T Cells. *Biophys. J.* 114, 2200–2211. doi: 10.1016/j.bpj.2018.02.044

Porath, J. (1992). Immobilized metal ion affinity chromatography. *Protein Expr. Purif.* 3, 263–281. doi: 10.1016/1046-5928(92)90001-D

Pottosin, I., Delgado-Enciso, I., Bonales-Alatorre, E., Nieto-Pescador, M. G., Moreno-Galindo, E. G., and Dobrovinskaya, O. (2015). Mechanosensitive Ca2+-permeable channels in human leukemic cells: pharmacological and molecular evidence for TRPV2. *Biochim. Biophys. Acta Biomembr.* 1848, 51–59. doi: 10.1016/j.bbamem.2014.09.008

Santos, A. M., Ponjavic, A., Fritzsche, M., Fernandes, R. A., de la Serna, J. B., Wilcock, M. J., et al. (2018). Capturing resting T cells: the perils of PLL. *Nat. Immunol.* 19, 203–205. doi: 10.1038/s41590-018-0048-8

Schneider, C. A., Rasband, W. S., and Eliceiri, K. W. (2012). NIH image to imagej: 25 years of image analysis. *Nat. Methods* 9, 671–675. doi: 10.1038/nmeth.2089

Zhu, D.-M., Dustin, M. L., Cairo, C. W., and Golan, D. E. (2007). Analysis of two-dimensional dissociation constant of laterally mobile cell adhesion molecules. *Biophys. J.* 92, 1022–1034. doi: 10.1529/biophysj.106.089649

Conflict of Interest: The authors declare that the research was conducted in the absence of any commercial or financial relationships that could be construed as a potential conflict of interest.

frontiers in Immunology

ORIGINAL RESEARCH
published: 12 February 2021
doi: 10.3389/fimmu.2020.613286

Characterization of the Signaling Modalities of Prostaglandin E2 Receptors EP2 and EP4 Reveals Crosstalk and a Role for Microtubules

Ward Vleeshouwers[1], Koen van den Dries[1], Sandra de Keijzer[1], Ben Joosten[1], Diane S. Lidke[2,3] and Alessandra Cambi[1]**

[1] Department of Cell Biology, Radboud Institute for Molecular Life Sciences, Radboud University Medical Center, Nijmegen, Netherlands, [2] Department of Pathology, University of New Mexico Health Sciences Center, Albuquerque, NM, United States, [3] Comprehensive Cancer Center, University of New Mexico Health Sciences Center, Albuquerque, NM, United States

OPEN ACCESS

Edited by:
Erdinc Sezgin, Karolinska Institutet (KI), Sweden

Reviewed by:
Mezida B. Saeed, Karolinska Institutet (KI), Sweden
Huw Colin-York, University of Oxford, United Kingdom

***Correspondence:**
Alessandra Cambi
alessandra.cambi@radboudumc.nl
Diane S. Lidke
dlidke@salud.unm.edu

Specialty section:
This article was submitted to Molecular Innate Immunity, a section of the journal Frontiers in Immunology

Received: *01 October 2020*
Accepted: *18 December 2020*
Published: *12 February 2021*

Citation:
Vleeshouwers W, van den Dries K, de Keijzer S, Joosten B, Lidke DS and Cambi A (2021) Characterization of the Signaling Modalities of Prostaglandin E2 Receptors EP2 and EP4 Reveals Crosstalk and a Role for Microtubules. Front. Immunol. 11:613286. doi: 10.3389/fimmu.2020.613286

Prostaglandin E2 (PGE2) is a lipid mediator that modulates the function of myeloid immune cells such as macrophages and dendritic cells (DCs) through the activation of the G protein-coupled receptors EP2 and EP4. While both EP2 and EP4 signaling leads to an elevation of intracellular cyclic adenosine monophosphate (cAMP) levels through the stimulating $G\alpha_s$ protein, EP4 also couples to the inhibitory $G\alpha_i$ protein to decrease the production of cAMP. The receptor-specific contributions to downstream immune modulatory functions are still poorly defined. Here, we employed quantitative imaging methods to characterize the early EP2 and EP4 signaling events in myeloid cells and their contribution to the dissolution of adhesion structures called podosomes, which is a first and essential step in DC maturation. We first show that podosome loss in DCs is primarily mediated by EP4. Next, we demonstrate that EP2 and EP4 signaling leads to distinct cAMP production profiles, with EP4 inducing a transient cAMP response and EP2 inducing a sustained cAMP response only at high PGE2 levels. We further find that simultaneous EP2 and EP4 stimulation attenuates cAMP production, suggesting a reciprocal control of EP2 and EP4 signaling. Finally, we demonstrate that efficient signaling of both EP2 and EP4 relies on an intact microtubule network. Together, these results enhance our understanding of early EP2 and EP4 signaling in myeloid cells. Considering that modulation of PGE2 signaling is regarded as an important therapeutic possibility in anti-tumor immunotherapy, our findings may facilitate the development of efficient and specific immune modulators of PGE2 receptors.

Keywords: membrane receptor, prostaglandin E2 signaling, myeloid cells, G protein-coupled receptor, podosome

INTRODUCTION

The ability of cells to respond to their environment is critical for their function. Important players for transmitting extracellular information into intracellular signaling events are the G protein-coupled receptors (GPCRs) (1). The spatiotemporal organization of GPCRs within the cell membrane allows these receptors to elicit fine-tuned cellular responses to different ligands.

Prostaglandins are lipid mediators that represent an abundant type of GPCR ligand. Prostaglandins are derived from cyclooxygenase (COX)-catalyzed metabolism of arachidonic acid and exhibit versatile actions in a wide variety of tissues (2, 3). Prostaglandin E2 (PGE2) signals *via* the four GPCRs EP1-4, expressed in various combinations at the plasma membrane of cells (4). PGE2 modulates several key immunological processes including the activation, migration and cytokine production of different immune cells such as dendritic cells (DCs), macrophages and T lymphocytes (3, 5–8). Despite being a known mediator of inflammation, increased PGE2 concentrations have been associated with a highly immunosuppressive tumor microenvironment (TME) of several cancer types (9–13).

DCs are commonly observed in the TME of solid tumors (14). Yet, despite their potential to generate anti-tumor immunity, TME-resident DCs often exhibit impaired or defective function (15). The high PGE2 levels in the TME might play a role in the suppression of DC phenotype since PGE2 promotes IL-10 production by DCs (16). On the other hand, by stimulating the dissolution of actin-rich adhesion structures called podosomes, PGE2 is also important for inducing the highly migratory phenotype typical of mature DCs and crucial in immunity (6). Understanding how PGE2 exerts its dual function in DCs can offer novel leads to reverse unwanted DC immunosuppression in the context of anti-tumor immunity.

PGE2 modulates DC function exclusively *via* EP2 and EP4 (6, 17, 18). For example, PGE2 has previously been shown to induce the dissolution of podosomes through the cAMP-PKA-RhoA signaling axis downstream of EP2 and EP4 (8). PGE2-induced podosome dissolution is an important step toward DC maturation and the acquisition of a highly migratory phenotype, but the receptor-specific contributions to these processes are still poorly defined.

Signaling *via* EP2 and EP4 is predominantly transduced by the stimulating Gα protein ($G\alpha_s$), leading to increased activity of adenylate cyclase (AC) and subsequent elevation of intracellular cyclic adenosine monophosphate (cAMP) levels (19, 20). An important difference between EP2 and EP4 is the reported capacity of EP4 to also couple to inhibitory Gα protein ($G\alpha_i$), thereby inhibiting cAMP formation and activating a phosphatidylinositol 3-kinase (PI3K) pathway (21, 22). Furthermore, in contrast to EP2, EP4 is rapidly internalized upon ligand binding (23–25). Altogether, these observations suggest that signal modalities (intensity, duration, downstream effectors) likely differ between EP2 and EP4 and that a better understanding of EP2 and EP4 differential signaling is key to understanding and predicting the effects of PGE2 in DC biology.

Here, we aimed to characterize EP2 and EP4 early signaling events in response to PGE2 in myeloid cells and link them to the dissolution of podosomes in DCs. We first demonstrate that in DCs, PGE2 leads to podosome dissolution primarily through EP4 signaling. Next, we show that selective EP2 and EP4 stimulation leads to distinct cAMP production profiles and suggest reciprocal control of receptor signaling efficiency. Finally, we demonstrate that the integrity of the cortical microtubule network is important for efficient EP2 and EP4 signaling. Modulation of PGE2 signaling is considered an important therapeutic possibility in anti-tumor immunotherapy. Our findings enhance our understanding of early EP2 and EP4 signaling and may thereby facilitate the development of efficient and specific modulators of PGE2 signaling receptors that can contribute to reverse tumor immunosuppression (26).

MATERIALS AND METHODS

Chemicals and Reagents

Cells were treated with several compounds that activated or inhibited EP2 and EP4 (see database of FDA-approved compounds at www.bindingdb.org for pharmacological details): EP2 agonist (R)-Butaprost (Sigma), EP4 agonist L-902688 (Cayman Chemicals), EP2 competitive antagonist AH6809 (Cayman Chemicals), EP4 competitive antagonist GW627368X (Cayman Chemicals) or AH23848 (Cayman Chemicals), pertussis toxin (TOCRIS biosciences), PGE2 (Cayman Chemicals), Pertussis Toxin (PTx, Calbiochem, San Diego, CA) and nocodazole (Sigma). Concentrations used for the various compounds are based on previous literature (27–31) in combination with viability assays (performed by Trypan Blue staining). Compounds used for immunofluorescence staining were mouse anti-vinculin antibody (Sigma, V9131), Goat anti-Mouse-(H&L)-Alexa488 and Goat anti-Mouse-(H&L)-Alexa647 secondary antibodies (Invitrogen), Alexa488-conjugated phalloidin (Invitrogen, A12379) and Texas Red-conjugated phalloidin (Invitrogen, T7471), Mowiol (Sigma).

Cell Culture

RAW 246.7 cells were cultured in RPMI-1640 medium (Gibco) supplemented with 10% Fetal Bovine Serum (FBS, Greiner Bio-one), 1mM Ultra-glutamine (BioWitthaker) and 0.5% Antibiotic-Antimytotic (AA, Gibco). iDCs were derived from PBMCs as described previously (32, 33) and cultured in RPMI 1640 medium (Gibco) supplied with 10% Fetal Bovine Serum (FBS, Greiner Bio-one). Transfections with t-Epac-vv (34) (gift from K. Jalink), $G\alpha_s$-GFP (gift from M. Rasenick), $G\alpha_i$-GFP and $G\alpha_{i1}$-Citrine (35) (gift from A. Gilman), $G\gamma_2$-CFP and $G\beta_1$ wildtype (both gifts from M. Adjobo-Hermans) were performed with Fugene HD (Roche) according to the manufacturer protocol and imaged after 24 h. Stable cell lines expressing $G\alpha_s$-GFP and $G\alpha_i$-GFP was maintained using the appropriate antibiotics. Cells were plated one day prior to measurements or transfection in Willco dishes (Willco Wells BV) at 400,000 cells/dish or in 96 well-plate (microplate BD Falcon) at 40,000 cells/well or in 4-well Lab-Tek II chambered coverglass (Nunc) at 100,000 cells/chamber. Prior to imaging, the medium was replaced with 1 ml RPMI medium without phenol red to avoid background fluorescence.

Podosome Dissolution Assay and Widefield Immunofluorescence

For agonist experiments, iDCs were treated with (R)-Butaprost, L-902688 or 10 μM PGE2 for 10 min. For antagonist and pertussis toxin experiments, iDCs were pretreated with 3 μM AH6809 for 1 h, 10 μM GW627368X for 1 h, 100 ng/ml pertussis toxin for 16 h as previously described (22) or left untreated prior to the addition of PGE2. After stimulation, iDCs were fixed in 3.7% (w/v) formaldehyde in PBS for 10 min. Cells were permeabilised in 0.1% (v/v) Triton X-100 in PBS for 5 min and blocked with 2% (w/v) BSA in PBS. The cells were incubated with mouse anti-vinculin antibody for 1 h. Subsequently, the cells were washed with PBS and incubated with GaM-(H&L) secondary antibody and phalloidin for 45 min. Lastly, samples were washed with PB prior to embedding in Mowiol. Cells were imaged on a Leica DM fluorescence microscope with a 63× PL APO 1.3 NA oil immersion lens and a COHU high-performance integrating CCD camera (COHU, San Diego, CA) or a Zeiss LSM 510 microscope equipped with a PlanApochromatic 63x/1.4 NA oil immersion objective. Images were analyzed using Fiji-based software (36).

Förster Resonance Energy Transfer Experiments

RAW macrophages expressing t-Epac-vv were imaged using a BD Pathway high-content imaging inverted widefield microscope (BD biosciences) equipped with a 20X 0.75 N.A. objective (Olympus LUCPLFLN). A mercury metal halide lamp combined with an excitation filter (440/10) was used to excite mTurqoise. The fluorescence emission was filtered using a dichroic mirror (458-DiO1) and filters (479/40 and 542/27 for mTurquoise and Venus emission, respectively). Emission was collected by a high-resolution cooled CCD camera (1344x1024 pix, 0.32 μm/pix). Samples were prepared in a 96 well-plate (microplate BD Falcon) from which the inner 60 wells were used. Cells were pretreated with 100 ng/ml pertussis toxin for 16 h or left untreated before adding 3 μM AH6809 for 1 h, or 10 μM GW627368X for 1 h, with and without 5 μM nocodazole for 20 min, Six mTurquoise and Venus emission images were acquired followed by automated addition of PGE2 and subsequent acquisition of another 20 mTurquoise and Venus emission images (t_{lag}=10 s). The mean fluorescence intensity of the Venus and mTurquoise signal in a cell was corrected by subtraction of the background signal in each image and channel before dividing the Venus over mTurquoise mean fluorescence intensity to obtain the FRET ratio. Values were normalized to the average ratio value of the first six pre-stimulus data points.

Fluorescence Lifetime Imaging Experiments

Frequency-domain FLIM experiments on transfected RAW macrophages were performed using a Nikon TE2000-U inverted widefield microscope and a Lambert Instruments Fluorescence Attachment (LIFA; Lambert Instruments) for lifetime imaging. A light-emitting diode (Lumiled LUXEON III, λ_{max} = 443 nm) modulated at 40 MHz was used to excite CFP. Fluorescence detection was performed by a combination of a modulated (40 MHz) image intensifier (II18MD; Lambert Instruments) and a 640x512 pixel CCD camera (CCD-1300QD; VDS Vosskühler). The emission of CFP was detected through a narrow emission filter (475/20 nm; Semrock) to suppress any fluorescence emission from the Citrine fluorophore. FLIM measurements were calibrated with a 1 μM solution of pyranine (HPTS), the lifetime of which was set to 5.7 ns. All FLIM images were calculated from phase stacks of 12 recorded images, with exposure times of individual images ranging from 200 to 400 ms. A USH-102DH 100 W mercury lamp (Nikon) was used for acceptor photobleaching. Cells were pretreated with 25 μM AH23848 for 1 h or left untreated and cells were stimulated with 10 μM PGE2 or 10 μM Butaprost.

Statistics and Reproducibility

All image processing was performed using Fiji/ImageJ software. Podosome count was performed semi-automatically. Briefly, a median filter (3 pixel radius) was applied to the phalloidin image after which the podosome clusters were manually selected. The Fiji maximum finder was subsequently used to detect and count the podosomes. Data from the podosome dissolution assay and the FRET experiments were processed using Microsoft Excel and GraphPad Prism 8 software. Data from the FLIM experiments were analyzed using OriginPro 8. All statistical analyses were performed using GraphPad Prism 8. The specific statistical test, the multiple testing corrections and the number of replicates used for each Figure are specified in the Figure legend. The normality of data distributions was assessed by visual data inspection and the Shapiro-Wilk normality test. *P*-values < 0.05 were considered statistically significant for all experiments. Statistical analyses were only performed for the comparisons indicated in the Figures.

RESULTS

EP4 Primarily Contributes to Prostaglandin E2-Induced Podosome Dissolution in Dendritic Cells

To assess the different contributions of EP2 and EP4 in mediating PGE2 signaling in DCs, we first determined whether both EP2 and EP4 signaling can lead to podosome dissolution. For this, we treated immature DCs (iDCs) with PGE2 or well-established and selective EP2 and EP4 agonists and quantified the number of podosomes per cell (**Figures 1A, B**). In line with our previous observations, the addition of PGE2 resulted in an almost complete loss of podosomes in iDCs. Interestingly, both EP2- and EP4-specific stimulation also reduced the number of podosomes, with EP4 agonist stimulation being slightly more efficient (**Figure 1B**). These results indicate that individual EP2 and EP4 downstream signaling can both lead to podosome dissolution.

After having established that both EP2 and EP4 signaling can lead to podosome dissolution, we aimed to investigate the

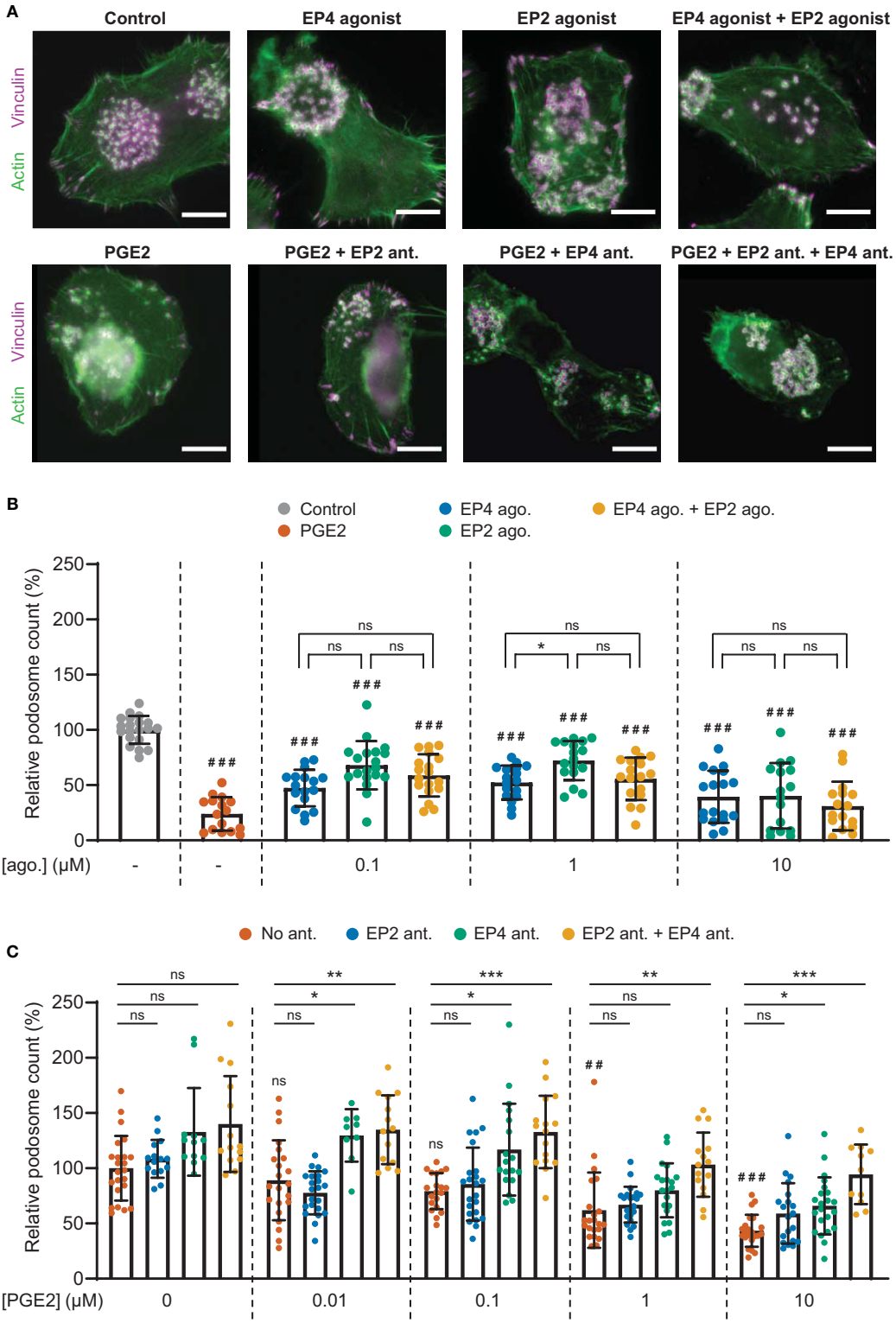

FIGURE 1 | Continued

FIGURE 1 | Prostaglandin E2 (PGE2)-induced podosome dissolution in human immature dendritic cells (iDCs) is mostly mediated by EP4. **(A)** Representative images of PBMC-derived iDCs that were left untreated or were treated with 1 μM EP4 agonist L-902688, 1 μM EP2 agonist (R)-Butaprost, both 1 μM L-902688 and 1 μM (R)-Butaprost, 1 μM PGE2 alone or 1 μM PGE2 after pretreatment with EP2 antagonist (ant.) AH6809, EP4 antagonist GW627368X or both AH6809 and GW627368X. Cells were stained for actin (green) and vinculin (magenta). Scale bar = 10 μm. **(B)** iDCs were treated with different concentrations of EP2 agonist (ago.) (R)-Butaprost, EP4 agonist L-902688 or both (R)-Butaprost and L-902688. Cells were stained for actin and vinculin and the number of podosomes per image was quantified and normalized to untreated control. Cells treated with 10 μM PGE2 were included as positive control. The error bars represent mean ± SD. Data presented are from two different donors. ns, not significant, *P<0.05; ###P<0.001 versus untreated control, Welch ANOVA with Dunnett's T3 multiple comparison test. **(C)** iDCs were treated with different concentrations of PGE2 with or without pretreatment with EP2 antagonist (ant.) AH6809, EP4 antagonist GW627368X or both AH6809 and GW627368X. Cells were stained for actin and vinculin and the number of podosomes per image was quantified and normalized to untreated control. The error bars represent mean ± SD. Data presented are from three different donors. ns, not significant, *P<0.05, **P<0.01, ***P<0.001; ##P<0.01, ###P<0.001 versus untreated control, Welch ANOVA with Dunnett's T3 multiple comparison test.

respective contribution of EP2 and EP4 signaling. We reasoned that this would be difficult to assess by using the agonists because of the different affinities for their respective receptor. Therefore, we instead pretreated the cells with well-characterized and selective competitive EP2 and EP4 antagonists to block signaling, followed by the stimulation with the natural ligand PGE2, and subsequently quantified podosome dissolution. **Figure 1C** shows that inhibition of EP4 attenuates podosome dissolution upon stimulation with 0.01–0.1 μM PGE2, while blocking of EP2 has no effect. This indicates that at lower PGE2 concentrations, EP4 is responsible for the induction of podosome loss. Interestingly, at 1 μM PGE2, EP4 blocking attenuates podosome dissolution only when EP2 antagonist is co-administered, suggesting that EP2 triggering by PGE2 could somehow influence EP4 activity. At the highest PGE2 concentration (10 μM), one cannot fully exclude that the antagonists are not displaced by the PGE2, which complicates the interpretation of these specific results.

Together, these results suggest that EP4 primarily contributes to PGE2-induced podosome dissolution. Importantly, in subsequent experiments we use selective receptor antagonists in combination with the natural ligand PGE2 to define the individual contributions of EP2 and EP4 in mediating PGE2 signaling.

EP2 and EP4 Differentially Stimulate cAMP Production

PGE2-induced podosome loss in DCs is mediated by the cAMP-PKA-RhoA signaling axis downstream of EP2 and EP4 (8). Since our results strongly suggest that EP4 is primarily responsible for podosome loss, we sought to determine whether EP4 induces stronger cAMP responses to PGE2 than EP2. To determine the individual contribution of EP2 and EP4 to the PGE2-induced increase of intracellular cAMP levels, we measured the onset of cAMP production in living RAW macrophages, which endogenously express both EP2 and EP4 (**Supplementary Figure 1**) (37) and are well-accepted as surrogate cell model to study DCs (38), using ratio measurements of the Förster Resonance Energy Transfer (FRET)-based cAMP sensor t-Epac-vv (34). Since the binding of cAMP to t-Epac-vv reduces FRET between the mTurquoise donor and Venus acceptor fluorophores, a decreased FRET ratio in the macrophages is a direct measure of cAMP production (**Figures 2A, B**). After the addition of PGE2, cAMP was produced immediately and reached a maximum concentration after about 40 seconds, subsiding to lower levels after 200 seconds (**Figure 2C**). To compare the cAMP kinetics across different treatment conditions, we quantified the peak of cAMP production and the production rate, as shown in **Figure 2D**. Both parameters scaled with increasing PGE2 concentrations, indicating that the rate and the magnitude of the induced cAMP response is dose-dependent (**Figure 2E**).

Compared to PGE2 only, EP2 inhibition led to higher cAMP levels at all tested PGE2 concentrations, while cAMP concentrations subsided to a similar extent (**Figure 2F**). The PGE2-induced cAMP production rate and cAMP peak remained dose-dependent upon EP2 inhibition as both parameters scaled with PGE2 concentration (**Figure 2G**). These results indicate that EP2 blockade increases the signaling efficiency of EP4 in response to PGE2. Inhibition of EP4 led to a dramatically different course of cAMP production. In contrast to EP2 inhibition, EP4 inhibition prevented robust cAMP production at PGE2 concentrations up to 0.1 μM but allowed a strong cAMP response at ≥ 1 μM (**Figures 2H, I**). Furthermore, this strong cAMP response did not attenuate as observed in the absence of EP4 inhibition. Compared to PGE2 only, the magnitude of the strong cAMP response observed upon EP4 inhibition suggests that EP4 activity may somehow impair the signaling efficiency of EP2. To ascertain that EP2 and EP4 are completely blocked by the antagonist concentrations used in our experiments, we measured cAMP production upon simultaneous inhibition of EP2 and EP4 (**Figure 2J**). Pretreatment with both antagonists effectively inhibited total cAMP production at 0.1 and 1 μM PGE2, showing that both receptors are completely blocked at physiological concentrations of PGE2 (**Figures 2J, K**). Importantly, since 10 μM PGE2 still induced a small amount of cAMP, even in the presence of both antagonists (**Figure 2J**), we decided to omit this condition in subsequent experiments, since either one or both of the antagonist may be displaced by the high concentration of PGE2.

Our results demonstrate that the selective stimulation of EP2 and EP4 by PGE2 induces kinetically distinct cAMP production profiles. While PGE2-EP4 signaling results in a fast and transient cAMP production that increases proportionally to the ligand concentrations, PGE2-EP2 signaling is induced only by PGE2 concentrations of 1 μM and higher, and cAMP elevation is more prolonged. We also show that co-stimulation of EP2 and EP4 mutually dampens their signaling efficiency, as both receptors induce higher cAMP production when they are individually triggered by PGE2.

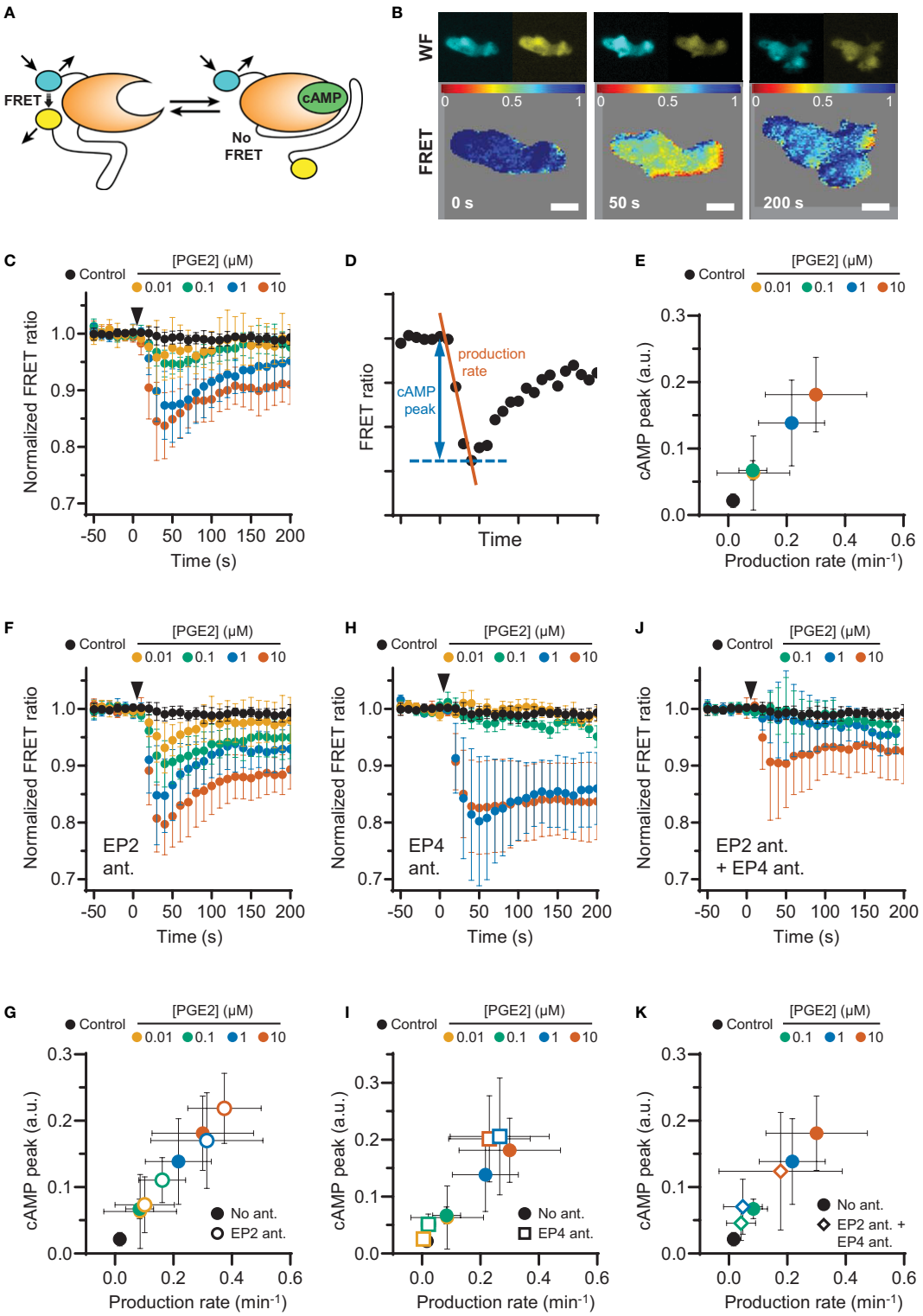

FIGURE 2 | Continued

FIGURE 2 | EP2 and EP4 induce distinct cyclic adenosine monophosphate (cAMP) responses. **(A)** Schematic illustration of intramolecular cAMP FRET sensor t-Epac-vv. Binding of cAMP to t-Epac-vv reduces Förster Resonance Energy Transfer (FRET) between the mTurquoise donor and Venus acceptor fluorophores of t-Epac-vv, making a decreased ratio of the fluorescent intensities a direct measure of cAMP accumulation [adapted from (34)]. **(B)** The mTurquoise (cyan) and Venus (yellow) signal were acquired with widefield microscopy (WF panels). After background subtraction in each image and channel, the FRET ratio was calculated as the Venus intensity over the mTurquoise intensity for each timepoint and was normalized to the average of prestimulus values (FRET panels). Normalized FRET values range from 0 (red) to 1 (blue). Scale bar = 5 μm. **(C)** FRET ratios of t-Epac-vv before and after the addition of different prostaglandin E2 (PGE2) concentrations were measured in transiently transfected RAW macrophages. A control was performed with the addition of buffer only. The data presented are mean ± SD from ≥5 cells per condition. **(D)** Example FRET curve that illustrates the definition of the relative cAMP peak and cAMP production rate. The amplitude of the cAMP peak was defined as the maximal decrease in FRET ratio. The cAMP production rate was quantified by determining the slope between the final prestimulus timepoint and the timepoint at which minimal FRET ratios were observed using a linear fit over all included timepoints. **(E)** The cAMP production peak and the cAMP production rate were measured from the FRET curve of individuals cells from **(C)** and the average peak was plotted as a function of the average production rate per condition. The error bars represent SD for both parameters. **(F, H, J)** FRET ratios were measured after the addition of PGE2 in cells pretreated with EP4 antagonist (ant.) GW627368X **(F)**, pretreated with EP2 antagonist AH6809 **(H)** or pretreated with both GW627368X and AH6809 **(J)**. The data presented are mean ± SD from ≥4 cells per condition. **(G, I, K)** The relative cAMP production peak and the cAMP production rate were measured from **(F, H, J)**, respectively. The error bars represent SD for both parameters.

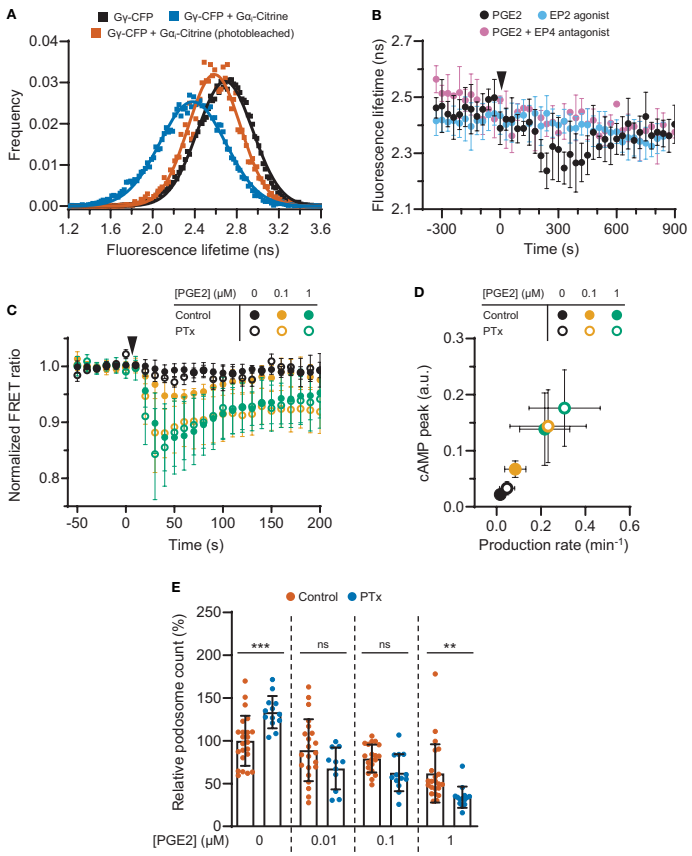

FIGURE 3 | EP4-coupled Ga_i dampens the prostaglandin E2 (PGE2)-induced cyclic adenosine monophosphate (cAMP) production. **(A)** RAW macrophages were transfected with Gγ-CFP only or with Gγ-CFP (donor), $G\alpha_i$-Citrine (acceptor) and Gβ wildtype together. The average lifetime of Gγ-CFP for individual cells were calculated from frequency-domain FLIM images and the distributions were fitted with a Gaussian profile (solid lines) to obtain the average lifetimes. Photobleaching of $G\alpha_i$-Citrine was used as a control for the occurrence of FRET. **(B)** The average donor lifetime in cells expressing both donor and acceptor is plotted before and after addition of 10 μM PGE2 in absence or presence of EP4 antagonist AH23848 or after addition of 10 μM EP2 agonist Butaprost. The data presented are mean ± SD from ≥2 cells. **(C)** FRET ratios of t-Epac-vv before and after addition of PGE2 were measured in transiently transfected RAW macrophages that were left untreated or were pretreated with $G\alpha_i$ inhibitor pertussis toxin (PTx). Controls were performed with the addition of buffer only. The data presented are mean ± SD of measurements from ≥4 cells per condition. **(D)** The cAMP peak and the cAMP production rate were quantified as described in **Figure 2D** from **(C)** and the average peak was plotted as a function of the average production rate per condition. The error bars represent SD for both parameters. **(E)** iDCs were treated with different concentrations of PGE2 with or without PTx pretreatment. Cells were stained for actin and vinculin and the number of podosomes per image was quantified and normalized to untreated control. The error bars represent mean ± SD. Data presented are from three different donors. **P<0.01, ***P<0.001, Welch ANOVA with Dunnett's T3 multiple comparison test.

EP4-Coupled Gαi Fine-Tunes the Prostaglandin E2-Induced cAMP Production

Given that EP2 and EP4 differentially control cAMP dynamics, we sought to identify factors that contribute to these differences. Since the inhibitory G protein $G\alpha_i$ has been shown to couple to EP4 (22), we hypothesized that $G\alpha_i$ dampens the PGE2-induced cAMP response in cells expressing EP4. To demonstrate that EP4 selectively activates $G\alpha_i$ also in macrophages, we performed fluorescence lifetime imaging (FLIM) to measure FRET between cyan fluorescent protein (CFP)-tagged Gγ (Gγ-CFP) and Citrine-tagged $G\alpha_i$ ($G\alpha_i$-Citrine). The fluorescent lifetime of the FRET donor (CFP) decreased upon co-expression with the acceptor (Citrine) and was restored to control levels upon acceptor photobleaching (**Figure 3A**), indicating that FRET occurred between Gγ-CFP and $G\alpha_i$-Citrine. Since $G\alpha_i$ is known to undergo conformational rearrangements upon activation (39) and FRET between Gγ-CFP and $G\alpha_i$-Citrine is likely affected by such rearrangements, a shift in fluorescence lifetime is expected upon EP4 stimulation. Treatment with PGE2 induced a gradual reduction in the lifetime of the donor fluorophore, whereas no shift in the lifetime phase was observed upon either inhibition of EP4 or selective stimulation of EP2 (**Figure 3B**). These findings confirm that PGE2 induces $G\alpha_i$ activation *via* EP4 only.

To determine the consequences of EP4-mediated $G\alpha_i$ activation on PGE2 signaling, we measured cAMP elevation using t-Epac-vv upon inhibition of $G\alpha_i$ with pertussis toxin (PTx). $G\alpha_i$ blockade significantly enhanced the cAMP peak concentrations and production induced by 0.1 μM PGE2 and to a lower extent also by 1 μM PGE2 (**Figure 3C**), indicating that $G\alpha_i$ attenuates cAMP production most strongly at lower PGE2 concentrations. The effect of $G\alpha_i$ inhibition on cAMP production is more clearly depicted in **Figure 3D**, where a higher cAMP peak and an increased production rate are observed after addition of PTx.

Next, to investigate whether EP4-mediated $G\alpha_i$ activation would dampen cAMP-dependent processes such as podosome dissolution, we determined PGE2-mediated podosome loss in iDCs with or without PTx treatment. We found that $G\alpha_i$ inhibition led to slightly increased podosome loss at all PGE2 concentrations tested, with 1 μM PGE2 being statistically significant while 0.01 and 0.1 μM PGE2 show a non-significant but clear trend (**Figure 3E**). It should be considered that such low concentrations of PGE2 are less powerful in inducing podosome dissolution (**Figure 1C**), making the effect of PTx treatment more difficult to assess. Nonetheless, this result indicates that the $G\alpha_i$-mediated dampening of cAMP production also affects cellular decisions downstream of EP2 and EP4.

Together, these findings show that $G\alpha_i$ dampens the onset of cAMP production, suggesting that the PGE2-EP4-$G\alpha_i$ axis might act as signaling gatekeeper when low PGE2 levels fluctuate slightly.

EP2- and EP4-Mediated Signaling Requires Cortical Microtubule Integrity

Since the interplay between G proteins and tubulin is well documented as well as their localization along microtubules (40–42), we investigated whether microtubule integrity is important for PGE2-induced cAMP production. We found that microtubule disruption (**Supplementary Figure 2**) deregulates PGE2-induced cAMP elevation (**Figure 4A**). More specifically, when both receptors are activated, attenuation of the cAMP response by nocodazole was only observed at 1 μM PGE2 and not at 0.1 μM PGE2 (**Figures 4A, B**). Upon EP2 inhibition, however, the cAMP production rate and the maximum cAMP levels induced by PGE2-EP4 were reduced at all PGE2 concentrations tested (**Figures 4C, D**). Finally, EP4 inhibition revealed that the strong and sustained cAMP response of PGE2-EP2 is completely prevented by microtubule disruption (**Figures 4E, F**). These results demonstrate that the $G\alpha_s$-mediated cAMP response to PGE2 relies on an intact microtubule network and that disruption of this network reduces the signaling efficiency of both EP2 and EP4, with EP2 activity being more sensitive to microtubule integrity than EP4 activity.

DISCUSSION

This study characterized the EP2 and EP4 signaling modalities to better understand DC and macrophage responses elicited by PGE2. Our first important observation is that selective activation of EP2 and EP4 by agonists leads to different outcomes compared to activation by PGE2 in the presence of selective receptor antagonists. More specifically, when the receptors are individually activated by a selective agonist, podosome dissolution is almost equally induced by EP2 and EP4, whereas podosome dissolution is mostly mediated by EP4 after the addition of natural ligand PGE2 in the presence of selective antagonists. Throughout this study, we consistently applied selective antagonists to determine individual receptor contributions to PGE2 signaling and show that 1) both EP2 and EP4 signal more efficiently when selectively activated by their natural ligand PGE2; 2) EP4 induces dose-dependent and transient cAMP production, whereas EP2 induces a sustained cAMP response only at high PGE2 concentration; 3) EP4-linked $G\alpha_i$ dampens both PGE2-induced cAMP generation and podosome dissolution; 4) microtubule disruption obstructs efficient signaling of both receptors, especially affecting EP2 strongly.

We here also show that PGE2-induced podosome loss in iDCs (18) is differentially controlled by EP2 and EP4. PGE2-induced podosome dissolution is a first step toward the acquisition of a fast migratory phenotype by DCs (18, 43). In fact, PGE2 is an important factor to induce DC maturation and by using selective agonists, both EP2 and EP4 have been proposed to play similar roles in this process (6, 16). Our results suggest that this might not be the case and that EP4 is likely the most predominant receptor in mediating the PGE2 signaling that leads to podosome dissolution and the induction of migratory mature DCs. This is in line with previous findings in gene-targeting experiments in mice, where PGE2-EP4 signaling was found to promote migration and maturation of Langerhans cells, thereby initiating skin immune responses (44). Similarly, other PGE2-mediated immunological processes such cytokine production and T cell activation have been reported to be controlled differently by EP2 and EP4 (45–47). Knockdown of

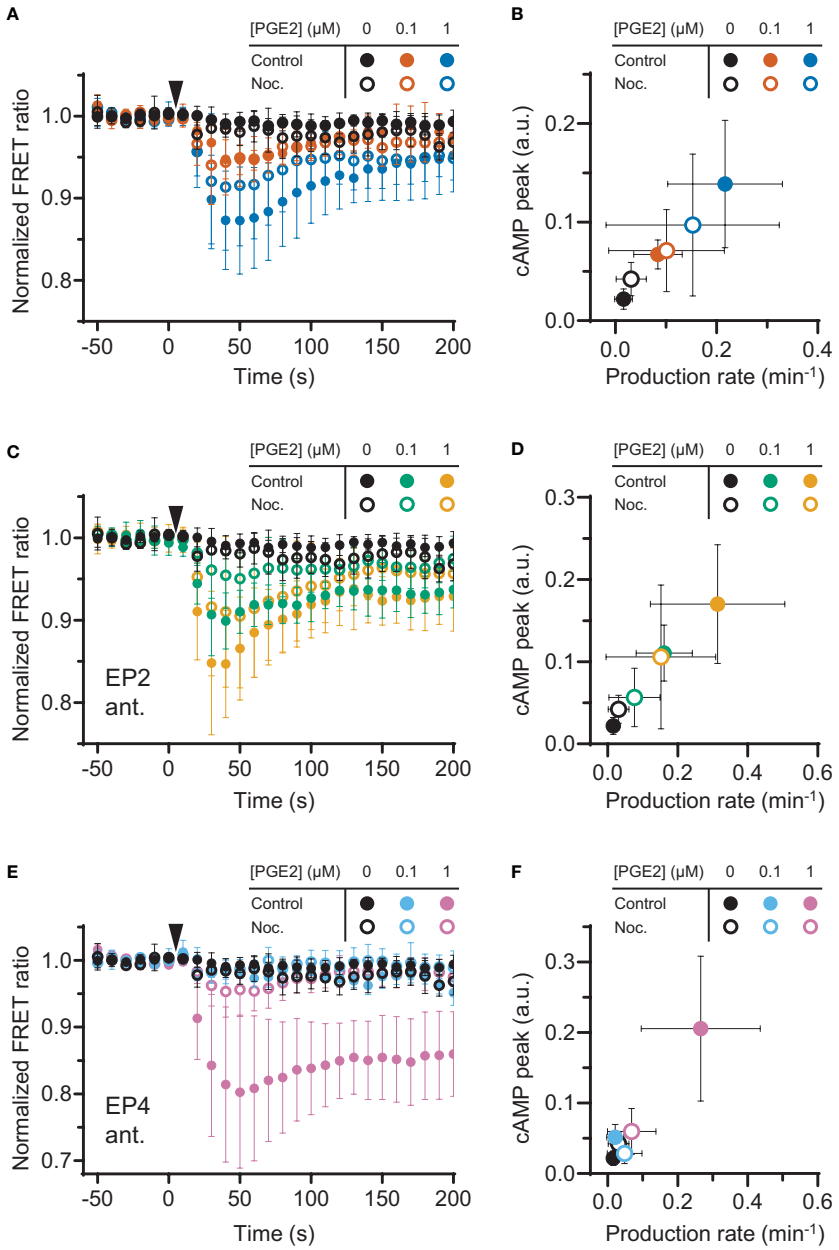

FIGURE 4 | Efficient signaling of EP2 and EP4 relies on microtubule integrity. **(A, C, E)** The Förster Resonance Energy Transfer (FRET) ratio of t-Epac-vv was measured in cells that were untreated or pretreated with nocodazole (Noc.) before and after addition of prostaglandin E2 (PGE2). Shown are the ratios obtained in cells in the absence of antagonists **(A)**, in the presence of EP2 antagonist AH6809 **(C)** or EP4 antagonist GW627368X **(E)**. Controls were performed with the addition of buffer only. The data are mean ± SD from ≥5 cells per condition. **(B, D, F)** The cyclic adenosine monophosphate (cAMP) production peak and the cAMP production rate were measured from the FRET curve of individual cells from **(A, C, E)**, respectively, and the average peak was plotted as a function of the average production rate per condition. The error bars represent SD for both parameters.

EP2 or EP4 in DCs possibly in combination with the use of agonists and antagonists might eventually help to clarify these differences. However, since EP2 and EP4 are always co-expressed in DCs, it remains to be determined whether the knockdown of one receptor does not affect expression patterns of the other receptor.

Early studies characterizing the EP receptor signaling capacity have mostly used cells that overexpress either EP2 or EP4 (22, 23, 25, 48–50), which makes it challenging to determine the differential contribution of the receptors when they are co-expressed. Here, we have addressed this question and measured the early onset of cAMP

production in cells that endogenously express both EP2 and EP4. Using selective EP2 and EP4 antagonists, we demonstrate that EP2 induces sustained cAMP, whereas EP4-mediated cAMP production is faster but more transient. This difference may partially be explained by the fact that EP4, and not EP2, is internalized shortly after stimulation with PGE2, which halts further signaling (23, 51). Furthermore, our results showing a sustained EP2-induced cAMP production are in line with the previous observation that EP2 is the main cAMP generator after extended PGE2 stimulation (48). We also know that EP4 can couple to both $G\alpha_s$ and $G\alpha_i$ (22). Here, we provide additional evidence that $G\alpha_i$ is only linked to EP4 and not to EP2, and that $G\alpha_i$ attenuates the cAMP response induced by low PGE2 concentrations. Given that several GPCRs do not precouple with $G\alpha_i$ (52), it would be important to determine how and when EP4 and $G\alpha_i$ interact. In a recent study, hidden Markov modeling classified G proteins into four diffusion states, of which the slowest two states represent G proteins that interact in hot spots for GPCR activation (53). The same study employed single-molecule tracking to show that adrenergic receptors and $G\alpha_i$ proteins interact only transiently within these hot spots (53). Single-molecule imaging methods are excellent tools to understand the fundamental principles of G protein dynamics and could be exploited to better understand the molecular mechanisms regulating the spatiotemporal interaction between EP4 and $G\alpha_s$ or $G\alpha_i$, which could shape the cAMP production profile.

Our FRET measurements also reveal that the cAMP response of EP4 is dose-dependent, whereas the EP2-induced cAMP production is negligible at low PGE2 concentrations and strong at high PGE2 concentrations. EP4 has a higher affinity for PGE2 than EP2, as indicated by dissociation constants of 0.59 nM and 13 nM, respectively (54). The high affinity of EP4 explains its responsiveness to low PGE2 concentrations, but the apparent irresponsiveness of EP2 to PGE2 concentrations below 1 μM cannot be explained by its lower affinity for PGE2, based on the magnitude of its dissociation constant. Therefore, additional mechanisms that mediate the all-or-nothing response of EP2 could exist and might include receptor hetero- or homo-oligomerization, which are documented for other GPCRs (55) but remain to be identified for EP2 and EP4. Importantly, our results indicate that EP4 is the main producer and regulator of cAMP production at low, possibly physiological, PGE2 concentrations, whereas EP2 boosts cAMP levels only when PGE2 concentration increases above a certain threshold, as could (locally) occur in inflamed or tumor tissues.

Interestingly, our experiments using a cAMP FRET biosensor show that EP2 and EP4 both signal more strongly when stimulated selectively. This indicates that simultaneous activation of both receptors limits efficient signaling and suggests the presence of signaling crosstalk between EP2 and EP4. Since both EP2 and EP4 couple to $G\alpha_s$, competition for downstream effectors could contribute to the attenuated cAMP response observed in the absence of receptor antagonists. Additionally, inhibitory interactions between activated receptors at the plasma membrane could attenuate the PGE2-induced cAMP response to establish an integrated signal that

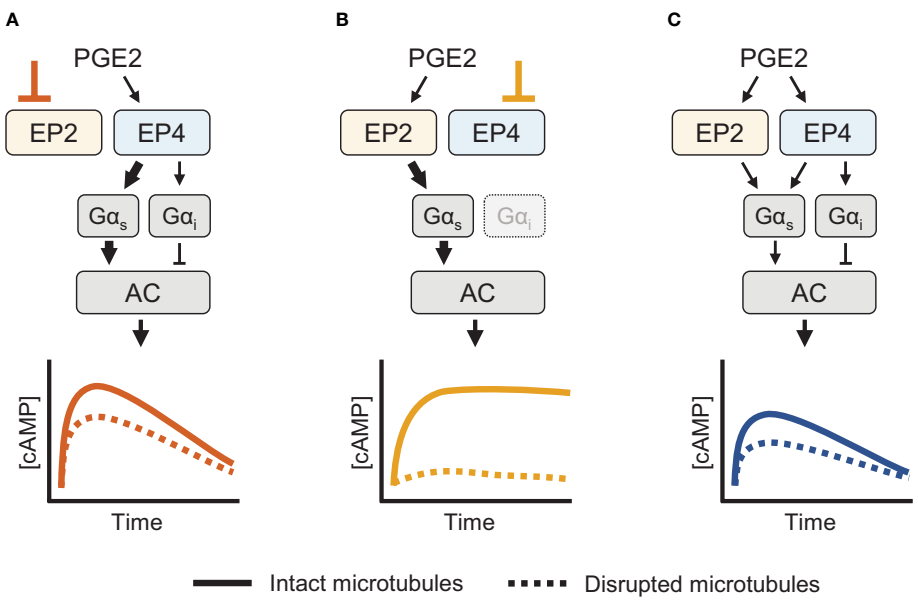

FIGURE 5 | Schematic overview of the cyclic adenosine monophosphate (cAMP) responses induced by EP2 and EP4. **(A)** When only EP4 is active, both $G\alpha_s$ and $G\alpha_i$ control AC activity. $G\alpha_s$ induces a dose-dependent cAMP response that is dampened by $G\alpha_i$. The cAMP signal subsides over time and is attenuated by microtubule disruption. **(B)** When EP2 is activated selectively, only $G\alpha_s$ modulates AC activity. The resulting cAMP response is either weak or strong, does not subside and completely relies on an intact microtubule network. **(C)** When both EP2 and EP4 are active, competition for $G\alpha_s$ dampens the integrated cAMP response. Signaling crosstalk between EP2 and EP4 allows the cell to respond differently to prostaglandin E2 (PGE2) depending on the organization and expression of EP2 and EP4.

fine-tunes downstream effects. Although the mechanisms underlying this potential crosstalk remains to be deciphered, our results strongly indicate that the EP2 and EP4 signaling axes may be closely intertwined.

The organization of GPCR signaling has previously been linked to membrane domains and the cortical microtubule network (56). Here, we show that an intact microtubule network (and possibly microtubule dynamic properties too, as shown in **Supplementary Figure 2B**) is necessary for efficient signaling of both EP2 and EP4. Remarkably, several other studies show that cAMP production is dampened by intact microtubules and lipid membrane domains (56–58). Specifically, microtubules were suggested to restrict the interactions of $G\alpha_s$ with GPCRs and AC, limiting the efficiency of cAMP responses (57, 59). Yet, most previous research focused on adrenergic receptors, which primarily localize to lipid-raft domains (60). By contrast, the insensitivity of EP receptors to cholesterol depletion suggests that EP2 and EP4 mainly localize in non-raft regions (61). Moreover, the AC isoform 2, which is the AC isoform that responds most strongly to PGE2, is also located in non-raft domains, further supporting the notion that PGE2 signaling occurs outside lipid rafts and possibly explaining their differential dependence on the microtubule network that was reported for the adrenergic receptors (61). Although a mechanistic explanation is still lacking, the different sensitivity of EP2 and EP4 to microtubule disruption is striking: whereas PGE2-EP4 signaling is partially reduced, PGE2-EP2 signaling is completely abolished by nocodazole treatment. Imaging of microtubules in combination with single-particle tracking of EP receptors could reveal the role of microtubules in PGE2 signaling. Furthermore, a detailed molecular investigation of $G\alpha_s$ and $G\alpha_i$ dynamics is required to accurately describe the organization and receptor-coupling of the different $G\alpha$ proteins involved. The different sensitivity of EP2 and EP4 to nocodazole together with the apparently contradictory results between adrenergic and prostaglandin receptors strongly emphasizes the complexity of GPCR spatiotemporal organization and the importance of studying the regulation of a specific receptor in its endogenous settings.

Based on our experimental observations, we here present a schematic model for the cAMP responses established by EP2 and EP4. Upon selective stimulation of EP4, both $G\alpha_s$ and $G\alpha_i$ proteins are activated (**Figure 5A**). Active $G\alpha_s$ proteins modulate the activity of AC, resulting in a strong cAMP response. $G\alpha_i$ functions to fine-tune the cAMP production at low PGE2 concentrations. As EP4 is subjected to desensitization and internalization (23, 25), the elicited cAMP response subsides over time. When EP2 is selectively stimulated instead, only $G\alpha_s$ controls AC activity (**Figure 5B**). The resulting cAMP response does not subside because EP2 is insensitive to receptor desensitization and internalization (23). Disruption of the microtubule network dampens the cAMP levels induced by both EP2 and EP4, albeit with different strength, showing that microtubules play an important role in the organization of EP receptor signaling. Upon simultaneous activation of EP2 and EP4, $G\alpha$ proteins are activated by both EP2 and EP4, resulting in an integrated cAMP response (**Figure 5C**). Competition between EP2 and EP4 for $G\alpha_s$ likely reduces the signaling efficiency of individual receptors and thereby moderates final cAMP levels. Since EP4 has a higher affinity for PGE2 than EP2 (54), EP4 is the main gatekeeper of cAMP levels, especially at low PGE2 concentrations, while EP2 becomes important only at high PGE2 concentrations that will result in strong and sustained cAMP production.

Increased PGE2 concentrations have been reported in the tumor microenvironment of several cancer types (9–12). Since PGE2 regulates immune cell function, the selective modulation of EP receptor signaling pathways has been proven to enhance the antitumor immune response (62–64). Further insight into the concerted action of EP2 and EP4 will be essential to efficiently control the cellular responses to PGE2.

DATA AVAILABILITY STATEMENT

The raw data supporting the conclusions of this article will be made available by the authors, without undue reservation.

AUTHOR CONTRIBUTIONS

WV, KD, BJ, SK performed the experiments and analyzed the data. DL provided the analytical tools. WV, KD, DL, and AC wrote the manuscript with input from all authors. DL and AC supervised the entire project. All authors contributed to the article and approved the submitted version.

FUNDING

This work was supported by a Human Frontiers Science Program grant awarded to DL and AC (RGY0074/2008) and by a NIH R35GM-126934 grant awarded to DL.

ACKNOWLEDGMENTS

The microscopy experiments were mostly conducted at the Radboudumc Technology Center Microscopy with the exception of the FLIM measurements that were performed at the University of Twente, Enschede, The Netherlands.

SUPPLEMENTARY MATERIAL

The Supplementary Material for this article can be found online at: https://www.frontiersin.org/articles/10.3389/fimmu.2020.613286/full#supplementary-material

REFERENCES

1. Pierce KL, Premont RT, Lefkowitz RJ. Seven-transmembrane receptors. *Nat Rev Mol Cell Biol* (2002) 3:639–50. doi: 10.1038/nrm908
2. Smith WL. Prostanoid biosynthesis and mechanisms of action. *Am J Physiol* (1992) 263:F181–91. doi: 10.1152/ajprenal.1992.263.2.F181
3. Coleman RA, Smith WL, Narumiya S. International Union of Pharmacology classification of prostanoid receptors: properties, distribution, and structure of the receptors and their subtypes. *Pharmacol Rev* (1994) 46:205–29.
4. Legler DF, Bruckner M, Uetz-von Allmen E, Krause P. Prostaglandin E2 at new glance: novel insights in functional diversity offer therapeutic chances. *Int J Biochem Cell Biol* (2010) 42:198–201. doi: 10.1016/j.biocel.2009.09.015
5. Narumiya S. Prostanoids in immunity: roles revealed by mice deficient in their receptors. *Life Sci* (2003) 74:391–5. doi: 10.1016/j.lfs.2003.09.025
6. Legler DF, Krause P, Scandella E, Singer E, Groettrup M. Prostaglandin E2 is generally required for human dendritic cell migration and exerts its effect via EP2 and EP4 receptors. *J Immunol* (2006) 176:966–73. doi: 10.4049/jimmunol.176.2.966
7. Gualde N, Harizi H. Prostanoids and their receptors that modulate dendritic cell-mediated immunity. *Immunol Cell Biol* (2004) 82:353–60. doi: 10.1111/j.0818-9641.2004.01251.x
8. van Helden SF, Oud MM, Joosten B, Peterse N, Figdor CG, van Leeuwen FN. PGE2-mediated podosome loss in dendritic cells is dependent on actomyosin contraction downstream of the RhoA-Rho-kinase axis. *J Cell Sci* (2008) 121:1096–106. doi: 10.1242/jcs.020289
9. Rasmuson A, Kock A, Fuskevåg OM, Kruspig B, Simón-Santamaría J, Gogvadze V, et al. Autocrine Prostaglandin E2 Signaling Promotes Tumor Cell Survival and Proliferation in Childhood Neuroblastoma. *PloS One* (2012) 7:e29331. doi: 10.1371/journal.pone.0029331
10. Rigas B, Goldman IS, Levine L. Altered eicosanoid levels in human colon cancer. *J Lab Clin Med* (1993) 122:518–23. doi: 10.5555/uri:pii:002221439390010V
11. Howe LR. Inflammation and breast cancer. Cyclooxygenase/prostaglandin signaling and breast cancer. *Breast Cancer Res* (2007) 9:210. doi: 10.1186/bcr1678
12. Huang M, Stolina M, Sharma S, Mao JT, Zhu L, Miller PW, et al. Non-Small Cell Lung Cancer Cyclooxygenase-2-dependent Regulation of Cytokine Balance in Lymphocytes and Macrophages: Up-Regulation of Interleukin 10 and Down-Regulation of Interleukin 12 Production. *Cancer Res* (1998) 58:1208–16.
13. Kobayashi K, Omori K, Murata T. Role of prostaglandins in tumor microenvironment. *Cancer Metastasis Rev* (2018) 37:347–54. doi: 10.1007/s10555-018-9740-2
14. Ma Y, Shurin GV, Peiyuan Z, Shurin MR. Dendritic cells in the cancer microenvironment. *J Cancer* (2013) 4:36–44. doi: 10.7150/jca.5046
15. Klarquist JS, Janssen EM. Melanoma-infiltrating dendritic cells: Limitations and opportunities of mouse models. *Oncoimmunology* (2012) 1:1584–93. doi: 10.4161/onci.22660
16. Kubo S, Takahashi HK, Takei M, Iwagaki H, Yoshino T, Tanaka N, et al. E-prostanoid (EP)2/EP4 receptor-dependent maturation of human monocyte-derived dendritic cells and induction of helper T2 polarization. *J Pharmacol Exp Ther* (2004) 309:1213–20. doi: 10.1124/jpet.103.062646
17. Harizi H, Grosset C, Gualde N. Prostaglandin E2 modulates dendritic cell function via EP2 and EP4 receptor subtypes. *J Leukoc Biol* (2003) 73:756–63. doi: 10.1189/jlb.1002483
18. van Helden SF, Krooshoop DJ, Broers KC, Raymakers RA, Figdor CG, van Leeuwen FN. A critical role for prostaglandin E2 in podosome dissolution and induction of high-speed migration during dendritic cell maturation. *J Immunol* (2006) 177:1567–74. doi: 10.4049/jimmunol.177.3.1567
19. Honda A, Sugimoto Y, Namba T, Watabe A, Irie A, Negishi M, et al. Cloning and expression of a cDNA for mouse prostaglandin E receptor EP2 subtype. *J Biol Chem* (1993) 268:7759–62. doi: 10.1016/S0021-9258(18)53022-2
20. Regan JW, Bailey TJ, Pepperl DJ, Pierce KL, Bogardus AM, Donello JE, et al. Cloning of a novel human prostaglandin receptor with characteristics of the pharmacologically defined EP2 subtype. *Mol Pharmacol* (1994) 46:213–20.
21. Leduc M, Breton B, Gales C, Le Gouill C, Bouvier M, Chemtob S, et al. Functional selectivity of natural and synthetic prostaglandin EP4 receptor ligands. *J Pharmacol Exp Ther* (2009) 331:297–307. doi: 10.1124/jpet.109.156398
22. Fujino H, Regan JW. EP_4 Prostanoid Receptor Coupling to a Pertussis Toxin-Sensitive Inhibitory G Protein. *Mol Pharmacol* (2006) 69:5–10. doi: 10.1124/mol.105.017749
23. Desai S, April H, Nwaneshiudu C, Ashby B. Comparison of agonist-induced internalization of the human EP2 and EP4 prostaglandin receptors: role of the carboxyl terminus in EP4 receptor sequestration. *Mol Pharmacol* (2000) 58:1279–86. doi: 10.1124/mol.58.6.1279
24. Penn RB, Pascual RM, Kim YM, Mundell SJ, Krymskaya VP, Panettieri RAJr, et al. Arrestin specificity for G protein-coupled receptors in human airway smooth muscle. *J Biol Chem* (2001) 276:32648–56. doi: 10.1074/jbc.M104143200
25. Desai S, Ashby B. Agonist-induced internalization and mitogen-activated protein kinase activation of the human prostaglandin EP4 receptor. *FEBS Lett* (2001) 501:156–60. doi: 10.1016/S0014-5793(01)02640-0
26. Mao Y, Sarhan D, Steven A, Seliger B, Kiessling R, Lundqvist A. Inhibition of tumor-derived prostaglandin-e2 blocks the induction of myeloid-derived suppressor cells and recovers natural killer cell activity. *Clin Cancer Res* (2014) 20:4096–106. doi: 10.1158/1078-0432.CCR-14-0635
27. Kiriyama M, Ushikubi F, Kobayashi T, Hirata M, Sugimoto Y, Narumiya S. Ligand binding specificities of the eight types and subtypes of the mouse prostanoid receptors expressed in Chinese hamster ovary cells. *Br J Pharmacol* (1997) 122:217–24. doi: 10.1038/sj.bjp.0701367
28. Wilson RJ, Giblin GM, Roomans S, Rhodes SA, Cartwright KA, Shield VJ, et al. GW627368X ((N-{2-[4-(4,9-diethoxy-1-oxo-1,3-dihydro-2H-benzo[f]isoindol-2-yl)phenyl]acetyl} benzene sulphonamide): a novel, potent and selective prostanoid EP4 receptor antagonist. *Br J Pharmacol* (2006) 148:326–39. doi: 10.1038/sj.bjp.0706726
29. Woodward DF, Pepperl DJ, Burkey TH, Regan JW. 6-Isopropoxy-9-oxoxanthene-2-carboxylic acid (AH 6809), a human EP2 receptor antagonist. *Biochem Pharmacol* (1995) 50:1731–3. doi: 10.1016/0006-2952(95)02035-7
30. Luschnig-Schratl P, Sturm EM, Konya V, Philipose S, Marsche G, Frohlich E, et al. EP4 receptor stimulation down-regulates human eosinophil function. *Cell Mol Life Sci* (2011) 68:3573–87. doi: 10.1007/s00018-011-0642-5
31. Turcotte C, Zarini S, Jean S, Martin C, Murphy RC, Marsolais D, et al. The Endocannabinoid Metabolite Prostaglandin E2 (PGE2)-Glycerol Inhibits Human Neutrophil Functions: Involvement of Its Hydrolysis into PGE2 and EP Receptors. *J Immunol* (2017) 198:3255–63. doi: 10.4049/jimmunol.1601767
32. Thurner B, Roder C, Dieckmann D, Heuer M, Kruse M, Glaser A, et al. Generation of large numbers of fully mature and stable dendritic cells from leukapheresis products for clinical application. *J Immunol Methods* (1999) 223:1–15. doi: 10.1016/S0022-1759(98)00208-7
33. de Vries IJ, Eggert AA, Scharenborg NM, Vissers JL, Lesterhuis WJ, Boerman OC, et al. Phenotypical and functional characterization of clinical grade dendritic cells. *J Immunother* (2002) 25:429–38. doi: 10.1097/00002371-200209000-00007
34. Klarenbeek JB, Goedhart J, Hink MA, Gadella TW, Jalink K. A mTurquoise-based cAMP sensor for both FLIM and ratiometric read-out has improved dynamic range. *PLoS One* (2011) 6:e19170. doi: 10.1371/journal.pone.0019170
35. Gibson SK, Gilman AG. Gialpha and Gbeta subunits both define selectivity of G protein activation by alpha2-adrenergic receptors. *Proc Natl Acad Sci USA* (2006) 103:212–7. doi: 10.1073/pnas.0509763102
36. De Keijzer S, Meddens MB, Torensma R, Cambi A. The multiple faces of prostaglandin E2 G-protein coupled receptor signaling during the dendritic cell life cycle. *Int J Mol Sci* (2013) 14:6542–55. doi: 10.3390/ijms14046542
37. Hubbard NE, Lee S, Lim D, Erickson KL. Differential mRNA expression of prostaglandin receptor subtypes in macrophage activation. *Prostaglandins Leukot Essent Fatty Acids* (2001) 65:287–94. doi: 10.1054/plef.2001.0327
38. van Helden SF, van Leeuwen FN, Figdor CG. Human and murine model cell lines for dendritic cell biology evaluated. *Immunol Lett* (2008) 117:191–7. doi: 10.1016/j.imlet.2008.02.003
39. Bünemann M, Frank M, Lohse MJ. Gi protein activation in intact cells involves subunit rearrangement rather than dissociation. *Proc Natl Acad Sci* (2003) 100:16077–82. doi: 10.1073/pnas.2536719100
40. Wang N, Yan K, Rasenick MM. Tubulin binds specifically to the signal-transducing proteins, Gs alpha and Gi alpha 1. *J Biol Chem* (1990) 265:1239–42. doi: 10.1016/S0021-9258(19)40002-1

41. Côté M, Payet MD, Gallo-Payet N. Association of αs-Subunit of the Gs Protein with Microfilaments and Microtubules: Implication during Adrenocorticotropin Stimulation in Rat Adrenal Glomerulosa Cells1. *Endocrinology* (1997) 138:69–78. doi: 10.1210/endo.138.1.4860
42. Sarma T, Voyno-Yasenetskaya T, Hope TJ, Rasenick MM. Heterotrimeric G-proteins associate with microtubules during differentiation in PC12 pheochromocytoma cells. *FASEB J* (2003) 17:848–59. doi: 10.1096/fj.02-0730com
43. Scandella E, Men Y, Gillessen S, Forster R, Groettrup M. Prostaglandin E2 is a key factor for CCR7 surface expression and migration of monocyte-derived dendritic cells. *Blood* (2002) 100:1354–61. doi: 10.1182/blood-2001-11-0017
44. Kabashima K, Sakata D, Nagamachi M, Miyachi Y, Inaba K, Narumiya S. Prostaglandin E2-EP4 signaling initiates skin immune responses by promoting migration and maturation of Langerhans cells. *Nat Med* (2003) 9:744–9. doi: 10.1038/nm872
45. Flórez-Grau G, Cabezón R, Borgman KJE, España C, Lozano JJ, Garcia-Parajo MF, et al. Up-regulation of EP2 and EP3 receptors in human tolerogenic dendritic cells boosts the immunosuppressive activity of PGE2. *J Leukoc Biol* (2017) 102:881–95. doi: 10.1189/jlb.2A1216-526R
46. Poloso NJ, Urquhart P, Nicolaou A, Wang J, Woodward DF. PGE(2) differentially regulates monocyte-derived dendritic cell cytokine responses depending on receptor usage (EP(2)/EP(4)). *Mol Immunol* (2013) 54:284–95. doi: 10.1016/j.molimm.2012.12.010
47. Yao C, Sakata D, Esaki Y, Li Y, Matsuoka T, Kuroiwa K, et al. Prostaglandin E2–EP4 signaling promotes immune inflammation through TH1 cell differentiation and TH17 cell expansion. *Nat Med* (2009) 15:633–40. doi: 10.1038/nm.1968
48. Fujino H, West KA, Regan JW. Phosphorylation of glycogen synthase kinase-3 and stimulation of T-cell factor signaling following activation of EP2 and EP4 prostanoid receptors by prostaglandin E-2. *J Biol Chem* (2002) 277:2614–9. doi: 10.1074/jbc.M109440200
49. Fujino H, Xu W, Regan JW. Prostaglandin E2 induced functional expression of early growth response factor-1 by EP4, but not EP2, prostanoid receptors via the phosphatidylinositol 3-kinase and extracellular signal-regulated kinases. *J Biol Chem* (2003) 278:12151–6. doi: 10.1074/jbc.M212665200
50. Fujino H, Salvi S, Regan JW. Differential regulation of phosphorylation of the cAMP response element-binding protein after activation of EP2 and EP4 prostanoid receptors by prostaglandin E2. *Mol Pharmacol* (2005) 68:251–9. doi: 10.1124/mol.105.011833
51. Hamdan FF, Rochdi MD, Breton B, Fessart D, Michaud DE, Charest PG, et al. Unraveling G Protein-coupled Receptor Endocytosis Pathways Using Real-time Monitoring of Agonist-promoted Interaction between β-Arrestins and AP-2. *J Biol Chem* (2007) 282:29089–100. doi: 10.1074/jbc.M700577200
52. Bondar A, Lazar J. G protein Gi1 exhibits basal coupling but not preassembly with G protein-coupled receptors. *J Biol Chem* (2017) 292:9690–8. doi: 10.1074/jbc.M116.768127
53. Sungkaworn T, Jobin M-L, Burnecki K, Weron A, Lohse MJ, Calebiro D. Single-molecule imaging reveals receptor–G protein interactions at cell surface hot spots. *Nature* (2017) 550:543–7. doi: 10.1038/nature24264
54. Abramovitz M, Adam M, Boie Y, Carriere M, Denis D, Godbout C, et al. The utilization of recombinant prostanoid receptors to determine the affinities and selectivities of prostaglandins and related analogs. *Biochim Biophys Acta* (2000) 1483:285–93. doi: 10.1016/S1388-1981(99)00164-X
55. Sleno R, Hebert TE. The Dynamics of GPCR Oligomerization and Their Functional Consequences. *Int Rev Cell Mol Biol* (2018) 338:141–71. doi: 10.1016/bs.ircmb.2018.02.005
56. Head BP, Patel HH, Roth DM, Murray F, Swaney JS, Niesman IR, et al. Microtubules and actin microfilaments regulate lipid raft/caveolae localization of adenylyl cyclase signaling components. *J Biol Chem* (2006) 281:26391–9. doi: 10.1074/jbc.M602577200
57. Pontier SM, Percherancier Y, Galandrin S, Breit A, Galés C, Bouvier M. Cholesterol-dependent Separation of the β2-Adrenergic Receptor from Its Partners Determines Signaling Efficacy: INSIGHT INTO NANOSCALE ORGANIZATION OF SIGNAL TRANSDUCTION. *J Biol Chem* (2008) 283:24659–72. doi: 10.1074/jbc.M800778200
58. Allen JA, Yu JZ, Dave RH, Bhatnagar A, Roth BL, Rasenick MM. Caveolin-1 and Lipid Microdomains Regulate Gs Trafficking and Attenuate Gs/Adenylyl Cyclase Signaling. *Mol Pharmacol* (2009) 76:1082–93. doi: 10.1124/mol.109.060160
59. Czysz AH, Schappi JM, Rasenick MM. Lateral Diffusion of Gαs in the Plasma Membrane Is Decreased after Chronic but not Acute Antidepressant Treatment: Role of Lipid Raft and Non-Raft Membrane Microdomains. *Neuropsychopharmacology* (2015) 40:766–73. doi: 10.1038/npp.2014.256
60. Agarwal SR, Yang P-C, Rice M, Singer CA, Nikolaev VO, Lohse MJ, et al. Role of Membrane Microdomains in Compartmentation of cAMP Signaling. *PloS One* (2014) 9:e95835. doi: 10.1371/journal.pone.0095835
61. Bogard AS, Adris P, Ostrom RS. Adenylyl Cyclase 2 Selectively Couples to E Prostanoid Type 2 Receptors, Whereas Adenylyl Cyclase 3 Is Not Receptor-Regulated in Airway Smooth Muscle. *J Pharmacol Exp Ther* (2012) 342:586–95. doi: 10.1124/jpet.112.193425
62. Ma X, Holt D, Kundu N, Reader J, Goloubeva O, Take Y, et al. (PGE) receptor EP4 antagonist protects natural killer cells from PGE-mediated immunosuppression and inhibits breast cancer metastasis. *Oncoimmunology* (2013) 2:e22647. doi: 10.4161/onci.22647
63. Majumder M, Xin X, Liu L, Girish GV, Lala PK. Prostaglandin E2 receptor EP4 as the common target on cancer cells and macrophages to abolish angiogenesis, lymphangiogenesis, metastasis, and stem-like cell functions. *Cancer Sci* (2014) 105:1142–51. doi: 10.1111/cas.12475
64. Albu DI, Wang Z, Huang KC, Wu J, Twine N, Leacu S, et al. EP4 Antagonism by E7046 diminishes Myeloid immunosuppression and synergizes with Treg-reducing IL-2-Diphtheria toxin fusion protein in restoring anti-tumor immunity. *Oncoimmunology* (2017) 6:e1338239. doi: 10.1080/2162402X.2017.1338239

Conflict of Interest: The authors declare that the research was conducted in the absence of any commercial or financial relationships that could be construed as a potential conflict of interest.

frontiers in Immunology

REVIEW
published: 19 February 2021
doi: 10.3389/fimmu.2021.613185

Plasma Membrane Integrates Biophysical and Biochemical Regulation to Trigger Immune Receptor Functions

Tongtong Zhang[1†], *Wei Hu*[2†] *and Wei Chen*[2,3*]

[1] Department of Hepatobiliary and Pancreatic Surgery, The Center for Integrated Oncology and Precision Medicine, Affiliated Hangzhou First People's Hospital, Zhejiang University School of Medicine, Hangzhou, China, [2] Department of Cell Biology and Department of Cardiology of the Second Affiliated Hospital, Zhejiang University School of Medicine, Hangzhou, China, [3] Key Laboratory for Biomedical Engineering of Ministry of Education, State Key Laboratory for Modern Optical Instrumentation, College of Biomedical Engineering and Instrument Science, Collaborative Innovation Center for Diagnosis and Treatment of Infectious Diseases, Zhejiang University, Hangzhou, China

OPEN ACCESS

Edited by:
Harry W. Schroeder,
University of Alabama at Birmingham,
United States

Reviewed by:
Michael Reth,
University of Freiburg, Germany
Wenxia Song,
University of Maryland, College Park,
United States

***Correspondence:**
Wei Chen
jackweichen@zju.edu.cn

[†]These authors have contributed equally to this work

Specialty section:
This article was submitted to B Cell Biology, a section of the journal Frontiers in Immunology

Received: 01 October 2020
Accepted: 06 January 2021
Published: 19 February 2021

Citation:
Zhang T, Hu W and Chen W (2021) Plasma Membrane Integrates Biophysical and Biochemical Regulation to Trigger Immune Receptor Functions. Front. Immunol. 12:613185. doi: 10.3389/fimmu.2021.613185

Plasma membrane provides a biophysical and biochemical platform for immune cells to trigger signaling cascades and immune responses against attacks from foreign pathogens or tumor cells. Mounting evidence suggests that the biophysical-chemical properties of this platform, including complex compositions of lipids and cholesterols, membrane tension, and electrical potential, could cooperatively regulate the immune receptor functions. However, the molecular mechanism is still unclear because of the tremendous compositional complexity and spatio-temporal dynamics of the plasma membrane. Here, we review the recent significant progress of dynamical regulation of plasma membrane on immune receptors, including T cell receptor, B cell receptor, Fc receptor, and other important immune receptors, to proceed mechano-chemical sensing and transmembrane signal transduction. We also discuss how biophysical-chemical cues couple together to dynamically tune the receptor's structural conformation or orientation, distribution, and organization, thereby possibly impacting their *in-situ* ligand binding and related signal transduction. Moreover, we propose that electrical potential could potentially induce the biophysical-chemical coupling change, such as lipid distribution and membrane tension, to inevitably regulate immune receptor activation.

Keywords: immune receptor, plasma membrane, biophysical-chemical coupling, electrical potential, mechanical force

INTRODUCTION

The plasma membrane (PM) of cells, mainly consisting of lipid, cholesterol, and protein, is a lipid bilayer structure. Its outer leaflet enriches phosphatidylcholine, sphingolipid, and cholesterol, and the inner leaflet mainly contains cholesterol and acidic phospholipids (e.g. phosphatidylserine, phosphatidylinositol, and phosphatidic acid) (1–3). The asymmetry mobility and dynamic organization of lipid and membrane proteins have been proposed in the Fluid-Mosaic model

(4–7). In this model, the PM is a very dynamic structure, where lipid-protein, lipid-lipid, and protein-protein interactions occur at all times, and all of these interactions regulate membrane receptor's ligand recognition and triggering (6, 8). Moreover, sphingolipid and cholesterol contribute to the formation of nanodomains or lipid rafts, which are highly dynamic in many receptor-activated cellular processes (9–12). It has been reported that the biophysical-chemical properties of the PM, including the asymmetry of lipid and protein distribution, the membrane curvature and mechanical tension, and the membrane electrical potential, could dynamically regulate diverse cellular processes (13–16).

For immune cells, the PM tunes their essential physiological processes. For example, the cholesterol accumulation could increase T cell differentiation and proliferation, whereas it also induces T cell exhaustion through T-cell receptor (TCR) signaling (17–20). Phosphatidylserine directly tunes T cell migration, adhesion, tissue infiltration, and rapid inflammatory response (21, 22). Moreover, PM's mechanical tension, driven by the cytoskeleton and its associated molecular motors, dynamically shapes PM morphology and regulates T cell adhesion, migration, and activation cooperatively *via* many immune receptors (e.g. TCR and integrin) (23–25). Also, PM morphology (e.g. microvilli) facilitates the discrimination of peptide major histocompatibility complex (pMHC) for TCR (26–28). Membrane potential, another PM biophysical property, might also regulate T cell proliferation and cytotoxicity through TCR activation (29, 30).

Here, we review how PM couples with biophysical and biochemical factors to regulate the functions of immune cells (e.g. T cell, B cell, and natural killer cell) through the respective immune receptor activation, such as TCR, B-cell receptor (BCR) or Fc receptor (FcR), and further discuss and propose the potential molecular mechanism.

DOUBLE-EDGED REGULATION OF CHOLESTEROL

It has been reported that many receptors (e.g. acetylcholine receptor and G protein-coupled receptor) contain the cholesterol recognition/interaction amino acid consensus (CARC, mainly containing Valine, Isoleucine, Alanine, Methionine, and Serine amino acids) motif in the transmembrane domain (TMD) which directly interacts with cholesterol (31, 32). This CARC motif might be conserved for many immune receptors. Based on previous findings, we propose a double-edged model of cholesterol regulation on receptor activation: 1) cholesterol directly binds TMD to keep immune receptors in an inactive (close conformation) state (33); 2) once the immune cell is stimulated, cholesterol indirectly mediates the clustering of immune receptors (34, 35), which might be in an activation (open conformation) state. Cholesterol might finely tune the activation threshold to avoid perturbations from non-specific noise signals. Once strong stimulation activates the conformational change of receptor TMD, cholesterol could facilitate immune receptors clustering to launch and amplify downstream signaling cascades. Therefore, whether and which residues of receptor TMD mediate direct interaction with cholesterol, and if so, how cholesterol keeps immune receptors in the close conformation or resting state, and how strong stimulation (e.g. ligand binding) could trigger the conformational change of immune receptors to form the cholesterol-mediated nano or micro clusters, need to be further investigated with atomic resolutions.

As a major biochemical component of the PM, cholesterol can bifunctionally regulate TCR dynamics and functions (**Figure 1A**). On one hand, it associates with the TMD of the TCR β chain and keeps TCR in a resting and inactive conformation, preventing CD3 phosphorylation and recruitment of downstream signaling components, such as ZAP70 and ERK (33). On the other hand, it can also enhance TCR nanoclustering to promote T cell activation (36–38). Moreover, cholesterol can regulate TCR clustering and signaling through dynamic lipid rafts (35, 39, 40). For example, the increased cholesterol level in the PM by inhibiting cholesterol esterification of $CD8^+$ T cell *in vivo* can promote TCR clustering, enhance immune synapse formation, and amplify the phosphorylation of CD3, ZAP70, and ERK to produce more cytokine, leading to T cell proliferation (41). Consistently, cholesterol sulfate can inhibit CD3 immunoreceptor tyrosine-based activation motif (ITAM) phosphorylation by replacing cholesterol to disrupt the formation of TCR nano-clustering (42). The depletion of cholesterol in T cells also drastically reduces *in-situ* TCR/pMHC binding affinities and association rates, potentially through regulating the conformation or orientation of TCR's TMD and ectodomains to impair TCR antigen recognition (43). In brief, cholesterol possibly tunes TCR initial allosteric switch and subsequent clustering, respectively. The detailed regulation mechanism remains ambiguous, which requires further investigation with atomic resolution to reveal how exactly cholesterol dynamically associates with the TCR/CD3 complex. The cryo-EM structure of TCR/CD3 complex with membrane lipid and cholesterol will provide us more meaningful insights.

During the antigen recognition process of B cells, the micro-cluster formation of the BCR complex is crucial to strengthen BCR activation signaling (44, 45). Cholesterol has been reported to regulate the distribution of BCRs in PM microdomains, and low cholesterol level impairs BCRs aggregation further to affect Vav and Rac1 phosphorylation (46, 47). Moreover, cholesterol may affect the formation of protein islands, nanodomains, or microvilli on the PM, which provides a platform for BCRs to form their unique signaling complex with coreceptors (28, 48–50). Meanwhile, cholesterol could also induce BCR endocytosis on anergic cells to inhibit BCR signaling (51). Therefore, cholesterol also has double-edged regulation (amplifying or attenuating) on BCR signaling. However, the detailed molecular mechanism of these two regulatory effects and their switching is still unclear.

The lipid raft, mainly consisting with cholesterol, can directly tune activating receptor FcγRIIA signaling (e.g. phosphorylation of CbI and NTAL) without ligand binding (52). The cholesterol depletion can impair FcγRIIA association with CD55, GM1, and Lyn kinase, and the related phosphorylation signaling (53). Similar to FcγRIIA, FcγRIIIA activation could also be inhibited

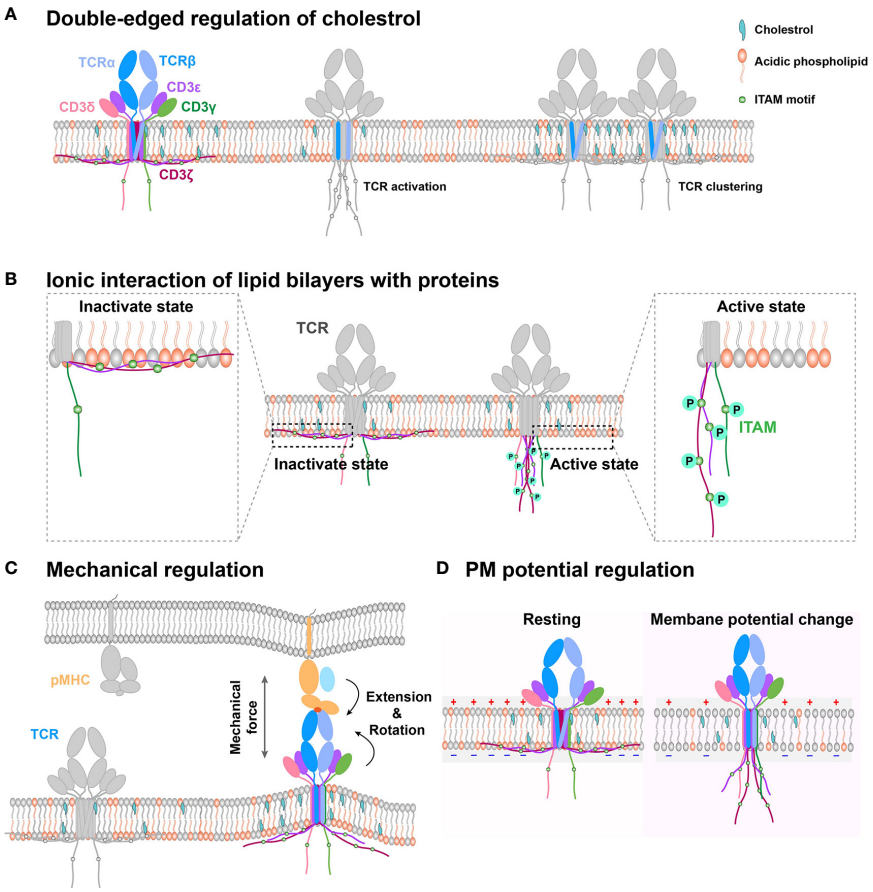

FIGURE 1 | Schematic models of PM regulation on TCR complex signaling. **(A)** Double-edged regulation of cholesterol on TCR activation. Cholesterol could directly bind with the TMD of the TCR β chain to keep TCR in an inactive state in the resting T cell. Cholesterol disassociation from the TCR β chain can switch the TCR complex to the activation state. Meanwhile, cholesterol also indirectly mediates TCR clustering, following TCR initial activation. **(B)** The interaction between negatively charged lipid and basic motif regulates CD3 ITAM motif exposure. TCR cytoplasmic domains contain polybasic regions, which directly interact with the negatively charged lipid in the membrane inner leaflet to embed the ITAM motif in hydrophobic core of the PM in resting cell. The disruption of this interaction can expose the signaling motif to amplify downstream signaling. **(C)** PM provides a platform to sense outside cues for immune receptors. On this platform, mechanical force regulates TCR/pMHC recognition through conformation change. **(D)** Electrical potential might directly trigger TCR signaling. Since TCR TMD contains several charged residues, PM potential depolarization might induce TMD titling conformation to further allosterically regulate dissociation of CD3 tails from inner leaflet and activate intracellular downstream signaling.

by cholesterol depletion to reduce ERK activation and prevent IFN-γ production (54). And the intracellular tyrosine phosphorylation of inhibitory receptor, FcγRIIIB, can also be significantly attenuated when the cholesterol level reduces (55, 56). Moreover, cholesterol can directly regulate the recognition of FcγRI to IgG (57). These detailed regulation molecular mechanisms still need to be further investigated.

SIGNALING MOTIFS PROTECTION BY NEGATIVELY CHARGED LIPID/BASIC MOTIF INTERACTION

The PM inner leaflet enriches negatively charged lipids (e.g. phosphatidylserine, phosphatidylinositol, etc.) that can interact with the polybasic regions of immune receptors to regulate their activation. Such interaction can embed the signaling motif of the immune receptors in the PM hydrophobic core. The positively charged Ca^{2+} ions flux, which is triggered by strong agonistic ligand stimulation, can disrupt this interaction to uncover the buried signaling site (58–61). The PM shields noise signal interference through their selective association with critical signaling motifs until strong stimulation is initiated. This mechanism of signaling shielding and amplification by regulating negatively charged lipid/basic motif interaction is potentially shared by many other immune receptors.

The inner leaflet of T cell PM mainly consists of negatively charged lipids, which associate with CD3ϵ/ζ cytoplasmic ITAM motif through electrostatic interactions (**Figure 1B**). These lipid and CD3 interactions protect CD3ϵ/ζ ITAMs from being recognized and phosphorylated by downstream kinase molecules, such as Lck (59, 60, 62, 63), thus keeping TCR/CD3

in the resting state and T cells in a quiescence state. As it has been extensively reviewed before (60), we here just briefly discuss it.

For the mIgG-BCR, PM's inner side could block non-specific stimulation and keep mIgG-BCR in a resting state, providing the critical activation thresholds for mIgG-BCRs (58). As the cytoplasmic region of the mIgG (mIgG-tail) contains several basic residues, it could electrostatically bind with negatively charged acidic phospholipids of the PM's inner leaflet to block the interference from noise signals and keep mIgG-BCR in a resting state in quiescent B cells (58). Ca^{2+} mobilization triggered by suitable antigenic stimulation on the mIgG-BCR complex could disrupt this protection, which further recruits pSyk, pBLNK, and pPI3K into the immunological synapse to induce a more potent Ca^{2+} mobilization response and B-cell hyperproliferation. Moreover, phosphatidylinositol (4,5)-bisphosphate (PIP2) triggers a signaling amplification loop to induce the initial formation of BCR micro-clusters upon B cell activation (64). PIP2 and phosphatidylinositol (3,4,5)-trisphosphate (PIP3) together tune the growth of BCR micro-clusters by recruiting Dock2 to remodel F-actin cytoskeleton (65). Remarkably, this electrostatical interaction mechanism might not be suitable for mIgG-associated Igα and Igβ as they contain polyacidic regions (58, 60).

MECHANICAL REGULATION AND ITS COUPLING WITH CHOLESTEROL AND NEGATIVELY CHARGED LIPID

In general, the PM provides a platform for immune receptors to sense outside physical and biochemical cues. Unlike biomolecules in solution that can freely rotate and adopt many different possible orientations, immune receptors' orientations are significantly restricted by the PM. They only can adopt limited protein topologies, which are essential for receptor-ligand binding and downstream signaling transduction. The membrane anchor pattern, extracellular length, and orientation of immune receptors all could influence the recognition of their ligands by affecting ligand accessibility and association kinetics. Meanwhile, the physical platform also tightly restricts immune receptors diffusion, which is distinct to that in solution, thereby drastically affecting immune receptor-ligand binding affinity (66). Moreover, the immune receptors also experience mechanical force induced by membrane tension and cytoskeleton contractions (23–25). The mechanical force has been reported to induce conformational changes of immune receptor and ligand to regulate their binding strength and immune functions. It is very likely that these mechanically regulated protein conformational changes could propagate across the PM and transduce toward the inside of the cell to allosterically regulate the conformation of the receptors' cytoplasmic tails and potentially their associated kinases or other adaptor molecules. Such propagation could provide a rapid physical activation of receptor signal transduction, other than traditionally accepted biochemical ways. This mechanical regulation might be universal in immune receptors. During cross-membrane mechanical propagation, cholesterol could inevitably be integrated with force to collectively regulate the conformation of receptor's TMD. For example, cholesterol can regulate PM tension, which in turn tunes cholesterol distribution, membrane stiffness and bending (67–69), thereby inducing immune receptors ectodomain conformational changes and TMD titling. Cholesterol could potentially prevent or facilitate the TMD tilting, which may be dependent on how cholesterol dynamically interacts with receptor's TMD. Collectively, the mechano-biochemical coupling could contribute to the conformational changes, triggering and clustering of immune receptors.

The PM provides a physical platform for TCR/CD3 complex to sense antigens (66). On this platform, TCR inevitably experiences external mechanical forces when T cells contact the antigen-presenting cell (APC) or migrate on the APC and the extracellular matrix (ECM), and the internal mechanical force produced by dynamic cytoskeleton contraction during T-cell searching for foreign antigens on the APC or membrane bending tension upon T-cell/APC contact formation (23, 70–73). For TCR recognition of pMHCs, the mechanical force can prolong the bond lifetimes for agonistic antigens but not antagonists by selectively inducing conformational changes (**Figure 1C**) of the agonistic pMHC to initiate the formation of new hydrogen bonds (electrostatic attraction between the hydrogen atom and negatively charged nitrogen or oxygen atom) (72, 73). This force induced by pMHC/TCR binding inevitably increases local membrane tension and further induces membrane bending, which might disrupt the interactions between CD3 polybasic regions and negatively charged lipids of the inner leaflet to expose ITAM motifs for Lck to phosphorylate and further trigger downstream signaling.

PM stiffness can also regulate the antigen discrimination of BCRs. BCR has stringent affinity discrimination when contacting with rigid APC PM during the invagination of antigens (74). Also, PM shape can regulate BCR stimulation by affecting the formation of BCR microclusters (75). On the PM platform, the mechanical force provides multiple effects on different isotyped BCRs, which influences the activation sensitivity of BCR by pathological antigens (antigens that can induce a specific immune response to cause the infectious, allergic or autoimmune diseases) (76). Low mechanical force (<12 pN) is enough to trigger the activation (e.g. BCR, pSyk, pPLCγ2, and pTyr clusters) of IgG- or IgE-BCR on memory B cells, but not IgM-BCR on mature naive B cells (76).

Besides, PM curvature causes the redistribution of FcεRI (77, 78). FcεRI bond with IgE always locates at the contact membrane regions which are less curved (79). Similarly, FcγRIIA also can be regulated by the mechanical force under the physiological flow conditions, which facilitates the capture of neutrophils directly by endothelial cells (80). Moreover, the recognition of FcγRII and FcγRIII to IgG is influenced by the anchor patterns (e.g. GPI and transmembrane domain) on the immune cell PM (81, 82).

It has been reported that high membrane tension or mechanical force helps CD28 (another costimulatory receptor

of TCR complex) to facilitate TCR signaling on the PM platform (83, 84). Also, LFA-1/ICAM-1 interaction is affected by the mechanical force to regulate T cell migration (85–88). For natural killer cells, PM stiffness can regulate the NKG2D/MICA interaction to determine the cell cytotoxic activity (89).

ELECTRICAL POTENTIAL REGULATION AND ITS COUPLING WITH MECHANICAL AND BIOCHEMICAL CUES

The PM electrical potential, which is commonly overlooked in the immunology field, is another essential biophysical factor that also potentially regulates immune receptor functions. It is generally defined as the electric potential difference between the intracellular and extracellular solution. PM potential depolarization can facilitate the opening of Ca^{2+} channels and initiate the mitotic activity to regulate the activation and proliferation of lymphocyte cells (90–92). The regulation of PM potential on neural activity and the networks has been widely reported. Its molecular regulation mechanism mainly divides into three ways (93). First, TMD conformational change of the voltage-dependent ion channels is triggered by PM potential depolarization (94). Considering that the TCR complex TMD contains several charged residues buried in the lipid bilayer, we propose that PM potential depolarization, which is triggered by T cell activation (95), might tilt the conformation of TCR TMD to further allosterically regulate the dissociation of CD3 tails from the inner leaflet of PM and activate intracellular downstream signaling (**Figure 1D**). However, this depolarization-induced TCR allosteric activation needs to be further investigated with detailed biophysical investigation. Second, ion influx, an indirect effect of depolarization, regulates transmembrane proteins. The possible mechanism might be that ion influx regulates ligand binding and tyrosine phosphorylation (96, 97). It has been reported that Ca^{2+} influx disrupts the interactions between CD3 cytoplasmic polybasic regions and negatively charged lipids to favor CD3 ITAMs phosphorylation. However, whether PM potential might directly tune CD3 ITAMs phosphorylation is still unknown. Third, the electro-osmosis or electrophoresis induced by local electric fields, re-distributes transmembrane protein on the PM (98). Like neural synapses, the immune synapses might also exist this electromigration to regulate immune receptor distribution pattern, which favors the recognition of APCs by T cells.

Notably, PM surface usually exists a ~2 nm electrical double layer (EDL, a layer formed by freely diffusing electrolyte ions in the nanometer range of the charged surface), which is regulated by lipid distribution and intracellular/extracellular ions concentration (16). Key proximal regions of TMD, usually containing acidic or basic amino acids and locating in the EDL, might respond to the electrical potential change to regulate immune receptor conformations. For example, Ca^{2+} influx of T cell activation indeed changes the ion distribution and reduces the interaction between the cytoplasmic domain of CD3 or CD28 and EDL, activating downstream signal transduction.

PM potential can also affect other chemical and biophysical properties, such as lipid distribution, membrane fluidity, tension, and curvature of PM (99, 100), dynamically changing the mechanical and biochemical environment where immune receptors reside (23). For example, PM potential depolarization can induce changes in PM curvature and tension, which could further regulate the mechano-dependent behavior of immune receptors, such as the conformational changes and ligand binding kinetics (23, 100, 101). Meanwhile, the depolarization also reduces the lateral diffusion of membrane components (e.g. cholesterol, phospholipids, and protein) to affect the formation of lipid rafts, receptor microclusters, and microvilli (12, 99, 102, 103), all of which are crucial for immune receptor activation (12, 26, 28).

Inversely, the compositions of lipids and cholesterols can directly affect the charge distribution on the PM surface, which further determines the PM potential (12, 16, 30). PM tension and curvature might also tune immune cell PM potential through mechanosensitive Piezo1 channel (104), causing a series of related regulation on immune receptor activation. However, the detailed mechanism still needs further investigation.

Based on the above elaboration, the PM platform provides mechanical-electric-chemical coupling to synergistically regulate immune receptor-ligand recognition, conformational changes, and cross-membrane activation. This is also exciting to be investigated in the future.

CONCLUSION

In recent decades, the regulation of immune cell PM chemical properties on the receptor activation has been broadly investigated, and some of them have been revealed. However, many other PM biophysical effects (e.g. membrane tension and electrical potential) have not been clearly examined. Especially, whether and how biophysical-chemical cues couple together to tune receptors, and their molecular mechanism of these regulation patterns all need to be further investigated. Answering all these above questions will improve our understanding of immune receptor activation, especially TCR, thus contributing to immunotherapies development [e.g. chimeric antigen receptor (CAR) T-cell design].

AUTHOR CONTRIBUTIONS

WC conceived the writing. TZ wrote the first version of the manuscript and prepared the figures. WH and WC revised the paper. All authors contributed to the article and approved the submitted version.

FUNDING

WC is funded by grants from the Ministry of Science and Technology of China (No. 2017ZX10203205), and the National Natural Science Foundation of China (No. 31971237). WH is

funded by grants from The National Natural Science Foundation of China (No. 12002307) and China Postdoctoral Science Foundation (No. 2020M671697).

ACKNOWLEDGMENTS

We thank Jizhong Lou for the thoughtful discussion.

REFERENCES

1. Sezgin E, Levental I, Mayor S, Eggeling C. The mystery of membrane organization: composition, regulation and roles of lipid rafts. *Nat Rev Mol Cell Biol* (2017) 18:361–74. doi: 10.1038/nrm.2017.16
2. Balla T. Phosphoinositides: tiny lipids with giant impact on cell regulation. *Physiol Rev* (2013) 93:1019–137. doi: 10.1152/physrev.00028.2012
3. Leventis PA, Grinstein S. The distribution and function of phosphatidylserine in cellular membranes. *Annu Rev Biophys* (2010) 39:407–27. doi: 10.1146/annurev.biophys.093008.131234
4. Mouritsen OG, Bloom M. Mattress model of lipid-protein interactions in membranes. *Biophys J* (1984) 46:141–53. doi: 10.1016/S0006-3495(84)84007-2
5. Singer S. A fluid lipid-globular protein mosaic model of membrane structure. *Ann N Y Acad Sci* (1972) 195:16–23. doi: 10.1111/j.1749-6632.1972.tb54780.x
6. Nicolson GL. The fluid-mosaic model of membrane structure: still relevant to understanding the structure, function and dynamics of biological membranes after more than 40 years. *Biochim Biophys Acta* (2014) 1838:1451–66. doi: 10.1016/j.bbamem.2013.10.019
7. Singer SJ, Nicolson GL. The fluid mosaic model of the structure of cell membranes. *Science* (1972) 175:720–31. doi: 10.1126/science.175.4023.720
8. Nicolson GL. Cell membrane fluid-mosaic structure and cancer metastasis. *Cancer Res* (2015) 75:1169–76. doi: 10.1158/0008-5472.CAN-14-3216
9. Tank DW, Wu ES, Webb WW. Enhanced molecular diffusibility in muscle membrane blebs: release of lateral constraints. *J Cell Biol* (1982) 92:207–12. doi: 10.1083/jcb.92.1.207
10. Bernardino de la Serna J, Schütz GJ, Eggeling C. Cebecauer MJFic, and biology d. There is no simple model of the plasma membrane organization. *Front Cell Dev Biol* (2016) 4:106. doi: 10.3389/fcell.2016.00106
11. Pike LJ. Rafts defined: a report on the keystone symposium on lipid rafts and cell function. *J Lipid Res* (2006) 47:1597–8. doi: 10.1194/jlr.E600002-JLR200
12. Cebecauer M, Amaro M, Jurkiewicz P, Sarmento MJ, Sachl R, Cwiklik L, et al. Membrane Lipid Nanodomains. *Chem Rev* (2018) 118:11259–97. doi: 10.1021/acs.chemrev.8b00322
13. Rothman JE, Lenard J. Membrane asymmetry. *Science* (1977) 195:743–53. doi: 10.1126/science.402030
14. Baumgart T, Capraro BR, Zhu C, Das SL. Thermodynamics and mechanics of membrane curvature generation and sensing by proteins and lipids. *Annu Rev Phys Chem* (2011) 62:483–506. doi: 10.1146/annurev.physchem.012809.103450
15. Yang M, Brackenbury WJ. Membrane potential and cancer progression. *Front Physiol* (2013) 4:185. doi: 10.3389/fphys.2013.00185
16. Savtchenko LP, Poo MM, Rusakov DA. Electrodiffusion phenomena in neuroscience: a neglected companion. *Nat Rev Neurosci* (2017) 18:598–612. doi: 10.1038/nrn.2017.101
17. Surls J, Nazarov-Stoica C, Kehl M, Olsen C, Casares S, Brumeanu TD. Increased membrane cholesterol in lymphocytes diverts T-cells toward an inflammatory response. *PloS One* (2012) 7:e38733. doi: 10.1371/journal.pone.0038733
18. Chyu KY, Lio WM, Dimayuga PC, Zhou J, Zhao X, Yano J, et al. Cholesterol lowering modulates T cell function *in vivo* and *in vitro*. *PloS One* (2014) 9:e92095. doi: 10.1371/journal.pone.0092095
19. Mailer RKW, Gistera A, Polyzos KA, Ketelhuth DFJ, Hansson GK. Hypercholesterolemia induces differentiation of regulatory T Cells in the liver. *Circ Res* (2017) 120:1740–53. doi: 10.1161/CIRCRESAHA.116.310054
20. Ma X, Bi E, Lu Y, Su P, Huang C, Liu L, et al. Cholesterol induces CD8(+) T cell exhaustion in the tumor microenvironment. *Cell Metab* (2019) 30:143–56. doi: 10.1016/j.cmet.2019.04.002
21. Elliott JI, Surprenant A, Marelli-Berg FM, Cooper JC, Cassady-Cain RL, Wooding C, et al. Membrane phosphatidylserine distribution as a non-apoptotic signalling mechanism in lymphocytes. *Nat Cell Biol* (2005) 7:808–16. doi: 10.1038/ncb1279
22. Rysavy NM, Shimoda LM, Dixon AM, Speck M, Stokes AJ, Turner H, et al. Beyond apoptosis: the mechanism and function of phosphatidylserine asymmetry in the membrane of activating mast cells. *Bioarchitecture* (2014) 4:127–37. doi: 10.1080/19490992.2014.995516
23. Zhu C, Chen W, Lou J, Rittase W, Li K. Mechanosensing through immunoreceptors. *Nuture Immunol* (2019) 20:1269–78. doi: 10.1038/s41590-019-0491-1
24. Rossy J, Laufer JM, Legler DF. Role of mechanotransduction and tension in T cell function. *Front Immunol* (2018) 9:2638. doi: 10.3389/fimmu.2018.02638
25. Dupre L, Houmadi R, Tang C, Rey-Barroso J. T lymphocyte migration: an action movie starring the actin and associated actors. *Front Immunol* (2015) 6:586. doi: 10.3389/fimmu.2015.00586
26. Cai E, Marchuk K, Beemiller P, Beppler C, Rubashkin MG, Weaver VM, et al. Visualizing dynamic microvillar search and stabilization during ligand detection by T cells. *Science* (2017) 356:6338. doi: 10.1126/science.aal3118
27. Jung YM, Riven I, Feigelson SW, Kartvelishvily E, Tohya K, Miyasaka M, et al. Three-dimensional localization of T-cell receptors in relation to microvilli using a combination of superresolution microscopies. *Proc Natl Acad Sci United States America* (2016) 113:E5916–24. doi: 10.1073/pnas.1605399113
28. Greicius G, Westerberg L, Davey EJ, Buentke E, Scheynius A, Thyberg J, et al. Microvilli structures on B lymphocytes: inducible functional domains? *Int Immunol* (2004) 16:353–64. doi: 10.1093/intimm/dxh031
29. Lewis RS, Cahalan MD. Subset-specific expression of potassium channels in developing murine T lymphocytes. *Science* (1988) 239:771–5. doi: 10.1126/science.2448877
30. Ma Y, Poole K, Goyette J, Gaus K. Introducing membrane charge and membrane potential to T cell signaling. *Front Immunol* (2017) 8:1513. doi: 10.3389/fimmu.2017.01513
31. Baier CJ, Fantini J, Barrantes FJ. Disclosure of cholesterol recognition motifs in transmembrane domains of the human nicotinic acetylcholine receptor. *Sci Rep* (2011) 1:69. doi: 10.1038/srep00069
32. Hedger G, Koldso H, Chavent M, Siebold C, Rohatgi R, Sansom MSP. Cholesterol interaction sites on the transmembrane domain of the hedgehog signal transducer and class F G protein-coupled receptor smoothened. *Structure* (2019) 27:549–59. doi: 10.1016/j.str.2018.11.003
33. Swamy M, Beck-Garcia K, Beck-Garcia E, Hartl FA, Morath A, Yousefi OS, et al. A cholesterol-based allostery model of T cell receptor phosphorylation. *Immunity* (2016) 44:1091–101. doi: 10.1016/j.immuni.2016.04.011
34. Fantini J, Di Scala C, Evans LS, Williamson PTF, Barrantes FJ. A mirror code for protein-cholesterol interactions in the two leaflets of biological membranes. *Sci Rep* (2016) 6:21906. doi: 10.1038/srep21907
35. Bietz A, Zhu H, Xue M, Xu C. Cholesterol Metabolism in T Cells. *Front Immunol* (2017) 8:1664. doi: 10.3389/fimmu.2017.01664
36. Molnar E, Swamy M, Holzer M, Beck-Garcia K, Worch R, Thiele C, et al. Cholesterol and sphingomyelin drive ligand-independent T-cell antigen receptor nanoclustering. *J Biol Chem* (2012) 287:42664–74. doi: 10.1074/jbc.M112.386045
37. Roh K-H, Lillemeier BF, Wang F, Davis M. The coreceptor CD4 is expressed in distinct nanoclusters and does not colocalize with T-cell receptor and active protein tyrosine kinase p56lck. *PNAS* (2015) 112:E1604–13. doi: 10.1073/pnas.1503532112
38. Hu YS, Cang H, Lillemeier BF. Superresolution imaging reveals nanometer- and micrometer-scale spatial distributions of T-cell receptors in lymph nodes. *Proc Natl Acad Sci United States America* (2016) 113:7201–6. doi: 10.1073/pnas.1512331113
39. Krishnan S, Nambiar MP, Warke VG, Fisher CU, Mitchell J, Delaney N, et al. Alterations in lipid raft composition and dynamics contribute to abnormal T cell responses in systemic lupus erythematosus. *J Immunol* (2004) 172:7821–31. doi: 10.4049/jimmunol.172.12.7821
40. Deng GM, Tsokos GC. Cholera toxin B accelerates disease progression in lupus-prone mice by promoting lipid raft aggregation. *J Immunol* (2008) 181:4019–26. doi: 10.4049/jimmunol.181.6.4019

41. Yang W, Bai Y, Xiong Y, Zhang J, Chen S, Zheng X, et al. Potentiating the antitumour response of CD8(+) T cells by modulating cholesterol metabolism. *Nature* (2016) 531:651–5. doi: 10.1038/nature17412
42. Wang F, Beck-Garcia K, Zorzin C, Schamel WW, Davis MM. Inhibition of T cell receptor signaling by cholesterol sulfate, a naturally occurring derivative of membrane cholesterol. *Nat Immunol* (2016) 17:844–50. doi: 10.1038/ni.3462
43. Liu B, Chen W, Natarajan K, Li Z, Margulies DH, Zhu C. The cellular environment regulates in situ kinetics of T-cell receptor interaction with peptide major histocompatibility complex. *Eur J Immunol* (2015) 45:2099–110. doi: 10.1002/eji.201445358
44. Tolar P, Sohn HW, Pierce SK. The initiation of antigen-induced B cell antigen receptor signaling viewed in living cells by fluorescence resonance energy transfer. *Nat Immunol* (2005) 6:1168–76. doi: 10.1038/ni1262
45. Tolar P, Hanna J, Krueger PD, Pierce SK. The constant region of the membrane immunoglobulin mediates B cell-receptor clustering and signaling in response to membrane antigens. *Immunity* (2009) 30:44–55. doi: 10.1016/j.immuni.2008.11.007
46. Karnell FG, Brezski RJ, King LB, Silverman MA, Monroe JG. Membrane cholesterol content accounts for developmental differences in surface B cell receptor compartmentalization and signaling. *J Biol Chem* (2005) 280:25621–8. doi: 10.1074/jbc.M503162200
47. Brezski RJ, Monroe JG. B cell antigen receptor-induced Rac1 activation and Rac1-dependent spreading are impaired in transitional immature B cells due to levels of membrane cholesterol. *J Immunol* (2007) 179:4464–72. doi: 10.4049/jimmunol.179.7.4464
48. Maity PC, Blount A, Jumaa H, Ronneberger O, Lillemeier BF, Reth M. B cell antigen receptors of the IgM and IgD classes are clustered in different protein islands that are altered during B cell activation. *Sci Signaling* (2015) 8:ra93–3. doi: 10.1126/scisignal.2005887
49. Becker M, Hobeika E, Jumaa H, Reth M, Maity PC. CXCR4 signaling and function require the expression of the IgD-class B-cell antigen receptor. *Proc Natl Acad Sci USA* (2017) 114:5231–6. doi: 10.1073/pnas.1621512114
50. Gold MR, Reth MG. Antigen Receptor Function in the Context of the Nanoscale Organization of the B Cell Membrane. *Annu Rev Immunol* (2019) 37:97–123. doi: 10.1146/annurev-immunol-042718-041704
51. Blery M, Tze L, Miosge LA, Jun JE, Goodnow CC. Essential role of membrane cholesterol in accelerated BCR internalization and uncoupling from NF-kappa B in B cell clonal anergy. *J Exp Med* (2006) 203:1773–83. doi: 10.1084/jem.20060552
52. Kulma M, Kwiatkowska K, Sobota A. Raft coalescence and FcgammaRIIA activation upon sphingomyelin clustering induced by lysenin. *Cell Signal* (2012) 24:1641–7. doi: 10.1016/j.cellsig.2012.04.007
53. Kwiatkowska K, Sobota A. The clustered Fcγ receptor II is recruited to Lyn-containing membrane domains and undergoes phosphorylation in a cholesterol-dependent manner. *Eur J Immunol* (2001) 31:989–98. doi: 10.1002/1521-4141(200104)31:4<989::aid-immu989>3.0.co;2-v
54. Kondadasula SV, Roda JM, Parihar R, Yu J, Lehman A, Caligiuri MA, et al. Colocalization of the IL-12 receptor and FcgammaRIIIa to natural killer cell lipid rafts leads to activation of ERK and enhanced production of interferon-gamma. *Blood* (2008) 111:4173–83. doi: 10.1182/blood-2007-01-068908
55. Fernandes MJ, Rollet-Labelle E, Pare G, Marois S, Tremblay ML, Teillaud JL, et al. CD16b associates with high-density, detergent-resistant membranes in human neutrophils. *Biochem J* (2006) 393:351–9. doi: 10.1042/BJ20050129
56. David A, Fridlich R, Aviram I. The presence of membrane Proteinase 3 in neutrophil lipid rafts and its colocalization with FcgammaRIIIb and cytochrome b558. *Exp Cell Res* (2005) 308:156–65. doi: 10.1016/j.yexcr.2005.03.034
57. Beekman JM, van der Linden JA, van de Winkel JG, Leusen JH. FcgammaRI (CD64) resides constitutively in lipid rafts. *Immunol Lett* (2008) 116:149–55. doi: 10.1016/j.imlet.2007.12.003
58. Chen X, Pan W, Sui Y, Li H, Shi X, Guo X, et al. Acidic phospholipids govern the enhanced activation of IgG-B cell receptor. *Nat Commun* (2015) 6:8552. doi: 10.1038/ncomms9552
59. Xu C, Gagnon E, Call ME, Schnell JR, Schwieters CD, Carman CV, et al. Regulation of T cell receptor activation by dynamic membrane binding of the CD3ε cytoplasmic tyrosine-based motif. *Cell* (2008) 135:702–13. doi: 10.1016/j.cell.2008.09.044
60. Li H, Yan C, Guo J, Xu C. Ionic protein-lipid interactions at the plasma membrane regulate the structure and function of immunoreceptors. *Adv Immunol* (2019) 144:65–85. doi: 10.1016/bs.ai.2019.08.007
61. Shi X, Bi Y, Yang W, Guo X, Jiang Y, Wan C, et al. Ca2+ regulates T-cell receptor activation by modulating the charge property of lipids. *Nature* (2013) 493:111–5. doi: 10.1038/nature11699
62. Kuhns MS, Davis MM. The safety on the TCR trigger. *Cell* (2008) 135:594–6. doi: 10.1016/j.cell.2008.10.033
63. Aivazian D, Stern LJ. Phosphorylation of T cell receptor ζ is regulated by a lipid dependent folding transition. *Nat Struct Biol* (2000) 7:1023–6. doi: 10.1038/80930
64. Xu C, Xie H, Guo X, Gong H, Liu L, Qi H, et al. A PIP2-derived amplification loop fuels the sustained initiation of B cell activation. *Sci Immunol* (2017) 2: eaan0787. doi: 10.1126/sciimmunol.aan0787
65. Wang J, Xu L, Shaheen S, Liu S, Zheng W, Sun X, et al. Growth of B cell receptor microclusters is regulated by PIP2 and PIP3 equilibrium and Dock2 recruitment and activation. *Cell Rep* (2017) 21:2541–57. doi: 10.1016/j.celrep.2017.10.117
66. Huang J, Zarnitsyna VI, Liu B, Edwards LJ, Jiang N, Evavold BD, et al. The kinetics of two-dimensional TCR and pMHC interactions determine T-cell responsiveness. *Nature* (2010) 464:932–6. doi: 10.1038/nature08944
67. Biswas A, Kashyap P, Datta S, Sengupta T, Sinha B. Cholesterol depletion by MβCD enhances cell membrane tension and Its variations-reducing integrity. *Biophys J* (2019) 116:1456–68. doi: 10.1016/j.bpj.2019.03.016
68. Petelska AD, Naumowicz M, Figaszewski ZA. The interfacial tension of the lipid membrane formed from lipid-cholesterol and lipid-lipid systems. *Cell Biochem Biophys* (2006) 44:205–11. doi: 10.1385/CBB:44:2:205
69. Nomoto T, Takahashi M, Fujii T, Chiari L, Toyota T, Fujinami M. Effects of cholesterol concentration and osmolarity on the fluidity and membrane tension of free-standing black lipid membranes. *Anal Sci* (2018) 34:1237–42. doi: 10.2116/analsci.18P200
70. Marshall BT, Long M, Piper JW, Yago T, McEver RP, Zhu C. Direct observation of catch bonds involving cell-adhesion molecules. *Nature* (2003) 423:190–3. doi: 10.1038/nature01605
71. Liu B, Chen W, Evavold BD, Zhu C. Accumulation of dynamic catch bonds between TCR and agonist peptide-MHC triggers T cell signaling. *Cell* (2014) 157:357–68. doi: 10.1016/j.cell.2014.02.053
72. Wu P, Zhang T, Liu B, Fei P, Cui L, Qin R, et al. Mechano-regulation of peptide-MHC class I conformations determines TCR antigen recognition. *Mol Cell* (2019) 73:1015–27. doi: 10.1016/j.molcel.2018.12.018
73. Das DK, Feng Y, Mallis RJ, Li X, Keskin DB, Hussey RE, et al. Force-dependent transition in the T-cell receptor beta-subunit allosterically regulates peptide discrimination and pMHC bond lifetime. *Proc Natl Acad Sci USA* (2015) 112:1517–22. doi: 10.1073/pnas.1424829112
74. Spillane KM, Tolar P. B cell antigen extraction is regulated by physical properties of antigen-presenting cells. *J Cell Biol* (2017) 216:217–30. doi: 10.1083/jcb.201607064
75. Treanor B, Depoil D, Bruckbauer A, Batista FD. Dynamic cortical actin remodeling by ERM proteins controls BCR microcluster organization and integrity. *J Exp Med* (2011) 208:1055–68. doi: 10.1084/jem.20101125
76. Wan Z, Chen X, Chen H, Ji Q, Chen Y, Wang J, et al. The activation of IgM- or isotype-switched IgG- and IgE-BCR exhibits distinct mechanical force sensitivity and threshold. *Elife* (2015) 4:e06925. doi: 10.7554/eLife.06925
77. Spendier K. N-terminal amphipathic helix of Amphiphysin can change the spatial distribution of immunoglobulin E receptors (FcepsilonRI) in the RBL-2H3 mast cell synapse. *Results Immunol* (2016) 6:1–4. doi: 10.1016/j.rinim.2015.11.001
78. Spendier K, Carroll-Portillo A, Lidke KA, Wilson BS, Timlin JA, Thomas JL. Distribution and dynamics of rat basophilic leukemia immunoglobulin E receptors (FcεRI) on planar ligand-presenting surfaces. *Biophys J* (2010) 99:388–97. doi: 10.1016/j.bpj.2010.04.029
79. Machado R, Bendesky J, Brown M, Spendier K, Hagen GM. Imaging membrane curvature inside a FcεRI-centric synapse in RBL-2H3 cells using TIRF microscopy with polarized excitation. *J Biol Chem* (2019) 5:63. doi: 10.3390/jimaging5070063
80. Nishi H, Furuhashi K, Cullere X, Saggu G, Miller MJ, Chen Y, et al. Neutrophil FcgammaRIIA promotes IgG-mediated glomerular neutrophil capture *via* Abl/Src kinases. *J Clin Invest* (2017) 127:3810–26. doi: 10.1172/JCI94039

81. Williams TE, Nagarajan S, Selvaraj P, Zhu C. Concurrent and independent binding of Fcgamma receptors IIa and IIIb to surface-bound IgG. *Biophys J* (2000) 79:1867–75. doi: 10.1016/S0006-3495(00)76436-8
82. Hu W, Zhang Y, Sun X, Zhang T, Xu L, Xie H, et al. FcgammaRIIB-I232T polymorphic change allosterically suppresses ligand binding. *Elife* (2019) 8: e46689. doi: 10.7554/eLife.46689
83. Bashour KT, Gondarenko A, Chen H, Shen K, Liu X, Huse M, et al. CD28 and CD3 have complementary roles in T-cell traction forces. *Proc Natl Acad Sci USA* (2014) 111:2241–6. doi: 10.1073/pnas.1315606111
84. Hong J, Ge C, Jothikumar P, Yuan Z, Liu B, Bai K, et al. A TCR mechanotransduction signaling loop induces negative selection in the thymus. *Nat Immunol* (2018) 19:1379–90. doi: 10.1038/s41590-018-0259-z
85. Chen W, Zhu C. Mechanical regulation of T-cell functions. *Immunol Rev* (2013) 256:160–76. doi: 10.1111/imr.12122
86. Chen W, Lou J, Zhu C. Forcing switch from short- to intermediate- and long-lived states of the alphaA domain generates LFA-1/ICAM-1 catch bonds. *J Biol Chem* (2010) 285:35967–78. doi: 10.1074/jbc.M110.155770
87. Xiang X, Lee CY, Li T, Chen W, Lou J, Zhu C. Structural basis and kinetics of force-induced conformational changes of an alphaA domain-containing integrin. *PloS One* (2011) 6:e27946. doi: 10.1371/journal.pone.0027946
88. Chen W, Lou J, Evans EA, Zhu C. Observing force-regulated conformational changes and ligand dissociation from a single integrin on cells. *J Cell Biol* (2012) 199:497–512. doi: 10.1083/jcb.201201091
89. Mordechay L, Edri A, Hadad U, Porgador A, Schvartzman M, Le Saux G. Mechanical regulation of the cytotoxic activity of natural killer cells. *bioRxiv* (2020) 7(1):122–32. doi: 10.1021/acsbiomaterials.0c01121
90. Kiefer H, Blume AJ, Kaback HR. Membrane potential changes during mitogenic stimulation of mouse spleen lymphocytes. *Proc Natl Acad Sci USA* (1980) 77:2200–4. doi: 10.1073/pnas.77.4.2200
91. Hess SD, Oortgiesen M, Cahalan MD. Calcium oscillations in human-T and natural-killer-cells depend upon membrane-potential and calcium influx. *J Immunol* (1993) 150:2620–33.
92. Monroe JG, Cambier JC. B cell activation. I. Anti-immunoglobulin-induced receptor cross-linking results in a decrease in the plasma membrane potential of murine B lymphocytes. *J Exp Med* (1983) 157:2073–86. doi: 10.1084/jem.157.6.2073
93. Zhang LI, Poo MM. Electrical activity and development of neural circuits. *Nat Neurosci* (2001) 4 Suppl:1207–14. doi: 10.1038/nn753
94. Zucker RS. Calcium- and activity-dependent synaptic plasticity. *Curr Opin Neurobiol* (1999) 9:305–13. doi: 10.1016/s0959-4388(99)80045-2
95. Felber SM, Brand MD. Early plasma-membrane-potential changes during stimulation of lymphocytes by concanavalin A. *Biochem J* (1983) 210:885–91. doi: 10.1042/bj2100885
96. Cooper DM, Schell MJ, Thorn P, Irvine RF. Regulation of adenylyl cyclase by membrane potential. *J Biol Chem* (1998) 273:27703–7. doi: 10.1074/jbc.273.42.27703
97. Reddy R, Smith D, Wayman G, Wu Z, Villacres EC, Storm DR. Voltage-sensitive adenylyl cyclase activity in cultured neurons. A calcium-independent phenomenon. *J Biol Chem* (1995) 270:14340–6. doi: 10.1074/jbc.270.24.14340
98. Poo M. In situ electrophoresis of membrane components. *Annu Rev Biophys Bioeng* (1981) 10:245–76. doi: 10.1146/annurev.bb.10.060181.001333
99. Oghalai JS, Zhao HB, Kutz JW, Brownell WE. Voltage- and tension-dependent lipid mobility in the outer hair cell plasma membrane. *Science* (2000) 287:658–61. doi: 10.1126/science.287.5453.658
100. Zhang PC, Keleshian AM, Sachs F. Voltage-induced membrane movement. *Nature* (2001) 413:428–32. doi: 10.1038/35096578
101. Todorov AT, Petrov AG, Fendler JH. Flexoelectricity of charged and dipolar bilayer-lipid membranes studied by stroboscopic interferometry. *Langmuir* (1994) 10:2344–50. doi: 10.1021/la00019a053
102. Poste G, Nicolson GL. *Membrane reconstitution*. North Holland: Elsevier Biomedical Press (1982).
103. Golan DE, Alecio MR, Veatch WR, Rando RR. Lateral mobility of phospholipid and cholesterol in the human erythrocyte membrane: effects of protein-lipid interactions. *Biochemistry* (1984) 23:332–9. doi: 10.1021/bi00297a024
104. Liu CSC, Raychaudhuri D, Paul B, Chakrabarty Y, Ghosh AR, Rahaman O, et al. Cutting edge: Piezo1 mechanosensors optimize human T cell activation. *J Immunol* (2018) 200:1255–60. doi: 10.4049/jimmunol.1701118

Conflict of Interest: The authors declare that the research was conducted in the absence of any commercial or financial relationships that could be construed as a potential conflict of interest.

frontiers in Immunology

REVIEW
published: 25 February 2021
doi: 10.3389/fimmu.2021.600829

Biomechanics of T Cell Dysfunctions in Chronic Diseases

Sachith D. Gunasinghe[1,2], *Newton G. Peres*[1,2], *Jesse Goyette*[1,2*] *and Katharina Gaus*[1,2*]

[1] EMBL Australia Node in Single Molecule Science, University of New South Wales, Sydney, NSW, Australia, [2] ARC Centre of Excellence in Advanced Molecular Imaging, University of New South Wales, Sydney, NSW, Australia

Understanding the mechanisms behind T cell dysfunctions during chronic diseases is critical in developing effective immunotherapies. As demonstrated by several animal models and human studies, T cell dysfunctions are induced during chronic diseases, spanning from infections to cancer. Although factors governing the onset and the extent of the functional impairment of T cells can differ during infections and cancer, most dysfunctional phenotypes share common phenotypic traits in their immune receptor and biophysical landscape. Through the latest developments in biophysical techniques applied to explore cell membrane and receptor–ligand dynamics, we are able to dissect and gain further insights into the driving mechanisms behind T cell dysfunctions. These insights may prove useful in developing immunotherapies aimed at reinvigorating our immune system to fight off infections and malignancies more effectively. The recent success with checkpoint inhibitors in treating cancer opens new avenues to develop more effective, targeted immunotherapies. Here, we highlight the studies focused on the transformation of the biophysical landscape during infections and cancer, and how T cell biomechanics shaped the immunopathology associated with chronic diseases.

Keywords: T cell dysfunction, chronic diseases, infections, cancer, tumor microenvironment, immune receptor landscape, biophysical landscape, biomechanics

OPEN ACCESS

Edited by:
Wei Chen,
Zhejiang University, China

Reviewed by:
John J. Miles,
James Cook University, Australia
Hanjie Li,
Shenzhen Institutes of Advanced Technology (CAS), China

****Correspondence:***
Jesse Goyette
j.goyette@unsw.edu.au
Katharina Gaus
k.gaus@unsw.edu.au

Specialty section:
This article was submitted to T Cell Biology, a section of the journal Frontiers in Immunology

Received: *31 August 2020*
Accepted: *12 January 2021*
Published: *25 February 2021*

Citation:
Gunasinghe SD, Peres NG, Goyette J and Gaus K (2021) Biomechanics of T Cell Dysfunctions in Chronic Diseases. Front. Immunol. 12:600829. doi: 10.3389/fimmu.2021.600829

INTRODUCTION

T cells are at the frontline of immune surveillance, acting against pathogens and malignancies to maintain host homeostasis. Upon recognition of antigenic peptides presented on major histocompatibility complex (MHC) or MHC-like molecules (1, 2), T cells become activated and undergo clonal expansion, resulting in the generation of effector cells that help contain the spread of the disease. During clonal expansion, changes can occur at transcriptional, epigenetic and metabolic levels that enhance the effector functions of T cells (3). Effector T cells produce high amounts of cytokines, including interferon (IFNγ) and tumor necrosis factor (TNFα), and cytoplasmic granules containing granzymes and perforin (4). During antigenic clearance, the majority of effector $CD8^+$ T cells follow an apoptotic cell death, but 5–10% of cells differentiate into memory T cells (5). Memory T cells are capable of rapidly executing their effector functions upon re-encounter of the same antigen or pathogen (6, 7). They have a unique transcriptional makeup, which allows them to be distinguished from naïve and effector T cells (8). This unique transcriptional profile shapes the functional characteristics of memory T cells as well as their phenotype to maintain the acquired

immunity. Hence, memory T cell differentiation is tightly regulated and any alterations to this process can manifest in various forms of T cell dysfunction (9).

Depending on phenotypic and functional features, T cell dysfunctions can be classified into ignorance, tolerance, exhaustion, anergy or senescence (**Table 1**). These different states of dysfunctions can operate as mechanisms to reduce autoimmunity (ignorance and tolerance), minimise repercussions from inappropriate T cell stimulation (anergy), or simply regulate T cell division (senescence) (9). However, exhaustion brings a unique perspective to the state of T cell dysfunction as it occurs despite physiologically appropriate T cell stimulation. During the transformation of effector T cells into dysfunctional phenotypes, the proliferative capacity along with cytokine production gets reduced (10–12). Moreover, alterations occur at the membrane level transform the immune receptor landscape of T cells (13) and their biophysical properties (14–16). This has ramifications in terms of maintaining optimal T cell responses against pathogens and malignancies. In this review, we highlight recent findings that helped to broaden our understanding on how T cell dysfunctions can reform the immune receptor and biophysical landscape of T cells, and how it can ultimately influence the state of disease progression. We primarily discuss dysfunctional T cell phenotypes in the context of chronic infections and cancer to draw our conclusions.

MECHANISMS OF T CELL DYSFUNCTION IN CHRONIC DISEASES

It is conceivable that all T cell dysfunctions stem from alterations occur in the biological process of T cell activation or differentiation. As a result, different dysfunctional T cells share common phenotypic traits, which make the differentiation between T cell dysfunctions subtypes difficult. However, in depth understanding of different molecular mechanisms driving T cell dysfunctions will help to identify signature phenotypic traits to build much clearer and distinguishable profiles for each subtype. Here, we attempt to highlight different mechanisms that drive T cell dysfunctions and the most commonly associated dysfunctional T cells found in chronic diseases.

TABLE 1 | Classification of dysfunctional T cells.

T cell dysfunction	Functional and Phenotypic features
Ignorance	Self-reactive T cells that do not sense self-antigens due to physical sequestration or low antigen expression.
Tolerance	Central tolerance accounts for negative selection of thymocytes expressing high-affinity TCRs to self-antigens. Thymocytes which escape negative selection are inactivated by different mechanisms of the peripheral tolerance.
Exhaustion	Persistent antigen stimulation of T cells during chronic diseases (infections or cancer) induce progressive loss of T cell effector functions and lead to exhaustion.
Anergy	A hyporesponsive state of T cells arise in suboptimal costimulatory signal during T cell-antigen recognition.
Senescence	State of non-reversible cell cycle arrest caused by telomere shortening.

T Cell Tolerance and Ignorance

Complete T cell activation requires three signals; first signal provided by TCR-cognitive pMHC interaction, the second is a costimulatory or coinhibitory receptor activation signal provided by APCs, and the third is provided by extracellular cytokines. Of these signals, the second signal becomes crucial in determining the functional outcome of T cell signaling, which may promote T cell effector functions (costimulation) or dampen excessive immune responses (coinhibition) to maintain immunological tolerance (17). Thus, both T cell activation and tolerance are interconnected to tightly regulate and maintain optimal immune responses against foreign antigens while preventing autoimmunity against self-antigens. Failure to maintain immunological tolerance may result in various types of autoimmune diseases. T cell tolerance is primarily enforced by central and peripheral tolerance. Central tolerance operates by eliminating self-reactive T cell through negative selection in the thymus during early stages of T cell development. These T cells express high-avidity TCRs to self-antigens and are mainly eliminated from the system *via* clonal deletion or diverted to differentiate into regulatory T cells (Treg) through thymic negative selection. These elimination mechanisms have been reviewed elsewhere (18). Although majority of self-reactive T cells get screened and eliminated though negative selection in the thymus, this process alone is not sufficient to safeguard against autoimmunity. Self-reactive T cells that escape thymic negative selection are eliminated by peripheral tolerance which acts as the second barrier to maintain immunological tolerance. It was shown that peripheral tolerance is most effective in detecting and eliminating mature T cells that express low-avidity self-reactive TCRs, while central tolerance is effective against eliminating thymocytes expressing high-avidity self-reactive TCRs (19). Peripheral tolerance operates with various mechanisms to inactivate self-reactive T cells that escaped central tolerance. These mechanisms include clonal deletion (20, 21), clonal suppression by Tregs (22–24) and induction of functional non-responsiveness *via* intrinsic cell programming mechanisms (25). It has been suggested that manifestation of a large proportion of autoimmune diseases are linked with the breakdown of peripheral tolerance mechanisms (26–29). In some instances, self-antigens fail to induce negative selection of self-reactive T cells and they become clonally ignorant (30–32). This can be due to low expression of the self-antigen or its physical sequestration at immune-privileged sites like the blood-brain barrier (31). During self-antigen encounter, unlike self-tolerant T cells, self-ignorant T cells remain functional. Most self-ignorant T cells in the periphery are naive, but given the right stimulatory conditions, they can initiate autoimmune responses (33–35).

T Cell Anergy

Another important state of T cell dysfunction is anergy. The consensus that describe the mechanism behind T cell anergy is based on T cell antigen-stimulation in the absence of the second signal i.e. costimulation, which drives T cells into a

hyporesponsive state for an extended period of time (36). Upon re-encounter of the same stimuli with optimal costimulation, anergic T cells fail to proliferate and produce cytokines (36). It has been shown that one of the hallmarks of T cell anergy is the reduced interleukin (IL)-2 production (37). T cell anergy has been broadly classified into clonal anergy and *in vivo* anergy (36). Clonal anergy can be induced in $CD4^+$ T cells when stimulated with a strong first signal (TCR-pMHC interaction) and in the absence of the second signal. Low doses of agonist in the presence of costimulation has also been shown to induce clonal anergy (38). *In vivo* anergy also known as adaptive tolerance can occur in the thymus or in the periphery and often associates with naïve T cells during self-antigen stimulation in a costimulation deficient or high coinhibition environment (37, 39). For example, cancer cells and tumor-antigen presenting cells are shown to express high levels of coinhibitory receptor ligands (PD-L1, PD-L2 and many other) with relatively low levels of costimulatory receptor ligands (CD80 and CD86) in the tumor microenvironment to promote T cell anergy (40–43). Despite overlapping functional and phenotypic features, clonal anergy and *in vivo* anergy are driven by distinct molecular mechanisms. For instance, while both anergic phenotypes display either impaired IL-2 production (clonal anergy) or impairment in all TCR-induced cytokine production (*in vivo* anergy) as a key dysfunctional feature during antigen stimulation, only clonal anergy can be rescued by the addition of exogenous IL-2 or by diacylglycerol kinase-α (DGK) inhibitor (44, 45). Clonal and *in vivo* anergy also differ in their signaling defects. TCR-based signaling pathway seems to have impairment in Zap-70 phosphorylation of LAT in the *in vivo* anergy model (37). The signaling pathway of clonal anergy shown to have defects in MAP-kinases activation and mobilisation of NF-κB to the nucleus (46). Anergic phenotypes are associated with a number of autoimmune diseases including human type-1 diabetes (26), systemic lupus erythematosus (47), autoimmune gastritis (48) and myasthenia gravis (49).

T Cell Senescence

Senescence is recognized as a T cell dysfunction that can play paradoxical roles in adaptive immunity. Based on the triggering mechanisms, T cell senescence can be classified into replicative senescence or premature senescence (50). Replicative senescence occurs as a consequence of telomere shortening after several rounds of cell division, which is associated with the natural aging process (51–53). Hence, an increased number of senescent T cells have been found in the elderly population, which increase their susceptibility for malignancies and chronic diseases (54, 55). However, a number of studies have shown that accumulation of senescent T cells is not limited to the ageing population, but can be found in younger patients with chronic infections and cancer (56–59). The second form of senescence: premature senescence is independent of telomere shortening, and is induced by external factors including cellular stress, particularly oncogenic stress (60, 61). During tumorigenesis, oncogenes become activated and promote uncontrolled cell division, which is commonly observed in many types of cancers. Adversely, a high proliferation rate in cancer cells can become a genetic and metabolic burden which triggers cellular senescence pathways, causing irreversible cell cycle arrest (62, 63). This demonstrates the paradoxical nature of cellular senescence. Moreover, by inducing DNA damage responses, both Tregs and tumor cells can convert T cells to become senescent (64–66). Transformation of effector to senescent T cells dramatically change the immune receptor landscape of T cells. The marked decline of costimulatory receptor expression (CD27 and CD28) (67, 68) is one of the main biomarkers of senescent T cells alongside higher expression of killer cell lectin-like receptor subfamily G member 1 (KLRG-1), Tim-3, CD57 and CD45RA (69–71).

T Cell Exhaustion

Since its first characterisation in lymphocytic choriomeningitis virus (LCMV) infection model in mice (72), T cell exhaustion has been the topic of much debate and is implicated in a number of chronic infections (primarily caused by viruses) and cancer (73–76) (**Figure 1**). Over the past few years, the topic of T cell exhaustion has become more relevant as we attempt to uncover the molecular mechanisms behind chronic T cell dysfunctions and develop effective immunotherapies to manage these conditions.

Although driving forces of T cell exhaustion may differ base on different pathological settings, most, if not all proposed mechanisms of T cell exhaustion centres around the three-signal model of T cell activation. Persistent antigen-stimulation, effects of native-regulatory cytokines and immune-suppressive influence of immunoregulatory cells like Tregs are known to promote exhaustion in effector T cells (79). Among these exhaustion inducible factors, persistent antigen-stimulation has been observed across several chronic infection and cancer models in humans and mice (80–82). Accordingly, the dose and the duration of antigen exposure can contribute to the degree of T cell exhaustion. This has been reviewed in later sections of the review.

A key difference has been identified in T cell differentiation during acute and chronic phases of a disease. In the acute phase, T cell mediated antigen clearance comprise of T cell expansion, contraction, and generation of memory T cells. This pattern diverges from the classic differentiation pathway during chronic infections and cancer as a consequence of persistent, higher prevalence of antigens. In this environment, T cells undergo persistent antigen stimulation, which progressively impair their effector functions and drive them to exhaustion. This functional impairment in exhausted T cells, however, does not describe a complete loss of effector functions. As reported by numerous accounts, exhausted T cells still retain some degree of effector functionality having control over the spread of the disease (83–85). Moreover, exhausted T cells share characteristics with memory T cells, which shows their capacity to survive long-term and respond to rechallenge of the antigen (86–89). An important differentiation arises from exhausted T cells having memory characteristics with those do not. Exhausted T cells with memory characteristics have shown to express transcription factor TCF1 (86, 87, 89–91). This subpopulation is responsible for maintaining immune responses during chronic diseases (86,

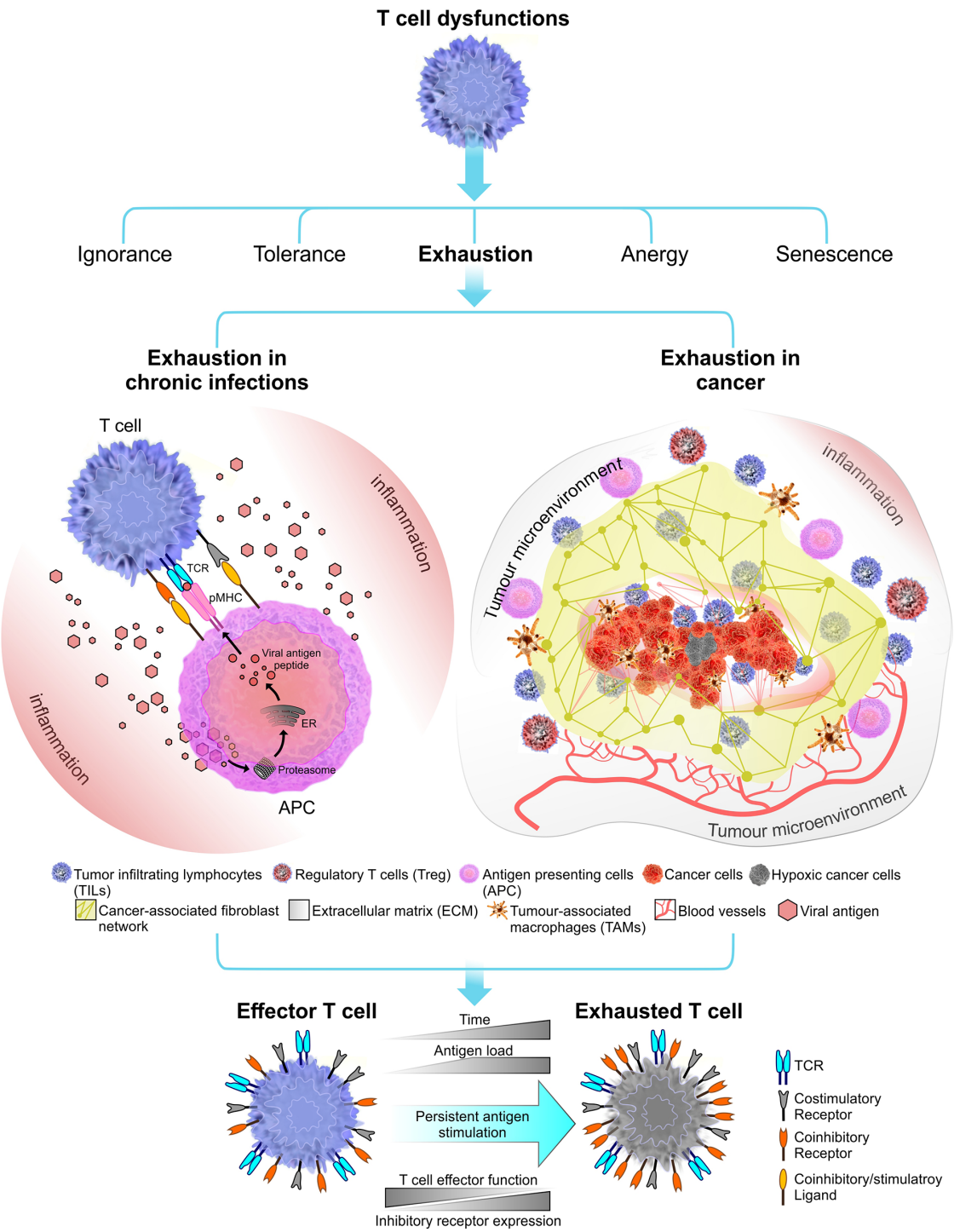

FIGURE 1 | Immune receptor landscape during T cell exhaustion. Exhaustion can be induced by chronic infections (in this instant viral infections) or cancer. Factors that influence the onset and the extent of T cell exhaustion differ in these two exhaustion models. During a chronic infection, pathogen clearance become inefficient, leading to persistent inflammation and chronic antigen stimulation of T cells which results in clonal deletion or exhaustion. In cancer, the immunosuppressive tumor microenvironment plays a crucial role in shaping the outcome of T cell exhaustion. Tumor microenvironment comprised of stroma containing a fibroblast network and a number of immune cells including regulatory T cells (Tregs) and tumor-associated macrophages (TAMs) which together promote tumorigenesis (77). Tumor microenvironment can induce stromal cells to secrete growth factor to promote angiogenesis (i.e. grow new blood vessels that feed the tumor) (78). Overall, T cell exhaustion in both chronic infections and cancer known to have several overlapping functional and phenotypic characteristics. The most common feature is sustained upregulation of inhibitory receptors during the course of the disease.

87, 92) and remains to be critical for the success of anit-PD-1 blockade therapy (87, 93, 94), while TCF1$^-$ exhausted T cells fail to provide such responses. In numerous studies TCF$^+$ exhausted T cells were described as "stem-like" T cells (87, 89) or "progenitor exhausted" cells (93) and more recently these terms have been unified under "precursor exhausted T cells" (T_{PEX}) in contrast to TCF$^-$ terminally exhausted effector T cells (T_{EX}) (95). Several other transcription factors have been identified to be coexpressed with TCF. Most notably, the T-box transcription factors T-bet and eomesodermin homologue (EOMES) which are known to regulate immune responses during acute and chronic infections (96–98). Their role in maintaining exhaustion phenotypes in both T_{PEX} and T_{EX} needs further investigation. B lymphocyte-induced maturation protein 1 (BLIMP1) is another critical transcription factor required in lymphocyte subset differentiation (99, 100). BLIMP1 suppresses multiple genes linked to T cell memory regulation, therefore, found to be partially expressed in T_{PEX} but not in T_{EX} (87, 91). Other transcription factors relevant in maintaining T cell exhaustion phenotype have been reviewed elsewhere (89, 101–103).

Cytokines play a major role in shaping the outcomes of T cell activation. During the acute phase of infection, proinflammatory cytokines (TNF-α, IL-1β, and IL-8) promote the development of effector T cells to fight off the infection. When the pathogen persists through to the chronic phase, negative regulatory cytokines like IL-10 and TGF-β target different pathways to suppress T cell activation and induce T cell exhaustion. IL-10 is produced by multiple different cells in the tumor microenvironment (TME) including Tregs, tumor-associated macrophages (TAM) and cancer cells (104–106). By inducing PD-L1 expression in dendritic cells, IL-10 promotes T cell exhaustion (107). Downregulation of MHCs, intercellular adhesion molecule 1 (ICAM-1) and costimulatory ligands (CD80 and CD86) on APCs promoted by IL-10 also contribute to immunosuppression (108). Importantly, previous studies have shown that IL-10 plays a role as an anti-inflammatory cytokine by demonstrating its capacity to inhibit or downregulate the production of proinflammatory cytokines (109). It is well known that the surface lattice formed by galectin-glycoprotein can influence membrane remodelling to suppress T cell mediated immune responses (110, 111). Recently, IL-10 was shown to be involved in an immune regulatory loop enhancing N-glycan branching, which heightened galectin-3 binding, thereby decreasing T cell antigen sensitivity (112). Although, IL-10 has been broadly characterized as an immune suppressor, at higher concentrations IL-10 and PEGylated IL-10 (pegilodecakin) has shown to have properties that enhance cytotoxicity and proliferative capacity of tumor-specific CD8$^+$ T cells (113–115). The mechanisms underlie this paradoxical nature of IL-10 remains to be investigated. TGF-β is a pleiotropic cytokine and is produced in large amounts in the TME. Generally, TGF-β restrict tumor growth in early stages by inducing the Smad signaling pathway (116). However, in late stages of the cancer, TGF-β has been linked to tumor progression by modulating immune responses most likely through a Smad-independent signaling pathway (117). Given the paradoxical role of TGF-β in cancer, makes it one of the most complex factors to be studied in the TME. Understanding how and when TGF-β switch from tumor suppressor to tumor promoter is being actively investigated.

Immunoregulatory cells including Tregs (CD4 and CD8), myeloid-derived suppressor cells (MDSC) and NK cells are shown to induce T cell exhaustion in effector T cells during chronic infections (118–122). Tregs at the site of the infection or at the TME secrete negative regulatory cytokines, IL-10 and TGF-β, to promote immune suppression (122), thereby limiting anti-pathogen or anti-tumor activity of effector T cells. The exact mechanism of how Treg induce immune suppression to drive effector T cells into exhaustion is still unclear. However, reinvigoration studies of exhausted CD8$^+$ T cells associated with chronic LCMV by blocking PD-1 signaling pathway and depleting Tregs simultaneously, suggest a role for Tregs in T cell exhaustion (123).

In summary, although persistent antigen stimulation remains as a key driving force for T cell exhaustion, numerous other factors differentially contribute to the development of exhaustion. In the next section we attempt to highlight two main models of T cell exhaustion found in chronic diseases.

T CELL EXHAUSTION MODELS

From studies reporting common phenotypic characteristics of exhausted T cells, there is an emerging profile that describes T cell exhaustion as a distinct state of cell differentiation. Accordingly, exhaustion phenotypes have been identified in both chronic viral infections and in cancer (**Figure 1**). Although these exhaustion models share common functional features, they differ substantially in some respects.

T Cell Exhaustion in Chronic Infections

The persistent overload of pathogens during chronic infections leads to persistent antigenic stimulation of T cells. This drive T cells into clonal deletion or exhaustion, both of which lead to reduced pathogen clearance. This is more commonly reported in infections associated with viruses, though T cell exhaustion has also been identified in bacterial and parasitic infections (124, 125). Here, our focus will be on T cell exhaustion during chronic viral infections. During chronic infections, reduced proliferative capacity and low interleukin-2 (IL-2) production (126) are known to be some of the earliest signs of loss of T cell effector functions. At the intermediate state, TNF-α and IFN-γ production are reduced (73). The low cytotoxicity in CD8$^+$ T cells is also observed at this stage. Loss of these functional properties occur partially or in severe exhaustion, completely. Finally, these exhausted virus-specific T cells are deleted from the system (72, 74). Hence, a stage-by-stage descent into exhaustion has been observed (10). The level of T cell exhaustion primarily depends on the amount and the strength of antigen stimulation (127). Although the "strength" of stimulus is difficult to define, prolonged exposure to a persistent viral load is an important determinant in the process of exhaustion. For example, higher

antigen load with prolong exposure results in severe exhaustion phenotypes seen in LCMV, untreated HBV, and HIV chronic infections (79, 128–130). The role of helper $CD4^+$ T cells are also important for promoting effector $CD8^+$ T cell functions, thus their low availability has been linked to T cell exhaustion (131, 132). Hence, high viral load and low availability of helper $CD4^+$ T cells generally correlates with severe exhaustion phenotype (75). Overall, a number of factors including the viral load, location of viral replication and the immunosuppressive environment, contribute to the level of effector function impairment in T cells during chronic infections.

Sustained Upregulation of Inhibitory Receptors

In addition to the gradual loss of effector functions, another classic feature of exhausted T cell is the sustained upregulation of inhibitory receptors (**Figure 1**). These surface expressed inhibitory receptors include programmed cell death protein 1 (PD-1) (133), cytotoxic T lymphocyte associated antigen 4 (CTLA-4), lymphocyte-activation gene 3 (LAG-3), T cell immunoglobulin and mucin-domain containing protein 3 (TIM-3), B and T lymphocyte attenuator (BTLA) and many others (13). In non-pathological settings, the transient expression of inhibitory receptors along with their co-stimulatory counterparts (CD28 and ICOS) serve a key role in maintaining the immunological tolerance. This is readily observed in acute infections where inhibitory receptors contribute to restrain immunopathology after pathogen clearance has been achieved. In fact, upregulation of inhibitory receptors are commonly observed during T cell activation (133–135), although steady-state expression levels may vary depending on the state of cell differentiation (136–138). As pathogen clearance progresses, inhibitory receptors are downregulated and maintained at low levels.

Many inhibitory receptors, including PD-1, can negatively regulate T cell receptor (TCR) signaling *via* immunoreceptor tyrosine-based inhibitory motifs (ITIM) or immunoreceptor tyrosine-based switch motifs (ITSM) found in their cytoplasmic tails (17). Upon binding ligands, ITIM/ITSM domains within the cytoplasmic tails of inhibitory receptors are phosphorylated and recruit Src homology region 2 domain-containing phosphatases (SHP-1 and SHP-2). Overall, PD-1/PD-L1 signaling pathway can regulate exhaustion phenotype by suppressing TCR signaling (139), inducing T cell suppressor genes (140) and by reducing T cell motility (141). TIGIT uses a similar strategy to negatively regulate T cell function (142). However, inhibitory receptors can engage more than one suppressive mechanism to attenuate T cell functions. In contrast to ITIM signaling, LAG-3 is known to function through KIEELE motifs located at its relatively short intracellular tail to negatively regulate cell cycle progression (143). Tim-3 also utilizes non-canonical inhibitory mechanisms that are distinct from, and complementary to, PD-1 (144). High surface expression of Tim-3 often correlates with severely exhausted T cell subsets during chronic infections (145, 146). The inhibitory receptor CTLA-4 functions by outcompeting CD28 stimulatory receptor by binding to their common ligands CD80 or CD86 to suppress T cell functions (147). Uniquely, CTLA-4 can utilize trans-endocytosis; a mechanism of capturing and removing common ligands from the surface of an antigen presenting cell (APC), thus making them unavailable for stimulatory receptor binding (148). All these inhibitory receptors can employ non-overlapping mechanisms of T cell suppression, making their functional role in promoting T cell exhaustion rather diverse and complex.

T Cell Exhaustion in Cancer

Immunosuppressive factors found in the tumor microenvironment and the tumor-antigen load greatly influence the degree of cancer-mediated T cell exhaustion. Similar to T cell exhaustion in chronic infections, tumor-infiltrating $CD8^+$ T cells display attenuated effector functions including impaired cytokine secretion and sustained high surface expression of inhibitory receptors (PD-1, CTLA-4, Tim-3, LAG-3, and others) (76, 149–151). However, exhausted T cells in cancer show subtle differences in their gene expression profiles from infection mediated T cell exhaustion. For example, tumor-specific $CD8^+$ T cells derived from a late stage melanoma cancer model showed overexpression of several genes involved in cell cycle regulation, DNA repair and immune responses which was comparatively different from gene expression profiles derived from EBV-specific and CMV-specific exhausted $CD8^+$ T cells (152). These differentially expressed genes were related to inhibitory receptors. Accordingly, CD160 and several other inhibitory receptors were not co-expressed in tumor-specific exhausted $CD8^+$ T cells compared to virus-specific exhausted $CD8^+$ T cells. Some inhibitory receptors like BTLA are upregulated in exhausted tumor-specific $CD8^+$ T cells and not in exhausted virus-specific $CD8^+$ T cells (76). These distinct gene expression profiles of multiple inhibitory receptors suggest different underlying mechanisms governing receptor upregulation in chronic viral infections and cancer mediated exhaustion. As such, the differential expression of inhibitory receptors may shape the extent of T cell exhaustion in each scenario and provide a molecular signature that will help to diagnose diseases.

Tumor Microenvironment

Despite several overlapping functional and phenotypic features found in exhausted T cells induced by chronic viral infections or cancer, the progression of cancer mediated T cell exhaustion is not fully understood. This is partly because of the complexity presented by the tumor microenvironment. The surrounding environment of a developing tumor is comprised of stroma (containing fibroblasts, immune cells, and extracellular matrix) (77), blood vessels, infiltrating inflammatory cells and a number of cells associated with host tissues (**Figure 1**). The cellular environment inside the tumor is not homogenous throughout the cancer (153–155). Hence, the tumor microenvironment (TME) is continuously evolving with tumor progression. Tumor-infiltrating lymphocytes, such as cytotoxic and regulatory T, B and natural killer (NK) cells, associated M2 macrophages (TAM) (156, 157), infiltrating dendritic cells

(TIDC) (158) make the TME a battle ground where highly dynamic cellular interactions that take place between the innate and adaptive immune system and the tumor (159). The process of antigen presentation can become impaired inside the TME which may result in incomplete T cell activation (160). Although some T cells are able to infiltrate the tumor, components surrounding the TME including malignant cells, inflammatory cells, stromal cells and cytokines can induce and maintain an immunosuppressive environment that would attenuate T cell effector functions which eventually drive them to exhaustion (153).

Immunoediting

With cancer progression, the intense pressure applied by the adaptive immune system and the antigenic heterogeneity of malignant cells allow rare cancer subclones to survive through the elimination phase, equilibrium phase and finally escape from T cell-mediated cytotoxicity (161, 162). In immune-oncology this is known as immunoediting. The theory of immunoediting explains how immunity can play a dual role as a suppressor and as a promoter in cancer (163). Cancer immunoediting is composed of the three phases: elimination, equilibrium and escape (164). In the first two phases, cancer is under control or at a dynamic equilibrium with the immune system, rendering it undetectable *via* clinical methods. As the cancer enters the final phase, it escapes immune surveillance, leading to becoming a clinically detectable progressing tumor.

Immunoediting comprises complex adaptive mechanisms where cancer reduce its immunogenicity to evade recognition and destruction of selected clones (162, 165). Examples of immunoediting are the loss of tumor-associated antigen (TAA) presentation or downregulation of PD-L1 driven by epigenetic changes on cancer cells and abrogated IFNγ—a key regulator of antigen process and presentation—delivered by tumor-infiltrating lymphocytes (TIL) in the TME (166–169), which can lead to incomplete elimination and persistence of adapted tumors becoming clinically evident (169). Insufficient TAA presentation poses a challenge for adaptive cytotoxicity by driving immunological ignorance (170, 171). The poor immunogenicity of transformed cells that escaped recognition can further promote insufficient activation of T cells, evident by unsuccessful immunotherapy treatments in some clinical settings (162). Thus, the selective advantage acquired by evasive cancer cells with impaired T cell responses would follow changes in the immune receptor landscapes on both sides of the immunological synapse. The biophysics of T cell-APC encounter is highly dynamic. The molecular forces at play during these encounters differ greatly in their nature and can trigger unique signaling pathways for cellular decision-making, which has been poorly discussed in the context of T cell dysfunctions.

BIOPHYSICAL LANDSCAPE OF DYSFUNCTIONAL T CELLS

T cell signaling and the cascade of events that follow T cell activation require close encounter of two cell membranes: the plasma membrane of the T cell and the APC. The dynamic and heterogeneous nature of the membrane environment, composed of different types of lipids, receptors and ligands makes the process of T cell-APC conjugation complex to understand. The close contact between the two opposing membranes is accompanied by the formation of unique structural features that promote information transfer through receptor–ligand interactions. The interface between a T cell and an APC is known as the immune synapse and its formation involves spatial redistribution of surface receptors and ligands to facilitate the initiation of immune responses (172). T cells continuously form membrane protrusions known as filopodia or microvilli which help them probe the surface of APCs and to sense biophysical properties in the surrounding environment (**Figure 2A**). Formation of these structural features require extensive membrane remodelling assisted by cytoskeleton rearrangements (178). Moreover, due to relatively high cell motility and relatively slow diffusion rates of engaged receptors and ligands, both cells experience pulling-pushing and shear forces. Recent studies have attempted to quantify these mechanical forces during immune synapse formation (179, 180). It is generally thought that these forces enable T cells to probe the surrounding environment and execute effector functions at optimal levels. Changes to this biophysical landscape could therefore abort T cell responses and disrupt host immune regulatory mechanisms. In this section we highlight the studies that attempt to unravel the link between changes in biophysical properties of the membrane and T cell dysfunction.

Structure and Functions of Immune Synapses

The immunological synapse is crucial for T cell activation and is sometimes referred to as an activation synapse. Immune receptors, signaling molecules, cytoskeletal components and cell organelles all participate in the formation of the immune synapse (181). In cytotoxic T cells (CTLs), the immune synapse is also the interface in which cytolytic granules are delivered to the target cells and in these cases they have also been referred to as cytotoxic synapses or lytic synapses (182).

Immunological Synapses for Activation

When forming activation synapses, key signaling molecules congregate to form a distinct sub-synaptic domain known as the supramolecular activation cluster (SMAC) (**Figure 2B**). The central region of SMAC (cSMAC) primarily contains TCRs and tyrosine kinases which are crucial for the initiation of TCR signaling. The peripheral SMAC (pSMAC) surrounds the cSMAC and contains integrins like LFA-1 which binds to ICAM-1 expressed on APCs, facilitating the adhesion of T cell to APC. Under some circumstances, T cell activation is achieved *via* TCR microclusters and without the need of classic immune synapse formation (183, 184). It has also been proposed that the cSMAC serves as the site for signal termination and receptor recycling (185). One of the main functions of activation synapse is the initiation and amplification of TCR signaling. Upon TCR

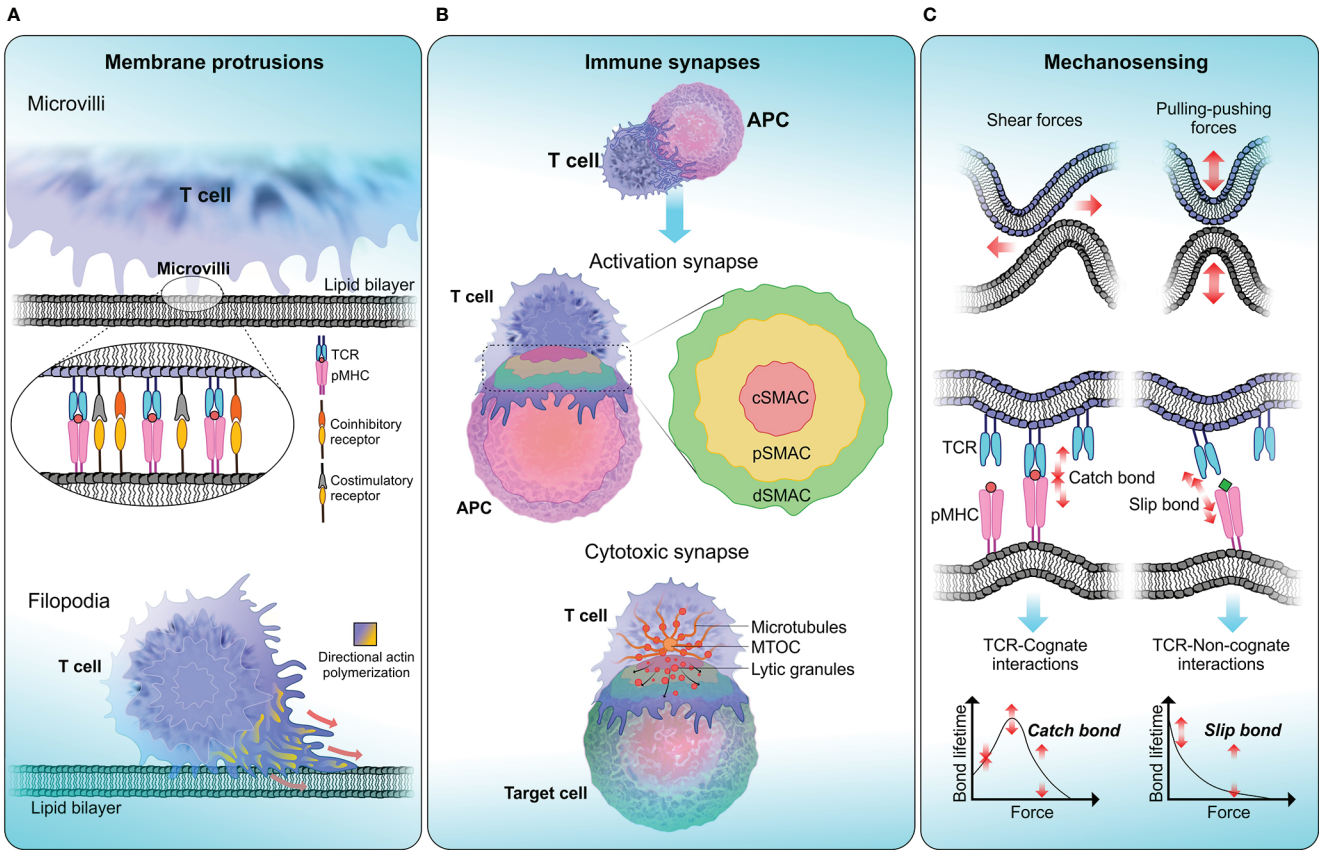

FIGURE 2 | T cell biophysical landscape. **(A)** Membrane protrusions. T cells continuously form actin-rich membrane protrusions known as filopodia or microvilli which help them to sense biophysical properties in the surrounding environment. Microvilli are involved in early T cell activation (173) and where signaling components including TCR and TCR-associated signaling molecules get accumulated (174, 175). The tip of a microvilli is zoomed in to illustrate the accumulation of T cell signaling molecules. Compared to microvilli, filopodium membrane projections are larger in size ranging from 10-40 μm in length in different cells (176). The function of filopodia is broad including crucial roles in cell-cell adhesion and cell migration (177). **(B)** Immune synapses. Formation of immune synapses are important steps in T cell activation and executing T cell effector functions through cytotoxicity. When forming activation synapses, signaling receptors (in T cells) and ligands (in APCs) spatially segregate into a bull's eye-like structure forming the supra-molecular activation cluster that is separated into central (cSMAC—red), peripheral (pSMAC—yellow) and distal (dSMAC—green) regions, where each zone preferentially recruit different signaling receptors to initiate T cell signaling. Cytotoxic synapses are formed when a CTL encounters a target cell. Cytotoxic synapses differ from activation synapses in the recruitment of lytic granules to the synaptic cleft with the help of Golgi apparatus and the microtubule organising centre (MTOC). Delivery of lytic granules and exocytosis of granule contents are highly depended on calcium influx. **(C)** Mechanosensing. T cells are constantly being subjected to mechanical stresses when undergoing kinapse formation with APCs. TCRs display mechanosensing properties by exerting pulling-pushing and shear forces on pMHC molecules on APCs. When a TCR engage with cognate-antigen peptide, a catch bond is formed, which triggers conformational changes in the TCR-CD3 complex and initiate T cell signaling. Conversely, TCR encounter with a non-cognate-antigen peptide results in a slip bond, where an exponential decay of bond lifetime is observed with increasing force. Slip bonds fail to trigger TCR signaling.

binding to its cognate pMHC, a cascade of signaling events take place leading to T cell activation, proliferation and execution of effector functions. TCR-pMHC ligation also triggers substantial structural alterations in the membrane (186). These changes permit the recruitment of crucial signaling molecules to the synapse along with accumulation of actin polymers at the pSMAC (187). The surge of F-actin facilitates the formation of membrane structures like lamellipodial which help T cells to spread across APC surface (188).

Overall, optimal T cell-APC contact and effective immune synapse formation is regulated by several cytoskeletal changes. The Vav family of proteins are involved in modulating these cytoskeletal changes at the immune synapse. As shown by previous studies, Vav1 mediates downstream signaling in T cells *via* PLCγ1 and TCR-induced calcium flux (189–191). The absence of Vav1 affects the stability of the TCR signaling clusters and impair both calcium flux and MAP kinase phosphorylation (192). By activating RHO GTPases such as RAC1 and CDC42 (193), Vav1 is implicated in series of events facilitating Wiskott-Aldrich syndrome protein (WASP) and WASP-family verprolin-homologous protein-2 (WAVE2) to activate actin-related protein 2 and 3 (ARP2/3), which leads to polymerisation and

accumulation of actin filaments at the immune synapses (194, 195).

Cytotoxic Immune Synapses

Cytotoxic synapses are crucial in executing T cell effector functions. One important difference between a cytotoxic synapse and an activation synapse is the recruitment of lytic granules to the synaptic cleft (**Figure 2B**). CTLs exert their cytotoxicity by first binding to the target cell and then releasing lytic granules containing perforin and granzymes *via* exocytosis, and finally detaching from the target cell (196). Similar to activation synapses, attachment to the target cell is primarily mediated by LFA-1 which also aids the formation of SMAC (197). Importantly, the pSMAC has been implicated in stabilising the cytotoxic synapses in CTLs, as the disruption of pSMAC formation results in impaired target cell lysis (198). During CTL mediated target cell lysis, granules containing cytotoxic enzymes (lytic granules) are recruited to the immune synapse with the help of the Golgi apparatus and the microtubule organising centre (MTOC). In NK cells, it was shown that dynein, a cytoskeletal motor protein is responsible for the transport of lytic granules to the MTOC and then MTOC polarises to deliver lytic granules to the synaptic cleft (199). Targeted delivery of lytic granules and exocytosis of granule contents are highly depended on calcium influx (200). Following the detachment from the target cell, CTLs are capable of effectively killing multiple targets sequentially (201).

Immune Synapse Dysfunctions in Chronic Diseases

Chronic diseases are often associated with the phenotype of T cell exhaustion. The root cause for a number of chronic diseases stems from the inability of T cells to form functional immune synapses with the target cells, leading to impaired T cell activation resulting suboptimal immune responses (202, 203). Understanding the mechanisms that induce impairments in immune synapse formation is an important step in developing effective therapeutics that can reverse T cell exhaustion by restoring effector functions.

Disruption of T cell and target cell contact during T cell activation or T cell-mediated cytotoxicity can impair the formation of functional immune synapses. This can be detrimental in terms of maintaining immunity against pathogens and cellular malignancies. Leukocyte adhesion disorder (LAD) is a classic example of a chronic disease caused by defective expression (LAD type-I) or activation (LAD type-III) of cell adhesion molecules, primarily β-2 integrins like LFA-1 (204). Since LFA-1 plays a crucial role in the assembly of immune synapses, LAD patients often have recurrent bacterial infections due to their compromised immune system (205). Similarly, defects in WASP family of proteins directly affect actin mediated cytoskeletal rearrangement during immune synapse formation. This was shown in Wiskott-Aldrich Syndrome where CTLs lose their cytotoxicity (206). In a rare type of non-Hodgkin lymphoma known as anaplastic large cell lymphoma (ALCL), it has been shown that WASP and WASP-interacting-protein (WIP) are expressed in low amounts (207). In WASP knockout (KO) mice, fast onset of tumor growth has been observed (208). In the same study, the metastatic rate of B16 melanoma was shown to be higher, indicating an overall loss of T cell tolerance towards the cancer. However, somewhat contradictory observations were made in mouse breast carcinoma, where the metastatic spread was decreased in the absence of WASP (209), suggesting differing roles for WASP in cancer progression depending on the cancer model. Interestingly, addition of exogenous IL-2 was able to rescue the cytotoxicity of WASP KO NK cells by restoring their ability to form immune synapses (210, 211). In fact, IL-2 treatment is commonly used as an immunotherapy treatment in the attempt to promote T cell proliferation and restore or enhance T cell effector functions (212). WASP is one of many proteins in which irregular protein expression can lead to immune dysfunctions because of cytoskeletal organisation defects during immune synapse formation. A growing number of putative proteins including Dock8, RAC2, RHOH, CORO1A, ACTB and many others have been implicated in modulating actin-dependent cytoskeleton organisation to promote efficient T cell activation. Their individual functions have been reviewed elsewhere (213).

Failure to deliver lytic granules to the synaptic cleft leave CTLs with impaired cytotoxicity and reduced pathogen clearance. The continual stimulation from the innate immune system together with dysfunctional adaptive immune responses can result in systemic inflammation which is detrimental to the host homeostasis. This is readily observed in herpes viral infections, particularly Epstein–Barr virus (EBV) and cytomegalovirus (CMV). These viruses with their lifelong latency in the host may result in persistent antigenic-stimulation mediated by the innate immune system (214). This has been linked to hemophagocytic lymphohistiocytosis (HLH), a life-threatening syndrome presented with attenuated killing capacity of T cells and NK cells (215).

In cancer models, much of the evidence for defects in the formation of immune synapses comes from haematological malignancies (15, 216, 217). For instance, one report demonstrated that $CD8^+$ and $CD4^+$ T cells are unable to form proper immune synapses with chronic lymphocytic leukemia (CLL) cells, which hindered anti-tumor activity (15). The authors show that when a healthy T cell encounters CLL-B cells, F-actin polymerisation was suppressed and there was impaired recruitment of key adhesion and signaling molecules to the immune synapse of the T cells (15). These observations agree with other cancer models where tumor-infiltrating lymphocytes (TIL) showed similar defects in actin polymerisation (218, 219). The exact mechanism behind tumor-induced immune synapse defects in T cells is not yet clear. However, immuno-modulatory drugs such as lenalidomide are shown to be effective in reversing actin polymerisation defects in patients with follicular lymphoma (216).

Human immunodeficiency virus type-1 (HIV-1) also induces signaling dysfunctions in $CD4^+$ T cells as a part of its viral pathogenesis. The abundantly expressed viral protein Nef plays a central role in impairing the immune synapse formation in HIV-

1 infected T cells (220). Nef achieves this by hijacking the host membrane protein trafficking machinery to promote the spread of infection (221). HIV-1 infected T cells showed poor cell spreading, suggesting a Nef-dependent inhibition of actin polymerisation. In parallel, a reduced recruitment of TCR-CD3 complex, Lck and other actin polymerisation-related proteins to the immune synapses was observed (222). Interestingly, Nef sequesters Lck away from TCR-CD3 complex, in both the presence or absence of CD4, and slows down TCR internalisation (220), thereby arresting TCR recycling and downregulation following TCR-pMHC ligation. This leads to accumulation of TCRs on the cell surface, resulting in T cell hyperactivation which is readily observed in untreated HIV-infection (223, 224). Previous reports also show that Nef has downstream effects on transcription factors like NFAT and NF-κB which are important to execute T cell mediated immune responses (225, 226).

From T cell-APC conjugation to T cell activation and cytolytic granule trafficking to targeted cytotoxicity, these chronic diseases highlight the importance of each stage in immune synapse formation for the execution of optimal T cell immune responses.

T Cell Mechanosensing

The initial contact between T cell and APC demonstrated by TCR binding to its cognate antigen-peptide triggers downstream signaling events that would activate T cells to efficiently execute their effector functions. However, the outcome of TCR signaling is largely impacted by mechanical forces applied to the TCR-pMHC complex (227, 228). Essentially, exogenous forces applied to TCR-pMHC interactions are transmitted into the cell as biochemical signals through mechanotransduction, the process which describes how physical perturbation experienced by receptors are translated into chemical signals (229). Conversely, biochemical signals generated by the cell is being translated into mechanical forces that are exerted on the surrounding environment.

Attempts to *ex vivo* activate and expand T cells utilising soluble anti-CD3 antibodies have largely failed (228, 230–232). TCR triggering *ex vivo* can be achieved by immobilising CD3 complex activating antibodies on rigid surfaces such as beads or tissue culture plates, as evidenced by the increased Ca^{2+} influx and phosphorylation of ZAP70 in T cells (233, 234). One explanation for why surface attached antibodies induce activation but those in solution do not is that surface association mimics mechanical forces created by the movements of synaptic membranes on TCR-pMHC complexes and suggests that TCR signaling cannot be initiated unless pulling-pushing stresses or shear forces are applied to the complex (**Figure 2C**) (234, 235).

Early studies showed that mechanical forces at the piconewton (pN) range applied through pMHC-coated beads were enough to induce Ca^{2+} influx and ERK phosphorylation in T cells (236). However, when similar forces were applied to CD28, CD62L, or ICAM-2 no significant increase in Ca^{2+} influx was observed (234). Since these mechanical forces involving antigen recognition by T cells operate at pN range, it poses technical challenges when elucidating them in biological systems. Recently, using biomembrane force probe (BFP) a number of studies have shown the threshold for cognate TCR-pMHC interaction to be at the scale of ~10 pN (237, 238). In addition to TCRs, other mechanosensors such as Piezo1 contributes to optimal T cell signaling (232). However, the extent of Piezo1 involvement in TCR signaling and T cell responses is yet to be elucidated. As the mechanical forces applied on TCR-pMHC require some level of rigidity from both biological supports (i.e. membranes), the stiffness of APC is expected to influence T cell responses. Stimulating substrates with anti-CD3 and anti-CD28 antibodies on supports with relatively high rigidity drive greater productions of IFN-γ, TNF-α and IL-2, up-regulation of activation markers and proliferative capacity compared with softer substrates (180, 228, 239–241). Furthermore, CTLs increase the stiffness of APC by stretching the synaptic region to modulate the speed of the perforin pore formation and consequently promote faster target cell lysis (242). These studies highlight the importance of fine tuning the rigidity of stimulating cultures for optimal T cell response which has implications in adoptive T cell immunotherapies (239, 240, 243, 244). One may also question whether subtle mechanical changes in TCR-pMHC affinity can trigger specific signal transduction pathways and affect downstream T cell responses.

Forces applied on TCR-pMHC complex can affect their bond lifetime in unexpected ways. For instance, catch bonds, where pulling forces applied to the bond, increases its bond lifetime (245), have been described for several receptor–ligand interactions (**Figure 2C**) (246, 247) and recently also for TCR-agonistic peptide MHC interactions (237, 238, 248). In contrast, antagonistic peptides form slip bonds characterized by short lifetimes (**Figure 2C**) (237). Independent reports using BFP (237, 238, 249, 250) and optical tweezers (248) on cell systems that express transgenic TCRs and cell-free experiments also using optical tweezers (248, 251) have demonstrated that while agonistic-peptides can increase TCR-pMHC binding lifetime, antagonistic-peptides tends to reduce it. These studies further demonstrated that catch bonds reach their maximum lifetime under a mechanical force in the range of ~10 pN and the lifetime of slip bonds decreases exponentially with increased mechanical force.

Another crucial aspect of T cell mechanosensing is to understand how TCR and cognate-pMHC binding events get translated into biochemical signals in T cells that are specific to the antigenic peptide. One theory suggests a conformational change of the TCR-CD3 complex during pMHC binding that would dislodge and release the cytoplasmic tails of CD3 from the inner leaflet of the plasma membrane. This would expose immunoreceptor tyrosine-based activation motifs (ITAMs) to get phosphorylated by tyrosine kinases Lck and Fyn. Accordingly, a TCR specific antigenic peptide would expose the cytoplasmic tails of CD3 for a longer period and permit more efficient phosphorylation by tyrosine kinases to generate a stronger signal to transduce (252, 253). A theory based on kinetic segregation model explains a local disruption of the kinase-phosphatase balance during TCR-pMHC binding is sufficient

to generate a productive signal as TCRs get phosphorylated by the segregation of phosphatase like CD45 (254, 255). Here, catch bonds (formed with cognate ligands) or slip bonds (formed with non-cognate ligands) formed during TCR-pMHC interactions (**Figure 2C**) may generate differential segregation patterns that would then be translated to a strong or weak signal, respectively (250).

In summary, regulating mechanosensing capacity of TCR is crucial to recognise and translate mechanical cues into cell signals during T cell activation and in execution of immune responses.

T Cell Mechanosensing in Chronic Diseases

T cells constantly patrol and migrate to different tissue compartments in search of cognate-antigens. This tissue migration involves continuous changes in T cell morphology driven by actin polymerisation which impose considerable mechanical force at the cellular level. During the contact between T cell and APC, the role played by mechanical forces in mediating immune responses are now becoming clear. The highly dynamic interactions between the extracellular matrix (ECM) and actin cytoskeleton is directly linked with translating mechanical cues from the environment into cell signals. Substrate stiffness is a mechanical cue that is implied to regulate number of cellular functions including proliferation, migration and differentiation (256–258). T cells are exposed to a range of substrate stiffnesses during their lifespan as stiffness values change substantially in different cells that T cells encounter. For example, while skeletal muscles have a stiffness in the range of ~10 kPa (259), elastic modulus of human bones may vary from 7–25 GPa (260).

A number of studies reported that reduced stiffness in cancer cells as a mechanism of promoting their growth independent of ECM stiffness (261, 262). Since optimal T cell responses require surfaces or biological membranes with relatively high rigidity, by reducing surface stiffness, cancer cells can effectively evade immune detection and subsequent cytotoxicity. Concurrently, a local increase in ECM stiffness is associated with disease progression (263). It has been reported that cancer cells are able to modify their surrounding ECM stiffness in order to promote metastasis (264). In fact, ECM associated adhesion proteins are known to play a vital role in different stages of cancer metastasis which overall influence the invasiveness of a cancer (265). In some cases, cancer cells are shown to synthesise their own ECM proteins to promote metastasis (266). Additionally, ECM stiffness influence the outcome of desmoplastic response (i.e. pervasive growth of dense collagen stroma around a tumor) associated with tumors (267). For instant, desmoplasia in pancreatic and breast cancer promote tumor progression and results in poor prognosis (268, 269). In mammary tumors, lysyl oxidase enzyme is linked to remodelling and increasing ECM stiffness as the inhibition of this enzyme reduced tissue stiffening and delayed tumor progression (270). Several studies have demonstrated a correlation between collagen density, a primary component of the ECM, and the infiltrative capacity of T cells into tumor islets (271–273). Densely packed collagen fibres are suggested to obstruct T cell entry into the tumor microenvironment, and overall reduce their proliferative and cytotoxic capacity (273). Recently, a study using confocal microscopy coupled with optical tweezers was able to track changes in biophysical properties of cancer cells in a multicellular 3D breast cancer model (274). The study was able to identify a stiffness gradient decreasing outward from the core of the growing tumor, suggesting cancer cells with softer biophysical characteristics are likely to be located at the periphery of the tumor. Moreover, this also implies that T cell mediated cytotoxicity become less efficient at the edge of the tumor, thereby increasing the invasiveness of the tumor at the periphery. Whether modulation of cell stiffness is a reliant mechanism for immune evasion during chronic infections is yet to be determined. Overall, understanding T cell responses to mechanical cues such as substrate stiffness may become crucial to understand the biophysical landscape of exhausted T cells.

TCR Diversity in Immune Responses

In adaptive immunity, the engagement of TCR with pMHC molecules plays a pivotal role in shaping the overall immune responses against foreign pathogens, malignancies and allergens. When TCRs recognise and bind to their cognate antigen, it triggers intracellular signaling pathways that activate the expression of multiple genes linked to several effector functions in T cells. Hence, the quality and magnitude of T cell effector functions are linked to the strength and quality of TCR-pMHC interactions. Primarily, the strength of these interactions are measured by TCR affinity to its antigen (275). T cell signaling is a complex function that involves the affinity of TCR-pMHC interactions, coreceptor binding and co-stimulatory and co-inhibitory signal integration (276), but in general, affinity of TCR-pMHC can predict the sensitivity of a T cell to a specific antigen (277). TCR affinity also dictates selective polyclonal expansion of antigen-specific T cells during immune responses.

Rearrangement within the variable regions of the TCR and thymic selection generates an immune repertoire of T cells with differing antigen specificities. During an infection, the expansion of T cell clones specific to a small number of immunodominant antigens can skew the immune repertoire (278). This form of TCR bias can be influenced by multiple factors ranging from thymic selection to initial immune response to an antigen (278). Overall, the adaptive immune system is shown to maintain a diversified population of antigen-specific T cell clones with varying affinities which possess the capacity to clonally expand and form memory T cells. In some cases a bias T cell clonal expansion, either towards high or low affinity has been observed (279, 280). During the acute phase of an infection, early models of clonal selection have shown that antigen-specific T cells with higher affinity are selectively expanded from the polyclonal T cell population to mediate immune responses and proceed to become memory T cells to retain acquired immunity (281–283). This selective enrichment of antigen-specific high-affinity clones has been described as a form of affinity maturation of T cells (284). During persistent antigen exposure, however, the profile of memory T cell clones shifts towards a low-affinity repertoire (16, 279, 285). Hence, distinct affinity profiles for antigen-specific T cells are generated and maintained during

acute and chronic phase of an infection. Elucidating the underline mechanisms behind this differential clonal expansion under different phases of antigen exposure proven to be beneficial in developing therapeutic interventions aimed at restoring T cell immune responses in chronic diseases.

Measuring TCR Affinity

TCR affinity to its cognate antigen-MHC complex is generally reported as the ratio of k_{off} and k_{on} rates, K_D: the equilibrium dissociation constant. In simple terms TCR-pMHC interactions with low K_D values (i.e. high affinity interactions) are typically associated with longer binding dwell times. Due to rapid dissociation (high k_{off}) of TCR-pMHC complex, it is often difficult to determine the affinity of TCR-pMHC interactions using conventional kinetic measurements. Generally, TCR-pMHC affinity is in the scale of micromolar range (1 to 300 μM), albeit with considerable variability (275, 286). Among several approaches which have been useful in characterising TCR-pMHC binding affinity, surface plasmon resonance (SPR), two-dimensional micropipette adhesion frequency assay (2D-MP) (287, 288) and pMHC multimer-binding have demonstrated their wide applicability in physiological settings (**Figure 3**).

The usage of SPR to determine TCR-pMHC affinity dates back three decades (290, 291). SPR measures a signal that correlates to a change in mass on a sensor-surface (i.e. sensor chip) where the binding partner, in this case pMHC molecules are immobilized on the senor-surface and TCR molecules flown over to bind (**Figure 3A**). SPR offers much lower sample requirement and versatility over earlier techniques like isothermal titration calorimetry (ITC), but with some drawbacks which have been reviewed elsewhere (292, 293). While SPR provides the means of directly measuring TCR-pMHC binding affinity, in physiological settings, the TCR is also attached to a surface where several other receptor–ligand interactions would take place simultaneously. Moreover, SPR would not account for the forces introduced with bystander TCRs, auxiliary receptors, cell adhesion molecules and membrane fluctuations which overall can modify TCR-pMHC

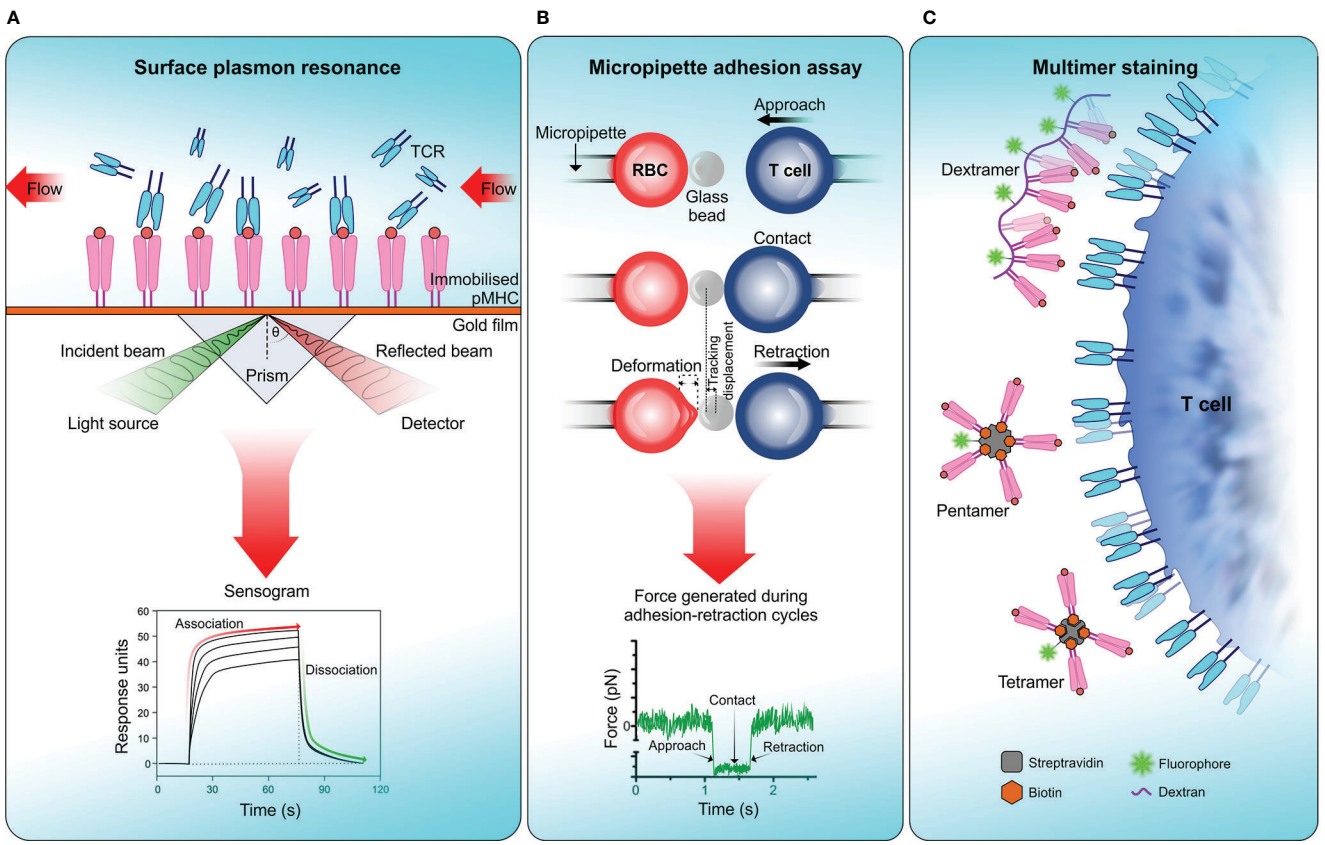

FIGURE 3 | Measuring TCR affinity. **(A)** Surface plasmon resonance (SPR). SPR measures the equilibrium dissociation constant (K_D) of TCR-pMHC interactions in which pMHC is immobilized on a sensor surface and TCR molecules are injected in a continuous flow. Binding of TCR to pMHC results in a change of mass on the sensor surface and is recorded in a sensogram which is then used to calculate K_D. **(B)** Micropipette adhesion assay. This technique uses two probes, one that is stationary which contains a red blood cell (RBC) attached to a functionalized glass bead to act as the adhesion force transducer and a mobile force probe bearing a T cell coupled to a piezotranslator. During adhesion-retraction cycles carried out by the mobile probe, the deformation of the RBC, displacement of the glass bead and the force generated in each cycle is recorded. **(C)** Multimer staining. This technique enhances the binding avidity of TCR-pMHC by increasing the valency of the interaction, results in more stable multimeric TCR-pMHC complexes for efficient labelling and detection. To date numerous forms of pMHC multimers have been reported which includes tetramers, pentamers, octamers, and dextramers (289).

binding affinity. Hence, measuring functional TCR-pMHC binding affinity in native cell membrane environment would be more physiologically relevant (288).

When predicting TCR-pMHC affinity in the context of T cell-APC interactions, the 2D micropipette adhesion assay (2D-MP) technique has proven to be useful. In 2D-MP, a human red blood cell (RBC) decorated with the ligand of interest acts as a sensor for measuring adhesion kinetics with the cell of interest expressing the cognate receptor (**Figure 3B**) (294). A micromanipulation device is used to bring these two cells into close proximity, in a tightly controlled environment enabling receptor–ligand binding. These binding events are captured as the degree of deformation of RBC membrane when the T cell is pulled away. These adhesion cycles were repeated and then translated into a binding curve which allows the calculation of binding kinetics for a given receptor–ligand interaction in two-dimensional space. By measuring affinity in the native membrane environment of a receptor, this method provides more physiologically relevant binding kinetics that have more applicability in cell biology. A modified version of 2D-MP known as the fluorescence biomembrane force probe (fBFP) uses osmolarity adjusted human red blood cell attached to a functionalized glass bead to act as the adhesion force transducer (**Figure 3B**) (237). This technique combined with single-molecule force spectroscopy and fluorescence microscopy enables the measurement of singular receptor–ligand binding event kinetics. Both 2D-MP and fBFP have measured much faster off-rates for TCR-pMHC interactions [30–8,300 fold faster (287)] than reported by 3D kinetic measurements derived from SPR. It should be noted that rapid 2D off-rates obtained for TCR-pMHC do not necessarily correlate with the rapid off-rates in 3D, indicating kinetics of TCR-pMHC interactions including off-rates and antigen-peptide affinity differ substantially from 2D to 3D space. A major drawback of these techniques is their requirement for highly specialized equipment to measure cellular level kinetics. This limits their usage in predicting population level kinetics during T cell-APC interactions.

Multimers of pMHC are the most commonly used method in identifying antigen-specific T cells from a polyclonal population. Due to their low affinity, monomeric pMHC are ineffective as a labelling probe in detecting antigen-specific T cell clones from a pool of other T cells. Multimer technology overcomes this by increasing the valency of TCR-pMHC interaction by multimerizing pMHC complexes to increasing avidity, which results in more stable multimeric TCR-pMHC complexes for efficient labelling and detection (295). The pMHC multimers can be in the form of tetramers, pentamers or octamers (**Figure 3C**) (296, 297). Recently, multimer labelling has been shown to introduce biases towards detection of high-affinity TCR-pMHC interactions and underestimation of interactions with low-affinity. This may distort the overall view of antigen-specific T cell diversity in a polyclonal population (298). Therefore, multimer binding intensity does not necessarily correlate with the functional responses produced by antigen-specific T cell population (299, 300).

It is evident that each affinity measurement technique in isolation overlooks the clonal diversity of T cell immune repertoire which is crucial to understand the full extent of immune responses during a disease. When combined, these techniques would resolve the shortcomings of affinity biases in predicting antigen-specific polyclonal T cell diversity.

T Cell Affinity Repertoire in Chronic Diseases

TCR affinity and signaling strength in response to a specific antigen sets the threshold for clonal selection to execute immune responses. Based on the premise that high-affinity TCR-pMHC interactions leads to efficient T cell activation, high-affinity T cell clones have a selective advantage over other clonotypes in mediating primary and secondary immune responses during the acute phase of a disease (281, 283, 301). This observed lack of affinity diversity becomes reduced when the disease progresses into a chronic phase. Mounting evidence suggest that this enhanced diversity in T cell clonal affinity is due to the recruitment of low-affinity TCR expressing T cells in the immune repertoire (280, 302–304). This distribution pattern of affinity clones of antigen-specific T cells can differ between disease models, and how this diversity is maintained to produce life-long immune responses is still under investigation. Moreover, screening affinity diversity in the T cell immune repertoire is challenging as current detection methods are suboptimal in identifying the full breadth of clonal diversity. Excluding low-affinity clones from the measured T cell repertoire will underestimate the full capacity of functional responses exerted by the immune system during chronic diseases.

A number of studies have demonstrated the effectiveness of low-affinity antigen-specific T cell clones in mediating immune responses, combating infections and preventing tumor progression similar to high-affinity counterparts (279, 280, 300, 305). Based on $CD4^+$ T cell responses to six different LCMV-antigens, Martinez et al. reported limited correlation between TCR affinity and dominance in clonal expansion (280). Moreover, both high and low-affinity T cell clones possess similar proliferative capacity (306, 307) and phenotypic characteristics (302) which all together challenge the prerequisite of high-affinity TCR-pMHC interaction dominance in driving clonal expansion and mediating immune responses. However, the strength of TCR-pMHC ligation may determine the magnitude of clonal expansion and the onset of contraction phase. This was demonstrated in *Listeria monocytogenes* infection model using altered peptide ligands with varying affinities (302). Despite the observed similarities in rapid proliferation rates in low and high-affinity antigen-specific T cell clones, Zehn et al. showed that weaker ligand interactions lead to early onset of contraction of T cell proliferation (302). In the same study, early appearance of low-affinity T cell clones in the blood stream after antigen-stimulation suggest a role for TCR-pMHC affinity in modulating the kinetics of T cell migration. Moreover, the reduced memory T cell expansion during successive challenge of a weak ligand/antigen indicates a correlation with the strength of recall stimulus and memory T cell responses.

Despite numerous attempts undertaken to predict the affinity diversity of T cells in different disease models, most clonal diversity observations of immune responsive T cells come from unrelated models of acute and chronic diseases. It would be highly

relevant to demonstrate the evolutionary trajectory of antigen-specific T cell affinity using longitudinal observations during acute and chronic phase of the same disease model. Using two LCMV infection models, Andargachew et al. showed that the overall affinity diversity of $CD4^+$ T cell clones were similarly maintained throughout acute and chronic antigen exposure along with effector and memory T cells showing similar affinity distribution patterns in both phases (308). Their study accompanied 2D-affinity kinetic measurements derived from 2D-MP assay. During the transition of effector to early memory $CD4^+$ T cells, both acute and chronic LCMV infection showed an increased functional avidity. However, the half-maximal effective concentration (EC_{50}) for IFN-γ and IL-2 production was much lower for acute-LCMV $CD4^+$ T cells compared to chronic exhausted $CD4^+$ T cells, which indicates a higher antigen sensitivity and functional avidity for $CD4^+$ T cells in the acute phase of LCMV infection. This study also drew parallels between chronic and acute-LCMV with their selective recruitment of low-affinity T cell clones into the immune repertoire.

More recently, a longitudinal study used memory T cell inflation to illustrate the evolutionary trajectory of cytomegalovirus (CMV)-specific $CD8^+$ effector memory T cell affinity during acute and chronic phase antigen exposure (16). T cell inflation is described as the atypical accumulation of memory T cells in blood and peripheral tissues in response to persistent low-level antigen exposure (309). Using both human and mouse CMV models, Schober et al. analyzed TCR affinity distribution among the $CD8^+$ T cell population. The TCR-pMHC dissociation rate (k_{off}) measurements obtained from real-time fluorescence microscopy (310) conclusively demonstrated that T cells with lower TCR affinity were enriched in the inflationary $CD8^+$ T cell pool compared to the acute phase. Moreover, in-depth analysis of CMV-specific TCR repertoire obtained from the mouse model showed clones under-represented in the acute phase of the infection (medium to low-affinity clones) were recruited at higher proportions to the immune repertoire at later stages *via* clonal succession (311). The authors also suggest that recruitment of low-affinity T cell clones compensated the loss of functional avidity provided by high-affinity clones which become senescent at late stages of the infection. This form of "reversed-affinity maturation" could be an important adaptation of the immune system to maintain life-long effective T cell responses against persistent viral infections which particularly exhibit low antigen expression levels. In the long-run, selective expansion of low-affinity T cell clones may provide an effective strategy in generating lasting pathogen control along with reduced immunopathology.

Whether the above mechanisms prove to be effective in regulating clonal diversity in T cell exhaustion related chronic diseases remains to be explored. T cells with high-functional avidity often exhibit exhaustion phenotypes under high levels of antigen exposure (312, 313). This can increase the probability of pathogen escape from the immune system, leaving low-avidity clones of antigen-specific T cells to take up the task of pathogen clearance or maintain a life-long host-pathogen equilibrium with reduced immunopathology. It should be noted that low-avidity T cell clones can also become functionally exhausted as reported by several tumor models (314, 315).

The affinity repertoire of effector T cells during cancer is less well understood than in chronic infections. Previous studies suggest that TILs with high-avidity are more likely show exhaustion markers albeit having superior control in eliminating tumor cells compared to their low-avidity counterparts (312, 316, 317). A growing number of studies have recognized a distinct role for low-avidity TILs in tumor clearance. Studies have shown low-affinity TCR interactions with tumor antigens activate tumor-specific T cells in a similar manner to high-affinity TCR interactions with the tumor antigen (317, 318). Moreover, with prolong exposure to the tumor, both clonotypes showed exhaustion markers including sustained upregulation of inhibitory receptors, with higher degree of exhaustion observed for high-avidity tumor-specific T cell clones (317). Another study using adoptive transfer of OT-I (high-affinity) and OT-3 (low-affinity) transgenic tumor-specific $CD8^+$ T cells was able to demonstrate that OT-3 T cells were able to mediate tumor regression in pancreas with minimum autoimmunity, contrast to OT-I T cells which in addition to the rapid eradication of the tumor, caused autoimmune diabetes in the mouse model (314). These studies suggest a necessary role for low-avidity tumor-specific T cells in anti-cancer immune responses. Thus, elucidating various mechanism underlying the expansion of T cell affinity repertoire during cancer progression is important to understand cancer immune surveillance and more complex immune-oncology concepts like immunoediting. Immunoediting of malignant cells can generate slightly variable neoantigen presented to the existing TCR repertoire in the TME causing decreases in the overall TCR affinities and T cell-cytolytic responses, and consequently tumor evasion (319–321).

Other Factors Influencing T Cell Affinity Diversity

Numerous other internal and external factors including the expression level of co-stimulatory/inhibitory receptors in T cells, co-stimulatory/inhibitory ligands on APC, and the dose and density of antigen presentation by APCs play a key role in shaping the functional avidity of antigen-specific T cell immune repertoire. For example, the CD27/CD70 mediated co-stimulation in T cells has been shown to lower the threshold of TCR activation to respond to low-affinity antigens, which promotes to generate a higher degree of memory T cell clonal diversity (322). Conversely, higher expression of B7-1 along with ICAM-1 and LFA-3 are linked to selectively enriching T cell clones with high functional avidity (323, 324). *De novo* expression of B7-1 by anti-myeloma cellular vaccines improves cytotoxicity and helper-dependent memory formation of subdominant $CD8^+$ T cell clones by avoiding tolerogenic effects (320). The antigen density presented by APCs during T cell priming and during infections has been shown to influence the functional avidity of immune responsive T cell populations (325). For instance, higher antigen density on APCs can compensate for low-affinity TCR-pMHC interactions. In human melanoma model it was demonstrated that low antigen doses presented by dendritic cells (DCs) produce melan-A-specific $CD8^+$ T cells with high functional avidity which had lower dependence on CD8 coreceptors (326). B cells in infection models like Friend virus (FV) are linked to efficient priming and subsequent expansion of T cells with low functional avidity,

overall diversifying $CD4^+$ T cell immune repertoire (327). Moreover, the degree of B cell activation correlates with B cell mediated clonal expansion of low-avidity $CD4^+$ T cells. Indeed, antigen specific B cells have long been speculated to drive clonal diversity in $CD4^+$ T cells (328).

CONCLUSION

Dysfunctional T cells are distinct from effector and memory T cells based on their functionality, metabolic activity, and epigenetic makeup. Recent findings strengthen the link between dysfunctional T cells and the progression of chronic diseases, thus, unravelling potential mechanisms behind the functional impairment of T cells with changes to its immune receptor and biophysical landscape during disease progression. In T cell exhaustion, the sustained upregulation of inhibitory receptors becomes a key feature that modifies the immune receptor landscape of T cells. Hence, these receptors have become primary targets in developing checkpoint blockade therapies aimed at restoring effector functions in non-responsive T cells. Although this has shown much clinical success in managing the progression of chronic diseases, there remains to be several limitations which hinder its wide applicability. Acquired resistance is one of the emerging challenges faced by checkpoint blockade therapy and may be overcome by combinatorial therapeutic strategies. The effectiveness of these therapeutic approaches in rescuing terminally exhausted T cells remains to be explored.

Apart from alterations in immune receptors expression profile, understanding changes to the cellular physiology of T cells during disease progression has become increasingly relevant to elucidate factors that promote T cell dysfunctions. Throughout their lifetime T cells are subjected to a myriad of mechanical forces experienced during cell migration, cell–cell interactions or exerted by the surrounding ECM. It is now becoming clear that these forces have important roles in T cell activation and the resultant effector functions, and may also play a central role in T cell dysfunctions. The concept of mechanotransduction as a mechanism of regulating cell behavior and function is not new (329), however, to understand this process at a subcellular level by means of measuring these infinitesimal forces require hypersensitive tools. As highlighted in this review, we have discussed the application of biophysical tools that can measure the strength of TCR-pMHC interactions as a proxy to predict the quality and magnitude of T cell mediated immune responses. Other techniques, including traction force microscopy (TFM) (180, 330), micro-pillar array detectors (mPADs) (331) and DNA-based molecular tension sensors (332, 333) have demonstrated to be useful in measuring mechanical forces experienced by TCRs *in vivo*. Importantly, DNA-based tension gauge tether was able to map mechanical forces during T cell activation modulated on a nanoparticle surface (332). This technique has been useful in determining T cell force threshold to distinguish functionally relevant mechanical forces from those do not trigger T cell activation, thus, providing a "fidelity checkpoint" for antigen discrimination (332). Utilization of these techniques to exploit single-molecule biomechanics of immune receptors may become useful in elucidating more complex cellular interactions faced by T cells such as found in the TME. Further, with the aid of these advanced biophysical tools, it is possible to develop new class of immunotherapies that aims to revamp T cell effector functions by recalibrating the mechanical force threshold of T cells to trigger more effective anti-tumor immune responses against the stiffness gradient of a growing tumor.

Lately, the usage of engineered chimeric antigen receptor (CAR) T cells as an effective immunotherapy has been useful in treating several cancer models (334–336). Importantly, previously observed non-classical immune synapses formation in CAR T cells correlates with the rapid recruitment of lytic granules to the synaptic cleft and killing the target cells much faster than classic CTLs (184). These unique functional features can be utilized to improve immunotherapy treatments against solid tumors. However, the potency of CAR T cells has been limited by several factors including T cell exhaustion (337, 338). The early constructs of CARs possessed affinities in the range of nano molar scale, rendering high-affinity interactions between CAR and antigens (339). These interactions are much stronger than physiologically relevant affinities displayed by TCR and pMHC, leading to off-target toxicities. This emphasises the role of affinity modulation in immunotherapy, which also becomes useful in designing prophylactic vaccine strategies to develop lasting immunity against pathogens. Immunotherapies aimed at treating patients in the acute phase of an infection should utilize the proliferative capacity of high-avidity T cell clones to achieve pathogen clearance. Accordingly, when an acute infection exacerbates into the chronic phase where pathogen clearance becomes inefficient, immunotherapies should make use of low-avidity clones to promote lasting host–pathogen equilibrium which delivers minimal immunopathology.

The importance of T cell biomechanics and how they differ between T cell subtypes needs further investigation. So far, much of the evidence of biomechanical influence in mediating T cell immune responses comes from expansion of clonal avidity of antigen-specific T cells during infections or cancer. Overall, in depth understanding of the biophysical properties behind mediating optimal immune reposes may help to identify broader principles governing T cell dysfunctions in chronic diseases and present new and improved avenues to develop clinical interventions in the future.

AUTHOR CONTRIBUTIONS

SG and NP reviewed the relevant literature and wrote the manuscript. JG and KG provided critical feedback and helped shape the manuscript. All authors contributed to the article and approved the submitted version.

FUNDING

The authors would like to acknowledge funding from the Australian Research Council (ARC) (CE140100011 to KG), the National Health and Medical Research Council of Australia (APP1155162 to KG), and Cancer Council New South Wales (APP1128488 to KG).

REFERENCES

1. Rock KL, Reits E, Neefjes J. Present Yourself! By MHC Class I and MHC Class II Molecules. *Trends Immunol* (2016) 37:724–37. doi: 10.1016/j.it.2016.08.010
2. Natarajan K, Jiang J, May NA, Mage MG, Boyd LF, McShan AC, et al. The role of molecular flexibility in antigen presentation and T cell receptor-mediated signaling. *Front Immunol* (2018) 9:1657. doi: 10.3389/fimmu.2018.01657
3. Masopust D, Schenkel JM. The integration of T cell migration, differentiation and function. *Nat Rev Immunol* (2013) 13:309–20. doi: 10.1038/nri3442
4. Cox MA, Harrington LE, Zajac AJ. Cytokines and the inception of CD8 T cell responses. *Trends Immunol* (2011) 32:180–6. doi: 10.1016/j.it.2011.01.004
5. Kalia V, Sarkar S, Ahmed R. CD8 T-cell memory differentiation during acute and chronic viral infections. *Adv Exp Med Biol* (2010) 684:79–95. doi: 10.1007/978-1-4419-6451-9_7
6. Wherry EJ, Ahmed R. Memory CD8 T-Cell Differentiation during Viral Infection. *J Virol* (2004) 78:5535–45. doi: 10.1128/jvi.78.11.5535-5545.2004
7. Williams MA, Bevan MJ. Effector and Memory CTL Differentiation. *Annu Rev Immunol* (2006) 25:171–92. doi: 10.1146/annurev.immunol.25.022106.141548
8. Kaech SM, Hemby S, Kersh E, Ahmed R. Molecular and functional profiling of memory CD8 T cell differentiation. *Cell* (2002) 111:837–51. doi: 10.1016/S0092-8674(02)01139-X
9. Schietinger A, Greenberg PD. Tolerance and exhaustion: Defining mechanisms of T cell dysfunction. *Trends Immunol* (2014) 35:51–60. doi: 10.1016/j.it.2013.10.001
10. Wherry EJ. T cell exhaustion. *Nat Immunol* (2011) 12:492–9. doi: 10.1038/ni.2035
11. Saeidi A, Zandi K, Cheok YY, Saeidi H, Wong WF, Lee CYQ, et al. Shankar EM. T-cell exhaustion in chronic infections: Reversing the state of exhaustion and reinvigorating optimal protective immune responses. *Front Immunol* (2018) 9:2569. doi: 10.3389/fimmu.2018.02569
12. Wang C, Singer M, Anderson AC. Molecular Dissection of CD8+ T-Cell Dysfunction. *Trends Immunol* (2017) 38:567–76. doi: 10.1016/j.it.2017.05.008
13. Blackburn SD, Shin H, Haining WN, Zou T, Workman CJ, Polley A, et al. Coregulation of CD8+ T cell exhaustion by multiple inhibitory receptors during chronic viral infection. *Nat Immunol* (2009) 10:29–37. doi: 10.1038/ni.1679
14. Duong MN, Erdes E, Hebeisen M, Rufer N, Chronic TCR-MHC. (self)-interactions limit the functional potential of TCR affinity-increased CD8 T lymphocytes. *J Immunother Cancer* (2019) 7:284. doi: 10.1186/s40425-019-0773-z
15. Ramsay AG, Johnson AJ, Lee AM, Gorgün G, Le DR, Blum W, et al. Chronic lymphocytic leukemia T cells show impaired immunological synapse formation that can be reversed with an immunomodulating drug. *J Clin Invest* (2008) 118:2427–37. doi: 10.1172/JC135017
16. Schober K, Voit F, Grassmann S, Müller TR, Eggert J, Jarosch S, et al. Reverse TCR repertoire evolution toward dominant low-affinity clones during chronic CMV infection. *Nat Immunol* (2020) 21:434–41. doi: 10.1038/s41590-020-0628-2
17. Chen L, Flies DB. Molecular mechanisms of T cell co-stimulation and co-inhibition. *Nat Rev Immunol* (2013) 13:227–42. doi: 10.1038/nri3405
18. Takaba H, Takayanagi H. The Mechanisms of T Cell Selection in the Thymus. *Trends Immunol* (2017) 38:805–16. doi: 10.1016/j.it.2017.07.010
19. Liu GY, Fairchild PJ, Smith RM, Prowle JR, Kioussis D, Wraith DC. Low avidity recognition of self-antigen by T cells permits escape from central tolerance. *Immunity* (1995) 3:407–15. doi: 10.1016/1074-7613(95)90170-1
20. Hernandez J, Aung S, Redmond WL, Sherman LA. Phenotypic and functional analysis of CD8+ T cells undergoing peripheral deletion in response to cross-presentation of self-antigen. *J Exp Med* (2001) 194:707–17. doi: 10.1084/jem.194.6.707
21. Kurts C, Kosaka H, Carbone FR, Miller JFAP, Heath WR. Class I-restricted cross-presentation of exogenous self-antigens leads to deletion of autoreactive CD8+ T cells. *J Exp Med* (1997) 186:239–45. doi: 10.1084/jem.186.2.239
22. Wing K, Sakaguchi S. Regulatory T cells exert checks and balances on self tolerance and autoimmunity. *Nat Immunol* (2010) 11:7–13. doi: 10.1038/ni.1818
23. Sakaguchi S. Naturally arising Foxp3-expressing CD25+ CD4+ regulatory T cells in immunological tolerance to self and non-self. *Nat Immunol* (2005) 6:345–52. doi: 10.1038/ni1178
24. Izcue A, Coombes JL, Powrie F. Regulatory lymphocytes and intestinal inflammation. *Annu Rev Immunol* (2009) 27:313–38. doi: 10.1146/annurev.immunol.021908.132657
25. Schietinger A, Delrow JJ, Basom RS, Blattman JN, Greenberg PD. Rescued tolerant CD8 T cells are preprogrammed to reestablish thetolerant state. *Science* (2012) (80-):723–7. doi: 10.1126/science.1214277
26. Burrack AL, Martinov T, Fife BT. T cell-mediated beta cell destruction: Autoimmunity and alloimmunity in the context of type 1 diabetes. *Front Endocrinol (Lausanne)* (2017) 8:343. doi: 10.3389/fendo.2017.00343
27. Skapenko A, Leipe J, Lipsky PE, Schulze-Koops H. The role of the T cell in autoimmune inflammation. *Arthritis Res Ther* (2005) 7:S4–14. doi: 10.1186/ar1505
28. Weiner HL. Multiple sclerosis is an inflammatory T-cell-mediated autoimmune disease. *Arch Neurol* (2004) 61:1613–5. doi: 10.1001/archneur.61.10.1613
29. Jabri B, Sollid LM. T Cells in Celiac Disease. *J Immunol* (2017) 198:3005–14. doi: 10.4049/jimmunol.1601693
30. Parish IA, Heath WR. Too dangerous to ignore: Self-tolerance and the control of ignorant autoreactive T cells. *Immunol Cell Biol* (2008) 86:146–52. doi: 10.1038/sj.icb.7100161
31. Ohashi PS, Oehen S, Buerki K, Pircher H, Ohashi CT, Odermatt B, et al. Ablation of "tolerance" and induction of diabetes by virus infection in viral antigen transgenic mice. *Cell* (1991) 65:305–17. doi: 10.1016/0092-8674(91)90164-T
32. Kurts C, Sutherland RM, Davey G, Li M, Lew AM, Blanas E, et al. (1999) CD8 T cell ignorance or tolerance to islet antigens depends on antigen dose. *Proc Natl Acad Sci USA* 96:12703–7.
33. Oldstone MBA, Nerenberg M, Southern P, Price J, Lewicki H. Virus infection triggers insulin-dependent diabetes mellitus in a transgenic model: Role of anti-self (virus) immune response. *Cell* (1991) 65:319–31. doi: 10.1016/0092-8674(91)90165-U
34. Millar DG, Garza KM, Odermatt B, Elford AR, Ono N, Li Z, et al. Hsp70 promotes antigen-presenting cell function and converts T-cell tolerance to autoimmunity in vivo. *Nat Med* (2003) 9:1469–76. doi: 10.1038/nm962
35. Ramanathan S, Dubois S, Chen X-L, Leblanc C, Ohashi PS, Ilangumaran S. Exposure to IL-15 and IL-21 Enables Autoreactive CD8 T Cells To Respond to Weak Antigens and Cause Disease in a Mouse Model of Autoimmune Diabetes. *J Immunol* (2011) 186:5131–41. doi: 10.4049/jimmunol.1001221
36. Schwartz RH. T cell anergy. *Annu Rev Immunol* (2003) 21:305–334. doi: 10.1146/annurev.immunol.21.120601.141110
37. Choi S, Schwartz RH. Molecular mechanisms for adaptive tolerance and other T cell anergy models. *Semin Immunol* (2007) 19:140–52. doi: 10.1016/j.smim.2007.02.005
38. Mirshahidi S, Huang C, Sadegh-Nasseri S. Anergy in peripheral memory CD4+ T cells induced by low avidity engagement of T cell receptor. *J Exp Med* (2001) 194:719–31. doi: 10.1084/jem.194.6.719
39. Jenkins MK, Schwartz RH. Antigen presentation by chemically modified splenocytes induces antigen-specific T cell unresponsiveness in vitro and in vivo. *J Exp Med* (1987) 165:302–19. doi: 10.1084/jem.165.2.302
40. Blank C, Brown I, Peterson AC, Spiotto M, Iwai Y, Honjo T, et al. PD-L1/B7H-1 Inhibits the Effector Phase of Tumor Rejection by T Cell Receptor (TCR) Transgenic CD8+ T Cells. *Cancer Res* (2004) 64:1140–5. doi: 10.1158/0008-5472.CAN-03-3259
41. Zou W, Chen L. Inhibitory B7-family molecules in the tumour microenvironment. *Nat Rev Immunol* (2008) 8:467–77. doi: 10.1038/nri2326
42. Kryczek I, Zou L, Rodriguez P, Zhu G, Wei S, Mottram P, et al. B7-H4 expression identifies a novel suppressive macrophage population in human ovarian carcinoma. *J Exp Med* (2006) 203:871–81. doi: 10.1084/jem.20050930

43. Curiel TJ, Wei S, Dong H, Alvarez X, Cheng P, Mottram P, et al. Blockade of B7-H1 improves myeloid dendritic cell-mediated antitumor immunity. *Nat Med* (2003) 9:562–67. doi: 10.1038/nm863
44. Boussiotis VA, Barber DL, Nakarai T, Freeman GJ, Gribben JG, Bernstein GM, et al. Prevention of T cell anergy by signaling through the γc chainof the IL-2 receptor. *Science* (1994) (80-):1039–42. doi: 10.1126/science.7973657
45. Zha Y, Marks R, Ho AW, Peterson AC, Janardhan S, Brown I, et al. T cell anergy is reversed by active Ras and is regulated by diacylglycerol kinase-α. *Nat Immunol* (2006) 7:1166–73. doi: 10.1038/ni1394
46. Chiodetti L, Choi S, Barber DL, Schwartz RH. Adaptive Tolerance and Clonal Anergy Are Distinct Biochemical States. *J Immunol* (2006) 176:2279–91. doi: 10.4049/jimmunol.176.4.2279
47. Moulton VR, Tsokos GC. Abnormalities of T cell signaling in systemic lupus erythematosus. *Arthritis Res Ther* (2011) 13:207. doi: 10.1186/ar3251
48. Harakal J, Rival C, Qiao H, Tung KS. Regulatory T Cells Control Th2-Dominant Murine Autoimmune Gastritis. *J Immunol* (2016) 197:27–41. doi: 10.4049/jimmunol.1502344
49. Reim J, McIntosh K, Martin S, Daniel BD. Specific immunotherapeutic strategy for myasthenia gravis: targeted antigen-presenting cells. *J Neuroimmunol* (1992) 41:61–70. doi: 10.1016/0165-5728(92)90196-R
50. Zhao Y, Shao Q, Peng G. Exhaustion and senescence: two crucial dysfunctional states of T cells in the tumor microenvironment. *Cell Mol Immunol* (2020) 17:27–35. doi: 10.1038/s41423-019-0344-8
51. Collado M, Blasco MA, Serrano M. Cellular Senescence in Cancer and Aging. *Cell* (2007) 99:1047–78. doi: 10.1016/j.cell.2007.07.003
52. Collado M, Serrano M. Senescence in tumours: Evidence from mice and humans. *Nat Rev Cancer* (2010) 10:51–7. doi: 10.1038/nrc2772
53. Kasakovski D, Xu L, Li Y. T cell senescence and CAR-T cell exhaustion in hematological malignancies. *J Hematol Oncol* (2018) 11:91. doi: 10.1186/s13045-018-0629-x
54. Chou JP, Effros RB. T Cell Replicative Senescence in Human Aging. *Curr Pharm Des* (2013) 19:1680–98. doi: 10.2174/138161213805219711
55. Weng N-P, Akbar AN, Goronzy J. CD28- T cells: their role in the age-associated decline of immune function. *Trends Immunol* (2009) 30:306–12. doi: 10.1016/j.it.2009.03.013
56. Tsukishiro T, Donnenberg AD, Whiteside TL. Rapid turnover of the CD8 +CD28- T-cell subset of effector cells in the circulation of patients with head and neck cancer. *Cancer Immunol Immunother* (2003) 52:599–607. doi: 10.1007/s00262-003-0395-6
57. Appay V, Nixon DF, Donahoe SM, Gillespie GMA, Dong T, King A, et al. HIV-specific CD8+ T cells produce antiviral cytokines but are impaired in cytolytic function. *J Exp Med* (2000) 192:63–75. doi: 10.1084/jem.192.1.63
58. Montes CL, Chapoval AI, Nelson J, Orhue V, Zhang X, Schulze DH, et al. Tumor-induced senescent T cells with suppressor function: A potential form of tumor immune evasion. *Cancer Res* (2008) 68:870–9. doi: 10.1158/0008-5472.CAN-07-2282
59. Wolfram RM, Budinsky AC, Brodowicz T, Kubista M, Köstler WJ, Kichler-Lakomy C, et al. Defective antigen presentation resulting from impaired expression of costimulatory molecules in breast cancer. *Int J Cancer* (2000) 88:239–44. doi: 10.1002/1097-0215(20001015)88:2<239::AID-IJC15>3.0.CO;2-Z
60. Zeng S, Shen W, Liu L. Senescence and Cancer. *Cancer Transl Med* (2018) 4:70–4. doi: 10.4103/ctm.ctm_22_18
61. Liu X-L, Ding J, Meng L-H. Oncogene-induced senescence: a double edged sword in cancer. *Acta Pharmacol Sin* (2018) 39:1553–8. doi: 10.1038/aps.2017.198
62. Sarkisian CJ, Keister BA, Stairs DB, Boxer RB, Moody SE, Chodosh LA. Dose-dependent oncogene-induced senescence in vivo and its evasion during mammary tumorigenesis. *Nat Cell Biol* (2007) 9:493–505. doi: 10.1038/ncb1567
63. Courtois-Cox S, Jones SL, Cichowski K. Many roads lead to oncogene-induced senescence. *Oncogene* (2008) 27:2801–9. doi: 10.1038/sj.onc.1210950
64. Liu X, Mo W, Ye J, Li L, Zhang Y, Hsueh EC, et al. Regulatory T cells trigger effector T cell DNA damage and senescence caused by metabolic competition. *Nat Commun* (2018) 9:249. doi: 10.1038/s41467-017-02689-5
65. Ye J, Peng G. Controlling T cell senescence in the tumor microenvironment for tumor immunotherapy. *Oncoimmunology* (2015) 4:e994398. doi: 10.4161/2162402X.2014.994398
66. Ye J, Ma C, Hsueh EC, Dou J, Mo W, Liu S, et al. TLR 8 signaling enhances tumor immunity by preventing tumor-induced T-cell senescence. *EMBO Mol Med* (2014) 6:1294–311. doi: 10.15252/emmm.201403918
67. Ye J, Huang X, Hsueh EC, Zhang Q, Ma C, Zhang Y, et al. Human regulatory T cells induce T-lymphocyte senescence. *Blood* (2012) 120:2021–31. doi: 10.1182/blood-2012-03-416040
68. Vallejo AN. CD28 extinction in human T cells: Altered functions and the program of T-cell senescence. *Immunol Rev* (2005) 205:158–69. doi: 10.1111/j.0105-2896.2005.00256.x
69. Li H, Wu K, Tao K, Chen L, Zheng Q, Lu X, et al. Tim-3/galectin-9 signaling pathway mediates T-cell dysfunction and predicts poor prognosis in patients with hepatitis B virus-associated hepatocellular carcinoma. *Hepatology* (2012) 56:1342–51. doi: 10.1002/hep.25777
70. Brenchley JM, Karandikar NJ, Betts MR, Ambrozak DR, Hill BJ, Crotty LE, et al. Expression of CD57 defines replicative senescence and antigen-induced apoptotic death of CD8+ T cells. *Blood* (2003) 101:2711–20. doi: 10.1182/blood-2002-07-2103
71. Heffner M, Fearon DT. Loss of T cell receptor-induced Bmi-1 in the KLRG1 + senescent CD8+ T lymphocyte. *Proc Natl Acad Sci USA* (2007) 104:13414–9. doi: 10.1073/pnas.0706040104
72. Moskophidis D, Lechner F, Pircher H, Zinkernagel RM. Virus persistence in acutely infected immunocompetent mice by exhaustion of antiviral cytotoxic effector T cells. *Nature* (1993) 362:758–61. doi: 10.1038/362758a0
73. Wherry EJ, Blattman JN, Murali-Krishna K, van der Most R, Ahmed R. Viral Persistence Alters CD8 T-Cell Immunodominance and Tissue Distribution and Results in Distinct Stages of Functional Impairment. *J Virol* (2003) 77:4911–27. doi: 10.1128/jvi.77.8.4911-4927.2003
74. Zajac AJ, Blattman JN, Murali-Krishna K, Sourdive DJD, Suresh M, Altman JD, et al. Viral immune evasion due to persistence of activated T cells without effector function. *J Exp Med* (1998) 188:2205–13. doi: 10.1084/jem.188.12.2205
75. McLane LM, Abdel-Hakeem MS, Wherry EJ. CD8 T Cell Exhaustion During Chronic Viral Infection and Cancer. *Annu Rev Immunol* (2019) 37:457–95. doi: 10.1146/annurev-immunol-041015-055318
76. Fourcade J, Sun Z, Pagliano O, Guillaume P, Luescher IF, Sander C, et al. CD8 + T cells specific for tumor antigens can be rendered dysfunctional by the tumor microenvironment through upregulation of the inhibitory receptors BTLA and PD-1. *Cancer Res* (2012) 72:887–96. doi: 10.1158/0008-5472.CAN-11-2637
77. Bremnes RM, Dønnem T, Al-Saad S, Al-Shibli K, Andersen S, Sirera R, et al. The Role of Tumor Stroma in Cancer Progression and Prognosis. *J Thorac Oncol* (2011) 6(1):209–17. doi: 10.1097/JTO.0b013e3181f8a1bd
78. Watnick RS. The role of the tumor microenvironment in regulating angiogenesis. *Cold Spring Harb Perspect Med* (2012) 2(12):a006676. doi: 10.1101/cshperspect.a006676
79. Wherry EJ, Kurachi M. Molecular and cellular insights into T cell exhaustion. *Nat Rev Immunol* (2015) 15(8):486–99. doi: 10.1038/nri3862
80. Shin H, Blackburn SD, Blattman JN, Wherry EJ. Viral antigen and extensive division maintain virus-specific CD8 T cells during chronic infection. *J Exp Med* (2007) 204(4):941–9. doi: 10.1084/jem.20061937
81. Wherry EJ, Ha SJ, Kaech SM, Haining WN, Sarkar S, Kalia V, et al. Molecular Signature of CD8+ T Cell Exhaustion during Chronic Viral Infection. *Immunity* (2007) 27(4):670–84. doi: 10.1016/j.immuni.2007.09.006
82. Schietinger A, Philip M, Krisnawan VE, Chiu EY, Delrow JJ, Basom RS, et al. Tumor-Specific T Cell Dysfunction Is a Dynamic Antigen-Driven Differentiation Program Initiated Early during Tumorigenesis. *Immunity* (2016) 45(2):389–401. doi: 10.1016/j.immuni.2016.07.011
83. Speiser DE, Utzschneider DT, Oberle SG, Münz C, Romero P, Zehn D. T cell differentiation in chronic infection and cancer: Functional adaptation or exhaustion? *Nat Rev Immunol* (2014) 14(11):768–74. doi: 10.1038/nri3740
84. Philip M, Schietinger A. Heterogeneity and fate choice: T cell exhaustion in cancer and chronic infections. *Curr Opin Immunol* (2019) 58:98–103. doi: 10.1016/j.coi.2019.04.014

85. Li H, van der Leun AM, Yofe I, Lubling Y, Gelbard-Solodkin D, van Akkooi ACJ, et al. Dysfunctional CD8 T Cells Form a Proliferative, Dynamically Regulated Compartment within Human Melanoma. *Cell* (2019) 176(4):775–89.e18. doi: 10.1016/j.cell.2018.11.043
86. Utzschneider DT, Charmoy M, Chennupati V, Pousse L, Ferreira DP, Calderon-Copete S, et al. T Cell Factor 1-Expressing Memory-like CD8+ T Cells Sustain the Immune Response to Chronic Viral Infections. *Immunity* (2016) 45(2):415–27. doi: 10.1016/j.immuni.2016.07.021
87. Im SJ, Hashimoto M, Gerner MY, Lee J, Kissick HT, Burger MC, et al. Defining CD8+ T cells that provide the proliferative burst after PD-1 therapy. *Nature* (2016) 537(7620):417–21. doi: 10.1038/nature19330
88. Utzschneider DT, Legat A, Fuertes Marraco SA, Carrié L, Luescher I, Speiser DE, et al. T cells maintain an exhausted phenotype after antigen withdrawal and population reexpansion. *Nat Immunol* (2013) 14(6):603–10. doi: 10.1038/ni.2606
89. Wu T, Ji Y, Ashley Moseman E, Xu HC, Manglani M, Kirby M, et al. The TCF1-Bcl6 axis counteracts type I interferon to repress exhaustion and maintain T cell stemness. *Sci Immunol* (2016) 1(6):eaai8593. doi: 10.1126/sciimmunol.aai8593
90. Brummelman J, Mazza EMC, Alvisi G, Colombo FS, Grilli A, Mikulak J, et al. High-dimensional single cell analysis identifies stemlike cytotoxic CD8 +T cells infiltrating human tumors. *J Exp Med* (2018) 215(10):2520–35. doi: 10.1084/JEM.20180684
91. Leong YA, Chen Y, Ong HS, Wu D, Man K, Deleage C, et al. CXCR5+ follicular cytotoxic T cells control viral infection in B cell follicles. *Nat Immunol* (2016) 17(10):1187–96. doi: 10.1038/ni.3543
92. He R, Hou S, Liu C, Zhang A, Bai Q, Han M, et al. Follicular CXCR5-expressing CD8+ T cells curtail chronic viral infection. *Nature* (2016) 537 (7620):412–28. doi: 10.1038/nature19317
93. Miller BC, Sen DR, Al Abosy R, Bi K, Virkud YV, LaFleur MW, et al. Subsets of exhausted CD8+ T cells differentially mediate tumor control and respond to checkpoint blockade. *Nat Immunol* (2019) 20(3):326–36. doi: 10.1038/s41590-019-0312-6
94. Siddiqui I, Schaeuble K, Chennupati V, Fuertes Marraco SA, Calderon-Copete S, Pais Ferreira D, et al. Intratumoral Tcf1 + PD-1 + CD8 + T Cells with Stem-like Properties Promote Tumor Control in Response to Vaccination and Checkpoint Blockade Immunotherapy. *Immunity* (2019) 50(1):195–211.e10. doi: 10.1016/j.immuni.2018.12.021
95. Kallies A, Zehn D, Utzschneider DT. Precursor exhausted T cells: key to successful immunotherapy? *Nat Rev Immunol* (2020) 20(2):128–36. doi: 10.1038/s41577-019-0223-7
96. Intlekofer AM, Takemoto N, Wherry EJ, Longworth SA, Northrup JT, Palanivel VR, et al. Effector and memory CD8+ T cell fate coupled by T-bet and eomesodermin. *Nat Immunol* (2005) 6(12):1236–44. doi: 10.1038/ni1268
97. Joshi NS, Cui W, Chandele A, Lee HK, Urso DR, Hagman J, et al. Inflammation Directs Memory Precursor and Short-Lived Effector CD8+ T Cell Fates via the Graded Expression of T-bet Transcription Factor. *Immunity* (2007) 27(2):281–95. doi: 10.1016/j.immuni.2007.07.010
98. Pearce EL, Mullen AC, Martins GA, Krawczyk CM, Hutchins AS, Zediak VP, et al. Control of Effector CD8+ T Cell Function by the Transcription FactorEomesodermin. *Science* (2003) (80-):1041–3. doi: 10.1126/science.1090148
99. Kallies A, Nutt SL. Terminal differentiation of lymphocytes depends on Blimp-1. *Curr Opin Immunol* (2007) 19(2):156–62. doi: 10.1016/j.coi.2007.01.003
100. Kallies A, Xin A, Belz GT, Nutt SL. Blimp-1 Transcription Factor Is Required for the Differentiation of Effector CD8+ T Cells and Memory Responses. *Immunity* (2009) 31(2):283–95. doi: 10.1016/j.immuni.2009.06.021
101. Khan O, Giles JR, McDonald S, Manne S, Ngiow SF, Patel KP, et al. TOX transcriptionally and epigenetically programs CD8+ T cell exhaustion. *Nature* (2019) 571(7764):211–8. doi: 10.1038/s41586-019-1325-x
102. Delpoux A, Michelini RH, Verma S, Lai CY, Omilusik KD, Utzschneider DT, et al. Continuous activity of Foxo1 is required to prevent anergy and maintain the memory state of CD8 + T cells. *J Exp Med* (2018) 215 (2):575–94. doi: 10.1084/jem.20170697
103. Seo H, Chen J, González-Avalos E, Samaniego-Castruita D, Das A, Wang YH, et al. TOX and TOX2 transcription factors cooperate with NR4A transcription factors to impose CD8+ T cell exhaustion. *Proc Natl Acad Sci USA* (2019) 116(25):12410–5. doi: 10.1073/pnas.1905675116
104. Qi L, Yu H, Zhang Y, Zhao D, Lv P, Zhong Y, et al. IL-10 secreted by M2 macrophage promoted tumorigenesis through interaction with JAK2 in glioma. *Oncotarget* (2016) 7(44):71673–85. doi: 10.18632/oncotarget.12317
105. Blackburn SD, Wherry EJ. IL-10, T cell exhaustion and viral persistence. *Trends Microbiol* (2007) 15(4):143–6. doi: 10.1016/j.tim.2007.02.006
106. Gastl GA, Abrams JS, Nanus DM, Oosterkamp R, Silver J, Liu F, et al. Interleukin-10 production by human carcinoma cell lines and its relationship to interleukin-6 expression. *Int J Cancer* (1993) 55(1):96–101. doi: 10.1002/ijc.2910550118
107. Kim Y-J, Park S-J, Broxmeyer HE. Phagocytosis, a Potential Mechanism for Myeloid-Derived Suppressor Cell Regulation of CD8 + T Cell Function Mediated through Programmed Cell Death-1 and Programmed Cell Death-1 Ligand Interaction. *J Immunol* (2011) 187(5):2291–301. doi: 10.4049/jimmunol.1002650
108. Asadullah K, Sterry W, Volk HD. Interleukin-10 therapy - Review of a new approach. *Pharmacol Rev* (2003) 55(2):241–69. doi: 10.1124/pr.55.2.4
109. Kessler B, Rinchai D, Kewcharoenwong C, Nithichanon A, Biggart R, Hawrylowicz CM, et al. Interleukin 10 inhibits pro-inflammatory cytokine responses and killing of Burkholderia pseudomallei. *Sci Rep* (2017) 7:42791. doi: 10.1038/srep42791
110. Rabinovich GA, Liu FT, Hirashima M, Anderson A. An emerging role for galectins in tuning the immune response: Lessons from experimental models of inflammatory disease, autoimmunity and cancer. *Scand J Immunol* (2007) 66(2-3):143–58. doi: 10.1111/j.1365-3083.2007.01986.x
111. Gilson RC, Gunasinghe SD, Johannes L, Gaus K. Galectin-3 modulation of T-cell activation: mechanisms of membrane remodelling. *Prog Lipid Res* (2019) 76:101010. doi: 10.1016/j.plipres.2019.101010
112. Smith LK, Boukhaled GM, Condotta SA, Mazouz S, Guthmiller JJ, Vijay R, et al. Interleukin-10 Directly Inhibits CD8+ T Cell Function by Enhancing N-Glycan Branching to Decrease Antigen Sensitivity. *Immunity* (2018) 48:299–312.e5. doi: 10.1016/j.immuni.2018.01.006
113. Naing A, Infante JR, Papadopoulos KP, Chan IH, Shen C, Ratti NP, et al. PEGylated IL-10 (Pegilodecakin) Induces Systemic Immune Activation, CD8+ T Cell Invigoration and Polyclonal T Cell Expansion in Cancer Patients. *Cancer Cell* (2018) 34(5):775–91.e3. doi: 10.1016/j.ccell.2018.10.007
114. Mumm JB, Emmerich J, Zhang X, Chan I, Wu L, Mauze S, et al. IL-10 Elicits IFNγ-Dependent tumor immune surveillance. *Cancer Cell* (2011) 20(6):781–96. doi: 10.1016/j.ccr.2011.11.003
115. Emmerich J, Mumm JB, Chan IH, LaFace D, Truong H, McClanahan T, et al. IL-10 directly activates and expands tumor-resident CD8+ T cells without De Novo infiltration from secondary lymphoid organs. *Cancer Res* (2012) 72 (14):3570–81. doi: 10.1158/0008-5472.CAN-12-0721
116. Massagué J. TGFβ in Cancer. *Cell* (2008) 134(2):215–30. doi: 10.1016/j.cell.2008.07.001
117. Yang L, Moses HL. Transforming growth factor β: Tumor suppressor or promoter? Are host immune cells the answer? *Cancer Res* (2008) 68:9107–11. doi: 10.1158/0008-5472.CAN-08-2556
118. Ng CT, Snell LM, Brooks DG, Oldstone MBA. Networking at the level of host immunity: Immune cell interactions during persistent viral infections. *Cell Host Microbe* (2013) 13:652–64. doi: 10.1016/j.chom.2013.05.014
119. Goh C, Narayanan S, Hahn YS. Myeloid-derived suppressor cells: The dark knight or the joker in viral infections? *Immunol Rev* (2013) 255:210–21. doi: 10.1111/imr.12084
120. Waggoner SN, Cornberg M, Selin LK, Welsh RM. Natural killer cells act as rheostats modulating antiviral T cells. *Nature* (2012) 481:394–8. doi: 10.1038/nature10624
121. Holderried TAW, Lang PA, Kim HJ, Cantor H. Genetic disruption of CD8+ Treg activity enhances the immune response to viral infection. *Proc Natl Acad Sci USA* (2013) 110:21089–94. doi: 10.1073/pnas.1320999110
122. Veiga-Parga T, Sehrawat S, Rouse BT. Role of regulatory T cells during virus infection. *Immunol Rev* (2013) 255:182–96. doi: 10.1111/imr.12085
123. Penaloza-MacMaster P, Kamphorst AO, Wieland A, Araki K, Iyer SS, West EE, et al. Interplay between regulatory T cells and PD-1 in modulating T cell exhaustion and viral control during chronic LCMV infection. *J Exp Med* (2014) 211:1905–18. doi: 10.1084/jem.20132577

124. Wong EA, Joslyn L, Grant NL, Klein E, Lin PL, Kirschner DE, et al. Low levels of T cell exhaustion in tuberculous lung granulomas. *Infect Immun* (2018) 86:e00426–18. doi: 10.1128/IAI.00426-18
125. Gigley JP, Bhadra R, Moretto MM, Khan IA. T cell exhaustion in protozoan disease. *Trends Parasitol* (2012) 28:377–84. doi: 10.1016/j.pt.2012.07.001
126. Yi JS, Cox MA, Zajac AJ. T-cell exhaustion: Characteristics, causes and conversion. *Immunology* (2010) 129:474–81. doi: 10.1111/j.1365-2567.2010.03255.x
127. Moskophidis D, Battegay M, Van den Broek M, Laine E, Hoffmann-Rohrer U, Zinkernagel RM. Role of virus and host variables in virus persistence or immunopathological disease caused by a non-cytolytic virus. *J Gen Virol* (1995) 76:381–91. doi: 10.1099/0022-1317-76-2-381
128. Shankar P, Russo M, Harnisch B, Patterson M, Skolnik P, Lieberman J. Impaired function of circulating HIV-specific CD8+ T cells in chronic human immunodeficiency virus infection. *Blood* (2000) 96:3094–101. doi: 10.1182/blood.v96.9.3094
129. Reignat S, Webster GJM, Brown D, Ogg GS, King A, Seneviratne SL, et al. Escaping high viral load exhaustion: CD8 cells with altered tetramer binding in chronic hepatitis B virus infection. *J Exp Med* (2002) 195:1089–101. doi: 10.1084/jem.20011723
130. Sandu I, Cerletti D, Claassen M, Oxenius A. Exhausted CD8+ T cells exhibit low and strongly inhibited TCR signaling during chronic LCMV infection. *Nat Commun* (2020) 11:4454. doi: 10.1038/s41467-020-18256-4
131. Matloubian M, Concepcion RJ, Ahmed R. CD4+ T cells are required to sustain CD8+ cytotoxic T-cell responses during chronic viral infection. *J Virol* (1994) 68:8056–63. doi: 10.1128/jvi.68.12.8056-8063.1994
132. Thomsen AR, Nansen A, Andreasen SO, Wodarz D, Christensen JP. Host factors influencing viral persistence. *Philos Trans R Soc B Biol Sci* (2000) 355:1031–41. doi: 10.1098/rstb.2000.0640
133. Sauce D, Almeida JR, Larsen M, Haro L, Autran B, Freeman GJ, et al. PD-1 expression on human CD8 T cells depends on both state of differentiation and activation status. *AIDS* (2007) 21:2005–13. doi: 10.1097/QAD.0b013e3282eee548
134. Agata Y, Kawasaki A, Nishimura H, Ishida Y, Tsubata T, Yagita H, et al. Expression of the PD-1 antigen on the surface of stimulated mouse T and B lymphocytes. *Int Immunol* (1996) 8:765–72. doi: 10.1093/intimm/8.5.765
135. Walunas TL, Lenschow DJ, Bakker CY, Linsley PS, Freeman GJ, Green JM, et al. CTLA-4 can function as a negative regulator of T cell activation. *Immunity* (1994) 1:405–13. doi: 10.1016/1074-7613(94)90071-X
136. Ahn E, Araki K, Hashimoto M, Li W, Riley JL, Cheung J, et al. Role of PD-1 during effector CD8 T cell differentiation. *Proc Natl Acad Sci USA* (2018) 115:4749–54. doi: 10.1073/pnas.1718217115
137. Baitsch L, Legat A, Barba L, Marraco SA, Rivals JP, Baumgaertner P, et al. Extended co-expression of inhibitory receptors by human CD8 T-cells depending on differentiation, antigen-specificity and anatomical localization. *PloS One* (2012) 7:e30852. doi: 10.1371/journal.pone.0030852
138. Duraiswamy J, Ibegbu CC, Masopust D, Miller JD, Araki K, Doho GH, et al. Phenotype, Function, and Gene Expression Profiles of Programmed Death-1 hi CD8 T Cells in Healthy Human Adults. *J Immunol* (2011) 186:4200–12. doi: 10.4049/jimmunol.1001783
139. Keir ME, Butte MJ, Freeman GJ, Sharpe AH. PD-1 and Its Ligands in Tolerance and Immunity. *Annu Rev Immunol* (2008) 26:677–704. doi: 10.1146/annurev.immunol.26.021607.090331
140. Quigley M, Pereyra F, Nilsson B, Porichis F, Fonseca C, Eichbaum Q, et al. Transcriptional analysis of HIV-specific CD8+ T cells shows that PD-1 inhibits T cell function by upregulating BATF. *Nat Med* (2010) 16:1147–51. doi: 10.1038/nm.2232
141. Zinselmeyer BH, Heydari S, Sacristán C, Nayak D, Cammer M, Herz J, et al. PD-1 promotes immune exhaustion by inducing antiviral T cell motility paralysis. *J Exp Med* (2013) 210:757–74. doi: 10.1084/jem.20121416
142. Johnston RJ, Comps-Agrar L, Hackney J, Yu X, Huseni M, Yang Y, et al. The Immunoreceptor TIGIT Regulates Antitumor and Antiviral CD8+T Cell Effector Function. *Cancer Cell* (2014) 26:923–37. doi: 10.1016/j.ccell.2014.10.018
143. Workman CJ, Dugger KJ, Vignali DAA. Cutting Edge: Molecular Analysis of the Negative Regulatory Function of Lymphocyte Activation Gene-3. *J Immunol* (2002) 169:5392–5. doi: 10.4049/jimmunol.169.10.5392
144. Kuchroo VK, Dardalhon V, Xiao S, Anderson AC. New roles for TIM family members in immune regulation. *Nat Rev Immunol* (2008) 8:577–80. doi: 10.1038/nri2366
145. Jin HT, Anderson AC, Tan WG, West EE, Ha SJ, Araki K, et al. Cooperation of Tim-3 and PD-1 in CD8 T-cell exhaustion during chronic viral infection. *Proc Natl Acad Sci USA* (2010) 107:14733–8. doi: 10.1073/pnas.1009731107
146. Chen JY, Feeney ER, Chung RT. HCV and HIV co-infection: Mechanisms and management. *Nat Rev Gastroenterol Hepatol* (2014) 11:362–71. doi: 10.1038/nrgastro.2014.17
147. Sansom DM. CD28, CTLA-4 and their ligands: Who does what and to whom? *Immunology* (2000) 101:169–77. doi: 10.1046/j.1365-2567.2000.00121.x
148. Qureshi OS, Zheng Y, Nakamura K, Attridge K, Manzotti C, Schmidt EM, et al. Trans-endocytosis of CD80 and CD86: A molecular basis for thecell-extrinsic function of CTLA-4. *Science* (2011) (80-):600–3. doi: 10.1126/science.1202947
149. Matsuzaki J, Gnjatic S, Mhawech-Fauceglia P, Beck A, Miller A, Tsuji T, et al. Tumor-infiltrating NY-ESO-1-specific CD8+ T cells are negatively regulated by LAG-3 and PD-1 in human ovarian cancer. *Proc Natl Acad Sci USA* (2010) 107:7875–80. doi: 10.1073/pnas.1003345107
150. Fourcade J, Sun Z, Benallaoua M, Guillaume P, Luescher IF, Sander C, et al. Upregulation of Tim-3 and PD-1 expression is associated with tumor antigen-specific CD8+ T cell dysfunction in melanoma patients. *J Exp Med* (2010) 72:917–27. doi: 10.1084/jem.20100637
151. Woo SR, Turnis ME, Goldberg MV, Bankoti J, Selby M, Nirschl CJ, et al. Immune inhibitory molecules LAG-3 and PD-1 synergistically regulate T-cell function to promote tumoral immune escape. *Cancer Res* (2012) 121:2350–60. doi: 10.1158/0008-5472.CAN-11-1620
152. Baitsch L, Baumgaertner P, Devêvre E, Raghav SK, Legat A, Barba L, et al. Exhaustion of tumor-specific CD8+ T cells in metastases from melanoma patients. *J Clin Invest* (2011) 6:209–17. doi: 10.1172/JCI46102
153. Bianchi G, Borgonovo G, Pistoia V, Raffaghello L. Immunosuppressive cells and tumour microenvironment: Focus on mesenchymal stem cells and myeloid derived suppressor cells. *Histol Histopathol* (2011) 26:941–51. doi: 10.14670/HH-26.941
154. Kouidhi S, Elgaaied AB, Chouaib S. Impact of Metabolism on T-Cell Differentiation and Function and Cross Talk with Tumor Microenvironment. *Front Immunol* (2017) 8:270. doi: 10.3389/fimmu.2017.00270
155. Leone RD, Powell JD. Metabolism of immune cells in cancer. *Nat Rev Cancer* (2020) 20:516–31. doi: 10.1038/s41568-020-0273-y
156. Kumar V, Donthireddy L, Marvel D, Condamine T, Wang F, Lavilla-Alonso S, et al. Cancer-Associated Fibroblasts Neutralize the Anti-tumor Effect of CSF1 Receptor Blockade by Inducing PMN-MDSC Infiltration of Tumors. *Cancer Cell* (2017) 32:654–68.e5. doi: 10.1016/j.ccell.2017.10.005
157. Ugel S, De Sanctis F, Mandruzzato S, Bronte V. Tumor-induced myeloid deviation: when myeloid-derived suppressor cells meet tumor-associated macrophages. *J Clin Invest* (2015) 125:3365–76. doi: 10.1172/JCI80006
158. Jiang L, Fang X, Wang H, Li D, Wang X. Ovarian Cancer-Intrinsic Fatty Acid Synthase Prevents Anti-tumor Immunity by Disrupting Tumor-Infiltrating Dendritic Cells. *Front Immunol* (2018) 9:2927. doi: 10.3389/fimmu.2018.02927
159. Gajewski TF, Schreiber H, Fu Y-X. Innate and adaptive immune cells in the tumor microenvironment. *Nat Immunol* (2013) 14:1014–22. doi: 10.1038/ni.2703
160. Baitsch L, Fuertes-Marraco SA, Legat A, Meyer C, Speiser DE. The three main stumbling blocks for anticancer T cells. *Trends Immunol* (2012) 33(7):364–72. doi: 10.1016/j.it.2012.02.006
161. Riaz N, Havel JJ, Makarov V, Desrichard A, Urba WJ, Sims JS, et al. Tumor and Microenvironment Evolution during Immunotherapy with Nivolumab. *Cell* (2017) 171:934–49.e16. doi: 10.1016/j.cell.2017.09.028
162. O'Donnell JS, Teng MWL, Smyth MJ. Cancer immunoediting and resistance to T cell-based immunotherapy. *Nat Rev Clin Oncol* (2019) 16:151–67. doi: 10.1038/s41571-018-0142-8
163. Dunn GP, Old LJ, Schreiber RD. The three Es of cancer immunoediting. *Annu Rev Immunol* (2004) 22:329–60. doi: 10.1146/annurev.immunol.22.012703.104803

164. Smyth MJ, Dunn GP, Schreiber RD. Cancer Immunosurveillance and Immunoediting: The Roles of Immunity in Suppressing Tumor Development and Shaping Tumor Immunogenicity. *Adv Immunol* (2006) 90:1–50. doi: 10.1016/S0065-2776(06)90001-7
165. Vesely MD, Kershaw MH, Schreiber RD, Smyth MJ. Natural innate and adaptive immunity to cancer. *Annu Rev Immunol* (2011) 29:235–71. doi: 10.1146/annurev-immunol-031210-101324
166. Dunn GP, Sheehan KCF, Old LJ, Schreiber RD. IFN unresponsiveness in LNCaP cells due to the lack of JAK1 gene expression. *Cancer Res* (2005) 65:3447–53. doi: 10.1158/0008-5472.CAN-04-4316
167. Takeda K, Nakayama M, Hayakawa Y, Kojima Y, Ikeda H, Imai N, et al. IFN-γ is required for cytotoxic T cell-dependent cancer genome immunoediting. *Nat Commun* (2017) 8:14607. doi: 10.1038/ncomms14607
168. Mandai M, Hamanishi J, Abiko K, Matsumura N, Baba T, Konishi I. Dual Faces of IFNγ in Cancer Progression: A Role of PD-L1 Induction in the Determination of Pro- and Antitumor Immunity. *Clin Cancer Res an Off J Am Assoc Cancer Res* (2016) 22:2329–34. doi: 10.1158/1078-0432.CCR-16-0224
169. Chang C-C, Pirozzi G, Wen S-H, Chung I-H, Chiu B-L, Errico S, et al. Multiple structural and epigenetic defects in the human leukocyte antigen class I antigen presentation pathway in a recurrent metastatic melanoma following immunotherapy. *J Biol Chem* (2015) 290:26562–75. doi: 10.1074/jbc.M115.676130
170. Sharma P, Hu-Lieskovan S, Wargo JA, Ribas A. Primary, Adaptive, and Acquired Resistance to Cancer Immunotherapy. *Cell* (2017) 168:707–23. doi: 10.1016/j.cell.2017.01.017
171. Ochsenbein AF, Klenerman P, Karrer U, Ludewig B, Pericin M, Hengartner H, et al. Immune surveillance against a solid tumor fails because of immunological ignorance. *Proc Natl Acad Sci USA* (1999) 96:2233–8. doi: 10.1073/pnas.96.5.2233
172. Dustin ML. The immunological synapse. *Cancer Immunol Res* (2014) 2 (11):1023–33. doi: 10.1158/2326-6066.CIR-14-0161
173. Razvag Y, Neve-Oz Y, Sajman J, Reches M, Sherman E. Nanoscale kinetic segregation of TCR and CD45 in engaged microvilli facilitates early T cell activation. *Nat Commun* (2018) 9(1):732. doi: 10.1038/s41467-018-03127-w
174. Jung Y, Riven I, Feigelson SW, Kartvelishvily E, Tohya K, Miyasaka M, et al. Three-dimensional localization of T-cell receptors in relation to microvilli using a combination of superresolution microscopies. *Proc Natl Acad Sci USA* (2016) 113(40):E5916–24. doi: 10.1073/pnas.1605399113
175. Ghosh S, Di Bartolo V, Tubul L, Shimoni E, Kartvelishvily E, Dadosh T, et al. ERM-Dependent Assembly of T Cell Receptor Signaling and Co-stimulatory Molecules on Microvilli prior to Activation. *Cell Rep* (2020) 30(10):3434–47.e6. doi: 10.1016/j.celrep.2020.02.069
176. Welch MD, Mullins RD. Cellular control of actin nucleation. *Annu Rev Cell Dev Biol* (2002) 18:247–88. doi: 10.1146/annurev.cellbio.18.040202.112133
177. Mattila PK, Lappalainen P. Filopodia: Molecular architecture and cellular functions. *Nat Rev Mol Cell Biol* (2008) 9(6):446–54. doi: 10.1038/nrm2406
178. Kumari S, Curado S, Mayya V, Dustin ML. T cell antigen receptor activation and actin cytoskeleton remodeling. *Biochim Biophys Acta - Biomembr* (2014) 1838(2):546–56. doi: 10.1016/j.bbamem.2013.05.004
179. Husson J, Chemin K, Bohineust A, Hivroz C, Henry N. Force generation upon T cell receptor engagement. *PloS One* (2011) 6:e19680. doi: 10.1371/journal.pone.0019680
180. Hui KL, Balagopalan L, Samelson LE, Upadhyaya A. Cytoskeletal forces during signaling activation in Jurkat T-cells. *Mol Biol Cell* (2015) 26:685–95. doi: 10.1091/mbc.E14-03-0830
181. Dustin ML. What counts in the immunological synapse? *Mol Cell* (2014) 54 (2):255–62. doi: 10.1016/j.molcel.2014.04.001
182. Dustin ML, Long EO. Cytotoxic immunological synapses. *Immunol Rev* (2010) 235:24–34. doi: 10.1111/j.0105-2896.2010.00904.x
183. Yokosuka T, Sakata-Sogawa K, Kobayashi W, Hiroshima M, Hashimoto-Tane A, Tokunaga M, et al. Newly generated T cell receptor microclusters initiate and sustain T cell activation by recruitment of Zap70 and SLP-76. *Nat Immunol* (2005) 6:1253–62. doi: 10.1038/ni1272
184. Davenport AJ, Cross RS, Watson KA, Liao Y, Shi W, Prince HM, et al. Chimeric antigen receptor T cells form nonclassical and potent immune synapses driving rapid cytotoxicity. *Proc Natl Acad Sci USA* (2018) 115: E2068–76. doi: 10.1073/pnas.1716266115
185. Varma R, Campi G, Yokosuka T, Saito T, Dustin ML. T Cell Receptor-Proximal Signals Are Sustained in Peripheral Microclusters and Terminated in the Central Supramolecular Activation Cluster. *Immunity* (2006) 25:117–27. doi: 10.1016/j.immuni.2006.04.010
186. Mariuzza RA, Agnihotri P, Orban J. The structural basis of T-cell receptor (TCR) activation: An enduring enigma. *J Biol Chem* (2020) 295:914–25. doi: 10.1074/jbc.REV119.009411
187. Acuto O, Cantrell D. T Cell Activation and the Cytoskeleton. *Annu Rev Immunol* (2000) 18:165–84. doi: 10.1146/annurev.immunol.18.1.165
188. Dupré L, Houmadi R, Tang C, Rey-Barroso J. T lymphocyte migration: An action movie starring the actin and associated actors. *Front Immunol* (2015) 6:586. doi: 10.3389/fimmu.2015.00586
189. Ksionda O, Saveliev A, Köchl R, Rapley J, Faroudi M, Smith-Garvin JE, et al. Mechanism and function of Vav1 localisation in TCR signalling. *J Cell Sci* (2012) 125(Pt 22):5302–14. doi: 10.1242/jcs.105148
190. Helou YA, Petrashen AP, Salomon AR. Vav1 Regulates T-Cell Activation through a Feedback Mechanism and Crosstalk between the T-Cell Receptor and CD28. *J Proteome Res* (2015) 14(7):2963–75. doi: 10.1021/acs.jproteome.5b00340
191. Reynolds LF, Smyth LA, Norton T, Freshney N, Downward J, Kioussis D, et al. Vav1 transduces T cell receptor signals to the activation ofphospholipase C-γ1 via phosphoinositide 3-kinase-dependent and -independentpathways. *J Exp Med* (2002) 195(9):1103–14. doi: 10.1084/jem.20011663
192. Costello PS, Walters AE, Mee PJ, Turner M, Reynolds LF, Prisco A, et al. The Rho-family GTP exchange factor Vav is a critical transducer of Tcell receptor signals to the calcium, ERK, and NF-κB pathways. *Proc Natl Acad Sci USA* (1999) 96:3035–40. doi: 10.1073/pnas.96.6.3035
193. Zeng R, Cannon JL, Abraham RT, Way M, Billadeau DD, Bubeck-Wardenberg J, et al. SLP-76 Coordinates Nck-Dependent Wiskott-Aldrich Syndrome Protein Recruitment with Vav-1/Cdc42-Dependent Wiskott-Aldrich Syndrome Protein Activation at the T Cell-APCContact Site. *J Immunol* (2003) 171:1360–8. doi: 10.4049/jimmunol.171.3.1360
194. Zipfel PA, Bunnell SC, Witherow DS, Gu JJ, Chislock EM, Ring C, et al. Role for the Abi/Wave protein complex in T cell receptor-mediatedproliferation and cytoskeletal remodeling. *Curr Biol* (2006) 16:35–46. doi: 10.1016/j.cub.2005.12.024
195. Nolz JC, Gomez TS, Zhu P, Li S, Medeiros RB, Shimizu Y, et al. The WAVE2 complex regulates actin cytoskeletal reorganization andCRAC-mediated calcium entry during T cell activation. *Curr Biol* (2006) 16:24–34. doi: 10.1016/j.cub.2005.11.036
196. Berke G. The CTL's kiss of death. *Cell* (1995) 81:9–12. doi: 10.1016/0092-8674(95)90365-8
197. Anikeeva N, Somersalo K, Sims TN, Thomas VK, Dustin ML, Sykulev Y. Distinct role of lymphocyte function-associated antigen-1 inmediating effective cytolytic activity by cytotoxic T lymphocytes. *Proc Natl Acad Sci USA* (2005) 102:6437–42. doi: 10.1073/pnas.0502467102
198. Beal AM, Anikeeva N, Varma R, Cameron TO, Norris PJ, Dustin ML, et al. Protein Kinase Cθ Regulates Stability of the Peripheral Adhesion Ring Junction and Contributes to the Sensitivity of Target Cell Lysis by CTL. *J Immunol* (2008) 181:4815–24. doi: 10.4049/jimmunol.181.7.4815
199. Mentlik AN, Sanborn KB, Holzbaur EL, Orange JS. Rapid lytic granule convergence to the MTOC in natural killer cellsis dependent on dynein but not cytolytic commitment. *Mol Biol Cell* (2010) 21:2241–56. doi: 10.1091/mbc.E09-11-0930
200. Pores-Fernando AT, Zweifach A. Calcium influx and signaling in cytotoxic T-lymphocyte lytic granuleexocytosis. *Immunol Rev* (2009) 231:160–73. doi: 10.1111/j.1600-065X.2009.00809.x
201. Wiedemann A, Depoil D, Faroudi M, Valitutti S. Cytotoxic T lymphocytes kill multiple targets simultaneously viaspatiotemporal uncoupling of lytic and stimulatory synapses. *Proc Natl Acad Sci USA* (2006) 103:10985–90. doi: 10.1073/pnas.0600651103
202. Kearney CJ, Brennan AJ, Darcy PK, Oliaro J. The role of the immunological synapse formed by cytotoxiclymphocytes in immunodeficiency and anti-tumor immunity. *Crit Rev Immunol* (2015) 35:325–47. doi: 10.1615/CritRevImmunol.2015014417
203. Kallikourdis M, Viola A, Benvenuti F. Human immunodeficiencies related to defective APC/T cellinteraction. *Front Immunol* (2015) 6:433. doi: 10.3389/fimmu.2015.00433

204. Hanna S, Etzioni A. Leukocyte adhesion deficiencies. *Ann N Y Acad Sci* (2012) 27:101–16. doi: 10.1111/j.1749-6632.2011.06389.x
205. Krensky AM, Mentzer SJ, Clayberger C, Anderson DC, Schmalstieg FC, Burakoff SJ, et al. Heritable lymphocyte function-associated antigen-1 deficiency: Abnormalities of cytotoxicity and proliferation associated with abnormal expression of LFA-1. *J Immunol* (1985) 135:3102–8.
206. Orange JS, Ramesh N, Remold-O'Donnell E, Sasahara Y, Koopman L, Byrne M, et al. Wiskott-Aldrich syndrome protein is required for NK cellcytotoxicity and colocalizes with actin to NK cell-activating immunologic synapses. *Proc Natl Acad Sci USA* (2002) 99:11351–6. doi: 10.1073/pnas.162376099
207. Menotti M, Ambrogio C, Cheong TC, Pighi C, Mota I, Cassel SH, et al. Wiskott–Aldrich syndrome protein (WASP) is a tumor suppressorin T cell lymphoma. *Nat Med* (2019) 25:130–40. doi: 10.1038/s41591-018-0262-9
208. Catucci M, Zanoni I, Draghici E, Bosticardo M, Castiello MC, Venturini M, et al. Wiskott-Aldrich syndrome protein deficiency in natural killer anddendritic cells affects antitumor immunity. *Eur J Immunol* (2014) 44:1039–45. doi: 10.1002/eji.201343935
209. Ishihara D, Dovas A, Hernandez L, Pozzuto M, Wyckoff J, Segall JE, et al. Wiskott-Aldrich syndrome protein regulates leukocyte-dependentbreast cancer metastasis. *Cell Rep* (2013) 4:429–36. doi: 10.1016/j.celrep.2013.07.007
210. Kritikou JS, Dahlberg CIM, Baptista MAP, Wagner AK, Banerjee PP, Gwalani LA, et al. IL-2 in the tumor microenvironment is necessary for Wiskott-Aldrichsyndrome protein deficient NK cells to respond to tumors in vivo article. *Sci Rep* (2016) 6:30636. doi: 10.1038/srep30636
211. Orange JS, Roy-Ghanta S, Mace EM, Maru S, Rak GD, Sanborn KB, et al. IL-2 induces a WAVE2-dependent pathway for actin reorganization thatenables WASp-independent human NK cell function. *J Clin Invest* (2011) 121:1535–48. doi: 10.1172/JCI44862
212. Klevorn LE, Berrien-Elliott MM, Yuan J, Kuehm LM, Felock GD, Crowe SA, et al. Rescue of tolerant CD8+ T cells during cancer immunotherapy withIL2: Antibody complexes. *Cancer Immunol Res* (2016) 4:1016–26. doi: 10.1158/2326-6066.CIR-16-0159
213. Moulding DA, Record J, Malinova D, Thrasher AJ. Actin cytoskeletal defects in immunodeficiency. *Immunol Rev* (2013) 256:282–99. doi: 10.1111/imr.12114
214. Dupont L, Reeves MB. Cytomegalovirus latency and reactivation: recent insights into anage old problem. *Rev Med Virol* (2016) 26:75–89. doi: 10.1002/rmv.1862
215. Brisse E, Wouters CH, Andrei G, Matthys P. How viruses contribute to the pathogenesis of hemophagocyticlymphohistiocytosis. *Front Immunol* (2017) 8:1102. doi: 10.3389/fimmu.2017.01102
216. Ramsay AG, Clear AJ, Kelly G, Fatah R, Matthews J, MacDougall F, et al. Follicular lymphoma cells induce T-cell immunologic synapsedysfunction that can be repaired with lenalidomide: Implications for the tumor microenvironment and immunotherapy. *Blood* (2009) 114:4713–20. doi: 10.1182/blood-2009-04-217687
217. Ramsay AG, Clear AJ, Fatah R, Gribben JG. Multiple inhibitory ligands induce impaired T-cell immunologicsynapse function in chronic lymphocytic leukemia that can be blocked with lenalidomide: Establishinga reversible immune evasion mechanism in human cancer. *Blood* (2012) 120(7):1412–21. doi: 10.1182/blood-2012-02-411678
218. Koneru M, Schaer D, Monu N, Ayala A, Frey AB. Defective Proximal TCR Signaling Inhibits CD8 + Tumor-Infiltrating Lymphocyte Lytic Function. *J Immunol* (2005)174(4):1830–40. doi: 10.4049/jimmunol.174.4.1830
219. Monu N, Frey AB. Suppression of proximal T cell receptor signaling and lytic functionin CD8+ tumor-infiltrating T cells. *Cancer Res* (2007) 67(23):11447–54. doi: 10.1158/0008-5472.CAN-07-1441
220. Thoulouze MI, Sol-Foulon N, Blanchet F, Dautry-Varsat A, Schwartz O, Alcover A. Human Immunodeficiency Virus Type-1 Infection Impairs the Formationof the Immunological Synapse. *Immunity* (2006) 24(5):547–61. doi: 10.1016/j.immuni.2006.02.016
221. Buffalo CZ, Iwamoto Y, Hurley JH, Ren X. How HIV Nef Proteins Hijack Membrane Traffic To PromoteInfection. *J Virol* (2019) 93(24):e01322–19. doi: 10.1128/jvi.01322-19
222. Haller C, Rauch S, Michel N, Hannemann S, Lehmann MJ, Keppler OT, et al. The HIV-1 pathogenicity factor Nef interferes with maturation ofstimulatory T-lymphocyte contacts by modulation of N-Wasp activity. *J Biol Chem* (2006) 281(28):19618–30. doi: 10.1074/jbc.M513802200
223. Ott M, Emiliani S, Van Lint C, Herbein G, Lovett J, Chirmule N, et al. Immune hyperactivation of HIV-1-infected T cells mediated by Tat andthe CD28 pathway. *Science* (1997) (80-):1481–5. doi: 10.1126/science.275.5305.1481
224. Haas A, Zimmermann K, Oxenius A. Antigen-Dependent and -Independent Mechanisms of T and B CellHyperactivation during Chronic HIV-1 Infection. *J Virol* (2011) 85(23):12102–13. doi: 10.1128/jvi.05607-11
225. Fortin JF, Barat C, Beauséjour Y, Barbeau B, Tremblay MJ. Hyper-responsiveness to stimulation of human immunodeficiencyvirus-infected CD4+ T cells requires Nef and Tat virus gene products and results from higher NFAT, NF-κB, and AP-1 induction. *J Biol Chem* (2004) 279 (38):39520–31. doi: 10.1074/jbc.M407477200
226. Manninen A, Huotari P, Hiipakka M, Renkema GH, Saksela K. Activation of NFAT-Dependent Gene Expression by Nef: Conservationamong Divergent Nef Alleles, Dependence on SH3 Binding and Membrane Association, and Cooperationwith Protein Kinase C-θ. *J Virol* (2001) 75(6):3034–7. doi: 10.1128/jvi.75.6.3034-3037.2001
227. Feng Y, Reinherz EL, Lang MJ. αβ T Cell Receptor Mechanosensing Forces out Serial Engagement. *Trends Immunol* (2018) 39:596–609. doi: 10.1016/j.it.2018.05.005
228. Judokusumo E, Tabdanov E, Kumari S, Dustin ML, Kam LC. Mechanosensing in T Lymphocyte Activation. *Biophys J* (2012) 102:L5–7. doi: 10.1016/j.bpj.2011.12.011
229. Orr AW, Helmke BP, Blackman BR, Schwartz MA. Mechanisms of mechanotransduction. *DevCell* (2006) 10(1):11–20. doi: 10.1016/j.devcel.2005.12.006
230. Minguet S, Swamy M, Alarcón B, Luescher IF, Schamel WWA. Full Activation of the T Cell Receptor Requires Both Clustering and Conformational Changes at CD3. *Immunity* (2007) 26:43–54. doi: 10.1016/j.immuni.2006.10.019
231. Li L, Guo X, Shi X, Li C, Wu W, Yan C, et al. Ionic CD3–Lck interaction regulates the initiation of T-cell receptor signaling. *Proc Natl Acad Sci* (2017) 114:E5891–9. doi: 10.1073/pnas.1701990114
232. Liu CSC, Raychaudhuri D, Paul B, Chakrabarty Y, Ghosh AR, Rahaman O, et al. Cutting Edge: Piezo1 Mechanosensors Optimize Human T Cell Activation. *J Immunol* (2018) 200:1255–60. doi: 10.4049/jimmunol.1701118
233. Malissen B, Bongrand P. Early T cell activation: integrating biochemical, structural, and biophysical cues. *Annu Rev Immunol* (2015) 33:539–61. doi: 10.1146/annurev-immunol-032414-112158
234. Li Y-C, Chen B-M, Wu P-C, Cheng T-L, Kao L-S, Tao M-H, et al. Cutting Edge: Mechanical Forces Acting on T Cells Immobilized via the TCR Complex Can Trigger TCR Signaling. *J Immunol* (2010) 184:5959–63. doi: 10.4049/jimmunol.0900775
235. Chen W, Zhu C. Mechanical regulation of T-cell functions. *Immunol Rev* (2013) 256:160–76. doi: 10.1111/imr.12122
236. Kim ST, Takeuchi K, Sun Z-YJ, Touma M, Castro CE, Fahmy A, et al. The alphabeta T cell receptor is an anisotropic mechanosensor. *J Biol Chem* (2009) 284:31028–37. doi: 10.1074/jbc.M109.052712
237. Liu B, Chen W, Evavold BD, Zhu C. Accumulation of dynamic catch bonds between TCR and agonistpeptide-MHC triggers T cell signaling. *Cell* (2014) 157(2):357–368. doi: 10.1016/j.cell.2014.02.053
238. Hong J, Persaud SP, Horvath S, Allen PM, Evavold BD, Zhu C. Force-Regulated In Situ TCR-Peptide-Bound MHC Class II Kinetics Determine Functions of CD4+ T Cells. *J Immunol* (2015) 195:3557–64. doi: 10.4049/jimmunol.1501407
239. O'Connor RS, Hao X, Shen K, Bashour K, Akimova T, Hancock WW, et al. Substrate rigidity regulates human T cell activation and proliferation. *J Immunol* (2012) 189:1330–9. doi: 10.4049/jimmunol.1102757
240. Saitakis M, Dogniaux S, Goudot C, Bufi N, Asnacios S, Maurin M, et al. Different TCR-induced T lymphocyte responses are potentiated by stiffness with variable sensitivity. *Elife* (2017) 6:e23190. doi: 10.7554/eLife.23190
241. Jin W, Tamzalit F, Chaudhuri PK, Black CT, Huse M, Kam LC. T cell activation and immune synapse organization respond to the microscale mechanics of structured surfaces. *Proc Natl Acad Sci USA* (2019) 116:19835–40. doi: 10.1073/pnas.1906986116

242. Basu R, Whitlock BM, Husson J, Le Floc'h A, Jin W, Oyler-Yaniv A, et al. Cytotoxic T Cells Use Mechanical Force to Potentiate Target Cell Killing. *Cell* (2016) 165:100–10. doi: 10.1016/j.cell.2016.01.021
243. Hickey JW, Dong Y, Chung JW, Salathe SF, Pruitt HC, Li X, et al. Engineering an Artificial T-Cell Stimulating Matrix for Immunotherapy. *Adv Mater* (2019) 31:e1807359. doi: 10.1002/adma.201807359
244. Aramesh M, Stoycheva D, Raaz L, Klotzsch E. Engineering T-cell activation for immunotherapy by mechanical forces. *Curr Opin BioMed Eng* (2019) 10:134–41. doi: 10.1016/j.cobme.2019.05.004
245. Dembo M, Torney DC, Saxman K, Hammer D. The reaction-limited kinetics of membrane-to-surface adhesion and detachment. *Proc R Soc London Ser B Biol Sci* (1988) 234:55–83. doi: 10.1098/rspb.1988.0038
246. Lee C, Lou J, Wen K, McKane M, Eskin SG, Ono S, et al. Actin depolymerization under force is governed by lysine 113:glutamic acid 195-mediated catch-slip bonds. *Proc Natl Acad Sci USA* (2013) 110:5022–7. doi: 10.1073/pnas.1218407110
247. Sundd P, Pospieszalska MK, Cheung LS-L, Konstantopoulos K, Ley K. Biomechanics of leukocyte rolling. *Biorheology* (2011) 48:1–35. doi: 10.3233/BIR-2011-0579
248. Das DK, Feng Y, Mallis RJ, Li X, Keskin DB, Hussey RE, et al. Force-dependent transition in the T-cell receptor β-subunit allosterically regulates peptide discrimination and pMHC bond lifetime. *Proc Natl Acad Sci USA* (2015) 112:1517–22. doi: 10.1073/pnas.1424829112
249. Kolawole EM, Andargachew R, Liu B, Jacobs JR, Evavold BD. 2D Kinetic Analysis of TCR and CD8 Coreceptor for LCMV GP33 Epitopes. *Front Immunol* (2018) 9:2348. doi: 10.3389/fimmu.2018.02348
250. Sibener LV, Fernandes RA, Kolawole EM, Carbone CB, Liu F, McAffee D, et al. Isolation of a Structural Mechanism for Uncoupling T Cell Receptor Signaling from Peptide-MHC Binding. *Cell* (2018) 174:672–87.e27. doi: 10.1016/j.cell.2018.06.017
251. Liu B, Chen W, Natarajan K, Li Z, Margulies DH, Zhu C. The cellular environment regulates in situ kinetics of T-cell receptor interaction with peptide major histocompatibility complex. *Eur J Immunol* (2015) 45:2099–110. doi: 10.1002/eji.201445358
252. Lee MS, Glassman CR, Deshpande NR, Badgandi HB, Parrish HL, Uttamapinant C, et al. A Mechanical Switch Couples T Cell Receptor Triggering to theCytoplasmic Juxtamembrane Regions of CD3ζζ. *Immunity* (2015) 43(2):227–39. doi: 10.1016/j.immuni.2015.06.018
253. Van Der Merwe PA, Dushek O. Mechanisms for T cell receptor triggering.*Nat Rev Immunol* (2011) 11(1):47–55. doi: 10.1038/nri2887
254. Chang VT, Fernandes RA, Ganzinger KA, Lee SF, Siebold C, McColl J, et al. Initiation of T cell signaling by CD45 segregation at "closecontacts." *Nat Immunol* (2016) 17(5):574–82. doi: 10.1038/ni.3392
255. James JR, Vale RD. Biophysical mechanism of T-cell receptor triggering in areconstituted system. *Nature* (2012) 487(7405):647–9. doi: 10.1038/nature11220
256. Higuchi A, Ling QD, Chang Y, Hsu ST, Umezawa A. Physical cues of biomaterials guide stem cell differentiationfate. *Chem Rev* (2013)113 (5):3297–328. doi: 10.1021/cr300426x
257. Yang Y, Wang K, Gu X, Leong KW. Biophysical Regulation of Cell Behavior —Cross Talk betweenSubstrate Stiffness and Nanotopography. *Engineering* (2017) 3(1):36–54. doi: 10.1016/J.ENG.2017.01.014
258. Tee SY, Fu J, Chen CS, Janmey PA. Cell shape and substrate rigidity both regulate cellstiffness. *Biophys J* (2011) 100(5):L25–7. doi: 10.1016/j.bpj.2010.12.3744
259. Uffmann K, Maderwald S, Ajaj W, Galban CG, Mateiescu S, Quick HH, et al. In vivo elasticity measurements of extremity skeletal muscle with MRelastography. *NMR BioMed* (2004) 17(4):181–90. doi: 10.1002/nbm.887
260. Gasiorowski JZ, Murphy CJ, Nealey PF. Biophysical cues and cell behavior: The big impact of littlethings. *Annu Rev BioMed Eng* (2013) 15:155–76. doi: 10.1146/annurev-bioeng-071811-150021
261. Friedl P, Alexander S. Cancer invasion and the microenvironment: Plasticity andreciprocity. *Cell* (2011)147(5):992–1009. doi: 10.1016/j.cell.2011.11.016
262. Tilghman RW, Cowan CR, Mih JD, Koryakina Y, Gioeli D, Slack-Davis JK, et al. Matrix rigidity regulates cancer cell growth and cellularphenotype. *PloS One* (2010) 5(9):e12905. doi: 10.1371/journal.pone.0012905
263. Handorf AM, Zhou Y, Halanski MA, Li WJ. Tissue stiffness dictates development, homeostasis, and diseaseprogression. *Organogenesis* (2015) 11(1):1–15. doi: 10.1080/15476278.2015.1019687
264. Wullkopf L, West AKV, Leijnse N, Cox TR, Madsen CD, Oddershede LB, et al. Cancer cells' ability to mechanically adjust to extracellularmatrix stiffness correlates with their invasive potential. *Mol Biol Cell* (2018) 29 (20):2378–85. doi: 10.1091/mbc.E18-05-0319
265. Hynes RO. Integrins: Bidirectional, allosteric signalingmachines. *Cell* (2002) 110(6):673–87. doi: 10.1016/S0092-8674(02)00971-6
266. Naba A, Clauser KR, Lamar JM, Carr SA, Hynes RO. Extracellular matrix signatures of human mammary carcinoma identifynovel metastasis promoters. *Elife* (2014) 3:e01308. doi: 10.7554/eLife.01308
267. Henke E, Nandigama R, Ergün S. Extracellular Matrix in the Tumor Microenvironment and Its Impact onCancer Therapy. *Front Mol Biosci* (2020) 6:160. doi: 10.3389/fmolb.2019.00160
268. Merika EE, Syrigos KN, Saif MW. Desmoplasia in pancreatic cancer. Can we fight it? *Gastroenterol Res Pract* (2012) 2012:781765. doi: 10.1155/2012/781765
269. Walker RA. The complexities of breast cancer desmoplasia. *Breast Cancer Res* (2001) 3(3):143–5. doi: 10.1186/bcr287
270. Levental KR, Yu H, Kass L, Lakins JN, Egeblad M, Erler JT, et al. Matrix Crosslinking Forces Tumor Progression by Enhancing IntegrinSignaling. *Cell* (2009) 139(5):891–906. doi: 10.1016/j.cell.2009.10.027
271. Hartmann N, Giese NA, Giese T, Poschke I, Offringa R, Werner J, et al. Prevailing role of contact guidance in intrastromal T-cell trappingin human pancreatic cancer. *Clin Cancer Res* (2014) 20(13):3422–33. doi: 10.1158/1078-0432.CCR-13-2972
272. Salmon H, Franciszkiewicz K, Damotte D, Dieu-Nosjean MC, Validire P, Trautmann A, et al. Matrix architecture defines the preferential localization andmigration of T cells into the stroma of human lung tumors. *J Clin Invest* (2012) 122(3):899–910. doi: 10.1172/JCI45817
273. Kuczek DE, Larsen AMH, Thorseth ML, Carretta M, Kalvisa A, Siersbæk MS, et al. Collagen density regulates the activity of tumor-infiltrating Tcells. *J Immunother Cancer* (2019) 7(1):68. doi: 10.1186/s40425-019-0556-6
274. Han YL, Pegoraro AF, Li H, Li K, Yuan Y, Xu G, et al. Cell swelling, softening and invasion in a three-dimensional breastcancer model. *Nat Phys* (2020) 16 (1):101–8. doi: 10.1038/s41567-019-0680-8
275. Stone JD, Chervin AS, Kranz DM. T-cell receptor binding affinities and kinetics: impact on T-cellactivity and specificity. *Immunology* (2009) 126 (2):165–76. doi: 10.1111/j.1365-2567.2008.03015.x
276. Zhong S, Malecek K, Johnson LA, Yu Z, De Miera EVS, Darvishian F, et al. T-cell receptor affinity and avidity defines antitumor response andautoimmunity in T-cell immunotherapy. *Proc Natl Acad Sci USA* (2013) 110(17):6973–8. doi: 10.1073/pnas.1221609110
277. Hu Z, Zhu L, Wang J, Wan Y, Yuan S, Chen J, et al. Immune Signature of Enhanced Functional Avidity CD8+ T Cells in vivoInduced by Vaccinia Vectored Vaccine. *Sci Rep* (2017) 7:41558. doi: 10.1038/srep41558
278. Turner SJ, Doherty PC, McCluskey J, Rossjohn J. Structural determinants of T-cell receptor bias inimmunity. *Nat Rev Immunol* (2006) 6(12):883–94. doi: 10.1038/nri1977
279. Sabatino JJ, Huang J, Zhu C, Evavold BD. High prevalence of low affinity peptide-MHC II tetramer-negativeeffectors during polyclonal CD4+ T cell responses. *J Exp Med* (2011) 208(1):81–90. doi: 10.1084/jem.20101574
280. Martinez RJ, Andargachew R, Martinez HA, Evavold BD. Low-affinity CD4+ T cells are major responders in the primary immuneresponse. *Nat Commun* (2016) 7:13848. doi: 10.1038/ncomms13848
281. Savage PA, Boniface JJ, Davis MM. A kinetic basis for T cell receptor repertoire selection during animmune response. *Immunity* (1999) 10 (4):485–92. doi: 10.1016/S1074-7613(00)80048-5
282. Malherbe L, Hausl C, Teyton L, McHeyzer-Williams MG. Clonal selection of helper T cells is determined by an affinitythreshold with no further skewing of TCR binding properties.*Immunity* (2004) 21(5):6697–79. doi: 10.1016/j.immuni.2004.09.008
283. Busch DH, Pamer EG. T cell affinity maturation by selective expansion duringinfection. *J Exp Med* (1999) 189(4):701–10. doi: 10.1084/jem.189.4.701
284. Kedl RM, Kappler JW, Marrack P. Epitope dominance, competition and T cell affinitymaturation. *Curr Opin Immunol* (2003) 15(1):1207–7. doi: 10.1016/S0952-7915(02)00009-2
285. Lichterfeld M, Yu XG, Mui SK, Williams KL, Trocha A, Brockman MA, et al. Selective Depletion of High-Avidity Human Immunodeficiency VirusType 1

(HIV-1)-Specific CD8+ T Cells after Early HIV-1 Infection. *J Virol* (2007) 81 (8):4199–214. doi: 10.1128/jvi.01388-06
286. Rossjohn J, Gras S, Miles JJ, Turner SJ, Godfrey DI, McCluskey J. T Cell Antigen Receptor Recognition of Antigen-PresentingMolecules. *Annu Rev Immunol* (2015) 33:169–200. doi: 10.1146/annurev-immunol-032414-112334
287. Huang J, Zarnitsyna VI, Liu B, Edwards LJ, Jiang N, Evavold BD, et al. The kinetics of two-dimensional TCR and pMHC interactions determineT-cell responsiveness. *Nature* (2010) 44(1):239–50. doi: 10.1038/nature08944
288. Liu B, Zhong S, Malecek K, Johnson LA, Rosenberg SA, Zhu C, et al. 2D TCR-pMHC-CD8 kinetics determines T-cell responses in a self-antigen-specific TCR system. *Eur J Immunol* (2014). doi: 10.1002/eji.201343774
289. Dolton G, Zervoudi E, Rius C, Wall A, Thomas HL, Fuller A, et al. Optimized peptide-MHC multimer protocols for detection and isolationof autoimmune T-cells. *Front Immunol* (2018) 9:1378. doi: 10.3389/fimmu.2018.01378
290. Corr M, Slanetz AE, Boyd LF, Jelonek MT, Khilko S, Al-Ramadi BK, et al. T cell receptor-MHC class I peptide interactions: Affinity,kinetics, and specificity. *Science* (1994) 80-):946–9. doi: 10.1126/science.8052850
291. Margulies DH, Plaksin D, Khilko SN, Jelonek MT. Studying interactions involving the T-cell antigen receptor bysurface plasmon resonance. *Curr Opin Immunol* (1996) 8(2):262–70. doi: 10.1016/S0952-7915(96)80066-5
292. Myszka DG. Improving biosensor analysis. *J MolRecognit* (1999) 12(5):279–84. doi: 10.1002/(SICI)1099-1352(199909/10)12:5<279::AID-JMR473>3.0.CO;2-3
293. Rich RL, Myszka DG. Survey of the 2009 commercial optical biosensorliterature. *J Mol Recognit* (2011) 24(6):892–914. doi: 10.1002/jmr.1138
294. Chesla SE, Selvaraj P, Zhu C. Measuring two-dimensional receptor-ligand binding kinetics bymicropipette. *Biophys J* (1998) 75(3):1553–72. doi: 10.1016/S0006-3495(98)74074-3
295. Boniface JJ, Rabinowitz JD, Wülfing C, Hampl J, Reich Z, Altman JD, et al. Initiation of signal transduction through the T cell receptorrequires the peptide multivalent engagement of MHC ligands.*Immunity* (1998) 9(4):459–66. doi: 10.1016/S1074-7613(00)80629-9
296. Bakker AH, Schumacher TNM. MHC multimer technology: Current status and futureprospects. *Curr Opin Immunol* (2005) 17(4):428–33. doi: 10.1016/j.coi.2005.06.008
297. Altman JD, Moss PAH, Goulder PJR, Barouch DH, McHeyzer-Williams MG, Bell JI, et al. Phenotypic analysis of antigen-specific Tlymphocytes. *Science* (1996) (80-):94–6. doi: 10.1126/science.274.5284.94
298. Rius C, Attaf M, Tungatt K, Bianchi V, Legut M, Bovay A, et al. Peptide–MHC Class I Tetramers Can Fail To Detect RelevantFunctional T Cell Clonotypes and Underestimate Antigen-Reactive T Cell Populations. *J Immunol* (2018) 200(7):2263–2279. doi: 10.4049/jimmunol.1700242
299. Al-Ramadi BK, Jelonek MT, Boyd LF, Margulies DH, Bothwell ALM. Lack of strict correlation of functional sensitization with theapparent affinity of MHC/peptide complexes for the TCR. *J Immunol* (1995) 155(2):662–73.
300. Dougan SK, Dougan M, Kim J, Turner JA, Ogata S, Il CH, et al. Transnuclear TRP1-specific CD8 T cells with high or low affinityTCRs show equivalent antitumor activity. *Cancer Immunol Res* (2013) 1(2):99–111. doi: 10.1158/2326-6066.CIR-13-0047
301. Cukalac T, Chadderton J, Handel A, Doherty PC, Turner SJ, Thomas PG, et al. Reproducible selection of high avidity CD8+ T-cell clones following secondary acute virus infection. *Proc Natl Acad Sci USA* (2014) 111(4):1485–90. doi: 10.1073/pnas.1323736111
302. Zehn D, Lee SY, Bevan MJ. Complete but curtailed T-cell response to very low-affinityantigen. *Nature* (2009) 458(7235):211–4. doi: 10.1038/nature07657
303. Krummey SM, Martinez RJ, Andargachew R, Liu D, Wagener M, Kohlmeier JE, et al. Low-Affinity Memory CD8 + T Cells Mediate Robust HeterologousImmunity. *J Immunol* (2016) 196(6):2838–46. doi: 10.4049/jimmunol.1500639
304. Martinez RJ, Evavold BD. Lower affinity T cells are critical components and activeparticipants of the immune response. *Front Immunol* (2015) 6:468. doi: 10.3389/fimmu.2015.00468
305. Caserta S, Kleczkowska J, Mondino A, Zamoyska R. Reduced Functional Avidity Promotes Central and Effector Memory CD4T Cell Responses to Tumor-Associated Antigens. *J Immunol* (2010) 185(11):6545–54. doi: 10.4049/jimmunol.1001867
306. Gallegos AM, Xiong H, Leiner IM, Sušac B, Glickman MS, Pamer EG, et al. Control of T cell antigen reactivity via programmed TCR downregulation. *Nat Immunol* (2016) 17(4):379–86. doi: 10.1038/ni.3386
307. Rosenthal KM, Edwards LJ, Sabatino JJ, Hood JD, Wasserman HA, Zhu C, et al. Low 2-dimensional CD4 T cell receptor affinity for myelin sets inmotion delayed response kinetics. *PloS One* (2012) 7(3):e32562. doi: 10.1371/journal.pone.0032562
308. Andargachew R, Martinez RJ, Kolawole EM, Evavold BD. CD4 T Cell Affinity Diversity Is Equally Maintained during Acute andChronic Infection. *J Immunol* (2018) 201(1):19–30. doi: 10.4049/jimmunol.1800295
309. Welten SPM, Baumann NS, Oxenius A. Fuel and brake of memory T cell inflation.*Med Microbiol Immunol* (2019) 208(3-4):329–38. doi: 10.1007/s00430-019-00587-9
310. Nauerth M, Weißbrich B, Knall R, Franz T, Dössinger G, Bet J, et al. TCR-ligand koff rate correlates with the protective capacity ofantigen-specific CD8 + T cells for adoptive transfer. *Sci Transl Med* (2013) 5(192):192ra87. doi: 10.1126/scitranslmed.3005958
311. Davenport MP, Fazou C, McMichael AJ, Callan MFC. Clonal Selection, Clonal Senescence, and Clonal Succession: TheEvolution of the T Cell Response to Infection with a Persistent Virus. *JImmunol* (2002) 168 (7):3309–17. doi: 10.4049/jimmunol.168.7.3309
312. Viganò S, Utzschneider DT, Perreau M, Pantaleo G, Zehn D, Harari A. Functional avidity: A measure to predict the efficacy of effector Tcells? *Clin Dev Immunol* (2012) 2012:153863. doi: 10.1155/2012/153863
313. Utzschneider DT, Alfei F, Roelli P, Barras D, Chennupati V, Darbre S, et al. High antigen levels induce an exhausted phenotype in a chronicinfection without impairing T cell expansion and survival. *J Exp Med* (2016) 213 (9):1819–34. doi: 10.1084/jem.20150598
314. Miller AM, Bahmanof M, Zehn D, Cohen EEW, Schoenberger SP. Leveraging TCR affinity in adoptive immunotherapy against sharedtumor/self-antigens. *Cancer Immunol Res* (2019) 7(1):40–49. doi: 10.1158/2326-6066.CIR-18-0371
315. Hoffmann MM, Slansky JE. T-cell receptor affinity in the age of cancerimmunotherapy. *Mol Carcinog* (2020) 59(7):862–870. doi: 10.1002/mc.23212
316. Bos R, Marquardt KL, Cheung J, Sherman LA. Functional differences between low- and highaffinity CD8+ T cells inthe tumor environment. *Oncoimmunology* (2012) 1(8):1239–47. doi: 10.4161/onci.21285
317. Shakiba M, Philip M, Camara S, Socci ND, Schietinger A. The impact of TCR affinity on T cell differentiation and dysfunctionin tumors. *J Immunol* (2018) 200(1 Supplement) 57.24.
318. Thaxton JE, Li Z. To affinity and beyond: Harnessing the T cell receptor for cancerimmunotherapy. *Hum Vaccines Immunother* (2014) 10(11):3313–21. doi: 10.4161/21645515.2014.973314
319. Beauchemin L, Slifker M, Rossell D, Font-Burgada J. Characterizing MHC-I Genotype Predictive Power for Oncogenic Mutation Probability in Cancer Patients. *Methods Mol Biol* (2020) 2131:185–98. doi: 10.1007/978-1-0716-0389-5_8
320. Mazzocco M, Martini M, Rosato A, Stefani E, Matucci A, Dalla Santa S, et al. Autologous cellular vaccine overcomes cancer immunoediting in a mouse model of myeloma. *Immunology* (2015) 146:33–49. doi: 10.1111/imm.12477
321. Qamra A, Xing M, Padmanabhan N, Kwok JJT, Zhang S, Xu C, et al. Epigenomic Promoter Alterations Amplify Gene Isoform and Immunogenic Diversity in Gastric Adenocarcinoma. *Cancer Discovery* (2017) 7:630–51. doi: 10.1158/2159-8290.CD-16-1022
322. van Gisbergen KPJM, Klarenbeek PL, Kragten NAM, Unger PPA, Nieuwenhuis MBB, Wensveen FM, et al. The costimulatory molecule CD27 maintains clonally diverse CD8+ Tcell responses of low antigen affinity to protect against viral variants. *Immunity* (2011) 35(1):97–108. doi: 10.1016/j.immuni.2011.04.020
323. Oh S, Hodge JW, Ahlers JD, Burke DS, Schlom J, Berzofsky JA. Selective Induction of High Avidity CTL by Altering the Balance ofSignals from APC. *J Immunol* (2003) 170(5):2523–30. doi: 10.4049/jimmunol.170.5.2523
324. Hodge JW, Chakraborty M, Kudo-Saito C, Garnett CT, Schlom J. Multiple Costimulatory Modalities Enhance CTLAvidity. *J Immunol* (2005) 174 (10):5994–6004. doi: 10.4049/jimmunol.174.10.5994
325. Viola A, Lanzavecchia A. T cell activation determined by T cell receptor number and tunablethresholds. *Science* (1996) (80-):104–6. doi: 10.1126/science.273.5271.104

326. Bullock TNJ, Mullins DW, Engelhard VH. Antigen Density Presented By Dendritic Cells In Vivo DifferentiallyAffects the Number and Avidity of Primary, Memory, and Recall CD8 + T Cells. *J Immunol* (2003) 170(4):1822–9. doi: 10.4049/jimmunol.170.4.1822
327. Merkenschlager J, Ploquin MJ, Eksmond U, Andargachew R, Thorborn G, Filby A, et al. Stepwise B-cell-dependent expansion of T helper clonotypesdiversifies the T-cell response. *Nat Commun* (2016) 7:10281. doi: 10.1038/ncomms10281
328. Mamula MJ, Janeway CA. Do B cells drive the diversification of immuneresponses? *Immunol Today* (1993) 14(4):151–2. doi: 10.1016/0167-5699(93)90274-O
329. Iskratsch T, Wolfenson H, Sheetz MP. Appreciating force and shape-the rise of mechanotransduction in cellbiology. *Nat Rev Mol Cell Biol* (2014) 15 (12):825–33. doi: 10.1038/nrm3903
330. Colin-York H, Javanmardi Y, Skamrahl M, Kumari S, Chang VT, Khuon S, et al. Cytoskeletal Control of Antigen-Dependent T CellActivation. *Cell Rep* (2019) 26(12):3369–79.e5. doi: 10.1016/j.celrep.2019.02.074
331. Bashoura KT, Gondarenko A, Chen H, Shen K, Liu X, Huse M, et al. CD28 and CD3 have complementary roles in T-cell tractionforces. *Proc Natl Acad Sci USA* (2014) 111(6):2241–6. doi: 10.1073/pnas.1315606111
332. Liu Y, Blanchfield L, Pui-Yan Ma V, Andargachew R, Galior K, Liu Z, et al. DNA-based nanoparticle tension sensors reveal that T-cell receptorstransmit defined pN forces to their antigens for enhanced fidelity. *ProcNatl Acad Sci USA* (2016) 113(20):5610–5. doi: 10.1073/pnas.1600163113
333. Ma VPY, Liu Y, Blanchfield L, Su H, Evavold BD, Salaita K. Ratiometric tension probes for mapping receptor forces andclustering at intermembrane junctions. *Nano Lett* (2016) 16(7):4552–9. doi: 10.1021/acs.nanolett.6b01817
334. Grupp SA, Kalos M, Barrett D, Aplenc R, Porter DL, Rheingold SR, et al. Chimeric antigen receptor-modified T cells for acute lymphoidleukemia. *N Engl J Med* (2013) 368(16):1509–18. doi: 10.1056/NEJMoa1215134
335. Maude SL, Teachey DT, Porter DL, Grupp SA. CD19-targeted chimeric antigen receptor T-cell therapy for acutelymphoblastic leukemia. *Blood* (2015) 125(26):4017–23. doi: 10.1182/blood-2014-12-580068
336. June CH, O'Connor RS, Kawalekar OU, Ghassemi S, Milone MC. CAR T cell immunotherapy for human cancer.*Science* (2018) (80-):1361–65. doi: 10.1126/science.aar6711
337. Long AH, Haso WM, Shern JF, Wanhainen KM, Murgai M, Ingaramo M, et al. 4-1BB costimulation ameliorates T cell exhaustion induced by tonicsignaling of chimeric antigen receptors. *Nat Med* (2015) 21(6):581–90. doi: 10.1038/nm.3838
338. Fraietta JA, Lacey SF, Orlando EJ, Pruteanu-Malinici I, Gohil M, Lundh S, et al. Determinants of response and resistance to CD19 chimeric antigenreceptor (CAR) T cell therapy of chronic lymphocytic leukemia. *Nat Med* (2018) 24(5):563–71. doi: 10.1038/s41591-018-0010-1
339. Watanabe K, Kuramitsu S, Posey AD, June CH. Expanding the therapeutic window for CAR T cell therapy in solidtumors: The knowns and unknowns of CAR T cell biology. *Front Immunol* (2018) 9:2486. doi: 10.3389/fimmu.2018.02486

Conflict of Interest: The authors declare that the research was conducted in the absence of any commercial or financial relationships that could be construed as a potential conflict of interest.

frontiers in Immunology

MINI REVIEW
published: 09 March 2021
doi: 10.3389/fimmu.2021.600961

The Role of Protein and Lipid Clustering in Lymphocyte Activation

*Rachel E. Lamerton†, Abbey Lightfoot†, Daniel J. Nieves and Dylan M. Owen**

Institute of Immunology and Immunotherapy, School of Mathematics and Centre of Membrane Proteins and Receptors (COMPARE), University of Birmingham, Birmingham, United Kingdom

Lymphocytes must strike a delicate balance between activating in response to signals from potentially pathogenic organisms and avoiding activation from stimuli emanating from the body's own cells. For cells, such as T or B cells, maximizing the efficiency and fidelity, whilst minimizing the crosstalk, of complex signaling pathways is crucial. One way of achieving this control is by carefully orchestrating the spatiotemporal organization of signaling molecules, thereby regulating the rates of protein-protein interactions. This is particularly true at the plasma membrane where proximal signaling events take place and the phenomenon of protein microclustering has been extensively observed and characterized. This review will focus on what is known about the heterogeneous distribution of proteins and lipids at the cell surface, illustrating how such distributions can influence signaling in health and disease. We particularly focus on nanoscale molecular organization, which has recently become accessible for study through advances in microscope technology and analysis methodology.

Keywords: nano-clustering, lymphocytes, T cell synapse, B cell synapse, lipid rafts

OPEN ACCESS

Edited by:
Erdinc Sezgin,
Karolinska Institutet (KI), Sweden

Reviewed by:
Iztok Urbancic,
Institut Jožef Stefan (IJS), Slovenia
Jorge Bernardino De La Serna,
Imperial College London,
United Kingdom

***Correspondence:**
Dylan M. Owen
d.owen@bham.ac.uk

†These authors have contributed equally to this work

Specialty section:
This article was submitted to B Cell Biology, a section of the journal Frontiers in Immunology

Received: *31 August 2020*
Accepted: *12 February 2021*
Published: *09 March 2021*

Citation:
Lamerton RE, Lightfoot A, Nieves DJ and Owen DM (2021) The Role of Protein and Lipid Clustering in Lymphocyte Activation. Front. Immunol. 12:600961. doi: 10.3389/fimmu.2021.600961

INTRODUCTION

In order for the immune system to effectively neutralize pathogens, cells must take part in complex cell-cell communication interactions, such as those occurring between T or B cells and antigen presenting cells (APCs), such as dendritic cells. At the level of whole cells, these interactions take place through the formation of the immunological synapse (IS). Rather than being uniformly distributed over the IS, proteins are segregated into a bullseye-like configuration, made up of three concentric sections (1) easily resolved by conventional fluorescence microscopy. Termed supramolecular activation clusters (SMACs), the original findings placed T cell receptor (TCR) complexes in the central SMAC (cSMAC), adhesion molecules, such as the integrin LFA-1 in a narrow ring-shaped peripheral SMAC (pSMAC) and negative regulators, such as the large phosphatase CD45, with a dense cortical actin meshwork in the distal SMAC (dSMAC). Since then, it has become widely accepted that actively signaling TCR molecules are more likely to be found in the distal regions of the synapse and subsequently migrate into the cSMAC (2–4).

Whilst macroscale organization is also observed in B and NK cells, they form their own uniquely structured IS for their specific functions. The B cell synapse typically lacks a well-defined dSMAC, with B cell receptors (BCRs) concentrated in a large cSMAC specialized for gathering antigen for internalization and further intracellular processing (5). The NK cell synapse is more complex, with differently structured synapses corresponding to different cellular outcomes—the lytic synapse, the inhibitory synapse and the regulatory synapse (6).

The lytic synapse is somewhat similar to the B cell arrangement, with a cSMAC containing lytic granules and the microtubule organizing center (MTOC) with adhesion molecules located in the pSMAC. The inhibitory IS differs, with killer immunoglobulin-like receptors (KIRs) gathering in the cSMAC. In each type of synapse, on top of these cell-scale organizational layers on the scale of microns, is nanoscale molecular organization—the clustering of proteins and lipids. The composition and properties of the membrane, therefore, have a profound effect on cell activation. These are reviewed in (7).

There are a number of ways of mathematically defining what we mean when we use the term "molecular clustering" (**Figure 1**). One of the simplest is that on average, the distance from one molecule, for example LAT, to its closest LAT neighbor is shorter than would be expected had all the LAT molecules been randomly distributed. Furthermore, the difference should be large enough that with a given statistical test and experimental power, we can distinguish the two cases, given the random degree of clustering that might occur in any control dataset.

The same concept can be applied to lipids—if the average distance from a sphingomyelin molecule to its nearest neighbor is smaller than had all the sphingomyelin lipids been randomly distributed, and by enough that this can be confirmed with statistical significance, then sphingomyelin is said to be clustered. In most biological scenarios almost all non-random distributions of molecules will probably result in clustering but not necessarily to a degree that chance clustering in a random distribution can be ruled out with a given statistical certainty.

Almost all descriptions of heterogeneous molecular distributions (proteins or lipids) are therefore descriptions of clustering. It should also be made clear that protein clustering does not imply any dynamic process or change in distribution, which would be correctly described as an increase or decrease in clustering. Here, we use clustering to denote a state, not a process.

PROTEIN CLUSTERING

In T cells, many of the key proximal signaling molecules; TCRs (8, 9), LAT (10, 11), Lck (12), and ZAP-70 (13, 14) have been shown to form nanoclusters. With the need for both sensitivity and selectivity in T cell responses, the spatial organization of TCRs is emerging as a key factor in appropriate and adequate T cell signaling. TCRs are generally thought to pre-cluster on resting cells with several studies detecting clusters using optical microscopy methods (8, 10), with approximately 7–30 TCRs per cluster, and an average radius of 35–70 nm (10). Upon cell activation, clusters become increasingly dense, with denser clusters being linked to phosphorylation, and higher signaling efficiency. Interestingly, cluster density appears to be determined by the dose and affinity of the MHC-antigen to the TCR, suggesting a relationship between antigen and signaling mediated through clustering (8).

Similar to T cells, studies have shown resting BCRs in IgM and IgG producing B cells cells are clustered with an average radius below 60 nm, though a much broader range of cluster sizes is observed in resting IgG producing cells (15). These clusters might be lipid dependent and exclude the phosphatase CD45 (16). In contrast to T cells, the density of clusters in B cells tends to decrease upon activation (15).

In NK cells, the nanoclustering properties differ again. Rather than relying on one dominant activating receptor being triggered, as occurs in T and B cells, the outcome of NK cell interactions is controlled by the balance of activating and inhibitory signals from multiple receptors. KIR2DL1 is an inhibitory receptor arranged in clusters on resting NK cells (17). Upon exposure to the activating receptor NKG2D, causing formation of the cytolytic immune synapse, the KIR2DL1 clusters become smaller and denser. Resting KIR2DL1 clusters, as measured on IgG1-coated control coverslips, were approximately 122 nm in diameter, decreasing in size by almost 20% in samples activated by the NKG2D receptor. There was also a 58% increase in KIR2DL1 cluster density between the IgG1 control and NKG2D receptor coverslips (17).

One of the key areas of debate is now whether important signaling molecules are pre-clustered on the surface of resting cells and if so, whether those pre-stimulus clusters are essential. In 2005, a FRET study suggested BCRs existed as monomers on resting cells (18), a finding that has also been shown by diffusion

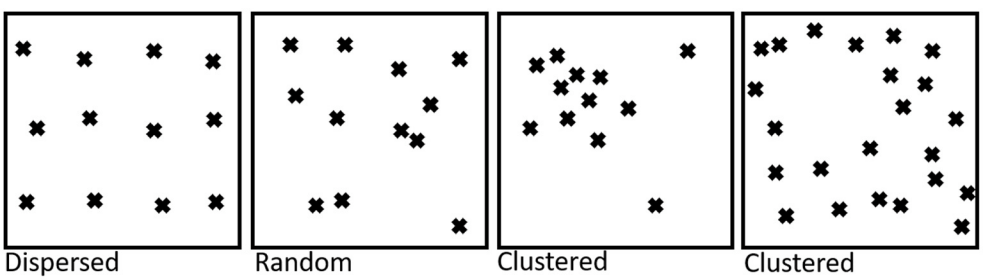

FIGURE 1 | Illustration of different molecule (protein or lipid) distributions on the cell surface. For dispersed distributions, the average distance between molecules is larger than would be expected for randomly distributed molecules. In both the clustered examples shown here, the average nearest neighbor distance is smaller than expected for randomly arranged molecules.

studies (19). More recent studies have shown pre-existing BCR clusters in resting cells using electron microscopy (20) and single molecule localization microscopy (SMLM) techniques, such as direct stochastic optical reconstruction microscopy (dSTORM) and photoactivated localization microscopy (PALM) (15). Rossboth et al. (21) suggest that clusters may be detected due to overcounting errors inherent to SMLM techniques. They carried out robust studies using dSTORM, PALM, and stimulated emission depletion (STED) to show that TCRs are distributed randomly across the membrane in resting cells. In a separate study, the notion that pre-clustering plays a role in antigen sensitivity and specificity was questioned. Using FRET and a single-molecule fluorescence brightness analysis method, monomeric TCR-CD3 complexes were found to initiate intracellular signaling, rather than TCR-CD3 oligomers (22).

Overall, much uncertainty about the presence or role of pre-clusters still exists. The fact that pre-clustering has been detected by independent techniques (SMLM, FRET, EM etc), and in different cell types suggests non-random distributions on the surface of non-stimulated cells is likely, at least for some molecules. As we discussed in the definition of clustering, different tests will have different statistical power and may have been testing different definitions of clustering. If clustering is low level with only small deviations from random distributions, these different tests could account for the discrepancies and controversy. Going forward, the community might agree a definition for molecular clustering and work to establish how clustering, by that definition, would be manifested in different data types. In parallel, work is needed on the experimental sample system to agree clear definitions of "resting cells" and other biological descriptors to foster consistency between systems used in competing claims.

LIPID CLUSTERING

The original "lipid raft hypothesis" suggested that interactions between cholesterol and lipids with highly saturated acyl chains can cause cholesterol clustering in which cholesterol-proximal lipid acyl tails become highly ordered, as opposed to the disordered tails in the surrounding membrane. These clusters, it was hypothesized, can also preferentially accommodate some proteins whilst excluding others (23), therefore leading to clustered distributions for both the "raft enriched" and excluded proteins (**Figure 1**). There is a wide variety of nomenclature in the literature for describing the lateral distribution of lipids—rafts, domains, territories, islands, and some open questions about whether lipids "cluster" in the same way as has been observed for proteins. Mathematically, however, the lipid raft hypothesis, ordered phase domains and other similar models are describing clustering, even if the particular lipid distribution involves areas of exclusion (**Figure 1**). If you were to take a particular lipid species, e.g., palmitoyl sphingomyelin (PSM) for example, and plot the coordinates of each molecule on the cell surface, almost all these membrane models would result in clustering—the distance to a nearest neighbor would be smaller than would be expected for a completely random distribution of the lipid in question. We therefore consider rafts, domains as well as concepts such as islands and territories—any area in which a specific type of lipid is "enriched" or "excluded" to be a form of clustering (which may or may not be detectable, depending on the statistical strength of the experiment and analysis). However, the exact properties of the clustering, the biophysical determinants and the functions of lipid clusters could be very diverse from protein clusters.

One method for studying such distributions is using detergents, where, under specific conditions, clusters of sterols and lipids with ordered acyl tails are resistant to solubilisation. Detergent solubilisation assays of T cell derived giant plasma-membrane vesicles (GPMVs), report that non-activated TCRs are absent from detergent-resistant fractions and that TCRs only translocate into detergent-insoluble fractions (i.e., co-cluster with ordered-tail lipids and sterols) upon receptor activation (24). In contrast, the adaptor protein LAT, the Src-family kinase Lck, and the CD4/CD8 co-receptors involved in TCR signaling can be recovered in detergent-resistant fractions independently of TCR triggering (25, 26). Similarly, in B cells, the BCR is not present in detergent-resistant fractions prior to crosslinking, and will translocate to detergent-resistant fractions which are also enriched with the Src-family kinase Lyn following BCR ligand binding (27). The discovery that signaling complexes co-cluster with sterols and ordered acyl tail lipids which are resistant to detergent solubilisation, following receptor activation suggests a functional role of lipid clusters as hotspots that compartmentalize and regulate immunoreceptor activation and subsequent downstream signaling events (26). The use of detergent resistance, however, has started to fall out of favor, mainly due to the potential artifacts of the procedure (for example due to using cold temperatures) and often contradictory results, reviewed in Lichtenberg et al. (28). Most studies now focus on the less invasive optical microscopy methods, reviewed in Sezgin et al. (29).

Environmentally-sensitive lipid dyes such as Laurdan and Di-4-ANEPPDHQ exhibit spectral shifts in their fluorescence emission dependent on the degree of lipid packing in the membrane. These probes are solvatochromic, sensing the polarity of their local solvent, and, in the case of membranes therefore, the relative penetration of polar water molecules into the bilayer. Multispectral imaging can therefore be used to probe and quantify membrane lipid packing, which is dependent on the ordering of the lipid tails by sterols (30). Inconsistent with detergent solubilisation assays, Laurdan labeling of cells shows that TCR proteins in resting cells co-localize with areas of dense lipid packing and aggregate into even larger TCR clusters following cross-linking (31). The disparity between results observed using microscopy and those found using detergent-resistant solubilisation assays might arise from the instability of dynamic nanoclusters or artifacts from the detergent solubilisation process, in particular when membrane constituents might be associated with cortical actin.

Probes such as these can be used to map membrane properties across the immunological synapse. Interestingly, condensation of the membrane surrounding the TCR complex at the T cell immunological synapse has been observed (32, 33). The pattern

of increased membrane ordering at the immunological synapse periphery supports the proposed pattern of actively signaling TCR microclusters within the SMACs (34). Furthermore, application of small molecule agents such as the cholesterol analog 7-ketocholesterol (7KC), which disrupts lipid ordering, also disrupts T cell activation and synapse formation (35). Methyl-β-cyclodextrin depletion of cholesterol in the plasma membrane has been shown to both inhibit and enhance the activation of T cells, depending on experimental conditions (36, 37). It was recently found that following cell treatment with the naturally occurring analog cholesterol sulfate, TCR nanoclusters were disrupted, leading to reduced avidity for peptide-MHC and reduced CD3 ITAM phosphorylation (38). This points the way toward potential manipulation of membrane lipids in order to control molecular distributions (clustering) and function and, therefore, lymphocyte signaling.

Another way membrane lipids can influence the distribution and dynamics of membrane proteins is via sub-synaptic vesicles. Using SMLM and total internal reflection fluorescence microscopy (TIRF), LAT-containing sub-synaptic vesicles were found to be recruited to the plasma membrane in early cell activation, and it was found that plasma-membrane associated LAT may not be involved in signaling (11). Since then, it is believed that two phases of T cell activation occurs, initiated first by pre-existing clusters on the plasma membrane and prolonged by the recruitment of LAT containing vesicles that were found to have higher membrane order than non-LAT containing vesicles (39, 40). Lipid composition, therefore, might represent a novel mechanism for organizing cargo transport by intracellular vesicles.

Finally, in addition to regulating protein distributions and function, high lipid tail order has also been proposed to play a protective role for cytotoxic CD8+ T cells, protecting against accidental death by repelling perforin (41). In these cells, phosphatidylserine is enriched at the immunological synapse following antigen recognition (42). The negative charge of phosphatidylserine was found to inactivate residual perforin as an additional mechanism to prevent accidental cell death and allow for successive killing of target cells (41). With this in mind, elevated levels of negatively charged lipids on virus envelopes and cancerous cell membranes may be immunoevasive.

PROTEIN AND LIPID CLUSTERING RELEVANT TO DISEASE

Understanding of lymphocyte signaling protein cluster properties, and their regulation, has significantly advanced over the last 20 years, however, the next challenge is to exploit this knowledge in the context of health and disease. There is currently a lack of knowledge as to how these clustering properties relate to disease states and whether their exploitation could improve current clinical treatments.

One study looking at diffuse large B-cell lymphomas (DLBCLs) has shown that, of the 5 activated B-cell-like DLBCL cell-lines studied, all had pronounced BCR clustering, a phenomenon that was not observed in the 16 other cell lines tested from a variety of different B cell cancer types (43). Furthermore, decreased BCR diffusion in these lines was also observed, and it was suggested these clusters were actively signaling, with phosphotyrosine accumulation in these cells. This so-called "chronic active" signaling was required for cell survival, therefore, highlighting a role for the BCR clusters and the signaling they induce in activated B-cell-like DLBCL, and revealing a possible new treatment target.

Inappropriate clustering has also been linked to autoimmune diseases. The R620W variant in protein tyrosine phosphatase non-receptor type 22 (PTPN22) is associated with rheumatoid arthritis, lupus and type one diabetes and is a mutation present in the human population (44). More recently, Burn et al. (45) showed that PTPN22 inhibits LFA-1 signaling, with the R620W variant being loss-of-function. It was found that the mutation, in a non-catalytic protein binding domain, alters the clustering profile of PTPN22 with a resulting failure to de-cluster upon cell stimulation. The R620W mutation was also shown to be associated with changes in LFA-1 integrin clustering in migrating T cells (46).

Lipid clustering has also been implicated in a number of lymphocyte-related diseases, including cancer and autoimmunity. Hallmarks of systemic lupus erythematosus (SLE) include chronic immune cell activation and increased serum lipids, with interplay between the two being demonstrated (47, 48). High membrane order and increased cholesterol and glycosphingolipid levels have been observed in the plasma membrane of T cells from SLE patients (49, 50). The altered lipid environment is believed to drive an increase in glycosphingolipid expression in CD4+ T cells in a liver X receptor (LXR) dependent manner.

In vitro studies suggest that T cell function in SLE patient derived cells can be restored through normalization of glycosphingolipid expression using LXR antagonists (51). Additionally, LXR activation of CD4+ T cells from healthy donors can also upregulate expression of glycosphingolipids leading to reduced membrane order at the TCR immunological synapse. Altered spatiotemporal distribution of lipids promoted Lck recruitment to the immunological synapse and increased phosphorylation of CD3 and LAT, dysregulating effector functions via disruption of ordered lipids (52). Additionally, kinase phosphorylation in SLE patient-derived T cells is restored by statin inhibition of cholesterol synthesis (53). The cytotoxic effects of CD8+ T cells can be heightened by ablation or inhibition of cholesterol esterification enzyme ACAT1, which is upregulated upon TCR activation (54). Together these findings suggest that tight regulation of lipid properties and distributions is necessary for normal T cell function. There are numerous processes that result in diseases associated with lymphocytes where cholesterol plays a role. For example HIV entry, associated with the surface marker CD4, is significantly impaired by cholesterol depletion from the plasma membrane (55). Further, although we have focussed on cholesterol here, many other lipids display clustering and for a more complete review, we point the reader to Wu et al. (56). Many of these are also involved in regulating membrane order and, therefore might be relevant

to human health and disease (57) including cancer and autoimmune disease.

CONCLUSIONS

In lymphocytes, protein clustering has been well-documented on the micron-scale and with the development of super-resolution microscopy, is beginning to be characterized on the nanoscale. The challenge remains as to what biophysical mechanisms are governing nanocluster formation and what the ultimate function of such protein distributions is.

Cluster formation is likely due to a variety of competing and non-exclusionary phenomena. Prominent among these are the clustering properties of the lipids themselves within the plasma membrane. This is important as it brings into play a number of small molecule pharmacological agents, and even genetic manipulations, to control the lipidome and, therefore, cell fate and function. Protein-protein interactions and corralling by the cortical actin meshwork are also potentially important mechanisms and, thus, therapeutic targets.

The function of protein clustering in T cells has only been minimally explored, in part due to the lack of molecular tools to selectively manipulate the systems. In other protein pathways clustering has been shown to create digital switches, for example, in Ras signaling (58). Signaling via two protein species is dependent on the frequency of collisions between them as they diffuse, say in a 2D membrane. A similar situation exists for example in the rate of a chemical reaction as two substrates diffuse and react to form a product. In reaction kinetics, whether a substrate is dimeric or oligomeric and whether there is cooperativity between sites (allostery) will change the rate of product production. In the same way, clustering will change the rate of protein-protein interactions in a signaling interaction (59).

The hypothesized role of clustering can be illustrated by considering a hypothetical experiment in which two types of interacting molecules–say kinases and their substrates (which may be proteins or lipids, such as inositides) are observed (**Figure 2**). The "input" to the system represents the amount of kinase activity e.g., it may represent kinase concentration, activation status or elapsed time through the experiment. The "output" here might represent the amount of phosphorylated substrate. We hypothesize that clustering determines the shape of the curve relating this input and output and in particular, that clustering produces more digital relationships featuring input thresholds required to achieve any significant output. On top of this, phosphorylation events are stochastic (because of the random nature of diffusion) and so if the experiment were repeated many times, different amounts of phosphorylation would be observed each time, for a given input. In **Figure 2**, this is represented by the hypothesised size of the error bars. We further hypothesize that clustering affects the size of these variances, decreasing "noise" in the system.

In reality of course, a cellular signaling pathway will have many members and might involve complex feedback processes. In addition, while many studies have been performed on proteins, here, lipids play a dual role. They may represent members of a signaling pathway themselves (e.g., phosphatidylinositol) and therefore their distribution/clustering may be directly important, or they may be indirectly involved by influencing the clustering of proteins. Despite the complexity of a complete signaling pathway, there will still be some input-output curve for the entire pathway. In lymphocytes, for example, the input might represent the number or strength of engaged TCRs/BCRs and the output might be the level of downstream phosphorylation or even gene expression. We hypothesize that even in this complex case, the shape of the curve will be influenced by the clustering properties of the many proteins and lipids that constitute the pathway. Since many pathologies, for example autoimmune disease, may be caused by modified immune cell activation thresholds, understanding molecular clustering, and how to manipulate it, may lead to new types of therapeutic interventions.

Clearly, several open questions remain to be answered. For example, to relate protein clustering to the concepts of allostery, stoichiometry and competition in classic enzyme kinetics, requires accurate measurements of protein oligomers even down to the level of dimers. In some contexts, this is possible, but precise molecular counting and localization on the scale of proteins is still difficult. Since much of the recent progress has been made using optical microscopy, **Table 1** summarizes

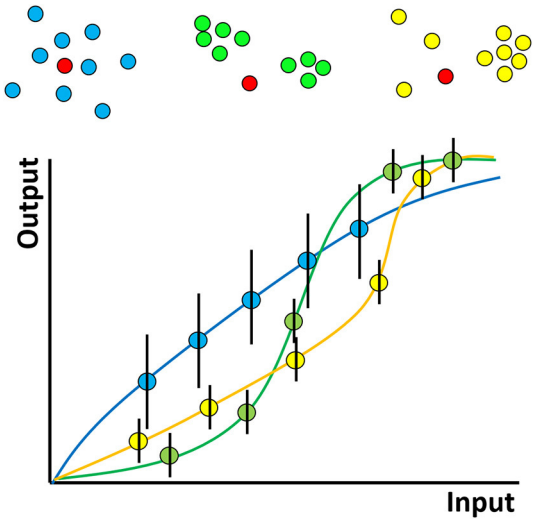

FIGURE 2 | Hypothesized effect of molecular nanoclustering on input-output relationship of a generalized signaling pathway for two proteins. A hypothetical kinase for example (red) can diffuse in the membrane and phosphorylate a substrate with different clustering properties (blue, green, yellow). The input can be conceptualized simply—as the amount of active kinase or more generally—say as the strength of antigen binding by a receptor. The output might be proximal downstream phosphorylation levels more distal, such as gene expression—analogous to the rate of production of product in a chemical reaction. The shape of the curve relating these two depends on the stoichiometry, oligermerisation and cooperativity of the molecules involved, just like a classical chemical reaction. In a cell signaling pathway however the situation will be complex, with many interacting partners, feedback and so on. The exact shapes of such hypothetical curves therefore remain an area for future study.

TABLE 1 | Fluorescence methods applied to study membrane protein and lipid clustering, their limitations and suggestions for future development.

Method	Limitations	Required developments
Fluorescence microscopy with environmentally sensitive probes	Dyes change the composition of the bilayers and may alter properties (60). They also do not generally allow the environment around specific molecules to be probed as the dyes are usually untargeted. Probes often have low brightness and photostability.	Targeted, leaflet specific probes compatible with super-resolution microscopy (61–63).
Single molecule localization microscopy (SMLM)	Overcounting due to multiple blinking makes quantifying small clusters challenging (64, 65). Labeling methodology generally limited to proteins.	New, smaller probes, with well-characterized photophysics and new analysis methods are needed. Further, the technology for labeling lipids—to allow lipid clustering to be analyzed in the same framework as proteins is also lacking and developments in this area would be a significant boon.
Diffusion measurements such as fluorescence correlation spectroscopy (FCS)	Generally, point measurements are used making mapping heterogeneity over the cell challenging. Can be difficult to interpret data in complex membrane geometries.	Area based FCS measurements such as Imaging FCS (66). Greater computational modeling approaches to single-molecule tracking data.
Whole cell imaging	Generally, artificial synapses are studied but more physiological insights could be derived from cell-cell conjugate systems (67).	Application of light-sheet based approaches for long term, 3D imaging.

the main methods that have been applied to study protein and lipid clustering in lymphocytes and, in our opinion, what developments are needed to further push the boundaries of our understanding.

In addition to microscopy, tools to specifically alter protein and lipid nanoscale clustering are required in order to better draw causal links with cell phenotypic outcomes. On the biological side, the role of pre-clustered surface proteins is an emerging topic, still controversial but has the potential to have a significant impact on our understanding of how B and T cells are regulated.

AUTHOR CONTRIBUTIONS

RL, AL, DN, and DO wrote the manuscript. All authors contributed to the article and approved the submitted version.

ACKNOWLEDGMENTS

We acknowledge funding from BBSRC grant BB/R007365/1 to DO, RL and AL acknowledge funding from the Wellcome Trust Mechanisms of Inflammatory Disease (MIDAS) PhD Program, grant code 108871/Z/15/Z, at the University of Birmingham.

REFERENCES

1. Monks CR, Freiberg BA, Kupfer H, Sciaky N, Kupfer A. Three-dimensional segregation of supramolecular activation clusters in T cells. *Nature.* (1998) 395:82–6. doi: 10.1038/25764
2. Bunnell SC, Hong DI, Kardon JR, Yamazaki T, McGlade CJ, Barr VA, et al. T cell receptor ligation induces the formation of dynamically regulated signaling assemblies. *J Cell Biol.* (2002) 158:1263–75. doi: 10.1083/jcb.200203043
3. DeMond AL, Mossman KD, Starr T, Dustin ML, Groves JT. T cell receptor microcluster transport through molecular mazes reveals mechanism of translocation. *Biophys J.* (2008) 94:3286–92. doi: 10.1529/biophysj.107.119099
4. Soares H, Henriques R, Sachse M, Ventimiglia L, Alonso MA, Zimmer C, et al. Regulated vesicle fusion generates signaling nanoterritories that control T cell activation at the immunological synapse. *J Exp Med.* (2013) 210:2415–33. doi: 10.1084/jem.20130150
5. Batista FD, Iber D, Neuberger MS. B cells acquire antigen from target cells after synapse formation. *Nature.* (2001) 411:489–94. doi: 10.1038/35078099
6. Mace EM, Orange JS. Multiple distinct NK-cell synapses. *Blood.* (2011) 118:6475–6. doi: 10.1182/blood-2011-10-381392
7. Pettmann J, Santos AM, Dushek O, Davis SJ. Membrane Ultrastructure and T Cell Activation. *Front Immunol.* (2018) 9:2152. doi: 10.3389/fimmu.2018.02152
8. Pageon SV, Tabarin T, Yamamoto Y, Ma YQ, Bridgeman JS, Cohnen A, et al. Functional role of T-cell receptor nanoclusters in signal initiation and antigen discrimination. *Proc Natl Acad Sci U S A.* (2016) 113:E5454–63. doi: 10.1073/pnas.1607436113
9. Goyette J, Nieves DJ, Ma YQ, Gaus K. How does T cell receptor clustering impact on signal transduction? *J Cell Sci.* (2019) 132:10. doi: 10.1242/jcs.226423
10. Lillemeier BF, Mortelmaier MA, Forstner MB, Huppa JB, Groves JT, Davis MM. TCR and Lat are expressed on separate protein islands on T cell membranes and concatenate during activation. *Nat Immunol.* (2010) 11:90–6. doi: 10.1038/ni.1832
11. Williamson DJ, Owen DM, Rossy J, Magenau A, Wehrmann M, Gooding JJ, et al. Pre-existing clusters of the adaptor Lat do not participate in early T cell signaling events. *Nat Immunol.* (2011) 12:655–62. doi: 10.1038/ni.2049
12. Rossy J, Owen DM, Williamson DJ, Yang ZM, Gaus K. Conformational states of the kinase Lck regulate clustering in early T cell signaling. *Nat Immunol.* (2013) 14:82–9. doi: 10.1038/ni.2488
13. Sherman E, Barr V, Manley S, Patterson G, Balagopalan L, Akpan I, et al. Functional nanoscale organization of signaling molecules downstream of the T cell antigen receptor. *Immunity.* (2011) 35:705–20. doi: 10.1016/j.immuni.2011.10.004
14. Neve-Oz Y, Razvag Y, Sajman J, Sherman E. Mechanisms of localized activation of the T cell antigen receptor inside clusters. *Biochim Biophys Acta Mol Cell Res.* (2015) 1853:810–21. doi: 10.1016/j.bbamcr.2014.09.025
15. Lee J, Sengupta P, Brzostowski J, Lippincott-Schwartz J, Pierce SK. The nanoscale spatial organization of B-cell receptors on immunoglobulin M- and G-expressing human B-cells. *Mol Biol Cell.* (2017) 28:511–23. doi: 10.1091/mbc.e16-06-0452
16. Nunez MF, Wisser K, Veatch SL. Synergistic factors control kinase-phosphatase organization in B-cells engaged with supported bilayers. *Mol Biol Cell.* (2020) 31:667–82. doi: 10.1091/mbc.E19-09-0507
17. Pageon SV, Cordoba SP, Owen DM, Rothery SM, Oszmiana A, Davis DM. Superresolution microscopy reveals nanometer-scale reorganization of inhibitory natural killer cell receptors upon activation of NKG2D. *Sci Signal.* (2013) 6:11. doi: 10.1126/scisignal.2003947
18. Tolar P, Sohn HW, Pierce SK. The initiation of antigen-induced B cell antigen receptor signaling viewed in living cells by fluorescence resonance energy transfer. *Nat Immunol.* (2005) 6:1168–76. doi: 10.1038/ni1262
19. Tolar P, Hanna J, Krueger PD, Pierce SK. The constant region of the membrane immunoglobulin mediates B cell-receptor clustering and

signaling in response to membrane antigens. *Immunity.* (2009) 30:44–55. doi: 10.1016/j.immuni.2008.11.007
20. Fiala GJ, Kaschek D, Blumenthal B, Reth M, Timmer J, Schamel WWA. Pre-clustering of the B cell antigen receptor demonstrated by mathematically extended electron microscopy. *Front Immunol.* (2013) 4:10. doi: 10.3389/fimmu.2013.00427
21. Rossboth B, Arnold AM, Ta H, Platzer R, Kellner F, Huppa JB, et al. TCRs are randomly distributed on the plasma membrane of resting antigen-experienced T cells. *Nat Immunol.* (2018) 19:821. doi: 10.1038/s41590-018-0162-7
22. Brameshuber M, Kellner F, Rossboth BK, Ta H, Alge K, Sevcsik E, et al. Monomeric TCRs drive T cell antigen recognition. *Nat Immunol.* (2018) 19:487. doi: 10.1038/s41590-018-0092-4
23. Simons K, Ikonen E. Functional rafts in cell membranes. *Nature.* (1997) 387:569–72. doi: 10.1038/42408
24. Beck-García K, Beck-García E, Bohler S, Zorzin C, Sezgin E, Levental I, et al. Nanoclusters of the resting T cell antigen receptor (TCR) localize to non-raft domains. *Biochim Biophys Acta (BBA) Mol Cell Res.* (2015) 1853:802–9. doi: 10.1016/j.bbamcr.2014.12.017
25. Zhang W, Trible RP, Samelson LE. LAT palmitoylation: its essential role in membrane microdomain targeting and tyrosine phosphorylation during T cell activation. *Immunity.* (1998) 9:239–46. doi: 10.1016/S1074-7613(00)80606-8
26. Harder T, Kuhn M. Selective accumulation of raft-associated membrane protein lat in T cell receptor signaling assemblies. *J Cell Biol.* (2000) 151:199–208. doi: 10.1083/jcb.151.2.199
27. Cheng PC, Brown BK, Song W, Pierce SK. Translocation of the B cell antigen receptor into lipid rafts reveals a novel step in signaling. *J Immunol.* (2001) 166:3693–701. doi: 10.4049/jimmunol.166.6.3693
28. Lichtenberg D, Goni FM, Heerklotz H. Detergent-resistant membranes should not be identified with membrane rafts. *Trends Biochem Sci.* (2005) 30:430–6. doi: 10.1016/j.tibs.2005.06.004
29. Sezgin E, Levental I, Mayor S, Eggeling C. The mystery of membrane organization: composition, regulation and roles of lipid rafts. *Nat Rev Mol Cell Biol.* (2017) 18:361–74. doi: 10.1038/nrm.2017.16
30. Owen DM, Rentero C, Magenau A, Abu-Siniyeh A, Gaus K. Quantitative imaging of membrane lipid order in cells and organisms. *Nat Protoc.* (2011) 7:24–35. doi: 10.1038/nprot.2011.419
31. Dinic J, Riehl A, Adler J, Parmryd I. The T cell receptor resides in ordered plasma membrane nanodomains that aggregate upon patching of the receptor. *Sci Rep.* (2015) 5:10082. doi: 10.1038/srep10082
32. Gaus K, Chklovskaia E, Fazekas de St Groth B, Jessup W, Harder T. Condensation of the plasma membrane at the site of T lymphocyte activation. *J Cell Biol.* (2005) 171:121–31. doi: 10.1083/jcb.200505047
33. Zech T, Ejsing CS, Gaus K, de Wet B, Shevchenko A, Simons K, et al. Accumulation of raft lipids in T-cell plasma membrane domains engaged in TCR signalling. *EMBO J.* (2009) 28:466–76. doi: 10.1038/emboj.2009.6
34. Owen DM, Oddos S, Kumar S, Davis DM, Neil MAA, French PMW, et al. High plasma membrane lipid order imaged at the immunological synapse periphery in live T cells. *Mol Membr Biol.* (2010) 27:178–89. doi: 10.3109/09687688.2010.495353
35. Rentero C, Zech T, Quinn CM, Engelhardt K, Williamson D, Grewal T, et al. Functional implications of plasma membrane condensation for T cell activation. *PLoS ONE.* (2008) 3:e2262. doi: 10.1371/journal.pone.0002262
36. Kabouridis PS, Janzen J, Magee AL, Ley SC. Cholesterol depletion disrupts lipid rafts and modulates the activity of multiple signaling pathways in T lymphocytes. *Eur J Immunol.* (2000) 30:954–63. doi: 10.1002/1521-4141(200003)30:3<954::AID-IMMU954>3.0.CO;2-Y
37. Swamy M, Beck-Garcia K, Beck-Garcia E, Hartl FA, Morath A, Yousefi OS, et al. A cholesterol-based allostery model of T cell receptor phosphorylation. *Immunity.* (2016) 44:1091–101. doi: 10.1016/j.immuni.2016.04.011
38. Wang F, Beck-García K, Zorzin C, Schamel WWA, Davis MM. Inhibition of T cell receptor signaling by cholesterol sulfate, a naturally occurring derivative of membrane cholesterol. *Nat Immunol.* (2016) 17:844–50. doi: 10.1038/ni.3462
39. Ashdown GW, Williamson DJ, Soh GHM, Day N, Burn GL, Owen DM. Membrane lipid order of sub-synaptic T cell vesicles correlates with their dynamics and function. *Traffic.* (2018) 19:29–35. doi: 10.1111/tra.12532
40. Balagopalan L, Yi J, Nguyen T, McIntire KM, Harned AS, Narayan K, et al. Plasma membrane LAT activation precedes vesicular recruitment defining two phases of early T-cell activation. *Nat Commun.* (2018) 9:17. doi: 10.1038/s41467-018-04419-x
41. Rudd-Schmidt JA, Hodel AW, Noori T, Lopez JA, Cho H-J, Verschoor S, et al. Lipid order and charge protect killer T cells from accidental death. *Nat Commun.* (2019) 10:5396. doi: 10.1038/s41467-019-13385-x
42. Fischer K, Voelkl S, Berger J, Andreesen R, Pomorski T, Mackensen A. Antigen recognition induces phosphatidylserine exposure on the cell surface of human CD8+ T cells. *Blood.* (2006) 108:4094–101. doi: 10.1182/blood-2006-03-011742
43. Davis RE, Ngo VN, Lenz G, Tolar P, Young RM, Romesser PB, et al. Chronic active B-cell-receptor signalling in diffuse large B-cell lymphoma. *Nature.* (2010) 463:88–92. doi: 10.1038/nature08638
44. Burn GL, Svensson L, Sanchez-Blanco C, Saini M, Cope AP. Why is PTPN22 a good candidate susceptibility gene for autoimmune disease? *FEBS Lett.* (2011) 585:3689–98. doi: 10.1016/j.febslet.2011.04.032
45. Burn GL, Cornish GH, Potrzebowska K, Samuelsson M, Griffie J, Minoughan S, et al. Superresolution imaging of the cytoplasmic phosphatase PTPN22 links integrin-mediated T cell adhesion with autoimmunity. *Sci Signal.* (2016) 9:ra99. doi: 10.1126/scisignal.aaf2195
46. Shannon MJ, Pineau J, Griffie J, Aaron J, Peel T, Williamson DJ, et al. Differential nanoscale organisation of LFA-1 modulates T-cell migration. *J Cell Sci.* (2019) 133:jcs232991. doi: 10.1101/602326
47. Moulton VR, Tsokos GC. Abnormalities of T cell signaling in systemic lupus erythematosus. *Arthritis Res Ther.* (2011) 13:207. doi: 10.1186/ar3251
48. Ali Abdalla M, Mostafa El Desouky S, Sayed Ahmed A. Clinical significance of lipid profile in systemic lupus erythematosus patients: relation to disease activity and therapeutic potential of drugs. *Egypt Rheumatol.* (2017) 39:93–8. doi: 10.1016/j.ejr.2016.08.004
49. Krishnan S, Nambiar MP, Warke VG, Fisher CU, Mitchell J, Delaney N, et al. Alterations in lipid raft composition and dynamics contribute to abnormal T cell responses in systemic lupus erythematosus. *J Immunol.* (2004) 172:7821–31. doi: 10.4049/jimmunol.172.12.7821
50. Miguel L, Owen DM, Lim C, Liebig C, Evans J, Magee AI, et al. Primary human $CD4^+$ T cells have diverse levels of membrane lipid order that correlate with their function. *J Immunol.* (2011) 186:3505–16. doi: 10.4049/jimmunol.1002980
51. McDonald G, Deepak S, Miguel L, Hall CJ, Isenberg DA, Magee AI, et al. Normalizing glycosphingolipids restores function in CD4+ T cells from lupus patients. *J Clin Investig.* (2014) 124:712–24. doi: 10.1172/JCI69571
52. Waddington KE, Robinson GA, Adriani M, Rubio-Cuesta B, Chrifi-Alaoui E, Andreone S, et al. Activation of the liver X receptors alters $CD4^+$ T cell membrane lipids and signalling through direct regulation of glycosphingolipid synthesis. *bioRxiv [Preprint].* (2019):721050. doi: 10.1101/721050
53. Jury EC, Isenberg DA, Mauri C, Ehrenstein MR. Atorvastatin restores lck expression and lipid raft-associated signaling in T cells from patients with systemic lupus erythematosus. *J Immunol.* (2006) 177:7416–22. doi: 10.4049/jimmunol.177.10.7416
54. Yang W, Bai Y, Xiong Y, Zhang J, Chen S, Zheng X, et al. Potentiating the antitumour response of CD8+ T cells by modulating cholesterol metabolism. *Nature.* (2016) 531:651–5. doi: 10.1038/nature17412
55. Ono A, Freed EO. Plasma membrane rafts play a critical role in HIV-1 assembly and release. *Proc Natl Acad Sci U S A.* (2001) 98:13925–30. doi: 10.1073/pnas.241320298
56. Wu W, Shi X, Xu C. Regulation of T cell signalling by membrane lipids. *Nat Rev Immunol.* (2016) 16:690–701. doi: 10.1038/nri.2016.103
57. Simons K, Ehehalt R. Cholesterol, lipid rafts, and disease. *J Clin Invest.* (2002) 110:597–603. doi: 10.1172/JCI0216390
58. Kenworthy AK. Nanoclusters digitize Ras signalling. *Nat Cell Biol.* (2007) 9:875–7. doi: 10.1038/ncb0807-875
59. Roob E III, Trendel N, Rein Ten Wolde P, Mugler A. Cooperative clustering digitizes biochemical signaling and enhances its fidelity. *Biophys J.* (2016) 110:1661–9. doi: 10.1016/j.bpj.2016.02.031
60. Suhaj A, Gowland D, Bonini N, Owen DM, Lorenz CD. Laurdan and Di-4-ANEPPDHQ influence the properties of lipid membranes: a classical molecular dynamics and fluorescence study. *J Phys Chem B.* (2020) 124:11419–30. doi: 10.1021/acs.jpcb.0c09496

61. Danylchuk DI, Moon S, Xu K, Klymchenko AS. Switchable solvatochromic probes for live-cell super-resolution imaging of plasma membrane organization. *Angew Chem Int Ed Engl.* (2019) 58:14920–4. doi: 10.1002/anie.201907690
62. Barbotin A, Urbancic I, Galiani S, Eggeling C, Booth M, Sezgin E. z-STED imaging and spectroscopy to investigate nanoscale membrane structure and dynamics. *Biophys J.* (2020) 118:2448–57. doi: 10.1016/j.bpj.2020.04.006
63. Danylchuk DI, Sezgin E, Chabert P, Klymchenko AS. Redesigning solvatochromic probe laurdan for imaging lipid order selectively in cell plasma membranes. *Anal Chem.* (2020) 92:14798–805. doi: 10.1021/acs.analchem.0c03559
64. Annibale P, Scarselli M, Kodiyan A, Radenovic A. Photoactivatable fluorescent protein mEos2 displays repeated photoactivation after a long-lived dark state in the red photoconverted form. *J Phys Chem Lett.* (2010) 1:1506–10. doi: 10.1021/jz1003523
65. Platzer R, Rossboth BK, Schneider MC, Sevcsik E, Baumgart F, Stockinger H, et al. Unscrambling fluorophore blinking for comprehensive cluster detection via photoactivated localization microscopy. *Nat Commun.* (2020) 11:4993. doi: 10.1038/s41467-020-18726-9
66. Veerapathiran S, Wohland T. The imaging FCS diffusion law in the presence of multiple diffusive modes. *Methods.* (2018) 140–141:140–50. doi: 10.1016/j.ymeth.2017.11.016
67. Ritter AT, Asano Y, Stinchcombe JC, Dieckmann NMG, Chen B-C, Gawden-Bone C, et al. Actin depletion initiates events leading to granule secretion at the immunological synapse. *Immunity.* (2015) 42:864–76. doi: 10.1016/j.immuni.2015.04.013

Conflict of Interest: The authors declare that the research was conducted in the absence of any commercial or financial relationships that could be construed as a potential conflict of interest.

frontiers in Immunology

PERSPECTIVE
published: 10 March 2021
doi: 10.3389/fimmu.2021.613591

Role of Lipids in Morphogenesis of T-Cell Microvilli

Marek Cebecauer *

Department of Biophysical Chemistry, J. Heyrovsky Institute of Physical Chemistry of the Czech Academy of Sciences (CAS), Prague, Czechia

T cells communicate with the environment *via* surface receptors. Cooperation of surface receptors regulates T-cell responses to diverse stimuli. Recently, finger-like membrane protrusions, microvilli, have been demonstrated to play a role in the organization of receptors and, hence, T-cell activation. However, little is known about the morphogenesis of dynamic microvilli, especially in the cells of immune system. In this review, I focus on the potential role of lipids and lipid domains in morphogenesis of microvilli. Discussed is the option that clustering of sphingolipids with phosphoinositides at the plasma membrane results in dimpling (curved) domains. Such domains can attract phosphoinositide-binding proteins and stimulate actin cytoskeleton reorganization. This process triggers cortical actin opening and bundling of actin fibres to support the growing of microvilli. Critical regulators of microvilli morphogenesis in T cells are unknown. At the end, I suggest several candidates with a potential to organize proteins and lipids in these structures.

Keywords: T cell, microvilli, sphingolipids, phosphoinositides, lipid rafts, membrane curvature, dimpling domains, membrane-associated proteins

OPEN ACCESS

Edited by:
Yan Shi,
Tsinghua University, China

Reviewed by:
Chang-Duk Jun,
Gwangju Institute of Science and Technology, South Korea
Matthew Tyska,
Vanderbilt University, United States

***Correspondence:**
Marek Cebecauer
marek.cebecauer@jh-inst.cas.cz

Specialty section:
This article was submitted to T Cell Biology, a section of the journal Frontiers in Immunology

Received: *02 October 2020*
Accepted: *13 January 2021*
Published: *10 March 2021*

Citation:
Cebecauer M (2021) Role of Lipids in Morphogenesis of T-Cell Microvilli. Front. Immunol. 12:613591. doi: 10.3389/fimmu.2021.613591

INTRODUCTION

T lymphocytes, important supervisors of the immune system, are activated and regulated through receptors expressed on their surface. Surface of lymphocytes is densely covered by membrane protrusions, mainly microvilli (1, 2), which allow for a more complex three-dimensional (3D) organization of receptors compared to a flat membrane. Indeed, critical receptors of T-cell activation, T cell receptor (TCR), CD2, CD4 and CD28 were shown to accumulate at the tips of microvilli in recent studies benefitting from 3D imaging at high resolution (1, 3–7). On the contrary, CD45 is excluded from these areas (6, 7). It was suggested that non-random 3D distribution of receptors is important for optimisation of signalling and cellular responses (8–10). However, little is known about the origin of microvilli and molecules involved in their formation and homeostasis in T lymphocytes. Insight into molecular biophysics and structural details of these membrane protrusions can help to better understand T-cell function in health and disease.

In this work, I suggest the role of lipids and lipid domains in deformation of membranes and their potential role in the formation and organization of microvilli. I start with a brief introduction to microvilli structure and function. These data almost exclusively originate from studies of microvilli in epithelial cells. It is thus important to note here that microvilli of epithelial cells are more stable and may differ in structural details when compared to microvilli on leukocytes. In the central sections, I hypothezise a role of curved lipid domains in microvilli formation and describe regulatory role of lipids for the function of proteins localized prevalently to these structures. I finish

by discussing a handful of molecules with a potential role in morphogenesis of T-cell microvilli. Like lipid domains, function of these proteins in T cells needs to be determined.

MICROVILLI AND THEIR STRUCTURE

Microvilli are finger-like membrane protrusions at the surface of metazoan cells (11). Microvilli consist of the tip, shaft, and base, which connects these structures to the plasma membrane and cortical actin (**Figure 1**). Actin bundles determine a shape of microvilli and are responsible for their stability, but also a dynamic character. In the shaft, the membrane is tightly linked to actin bundles *via* actin- and membrane-binding proteins [e.g., myosins and ERM proteins; see **Figure 1** (12)]. At the base, at least in epithelial cells, actin bundle terminates in the network of intermediate filaments known as 'terminal web' (13, 14). The size of microvilli is regulated by the growth of actin fibres at the tip (15). Microvilli on the surface of polarized epithelial cells covering organs in direct contact with the exterior are rather stable and long (11). Microvilli on T cells are smaller and highly dynamic (1, 2, 16, 17). With ~100 nm in a diameter and a length of 0.5–5 μm, they represent rather small surface structures [Figure 1 in (17) and Figure 1 in (1)]. It is their abundance and flexibility, which makes these structures important for T-cell function. For example, vesicles with receptors and other effector molecules can be shed off the microvilli tips. This phenomenon was observed in epithelia, as well as in T cells, and can be part of complex regulatory mechanisms in multicellular organisms (1, 18).

The accumulation of receptors at the tip of microvilli is beneficiary for an easy access to ligands, substrates or mechanical forces and can determine cellular responses to such stimuli (8, 9, 11). The shaft and the base potentially function as a selecting region, segregating molecules to different membrane environments. However, physico-chemical basis of such selection remains unknown. Importantly, it is still unclear what defines a local onset and chemical composition of microvilli. In the following sections, I suggest a model (**Figure 1**), in which membrane lipids and their physico-chemical properties trigger the onset of microvilli formation.

LIPID DOMAINS AND LOCAL BENDING OF MEMBRANES

In our review on membrane lipid nanodomains [(19), Section 8.4], we discussed a role of curvature in stabilization of domains and prevention of their fusion. In general, formation of a lipid domain with different properties (e.g., rigidity and thickness) compared to the adjacent membrane results in line tension at the boundary (borderline) between the two 'phases' (**Figure 2A**). In

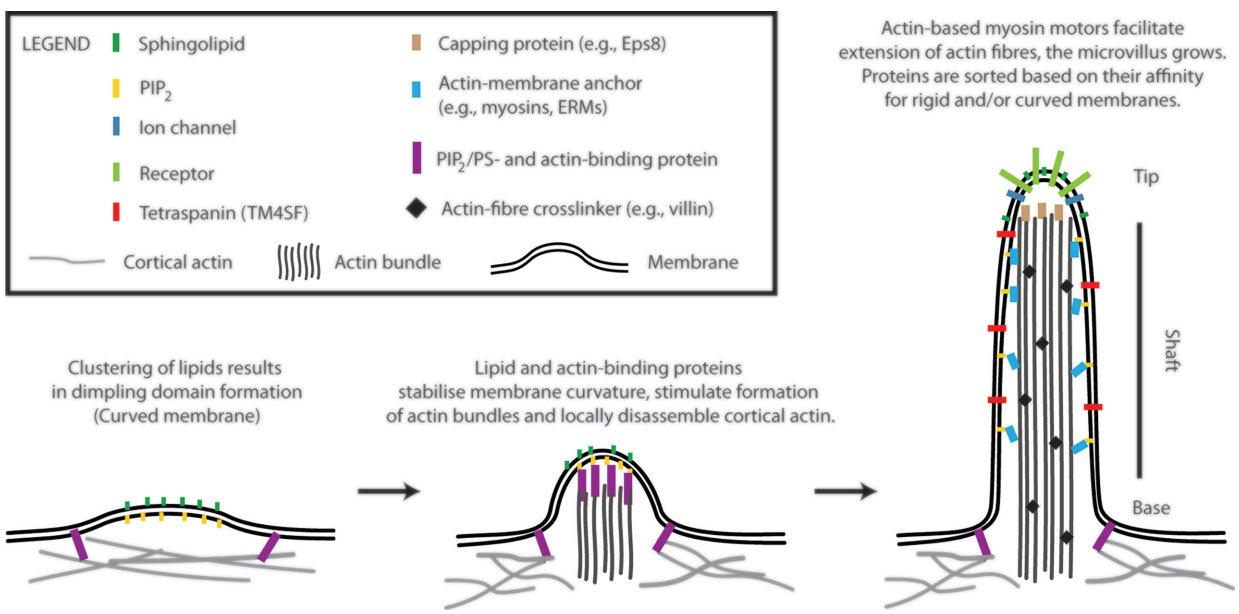

FIGURE 1 | A model of T-cell microvilli morphogenesis. The onset of microvilli can be triggered by transient formation of dimpling lipid domains (see also **Figure 2**). Sphingolipids together with phosphoinositides (e.g., phosphatidylinositol 4,5-bisphosphate; PIP_2) own a high potential to form dimpling domains in asymmetric membranes. Later, actin-binding proteins, which associate with plasma membrane *via* PIP_2 (or phosphatidylserine), induce cortical actin opening and stabilize dimpling domains. Similar proteins can stimulate bundling of actin fibres. The growth of microvilli is driven by polymerization of actin at the plus end of the fibres (distal end of microvilli). Myosins dynamically anchor actin bundles to the membrane at the shaft. ERM (ezrin, radixin, and moesin) proteins function in a similar fashion (membrane anchor) and regulate stability of microvilli. Proteins with affinity for rigid (sphingolipid-enriched) and/or for curved membranes accumulate at the tip or shaft of microvilli. Little is known about T-cell signalling molecules in the lumen of microvilli. The existence of terminal web in microvilli of leukocytes remains unknown. Components of microvilli are not drawn in scale.

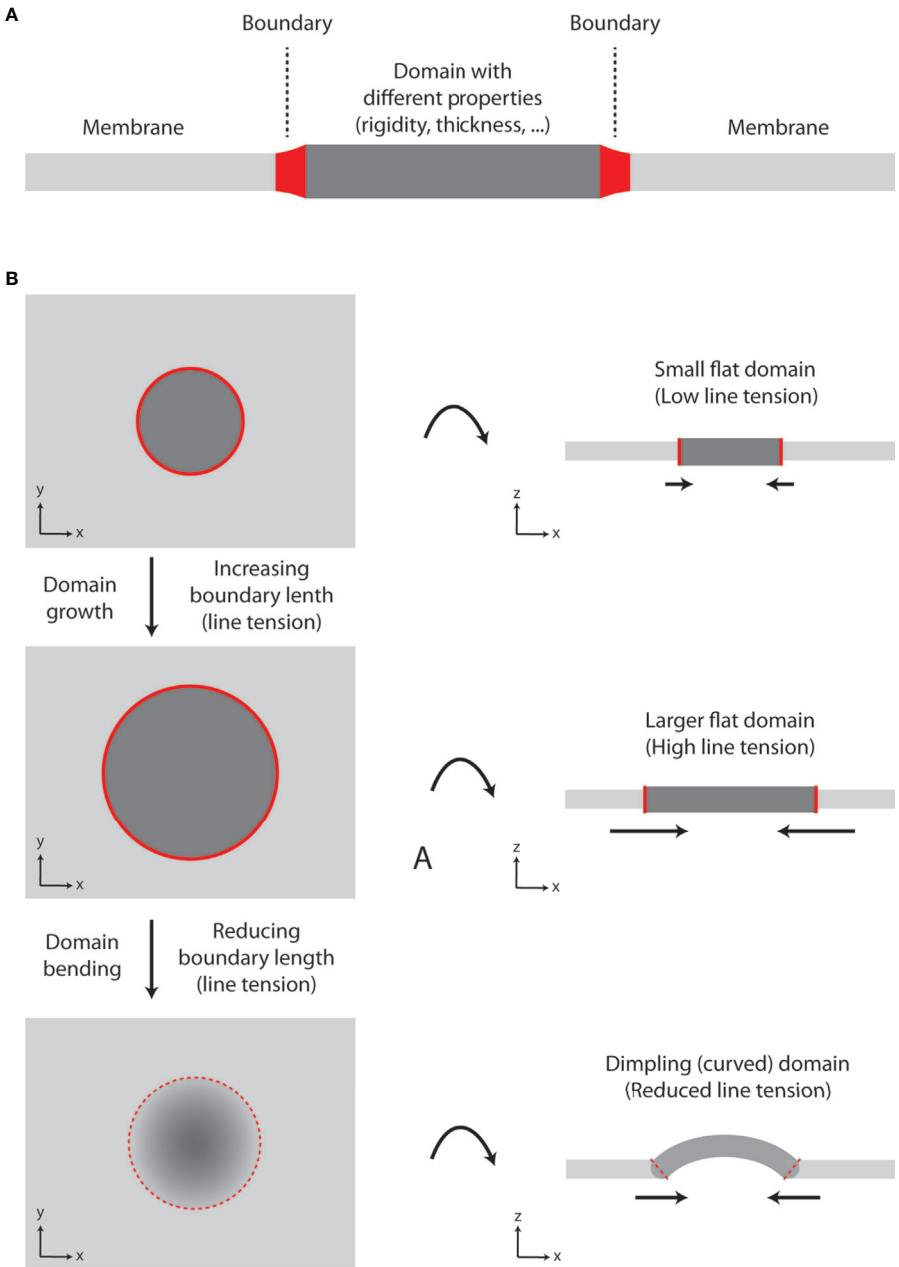

FIGURE 2 | Growth of lipid nanodomains and dimpling (curved) domain formation. **(A)** Schematic illustration of lipid membrane with a domain. The domain has different physico-chemical properties (e.g., rigidity-conformational order, thickness) compared to the surrounding lipid bilayer. The two environments are separated by the boundary. **(B)** Schematic illustration of a domain growth and formation of a dimpling domain. Certain lipids (e.g., sphingolipids and cholesterol) tend to segregate into circular domains in synthetic membranes containing unsaturated glycerophospholipids due to their immiscibility at lower temperatures or in the presence of other clustering factors (e.g., proteins). As the domain grows, line tension at the boundary increases, until it reaches the point, at which it exceeds bending energy required for membrane deformation and dimpling domain is formed. The length of the boundary is reduced, and further growth of the membrane is accompanied by membrane tubulation, but not increase in line tension. Hence, domain formation can lead to induction of membrane curvature and its tubulation.

a growing domain, the length of boundary increases, and line tension rises. However, lipid membranes prefer to minimize tensions associated with their organization (20, 21). Since elastic properties (bending modulus) of membranes are not changing significantly, the size of a domain can reach the point, at which membrane starts to bend and form dimpling domains [**Figure 2B** (22, 23)]. This is caused by the fact that line tension at the boundary exceeds the bending energy (resistance) of a membrane required for its deformation. Membrane bending reduces the boundary length and, thus, line tension. Further

growth of a domain is enabled by enhanced curvature, which can result in membrane tubulation. The length of boundary and line tension remain constant for such growing domain/protrusion (21).

In flat membranes, small domains diminish due to their fusion into larger entities, as observed in model, phase-separated giant unilamellar vesicles (24). Fusion of small domains reduces the length of boundary and line tension (23). However, large lipid domains are not frequent in cells. It is currently agreed that the plasma membrane is highly heterogenous due to the presence of small (nanometric) domains (25, 26). One can thus speculate that plasma membrane is prone to form dimpling domains, which cannot fuse due to repulsive forces at their boundaries (19, 22).

CLUSTERING OF SPHINGOLIPIDS AND PHOSPHOINOSITIDES TRIGGERS MICROVILLI FORMATION

Cellular membranes are composed of a large variety of lipid species. Among those, sphingolipids, with their long and saturated acyl chains and affinity to cholesterol, are prone to segregate from unsaturated glycerophospholipids and form nanodomains (19, 27–29). Ikenouchi and colleagues suggested that sphingolipids are required for the existence of microvilli and, potentially, also initiation of their formation in epithelial cells (30). Conversion of sphingomyelin to ceramides by acidic sphingomyelinase in these cells led to impaired microvilli. In untreated cells, sphingolipids accumulated on microvilli (30). Accumulation of sphingomyelin (and cholesterol) in microvilli was confirmed in another study, which employed lysenin labeling of sphingomyelin (perfolysin *O* for cholesterol) and sensitive nanoSIMS imaging in CHO-K1 epithelial-like cells (31). Of note, only freely accessible lipids could be detected using this method. In another study, interference with sphingolipid or cholesterol synthesis lead to reduced presence of microvilli on epithelial cells (32). All these studies indicate that sphingolipids are essential for the morphogenesis of microvilli.

Membrane lipid composition considerably differs between various cell types. Though sphingolipids consistently constitute 20-40% of plasma membrane lipids (33, 34). Local concentration of sphingolipids is even higher due to chemical asymmetry of the plasma membrane (lipid bilayer). Such high content of sphingolipids in the outer leaflet can lead to their transient clustering and, occasionally, formation of dimpling domains. Indeed, bilayer asymmetry reduces bending modulus of a membrane and, thus, facilitates its deformation (22, 35). In cells, phosphatidylinositol 4,5-bisphosphate (PIP_2) molecules were found to cluster underneath sphingolipid domains during membrane deformation induced by viral proteins [virion budding (36, 37)]. PIP_2 was also found to accumulate in microvilli (30). But comprehensive analysis of lipids in microvilli has not been performed to date (38). Therefore, it is unclear what is the content of PIP_2, sphingolipids and other lipids (e.g., cholesterol) in these structures.

The presence of PIP_2 in the apical membrane of epithelial cells, but of phosphatidylinositol 3,4,5-trisphosphate (PIP_3) in basolateral membrane, further supports the involvement of this lipid in microvilli formation (39). Microvilli can be found only on the apical surface of epithelial cells. Apical membrane of polarized cells is also enriched in sphingomyelin and cholesterol (40). Moreover, PIP_2 accumulates in the uropod of motile cells, whereas PIP_3 can be found in the leading edge. Microvilli are often observed at the back of motile cells, including T cells (17, 41, 42). In analogy to sphingomyelin domains, cholesterol facilitates clustering of PIP_2 (43). Due to its high lateral and transbilayer mobility (44, 45), cholesterol is expected to freely access dimpling domains. Interestingly, cholesterol does not influence bending modulus of synthetic membranes with diverse lipid composition (46, 47). Thus, cholesterol does not directly raise the energy required for membrane deformation and establishment of dimpling membranes, but the effect can depend on its intramembrane orientation and distribution between the outer and inner leaflet (45).

LIPID-PROTEIN CROSSTALK IN MICROVILLAR MORPHOGENESIS AND FUNCTION

To further highlight the importance of lipids in microvilli morphogenesis, I will describe three examples where lipid metabolism determines the function of critical proteins in microvilli. The examples were selected based on the depth of our understanding of these regulatory processes. As in the case of microvilli structure, this knowledge comes from microvilli of epithelial cells, but similar regulatory mechanisms can be expected in T-cells.

ERM family proteins (ezrin, radixin, and moesin) tightly anchor actin-bundles to the membrane of microvilli. This is facilitated by binding of their FERM domain to PIP_2 (48). The process is regulated by a local lipid environment. Conversion of sphingomyelin to ceramide and of sphingosine to sphingosine-1-phosphate negatively and positively, respectively, regulate membrane-association of ERM proteins and, thus, stability of microvilli (49, 50). The role of ERM proteins for microvilli is evidently critical, since their knock-down leads to their reduced size and number (51, 52).

Podocalyxin-1 accumulates in microvilli of epithelial cells. Podocalyxin-1 interacts with ERM proteins *via* EBP50 (53). It further interacts with phosphoinositide-4-phosphate 5-kinase (PI5K) β and delivers this critical enzyme to microvilli. The formation of podocalyxin-1 multiprotein complex with PI5K leads to a local increase in PIP_2 synthesis and stability of microvilli (30). Interestingly, podocalyxin-1 associates with sphingolipid domains, probably upon its palmitoylation (54). The crosstalk of diverse lipids in the regulation of this protein remains unknown.

Another protein associating with sphingolipid domains on microvilli is prominin-1 [also called CD133 (55)]. Overexpression of prominin-1 increases a number of microvilli (56). This protein directly binds cholesterol and GM1 ganglioside (57). These lipid-

protein interactions were found essential for fine tuning of microvillar structure. The protein is further regulated by phosphorylation of its regulatory tyrosines [Y_{817}/Y_{828} (56)]. Phosphorylation of these tyrosines regulates interaction of prominin-1 with phosphoinositide 3-kinase (PI3K). In contrast to PI5K, PI3K locally reduces available PIP_2 by its conversion to PIP_3 and destabilizes the anchorage of actin bundles to the membrane (56).

POTENTIAL REGULATORS OF MICROVILLI IN T CELLS

I have argued above that lipid domains induce curvature in flat regions of the plasma membrane. Such domains would be transient in the absence of supporting proteins (**Figure 1**). The process is well described for the endocytosis or viral budding (36, 37, 58–61). For example, matrix proteins (e.g., Gag of HIV-1) form a dome-like structure under the curved membrane of nascent viral particles.

Proteins stabilizing dimpling domains at the sites of newly assembling microvilli have not been described yet. A few proteins (e.g., prominin-1/CD133, podocalyxin-1) reported to regulate microvilli morphogenesis in epithelial cells (30, 55), are not expressed in T cells or at highly variable levels in diverse T-cell subsets. Their role in microvilli morphogenesis in T cells is thus questionable. Here, I will focus on four proteins (protein families), which exhibit great potential to induce or stabilize microvilli in T cells.

The geometry and chemistry of dimpling domains delineates properties of potential supporting proteins. These must interact with negative curvature and anionic lipids. I-BAR domain proteins exhibit such properties. IRSp53 contains I-BAR domain and was shown to induce negative curvature and tubulation in synthetic vesicles (62). IRSp53 localizes to curved membranes of neuronal cells (63) and filopodia of motile fibroblasts (64). It supports membrane ruffling and protrusions in T cells (65). In epithelial cells, it is expressed at the microvilli-containing apical membrane and functionally associates with podocalyxin-1 (66). As a protein of countless functions, it will be important to characterize its specific role in microvilli of T cells. Alternatively, other I-BAR domain-containing proteins can fulfil this function in lymphoid cells.

Tetherin (also called CD317) with affinity for ordered, sphingolipid-rich membranes interacts with BAR domain-containing RICH family proteins (67). Tetherin/RICH-2 complex forms a mechanical support of epithelial microvilli (68). Its analog, RICH-1, is expressed in T-cells (Human Protein Atlas). BAR domain of RICH proteins can induce positive curvature and tubulate lipid vesicles containing PIP_2 in the absence of tetherin (69). The potential of tetherin/RICH complex thus lies at the neck connecting microvilli (or dimpling domains) to membrane base *via* a positively curved segment (**Figure 1**).

Unconventional myosins (e.g., myo1a, myo7b) link actin fibres to membrane by their interaction with anionic lipids, PIP_2 or phosphatidylserine (70). Myosins also contribute to the formation of a 'hole' in the cortical actin at the site of new microvillus formation (71). Such local depletion of cortical actin is essential for the initiation of membrane protrusions (72). This process may be also connected to the formation and stabilization of dimpling lipid domains.

Members of tetraspanin protein superfamily (TM4SF) accumulate at the microvilli of diverse cells. CD9, CD81, CD82, and TSPAN33 were shown to control the size and shape of microvilli in both, leukocytes and epithelial cells (73–75). TM4SF proteins (e.g., CD81) require highly curved membrane for their assembly into virus-like particles induced by HIV-1 Gag protein (37, 76). The main role of TM4SF is thus expected for growing or established microvilli with highly curved tubular membrane.

None of the proteins mentioned in this section was already determined as a microvilli regulator in T cells. However, I believe that intense research in this direction may soon offer interesting discoveries related not only to microvilli, but also to T-cell signaling and function.

CONCLUSIONS

Recent observations demonstrate that microvilli play essential role in T-cell activation. Key signalling molecules were found to accumulate in different parts of these morphological structures. Theoretical and biophysical studies indicate that sphingolipids and phosphoinositides in complex asymmetric membranes tend to generate dimpling domains. In the plasma membrane of T cells, dimpling domains can be the sites of an onset of microvilli, as indicated in the presented model. Specific lipids also fine tune behaviour of critical regulatory proteins in microvilli. These data substantiate the role of lipids in morphogenesis and function of microvilli. However, in T cells, the identity of key proteins (and lipids) in microvilli remains unknown. Future works are required to discover these important organizers of signalling receptors at the plasma membrane of T cells. Such research may open new avenues for treatment of many human diseases, which are associated with the malfunction of these critical immune cells.

AUTHOR CONTRIBUTIONS

The author confirms being the sole contributor of this work and has approved it for publication.

FUNDING

This work was supported by Czech Science Foundation (19-07043S).

ACKNOWLEDGMENTS

I would like to thank Zuzana Kvíčalová, Harsha Mavila, Piotr Jurkiewicz and Tomáš Chum for excellent discussions, which stimulated and shaped this work.

REFERENCES

1. Kim HR, Mun Y, Lee KS, Park YJ, Park JS, Park JH, et al. T cell microvilli constitute immunological synaptosomes that carry messages to antigen-presenting cells. *Nat Commun* (2018) 9(1):3630. doi: 10.1038/s41467-018-06090-8
2. Majstoravich S, Zhang J, Nicholson-Dykstra S, Linder S, Friedrich W, Siminovitch KA, et al. Lymphocyte microvilli are dynamic, actin-dependent structures that do not require Wiskott-Aldrich syndrome protein (WASp) for their morphology. *Blood* (2004) 104(5):1396–403. doi: 10.1182/blood-2004-02-0437
3. Cai E, Marchuk K, Beemiller P, Beppler C, Rubashkin MG, Weaver VM, et al. Visualizing dynamic microvillar search and stabilization during ligand detection by T cells. *Science* (2017) 356(6338):598. doi: 10.1126/science.aal3118
4. Jung Y, Riven I, Feigelson SW, Kartvelishvily E, Tohya K, Miyasaka M, et al. Three-dimensional localization of T-cell receptors in relation to microvilli using a combination of superresolution microscopies. *Proc Natl Acad Sci USA* (2016) 113(40):E5916–24. doi: 10.1073/pnas.1605399113
5. Ghosh S, Di Bartolo V, Tubul L, Shimoni E, Kartvelishvily E, Dadosh T, et al. ERM-Dependent Assembly of T Cell Receptor Signaling and Co-stimulatory Molecules on Microvilli prior to Activation. *Cell Rep* (2020) 30(10):3434–47 e6. doi: 10.1016/j.celrep.2020.02.069
6. Franke C, Chum T, Kvíčalová Z, Glatzová D, Rodriguez A, Helmerich DA, et al. Unraveling nanotopography of cell surface receptors. *Biorxiv (Preprint)* (2019). doi: 10.1101/2020.08.10.244251
7. Jung Y, Wen L, Altman A, Ley K. CD45 pre-exclusion from the tips of microvilli establishes a phosphatase-free zone for early TCR triggering. *Biorxiv (Preprint)* (2020). doi: 10.1101/2020.05.21.109074
8. Kim HR, Jun CD. T Cell Microvilli: Sensors or Senders? *Front Immunol* (2019) 10:1753. doi: 10.3389/fimmu.2019.01753
9. Glatzova D, Cebecauer M. Dual Role of CD4 in Peripheral T Lymphocytes. *Front Immunol* (2019) 10:618. doi: 10.3389/fimmu.2019.00618
10. Garcia E, Ismail S. Spatiotemporal Regulation of Signaling: Focus on T Cell Activation and the Immunological Synapse. *Int J Mol Sci* (2020) 21(9):3283. doi: 10.3390/ijms21093283
11. Lange K. Fundamental role of microvilli in the main functions of differentiated cells: Outline of an universal regulating and signaling system at the cell periphery. *J Cell Physiol* (2011) 226(4):896–927. doi: 10.1002/jcp.22302
12. Sauvanet C, Wayt J, Pelaseyed T, Bretscher A. Structure, regulation, and functional diversity of microvilli on the apical domain of epithelial cells. *Annu Rev Cell Dev Biol* (2015) 31:593–621. doi: 10.1146/annurev-cellbio-100814-125234
13. Hirokawa N, Tilney LG, Fujiwara K, Heuser JE. Organization of actin, myosin, and intermediate filaments in the brush border of intestinal epithelial cells. *J Cell Biol* (1982) 94(2):425–43. doi: 10.1083/jcb.94.2.425
14. Beer AJ, Gonzalez Delgado J, Steiniger F, Qualmann B, Kessels MM. The actin nucleator Cobl organises the terminal web of enterocytes. *Sci Rep* (2020) 10 (1):11156. doi: 10.1038/s41598-020-66111-9
15. Faust JJ, Millis BA, Tyska MJ. Profilin-Mediated Actin Allocation Regulates the Growth of Epithelial Microvilli. *Curr Biol* (2019) 29(20):3457–65.e3. doi: 10.1016/j.cub.2019.08.051
16. Gorelik J, Shevchuk AI, Frolenkov GI, Diakonov IA, Lab MJ, Kros CJ, et al. Dynamic assembly of surface structures in living cells. *Proc Natl Acad Sci USA* (2003) 100(10):5819–22. doi: 10.1073/pnas.1030502100
17. Brown MJ, Nijhara R, Hallam JA, Gignac M, Yamada KM, Erlandsen SL, et al. Chemokine stimulation of human peripheral blood T lymphocytes induces rapid dephosphorylation of ERM proteins, which facilitates loss of microvilli and polarization. *Blood* (2003) 102(12):3890–9. doi: 10.1182/blood-2002-12-3807
18. Shifrin DA, Jr., McConnell RE, Nambiar R, Higginbotham JN, Coffey RJ, Tyska MJ. Enterocyte microvillus-derived vesicles detoxify bacterial products and regulate epithelial-microbial interactions. *Curr Biol* (2012) 22(7):627–31. doi: 10.1016/j.cub.2012.02.022
19. Cebecauer M, Amaro M, Jurkiewicz P, Sarmento MJ, Sachl R, Cwiklik L, et al. Membrane Lipid Nanodomains. *Chem Rev* (2018) 118(23):11259–97. doi: 10.1021/acs.chemrev.8b00322
20. Lipowsky R. Domain-induced budding of fluid membranes. *Biophys J* (1993) 64(4):1133–8. doi: 10.1016/S0006-3495(93)81479-6
21. Lipowsky R. Budding of Membranes Induced by Intramembrane Domains. *J Phys Ii* (1992) 2(10):1825–40. doi: 10.1051/jp2:1992238
22. Ursell TS, Klug WS, Phillips R. Morphology and interaction between lipid domains. *Proc Natl Acad Sci USA* (2009) 106(32):13301–6. doi: 10.1073/pnas.0903825106
23. Rim JE, Ursell TS, Phillips R, Klug WS. Morphological Phase Diagram for Lipid Membrane Domains with Entropic Tension. *Phys Rev Lett* (2011) 106 (5):057801. doi: 10.1103/PhysRevLett.106.057801
24. Veatch SL, Keller SL. Seeing spots: complex phase behavior in simple membranes. *Biochim Biophys Acta* (2005) 1746(3):172–85. doi: 10.1016/j.bbamcr.2005.06.010
25. Bernardino de la Serna J, Schutz GJ, Eggeling C, Cebecauer M. There Is No Simple Model of the Plasma Membrane Organization. *Front Cell Dev Biol* (2016) 4:106. doi: 10.3389/fcell.2016.00106
26. Levental I, Levental KR, Heberle FA. Lipid Rafts: Controversies Resolved, Mysteries Remain. *Trends Cell Biol* (2020) 30(5):341–53. doi: 10.1016/j.tcb.2020.01.009
27. Bjorkbom A, Rog T, Kaszuba K, Kurita M, Yamaguchi S, Lonnfors M, et al. Effect of sphingomyelin headgroup size on molecular properties and interactions with cholesterol. *Biophys J* (2010) 99(10):3300–8. doi: 10.1016/j.bpj.2010.09.049
28. Lonnfors M, Doux JP, Killian JA, Nyholm TK, Slotte JP. Sterols have higher affinity for sphingomyelin than for phosphatidylcholine bilayers even at equal acyl-chain order. *Biophys J* (2011) 100(11):2633–41. doi: 10.1016/j.bpj.2011.03.066
29. Simons K, Ikonen E. Functional rafts in cell membranes. *Nature* (1997) 387 (6633):569–72. doi: 10.1038/42408
30. Ikenouchi J, Hirata M, Yonemura S, Umeda M. Sphingomyelin clustering is essential for the formation of microvilli. *J Cell Sci* (2013) 126(Pt 16):3585–92. doi: 10.1242/jcs.122325
31. He C, Hu X, Jung RS, Weston TA, Sandoval NP, Tontonoz P, et al. High-resolution imaging and quantification of plasma membrane cholesterol by NanoSIMS. *Proc Natl Acad Sci USA* (2017) 114(8):2000–5. doi: 10.1073/pnas.1621432114
32. Poole K, Meder D, Simons K, Muller D. The effect of raft lipid depletion on microvilli formation in MDCK cells, visualized by atomic force microscopy. *FEBS Lett* (2004) 565(1-3):53–8. doi: 10.1016/j.febslet.2004.03.095
33. van Meer G, Voelker DR, Feigenson GW. Membrane lipids: where they are and how they behave. *Nat Rev Mol Cell Biol* (2008) 9(2):112–24. doi: 10.1038/nrm2330
34. Lorent JH, Levental KR, Ganesan L, Rivera-Longsworth G, Sezgin E, Doktorova M, et al. Plasma membranes are asymmetric in lipid unsaturation, packing and protein shape. *Nat Chem Biol* (2020) 16(6):644–52. doi: 10.1038/s41589-020-0529-6
35. Perlmutter JD, Sachs JN. Interleaflet interaction and asymmetry in phase separated lipid bilayers: molecular dynamics simulations. *J Am Chem Soc* (2011) 133(17):6563–77. doi: 10.1021/ja106626r
36. Romer W, Berland L, Chambon V, Gaus K, Windschiegl B, Tenza D, et al. Shiga toxin induces tubular membrane invaginations for its uptake into cells. *Nature* (2007) 450(7170):670–5. doi: 10.1038/nature05996
37. Hogue IB, Grover JR, Soheilian F, Nagashima K, Ono A. Gag induces the coalescence of clustered lipid rafts and tetraspanin-enriched microdomains at HIV-1 assembly sites on the plasma membrane. *J Virol* (2011) 85(19):9749–66. doi: 10.1128/JVI.00743-11
38. Kaiser F, Huebecker M, Wachten D. Sphingolipids controlling ciliary and microvillar function. *FEBS Lett* (2020) 594:3652–67. doi: 10.1002/1873-3468.13816
39. Martin-Belmonte F, Gassama A, Datta A, Yu W, Rescher U, Gerke V, et al. PTEN-mediated apical segregation of phosphoinositides controls epithelial morphogenesis through Cdc42. *Cell* (2007) 128(2):383–97. doi: 10.1016/j.cell.2006.11.051
40. Schuck S, Simons K. Polarized sorting in epithelial cells: raft clustering and the biogenesis of the apical membrane. *J Cell Sci* (2004) 117(Pt 25):5955–64. doi: 10.1242/jcs.01596
41. Iijima M, Devreotes P. Tumor suppressor PTEN mediates sensing of chemoattractant gradients. *Cell* (2002) 109(5):599–610. doi: 10.1016/s0092-8674(02)00745-6
42. Lokuta MA, Senetar MA, Bennin DA, Nuzzi PA, Chan KT, Ott VL, et al. Type Igamma PIP kinase is a novel uropod component that regulates rear retraction

during neutrophil chemotaxis. *Mol Biol Cell* (2007) 18(12):5069–80. doi: 10.1091/mbc.e07-05-0428
43. Jiang Z, Redfern RE, Isler Y, Ross AH, Gericke A. Cholesterol stabilizes fluid phosphoinositide domains. *Chem Phys Lipids* (2014) 182:52–61. doi: 10.1016/j.chemphyslip.2014.02.003
44. Pinkwart K, Schneider F, Lukoseviciute M, Sauka-Spengler T, Lyman E, Eggeling C, et al. Nanoscale dynamics of cholesterol in the cell membrane. *J Biol Chem* (2019) 294(34):12599–609. doi: 10.1074/jbc.RA119.009683
45. Allender DW, Sodt AJ, Schick M. Cholesterol-Dependent Bending Energy Is Important in Cholesterol Distribution of the Plasma Membrane. *Biophys J* (2019) 116(12):2356–66. doi: 10.1016/j.bpj.2019.03.028
46. Sorre B, Callan-Jones A, Manneville JB, Nassoy P, Joanny JF, Prost J, et al. Curvature-driven lipid sorting needs proximity to a demixing point and is aided by proteins. *Proc Natl Acad Sci USA* (2009) 106(14):5622–6. doi: 10.1073/pnas.0811243106
47. Pan J, Mills TT, Tristram-Nagle S, Nagle JF. Cholesterol perturbs lipid bilayers nonuniversally. *Phys Rev Lett* (2008) 100(19):198103. doi: 10.1103/PhysRevLett.100.198103
48. Blin G, Margeat E, Carvalho K, Royer CA, Roy C, Picart C. Quantitative analysis of the binding of ezrin to large unilamellar vesicles containing phosphatidylinositol 4,5 bisphosphate. *Biophys J* (2008) 94(3):1021–33. doi: 10.1529/biophysj.107.110213
49. Adada M, Canals D, Hannun YA, Obeid LM. Sphingolipid regulation of ezrin, radixin, and moesin proteins family: implications for cell dynamics. *Biochim Biophys Acta* (2014) 1841(5):727–37. doi: 10.1016/j.bbalip.2013.07.002
50. Canals D, Jenkins RW, Roddy P, Hernandez-Corbacho MJ, Obeid LM, Hannun YA. Differential effects of ceramide and sphingosine 1-phosphate on ERM phosphorylation: probing sphingolipid signaling at the outer plasma membrane. *J Biol Chem* (2010) 285(42):32476–85. doi: 10.1074/jbc.M110.141028
51. Bonilha VL, Finnemann SC, Rodriguez-Boulan E. Ezrin promotes morphogenesis of apical microvilli and basal infoldings in retinal pigment epithelium. *J Cell Biol* (1999) 147(7):1533–48. doi: 10.1083/jcb.147.7.1533
52. Crepaldi T, Gautreau A, Comoglio PM, Louvard D, Arpin M. Ezrin is an effector of hepatocyte growth factor-mediated migration and morphogenesis in epithelial cells. *J Cell Biol* (1997) 138(2):423–34. doi: 10.1083/jcb.138.2.423
53. Hsu YH, Lin WL, Hou YT, Pu YS, Shun CT, Chen CL, et al. Podocalyxin EBP50 ezrin molecular complex enhances the metastatic potential of renal cell carcinoma through recruiting Rac1 guanine nucleotide exchange factor ARHGEF7. *Am J Pathol* (2010) 176(6):3050–61. doi: 10.2353/ajpath.2010.090539
54. Marin EP, Derakhshan B, Lam TT, Davalos A, Sessa WC. Endothelial cell palmitoylproteomic identifies novel lipid-modified targets and potential substrates for protein acyl transferases. *Circ Res* (2012) 110(10):1336–44. doi: 10.1161/CIRCRESAHA.112.269514
55. Roper K, Corbeil D, Huttner WB. Retention of prominin in microvilli reveals distinct cholesterol-based lipid micro-domains in the apical plasma membrane. *Nat Cell Biol* (2000) 2(9):582–92. doi: 10.1038/35023524
56. Thamm K, Simaite D, Karbanova J, Bermudez V, Reichert D, Morgenstern A, et al. Prominin-1 (CD133) modulates the architecture and dynamics of microvilli. *Traffic* (2019) 20(1):39–60. doi: 10.1111/tra.12618
57. Taieb N, Maresca M, Guo XJ, Garmy N, Fantini J, Yahi N. The first extracellular domain of the tumour stem cell marker CD133 contains an antigenic ganglioside-binding motif. *Cancer Lett* (2009) 278(2):164–73. doi: 10.1016/j.canlet.2009.01.013
58. Romer W, Pontani LL, Sorre B, Rentero C, Berland L, Chambon V, et al. Actin dynamics drive membrane reorganization and scission in clathrin-independent endocytosis. *Cell* (2010) 140(4):540–53. doi: 10.1016/j.cell.2010.01.010
59. Ewers H, Romer W, Smith AE, Bacia K, Dmitrieff S, Chai W, et al. GM1 structure determines SV40-induced membrane invagination and infection. *Nat Cell Biol* (2010) 12(1):11–8. doi: 10.1038/ncb1999
60. Parton RG, Simons K. The multiple faces of caveolae. *Nat Rev Mol Cell Biol* (2007) 8(3):185–94. doi: 10.1038/nrm2122
61. Briggs JA, Riches JD, Glass B, Bartonova V, Zanetti G, Krausslich HG. Structure and assembly of immature HIV. *Proc Natl Acad Sci USA* (2009) 106(27):11090–5. doi: 10.1073/pnas.0903535106
62. Barooji YF, Rorvig-Lund A, Semsey S, Reihani SN, Bendix PM. Dynamics of membrane nanotubes coated with I-BAR. *Sci Rep* (2016) 6:30054. doi: 10.1038/srep30054
63. Choi J, Ko J, Racz B, Burette A, Lee JR, Kim S, et al. Regulation of dendritic spine morphogenesis by insulin receptor substrate 53, a downstream effector of Rac1 and Cdc42 small GTPases. *J Neurosci* (2005) 25(4):869–79. doi: 10.1523/JNEUROSCI.3212-04.2005
64. Nakagawa H, Miki H, Nozumi M, Takenawa T, Miyamoto S, Wehland J, et al. IRSp53 is colocalised with WAVE2 at the tips of protruding lamellipodia and filopodia independently of Mena. *J Cell Sci* (2003) 116(Pt 12):2577–83. doi: 10.1242/jcs.00462
65. Rajagopal S, Ji Y, Xu K, Li Y, Wicks K, Liu J, et al. Scaffold proteins IRSp53 and spinophilin regulate localized Rac activation by T-lymphocyte invasion and metastasis protein 1 (TIAM1). *J Biol Chem* (2010) 285(23):18060–71. doi: 10.1074/jbc.M109.051490
66. Bisi S, Marchesi S, Rizvi A, Carra D, Beznoussenko GV, Ferrara I, et al. IRSp53 controls plasma membrane shape and polarized transport at the nascent lumen in epithelial tubules. *Nat Commun* (2020) 11(1):3516. doi: 10.1038/s41467-020-17091-x
67. Billcliff PG, Rollason R, Prior I, Owen DM, Gaus K, Banting G. CD317/tetherin is an organiser of membrane microdomains. *J Cell Sci* (2013) 126(Pt 7):1553–64. doi: 10.1242/jcs.112953
68. Rollason R, Korolchuk V, Hamilton C, Jepson M, Banting G. A CD317/tetherin-RICH2 complex plays a critical role in the organization of the subapical actin cytoskeleton in polarized epithelial cells. *J Cell Biol* (2009) 184(5):721–36. doi: 10.1083/jcb.200804154
69. Richnau N, Fransson A, Farsad K, Aspenstrom P. RICH-1 has a BIN/Amphiphysin/Rvsp domain responsible for binding to membrane lipids and tubulation of liposomes. *Biochem Biophys Res Commun* (2004) 320(3):1034–42. doi: 10.1016/j.bbrc.2004.05.221
70. Weck ML, Grega-Larson NE, Tyska MJ. MyTH4-FERM myosins in the assembly and maintenance of actin-based protrusions. *Curr Opin Cell Biol* (2017) 44:68–78. doi: 10.1016/j.ceb.2016.10.002
71. Bisaria A, Hayer A, Garbett D, Cohen D, Meyer T. Membrane-proximal F-actin restricts local membrane protrusions and directs cell migration. *Science* (2020) 368(6496):1205–10. doi: 10.1126/science.aay7794
72. Welf ES, Miles CE, Huh J, Sapoznik E, Chi J, Driscoll MK, et al. Actin-Membrane Release Initiates Cell Protrusions. *Dev Cell* (2020) 55:P723–36. doi: 10.1016/j.devcel.2020.11.024
73. Navarro-Hernandez IC, Lopez-Ortega O, Acevedo-Ochoa E, Cervantes-Diaz R, Romero-Ramirez S, Sosa-Hernandez VA, et al. Tetraspanin 33 (TSPAN33) regulates endocytosis and migration of human B lymphocytes by affecting the tension of the plasma membrane. *FEBS J* (2020) 287(16):3449–71. doi: 10.1111/febs.15216
74. Runge KE, Evans JE, He ZY, Gupta S, McDonald KL, Stahlberg H, et al. Oocyte CD9 is enriched on the microvillar membrane and required for normal microvillar shape and distribution. *Dev Biol* (2007) 304(1):317–25. doi: 10.1016/j.ydbio.2006.12.041
75. Bari R, Guo Q, Xia B, Zhang YH, Giesert EE, Levy S, et al. Tetraspanins regulate the protrusive activities of cell membrane. *Biochem Biophys Res Commun* (2011) 415(4):619–26. doi: 10.1016/j.bbrc.2011.10.121
76. Sengupta P, Seo AY, Pasolli HA, Song YE, Johnson MC. Lippincott-Schwartz J. A lipid-based partitioning mechanism for selective incorporation of proteins into membranes of HIV particles. *Nat Cell Biol* (2019) 21(4):452–61. doi: 10.1038/s41556-019-0300-y

Conflict of Interest: The author declares that the research was conducted in the absence of any commercial or financial relationships that could be construed as a potential conflict of interest.

Advantages of publishing in Frontiers

OPEN ACCESS
Articles are free to read for greatest visibility and readership

FAST PUBLICATION
Around 90 days from submission to decision

HIGH QUALITY PEER-REVIEW
Rigorous, collaborative, and constructive peer-review

TRANSPARENT PEER-REVIEW
Editors and reviewers acknowledged by name on published articles

Frontiers
Avenue du Tribunal-Fédéral 34
1005 Lausanne | Switzerland

Visit us: www.frontiersin.org
Contact us: frontiersin.org/about/contact

REPRODUCIBILITY OF RESEARCH
Support open data and methods to enhance research reproducibility

DIGITAL PUBLISHING
Articles designed for optimal readership across devices

FOLLOW US
@frontiersin

IMPACT METRICS
Advanced article metrics track visibility across digital media

EXTENSIVE PROMOTION
Marketing and promotion of impactful research

LOOP RESEARCH NETWORK
Our network increases your article's readership